INFLUENCE OF MINERAL ADMIXTURE TYPE AND AMOUNT ON RHEOLOGICAL PROPERTIES OF MORTARS

A THESIS SUBMITTED TO

THE GRADUATE SCHOOL OF NATURAL AND APPLIED SCIENCES

OF

MIDDLE EAST TECHNICAL UNIVERSITY

BY

MARIA IDREES

IN PARTIAL FULFILLMENT OF THE REQUIREMENT

FOR

THE DEGREE OF DOCTOR OF PHILOSOPHY

IN

CIVIL ENGINEERING

NOVEMBER 2016

Approval of the thesis:

INFLUENCE OF MINERAL ADMIXTURE TYPE AND AMOUNT ON RHEOLOGICAL PROPERTIES OF MORTARS

submitted by **MARIA IDREES** in partial fulfillment of the requirements for the degree of **Doctor of Philosophy in Civil Engineering, Middle East Technical University** by,

Prof. Dr. Gülbin Dural Ünver ____________________
Dean, Graduate School of **Natural and Applied Sciences**

Prof. Dr. İsmail Özgür Yaman ____________________
Head of Department, **Civil Engineering**

Prof. Dr. Mustafa Tokyay ____________________
Supervisor, **Civil Engineering Dept., METU**

Examining Committee Members:

Prof. Dr. Kabiz Ramyar ____________________
Civil Eng. Dept., Ege University

Prof. Dr. Mustafa Tokyay ____________________
Civil Eng. Dept., METU

Prof. Dr. İsmail Özgür Yaman ____________________
Civil Eng. Dept., METU

Assoc. Prof. Dr. Mustafa Şahmaran ____________________
Civil Eng. Dept., Gazi University

Assist. Prof. Dr. Cağla Meral ____________________
Civil Eng. Dept., METU

Date: 18.11.2016

I hereby declare that all information in this document has been obtained and presented in accordance with academic rule and ethical conduct . I also declare that, as required by the rules and conducts, I have fully cited and referenced all material and results that are not original to this work.

Name, Last Name: Maria Idrees

Signature:-------------------

ABSTRACT

INFLUENCE OF MINERAL ADMIXTURE TYPE AND AMOUNT ON RHEOLOGICAL PROPERTIES OF MORTARS

Maria Idrees

PhD., Department of Civil Engineering
Supervisor: Prof. Dr. Mustafa TOKYAY

November 2016, 241 pages

Fly ash (FA), silica fume (SF) and ground granulated blast furnace slag (BFS) are used in different amounts to partially replace portland cement (PC) on mass basis to prepare mortars mixtures with different water-binder ratios. In all mixtures, a constant amount of a polycarboxylate based high range water reducing admixture was used. The rheological measurements of fresh mortars were taken right after mixing and at 10 and 20 minutes after mixing by using a two-probe eBT2 rheometer.

The effect of each mineral admixture amount on relative yield stress and relative viscosity of mortars were determined and compared with those of the control mixtures without any mineral admixture. General rheological behavior of these mixtures were determined and analyzed.

Eight different flow models proposed by other researchers are checked for suitability to the experimental data obtained and a new model is proposed. The suitability of the proposed model was checked both for portland cement and mineral admixture-incorporated cement mortars and it was found to be a better model than all other models when compared to the other proposed models, so far.

Key words: Rheology, mortar, mineral admixtures, flow models, relative yield stress, relative plastic viscosity.

ÖZ

MİNERAL KATKI TÜR VE MİKTARININ HARÇLARIN REOLOJİK ÖZELLİKLERİNE ETKİLERİ

Maria Idrees

Doktora., İnşaat Mühendisliği Bölümü
Danışman: Prof. Dr. Mustafa TOKYAY

Kasım 2016,   241 sayfa

Uçucu kül (FA), silis dumanı (SF) ve öğütülmüş granule yüksek fırın cürufu (BFS) portland çimentosunun (PÇ) bir kısmını ikame etmek üzere değişik miktarlarda kullanılarak farklı su-bağlayıcı oranına sahip harçlar üretilmiştir. Tüm karışımlarda sabit miktarda polikarboksilat esaslı bir yüksek akışkanlaştırıcı katkı kullanılmıştır. Taze harçların rheolojik ölçümleri karıştırma işleminden hemen ardından ve 10 ve 20 dakika sonra iki ölçüm ucu olan eBT2 reometresi kullanılarak yapılmıştır.

Kullanılan mineral katkıların miktarının harçların göreli akma gerilmesi ve göreli viskozitesine olan etkileri saptanmış ve mineral katkı içermeyen control karışımlarıyla karşılaştırılmıştır. Harç karışımlarının genel reolojik davranışları belirlenmiş ve analiz edilmiştir.

Başka araştırmacılar tarafından daha önce önerilmiş olan akma modellerinin uygunluğu bu araştırmada elde edilen deneysel sonuçlar kullanılarak kontrol edilmiş ve yeni bir model önerilmiştir. Önerilen modelin uygunluğu hem Portland çimentosu harçları hem de mineral katkı içeren harçlar için control edilmiş ve diğer modellerle kıyaslanmıştır. Önerilen modelin başarıyla kullanılabileceği belirlenmiştir.

Anahtar Sözcükler: Reoloji, harç, mineral katkılar, akma modelleri, göreli akma gerilmesi, göreli plastik viskozite.

To my parents

Sadia Idrees and Idrees Ahmed CH.

ACKNOWLEDGEMENT

Thanks to my advisor "Dr. Mustafa Tokyay" for his guidance and Dr. İÖ Yaman for providing apparatus, to all of my teachers, professors and father "Idrees Ahmad Ch." for their guidance throughout my life.

Special thanks to my mother Sadia Idrees, who is the original support for me.

Alhamdulillah

TABLE OF CONTENT

LIST OF TABLES

TABLES

LIST OF FIGURES

FIGURES

LIST OF ABBREVIATIONS

ABREVIATIONS

µ	**Relative viscosity**
BFS	**Ground blast furnace slag**
PC	**Portland cement**
PC0.3	**Portland cement at w/c0.3**
PC0.4	**Portland cement at w/c0.4**
PC0.6	**Portland cement at w/c0.6**
MSE	**Mean square error**
SF	**Silica fume**
T	**Torque**
To	**Yield Stress**
V	**Velocity**
w/c	**Water cementitious material ratio**
xBFSy(z)	**Mortar with x% slag replacement at w/c y after z minutes mix.**
xFAy(z)	**Mortar with x% Fly ash replacement at w/c y, after z minutes mix.**
xSFy(z)	**Mortar with x% Silica fume replacement at w/c y, after z minutes of mixing.**

CHAPTER 1

INTRODUCTION

1.1 General

The required hardened properties of cement-based materials are achieved after an initial period of plasticity within which the pastes, mortars, or concretes are to be (1) easily mixed and transported, (2) uniform within batch and between batches, (3) compacted without excessive effort, and (4) finished properly without significant segregation during placing and compaction (Mindess and Young, 1981). In other words, the properties of fresh concrete are important since they affect almost all of the properties in the hardened state.

The requirements stated above are not easily quantifiable and they may vary from one set of job conditions to another. Therefore, the term workability that covers all these properties of cementitious systems is being used to describe their behavior within the plastic stage. Workability of concrete is defined as that property which determines the effort required to place, compact, and finish a freshly mixed concrete with minimum loss of homogeneity (ASTM C 125, 2000). Two basic components of workability are consistency and cohesiveness which are, in a sense, counteracting with each other. In other words, fresh cementitious systems in plastic stage should be mobile and stable. Mobility of fresh mortar or concrete depends predominantly on the water content whereas stability has to do with the water-holding and aggregate-holding capacities of the mix. The first aspect of the stability of a fresh cementitious mixture is a measure of the resistance to bleeding which is the appearance of water and some fine cement and sand particles on the surface and the second one shows the resistance to segregation which is the settlement of coarse or heavy aggregate particles after compaction and finishing. Both phenomena lead to the separation of mortar or concrete components during placing and compaction.

Workability of concrete is affected by (1) water content of the mix, (2) relative proportions of the ingredients, (3) shape, surface texture, and porosity of the aggregates, (4) characteristics of the cement and mineral and chemical admixtures used, and (5) time and ambient temperature (Mehta and Monteiro, 2006).

Workability of fresh concrete can be measured by numerous different test methods which are generally categorized as (a) slump test, (b) compaction tests, (c) flow tests, (d) remolding tests, (e) penetration tests, (f) mixer tests (Mindess and Young, 1981) and (g) rheometer tests (Banfill, et al, 2001). Although almost all of these tests are empirical, it is significant to measure the workability and the available methods provide at least some information on its variations.

The slump test is a simple therefore the most popular method. It measures the resistance of fresh concrete to flow under its own weight. It is basically a consistency measurement. The compaction tests measure the compactibility of fresh concrete for a specified amount of work. A common example in this category is the compacting factor test which measures the degree of compaction by relating the density of uncompacted fresh concrete to that of the compacted one. Flow tests measure the flowability of fresh concrete upon jolting or vibration. Remolding tests were developed to measure the work required to make the concrete flow and change its shape from a frustum of a cone to a cylinder. VeBe test and Thaulow Drop Table test are the common examples for this category. The time required for the shape change stated above upon applying a vibration of controlled frequency and amplitude is recorded in the former whereas number drops to achieve the shape change is recorded in the latter. Penetration tests measure the depth of penetration of an indenter into concrete. The most commonly used method in this category is the Kelly Ball test which measures the penetration of a hemisphere shaped apparatus into concrete. Mixer tests measure the power required to turn a concrete mixer filled with concrete (Mindess and Young, 1981; Mehta and Monteiro, 2006). As the demand for control of workability increased with the development of new and special concretes such as self-compacting concrete and high performance concrete more sophisticated tools were started to be designed. The devices which are called concrete rheometers make use of rheology methods to measure the flow properties of fresh concretes. Basically, they measure the shear stress at varying shear rates (Banfill et al, 2001).

It is a common practice to approximate the flow behavior of fresh mortar or concrete which may be considered as heavily concentrated suspensions of cement and aggregate particles in water by Bingham Model which is described by Equation 1.1:

$$\tau - \tau_y = \eta \frac{d\gamma}{dt} \tag{1.1}$$

Where τ_y is the yield stress, η is the coefficient of viscosity, and $\frac{d\gamma}{dt}$ is the time rate of shear strain. Such behavior is shown in Figure 1.1. Flow takes place only at stresses above the yield value. It also follows that upto the yield stress the material behaves as elastic solid which is able to carry loads without permanent deformation. Materials that show this behavior are named as Bingham bodies (Jastrzebski, 1959).

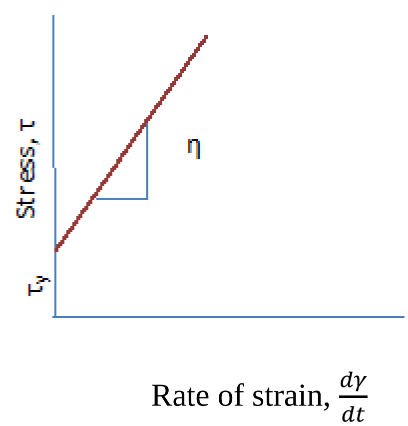

Figure 1.1. Flow behavior of the Bingham body.

The actual rheology of cementitious systems, however, is more complex than that can be described by Bingham Model. The rheological properties are time dependent because of the continuing hydration reactions in the very early stages even right after mixing cement with water. Furthermore, shear thinning or shear thickening phenomena may usually be observed. Fresh cementitious may also show thixotropy which is decrease of coefficient of viscosity under stress or sometimes anti-thixotropy (Mindess and Young, 1981). Besides these, there are several other parameters of cementitious materials such as (1) interparticle forces like Brownian, van der Waals, viscous, and liquid bridging forces, (2) particle shape, (3) particle size distribution and fineness, and (4) surface charge which may result in the flocculation or dispersion of particles that may affect the rheological behavior of cementitious systems (Nehdi et al, 1998; Moosberg-Bustnes, 2003). Consequently, numerous other models have been proposed by different researchers to predict the rheological properties of fresh cementitious systems (Hu, 2005).

The use of mineral admixtures in cementitious systems had long been a common practice due to economical, ecological, and technical advantages that they may provide. Whether they are used to partially replace the portland cement or as an addition in concrete they affect the workability and rheological properties as well as the rest of the fresh and hardened properties. Effects of mineral admixtures on concrete workability are usually related to the changes they cause in the water requirement of the mixture. Generally speaking, given a constant volume of cementitious material, mineral admixture incorporation would result in lower workability than an equivalent portland cement mixture due to the higher fineness of the mineral admixtures (Ferraris et al, 2001). The higher specific surface area of the mineral admixtures increases the interparticle forces that lead to higher cohesiveness. However, there are many cases in the literature that report the opposite. Most of such reports are on fly ashes and silica fume which are generally composed of spherical particles. The suggestions related with the improved workability are (1) the spherical particles roll over each other and reduce the interparticle friction (Ramachandran, 1995) and act as ball bearings giving the mix more mobility (Fidjestøl and Lewis, 1988); (2) having the shape that has the least surface area-volume ratio, the particles result in less water requirement; (3) spherical particles result in denser packing than angular particles causing lower water retention thus, lower water demand (Sakai et al, 1995). The idea of improved particle packing was also used in several reports to explain the reduced water demand upon BFS and limestone powder incorporations (Meusel and Rose, 1983; Lange et al, 1997; Ellerbrock et al, 1985).

1.2. Objectives

The goal of this study is to determine (1) the effect of mineral admixture type and amount on the rheological properties of mortars and (2) the suitability of some of the rheological models previously proposed by other researchers to the mineral admixture-incorporated mortars and (3) to propose a new model based on the experimental data obtained.

1.3. Research Approach

In order to ensure the objectives stated above the research strategy shown in Figure 1.2 was used. Three control mortar mixes were prepared by using portland cement (PC) as the only cementitious material. Fly ash (FA), silica fume (SF) and ground granulated blast furnace slag (BFS) were used in different amounts to partially replace PC on mass basis. All mixtures had a constant amount of polycarboxylate based high range water reducing admixture. Rheology measurements were taken as rotational speed and corresponding torque by a two-probe eBT2 rheometer. The measurements were taken initially, right after mixing, and at 10 and 20 minutes after mixing. The data obtained were statistically analyzed and yield stresses and plastic coefficients of viscosity were determined. Eight different rheological models proposed by other researchers were checked for suitability to the experimental data obtained and a new model is proposed.

Research approach adapted is presented in Figure 1.2.

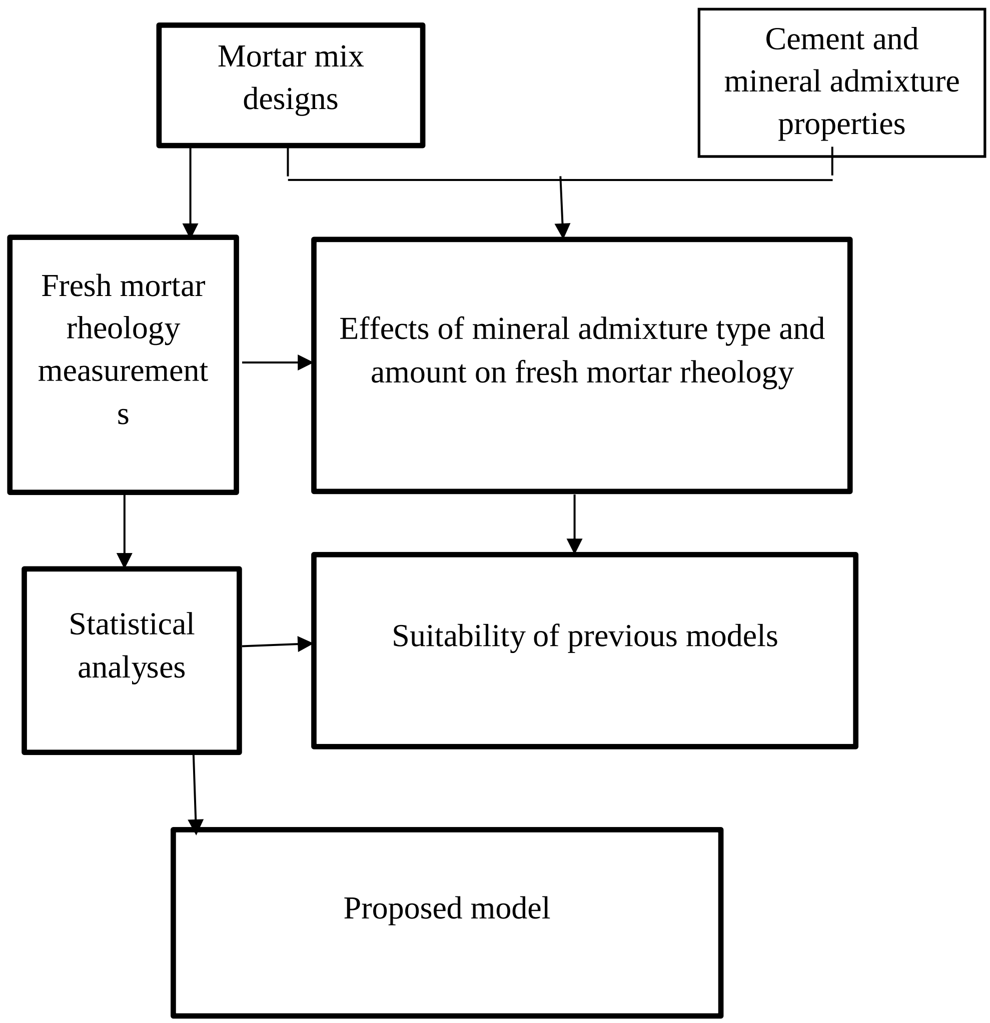

Figure 1.2. Outline of the research approach adapted.

CHAPTER 2

THEORETICAL BACKGROUND AND LITERATURE REVIEW

Workability of fresh concrete is related to two counteracting aspects: Mobility and stability which are termed as consistency and cohesiveness, respectively. Generally consistency depends on the amount of water in the mix and cohesiveness depends on water-holding and coarse aggregate-holding capacities which are related with two rather undesirable phenomena in fresh concrete which are known as bleeding and segregation, respectively. Bleeding is the appearance of water (with some very fine particles) on the surface after compaction while Segregation is the separation of coarse aggregate particles from the concrete. Both of the phenomenon result in non-uniformity.

As already stated above, a concrete with inadequate workability in fresh state will not be able to result in desired characteristics in hardened state. On the other hand, it should be stated that, although workability is a concrete property for concrete, it is not the fundamental property. In other words, workability of concrete should always be associated with the type of construction and method of concreting. (Mehta and & Monteiro 2006).

Since workability is a primary criterion for a good concrete and it has a direct effect on the strength, durability, appearance, and cost of concrete, it should be determined properly with due care. For more than a century, the workability of fresh concrete has been predominantly measured by the simple slump test, throughout the world (Koehler and Fowler, 2004). Flow table tests, VeBe test, etc. are also being used for many years (Hočevar et al, 2013). These empirical methods are currently viewed as not being sufficiently capable of providing a full characterization of the workability of today's advanced concrete mixtures (Koehler and Fowler, 2004). Furthermore, the common conventional workability test methods are considered as operator-sensitive and sometimes subjective (Hu, 2005). Therefore, test methods (rheometer tests) that are based on the established rheological techniques are taking more and more attention, nowadays.

2.1. Basics of Rheology

Rheology, the science of flow, may be used as an appropriate tool for describing workability and mobility of fresh cement-based materials like cement paste, mortar or concrete. By using the rheological methods, the elastic and viscous properties can be determined. The yield stress and plastic viscosity are two main parameters describing the rheological properties.

The shear rate is the change in velocity or a velocity gradient measured perpendicular to the flow. It is calculated by measuring the change in this velocity/distance ratio. The unit of shear rate is the inverse of time.

In laminar flow, the resistance to flow in the fluid layers, due to the shear rate, is called the shear stress and its unit is force per unit area.

Pump pressure is also related to the total amount of shear stress developed. The velocity and the shear rate increase cause the shear stress and hence the pressure required increase for maintaining the flow rate from the pumps.

Viscosity (μ) is a measure of the relative thinness or thickness of a fluid. It is the ratio of the shear stress to the shear rate. Viscosity is not usually constant. The viscosity changes with the flow velocity.

A Newtonian fluid is a fluid in which the stresses arising due to its flow, at each point, are linearly proportional to the strain rate at that point. Newtonian fluids can be characterized by a single coefficient of viscosity at a specific temperature. This viscosity will change with temperature, but it will not change with the strain rate. Newtonian flow can be described by using Figure 2.1 and 2.2.

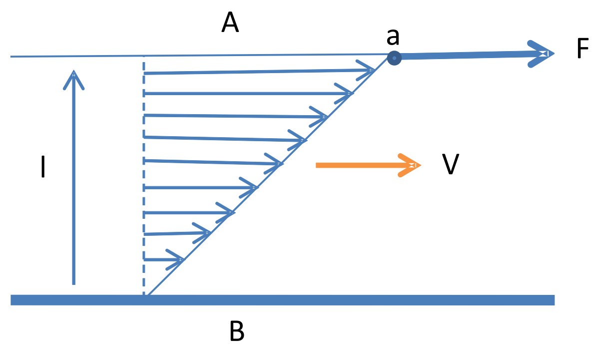

Figure 2.1. Laminar flow to describe Newton's Law of viscous flow.

When a tangential force, F applies on plane A, it moves with respect to the stationary plane B and carries the parallel layers of liquid between A and B. Thus the velocity of the liquid particles in each layer is a function of the distance, between the planes A and B. Newton showed the relationship between the tangential force and the velocity gradient as follow.

$$F = \mu \frac{dV}{dl} A \tag{2.1}$$

$$\tau = \mu \frac{dV}{dl} \tag{2.2}$$

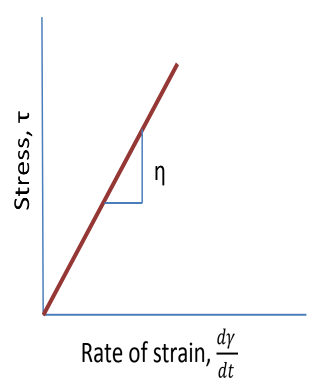

Figure 2.2. Stress-rate of strain relationship of Newtonian liquids.

Newtonian law is applicable to dilute suspensions as well as simple liquids. The only effect of solid suspended particles is the increase in viscosity. Coefficient of viscosity increases with increasing amount of suspended particles. On the other hand, the flow behaviour of concentrated suspensions is different than Newtonian flow. Flow of such materials is commonly described by Bingham Model:

$$\tau - \tau_y = \eta \frac{d\gamma}{dt} \tag{2.3}$$

Where τ_y is the yield stress. Such behaviour is illustrated in figure 1.1.

Flow takes place only at stresses above the yield value. It also follows that upto the yield stress the material behaves as elastic solid which is able to carry loads without permanent deformation.

Furthermore, non-Newtonian behaviour may show itself in many viscoelastic bodies either as pseudoplastic flow (shear-thinning) or dilatant flow (shear-thickening). Coefficient of viscosity decreases in the former and increases the latter with increasing shear rate or stress as shown in Figure 2.3 and mathematically described by Equation 2.4.

$$\tau - \tau_y = K\left(\frac{d\gamma}{dt}\right)^n \tag{2.4}$$

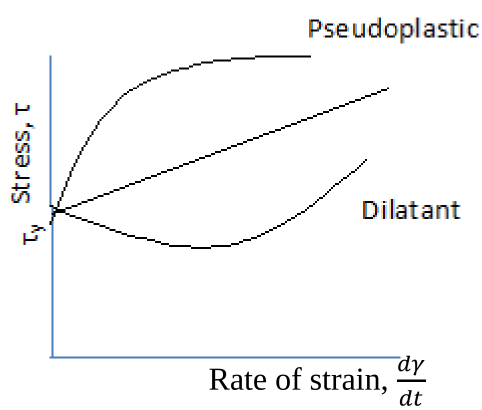

Figure 2.3. Pseudoplastic and dilatant flow behaviors.

2.2. Rheology of Fresh Concrete

Workability of fresh concrete is a complex property and the common terms or methods of measurement that are being used are generally found insufficient to describe this property as they usually do not quantify the property and therefore may be subjective. In order to "understand" the workability, as Banfill (2006) pointed out, there are three "levels" of identification: In level 1, workability is described in comparative terms such as stiff, semi.dry, or highly workable which are based on subjective assessment. Level 2 empirical methods of measurement such as slump test, flow test, etc which give quantitative results. However, these measurements are very often operator-sensitive. Level 3, on the other hand, defines the workability in terms of physical quantities such as yield stress and coefficient of viscosity that describe the fresh concrete rheology and the test methods developed do not depend on human factors.

Setting the first level aside, there are numerous different test methods proposed to measure the workability of fresh concrete. Some of them are standardized and most of them are empirical. Nevertheless, it is significant to have some measure of workability and the available measurement methods, at least, provide some information on the variations in workability and can at least be used for comparative purposes. On the other hand, it should be kept in mind that none of them can be used to measure the workability of the whole range of fresh concretes from very stiff to very fluid.

The methods to measure the workability of fresh concrete are grouped into different categories as (a) slump test, (b) compaction tests, (c) flow tests, (d) remolding tests, (e) penetration tests, (f) mixer tests (Mindess and Young, 1981), and (g) concrete rheometers (Banfill et al, 2001).

The slump test is the most popular method due to its simplicity. However, it is basically a consistency measurement and may not be suitable for very dry or very wet concretes. It may be considered as the measurement of the resistance of concrete to flow under its own weight. The compaction tests measure the compactibility of fresh concrete for a specified amount of work. The most common method in this category is the compacting factor test which measures the degree of compaction by relating the density of uncompacted fresh concrete to that of the compacted one. Flow tests measure the flowability of fresh concrete upon jolting or vibration. Remolding tests measure the work required to make the concrete flow and change its shape from a frustum of a cone to a cylinder. VeBe test and Thaulow Drop Table test are the common examples for this category. The time required for the shape change stated above upon applying a vibration of controlled frequency and amplitude is recorded in the former whereas number of drops to achieve the shape chance is recorded in the latter. Penetration tests measure the depth of penetration of an indenter into concrete. The most commonly used method in this category is the Kelly Ball test which measures the penetration of a hemispherical shaped apparatus into concrete. Mixer tests measure the power required to turn a concrete mixer filled with concrete (Mindess and Young, 1981; Mehta and Monteiro, 2006). As the demand for control of workability increased with the development of new and special concretes such as self-compacting concrete and high performance concrete more sophisticated tools were started to be designed. The devices which are called as concrete rheometers make use of rheology principles to measure the flow properties of fresh concretes. Basically, they measure the shear stress at varying shear rates (Banfill et al, 2001).

Most of the methods listed above are considered as "single point tests" since they measure the flow under a single set of conditions (Banfill, 2006) such as V-funnel test for self-compacting concretes which measures the time for flow of fresh concrete under gravity or slump test which measures the flow of fresh concrete under self weight. Single point tests give an indication of apparent viscosity assuming Newtonian behavior:

$$\eta_{app} = \frac{\tau}{\dot{\gamma}} \tag{2.5}$$

However, this assumption is not correct since fresh concrete, mortar, or even the cement paste exhibit a yield stress. In other words, fresh concrete flow has to be characterized by more than one parameter because it is a Non-Newtonian material. The most commonly used model is the Bingham Model that requires two parameters which are the yield stress and the plastic viscosity. The former is the stress beyond which the material starts to behave as a fluid and the latter is the measure of the ease of flow. Nevertheless, single point tests should not be underestimated since they can successfully be used as quality control tools (Ferraris, 1999).

In early 1970s, Tattersal developed a workability testing apparatus which was similar in nature to the rotational viscometers that measure the flow properties of Newtonian bodies but much larger in size. It was named as “two point test” apparatus because in order to describe the behavior of Bingham body measurements at a minimum of two points is necessary. Actually, in Tattersall’s apparatus and all the other two point test methods developed later, measurements are taken at much more than two points. In other words, a large number of different shear rates at different shear stresses are measured (Roy and Idorn, 1993; Banfill, 2006). Since then, many other researchers have proposed a number of other apparatus to describe the flow behavior of fresh concretes (Yen et al, 1999).

Two point tests gather data as a plot of torque versus rotational speed which are then converted to shear stress (τ) versus shear rate ($\dot{\gamma}$). As it was stated earlier, Bingham Model is considered to be valid for most fresh concretes. However, there are numerous other material equations proposed. Herschel Bulkley Model (Eq’n 2.4), for example, is found to be more suitable in describing the nonlinear behaviour often encountered. Furthermore, it was found that the negative yield stress which sometimes occurs when Bingham Model is applied is less likely in Herschel Bulkley Model (Wallevik and Wallevik, 2011).

The rheological behavior of fresh concrete can be approximated by two physical quantities: The yield stress (τ_y) and plastic viscosity (μ). Wallevik (1983), in his extensive research on the workability of fresh concrete, studied the change in these quantities with the changing amounts of water, entrained air, water reducing agent, and silica fume and obtained rheological graphs which are the plots of changes in τ_y-μ as a function of material properties, admixtures, etc. A summary of his results is shown in Figure 2.4.

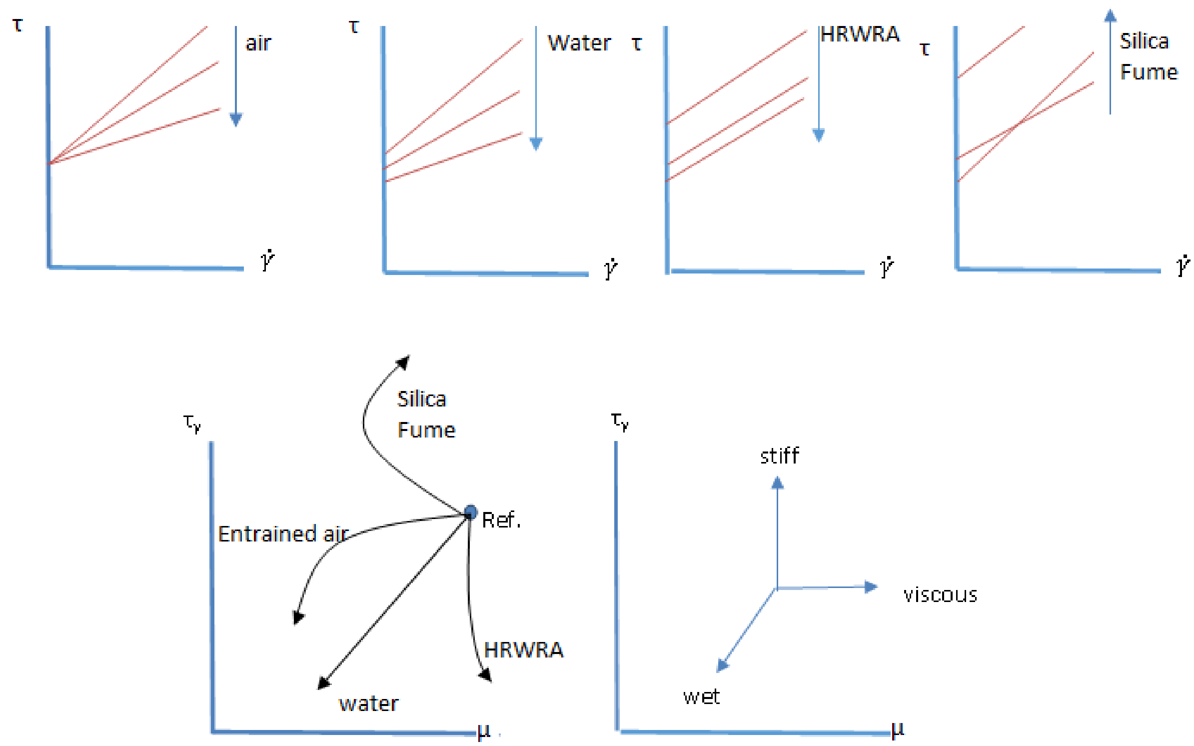

Figure 2.4. Effect of different constituents on shear stress rate of strain relations (top) and rheological graphs illustrating the effects on yield stress-plastic viscosity relations (bottom) (Wallevik and Wallevik, 2011).

2.3. Flow Curve Equations

In concentrated suspensions like cementitious systems, interactions between the solid particles may arise and the intensity of those interactions may depend on the shape of the particles, their size distributions, concentrations, surface properties, and the composition of the parent liquid they are incorporated. All these factors and the differences in the testing methods and the devices used to monitor the flow lead to many complications in mathematical description of the flow of fresh cement paste, mortar, and concrete.

Although there are qualitative and quantitative disagreements between the mathematical expressions proposed by different researchers for the flow of fresh cementitious systems, almost all of them indicate the existence of a yield stress (Banfill, 2003). Different mathematical forms that the flow curves have been reported to fit are given below:

Bingham Equation : $$\tau = \tau_y + \mu\dot{\gamma} \tag{2.6}$$

Herschel Bulkley Equation: $$\tau = \tau_y + A\dot{\gamma}^B \tag{2.7}$$

Robertson-Stiff Equation: $$\tau = A(\dot{\gamma} + B)^C \tag{2.8}$$

Modified Bingham Equation: $$\tau = \tau_y + \mu\dot{\gamma} + B\dot{\gamma}^2 \tag{2.9}$$

Casson Equation: $$\sqrt{\tau} = \sqrt{\tau_y} + \sqrt{\mu\dot{\gamma}} \tag{2.10}$$

De Kee Equation: $$\tau = \tau_y + \mu\dot{\gamma}e^{-A\dot{\gamma}} \tag{2.11}$$

Yahya and Khayat Equation: $$\tau = \tau_y + 2\sqrt{\tau_y\mu\dot{\gamma}e^{-A\dot{\gamma}}} \tag{2.12}$$

Vom Berg Equation: $$\tau = \tau_y + A\sinh^{-1}(B\dot{\gamma}) \tag{2.13}$$

In the equations given above, A, B, and C are constants.

Bingham equation (2.6) is preferred to describe the flow behavior of most of the cementitious materials in fresh state. However, there are numerous cases which it was found to give inaccurate results and a third parameter was required (Wallevik et al, 2015). Sometimes, for shear thickening or shear thinning phenomena, the third parameter becomes the power function of the shear rate as in Herschel Bulkley equation (2.7) or a second order term of the shear rate as in Modified Bingham equation (2.9).

When $B < 1$ in Eq'n 2.7 or $B/\mu < 0$ in Eq'n 2.9, shear thinning occurs. When $B > 1$ in Eq'n 2.7 or $B/\mu > 0$ in Eq'n 2.9, shear thickening occurs. Obviously, for $B=1$ or $B/\mu = 0$, in respective equations, the Bingham Equation is obtained.

The main reason why the Bingham Equation is the most preferred one is that using nonlinear equations result in difficulty in defining the viscosity of the system which is simply obtained as the slope of the line in Bingham Equation. Besides that, the yield stress values obtained by these three equations for a shear thickening material are ordered from highest to lowest as Herschel-Bulkley, Modified Bingham, and Bingham whereas the opposite is obtained for shear thinning materials (Wallevik et al, 2015). Nevertheless, these three equations are being more commonly used than the others listed above. It should also be stated that the rest of the flow curve equations listed above (2.8, 2.10-2.13) were found to be more appropriate for cement pastes and slurries (Ochoa, 2006).

2.4. Changes in Concrete Workability upon Mineral Admixture Incorporation

Mineral admixtures have lower densities than ordinary Portland cements. So the amount of paste becomes more at given water content and the cohesiveness and plasticity of the fresh concrete increases. There are other characteristics of the mineral admixtures which affect the workability of concretes.

2.4.1. Water Demand

The mineral admixtures change the workability of concrete by changing the water demand of the mixture. Considering a constant volume of cement based material, by adding mineral admixture, concretes show less workability than similar Portland cement concretes. The higher specific surface area of mineral admixture causes the water demand to increase (Ferraris et al, 2001). The higher surface area means more interparticle surface forces which increases the cohesiveness of the mix and decreases its mobility. For the finer mineral admixtures water content must be increased for a specified workability. This is why that silica fume has high water demand. (Fidjestøl and Lewis, 1988).

However, sometimes reduced water demand is also observed when mineral admixture is used along cement. It is reported for low lime fly ashes and sometimes silica fume too.

The reason may be the presence of spherical particles which makes the flow easy by rolling over each other and by reducing the friction between particles. These spherical particles act as ball bearings and increase the mobility (Fidjestøl and Lewis, 1988);

If the shape of mineral admixture particles is such that it has the least surface area-volume ratio, then less water is required for wetting. Additionally spherical particles has denser packing than angular particles, causing lower water retention in wet state, so water demand is lowered (Sakai et al, 1997). The improved particle packing, in several reports, explains the reduced water demand for BFS addition (Meusel and Rose, 1983; Lange et al, 1997; Ellerbrock et al, 1985).

2.4.1.1. Effect of Fly Ashes

The fly ash decreases the water demand of concrete, for a specified workability, (Davis et al, 1937). This has been verified by certain researchers (von Berg and Kukko, 1991; Dhir, 1986). Yet the other factors like amount, fineness, particle shape, and loss on ignition of Fly ash also affect the rheological properties and water demand. (Von Berg and Kukko, 1991). These factors are illustrated in Figures 2.5 to.2.8.

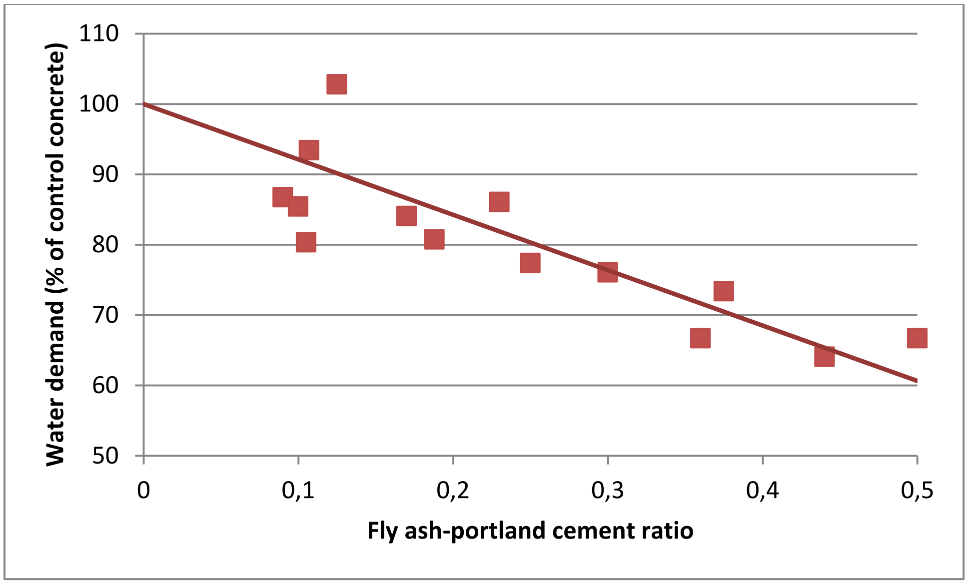

Figure 2.5. Water demand of the fly ash and portland cement blends in concrete (Adapted from von Berg and Kukko, 1991).

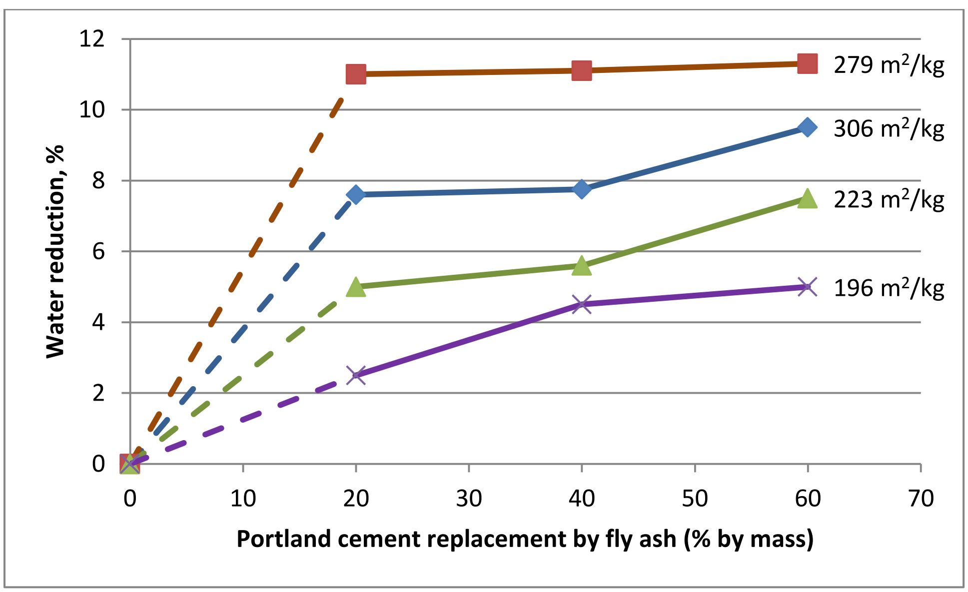

Figure 2.6 Water demand of fly ash mortars for different Blaine fineness of fly ashes (Helmuth, 1986).

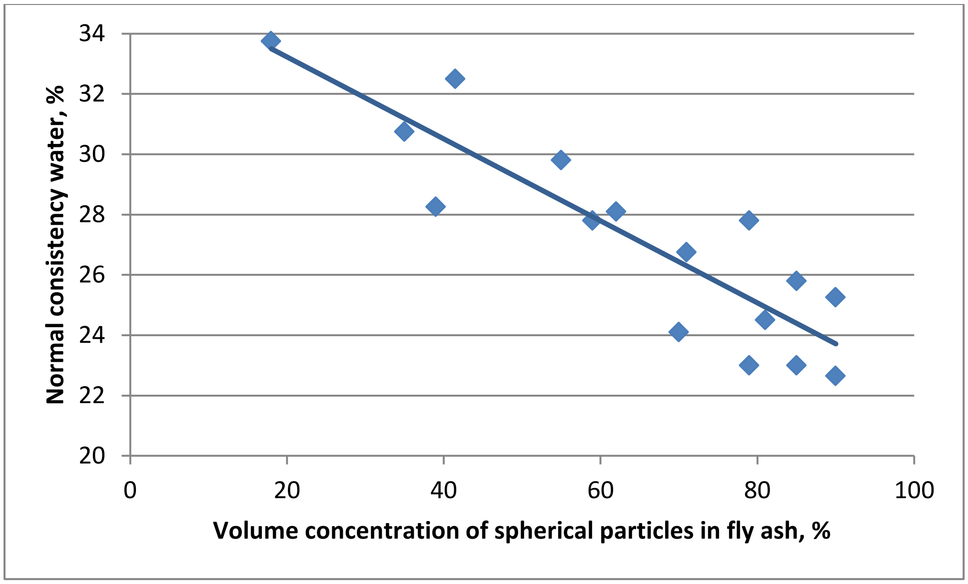

Figure 2.7. Change in normal consistency water requirement of 70:30 portland cement: fly ash pastes with increasing amount of spherical particles in the fly ash (Braun and Gebauer, 1983).

Figure 2. 8. Effect of loss on ignition of fly ash on the flow of mortars made with blended cements having 25:75 fly ash: portland cement ratio, by mass (Adapted from von Berg and Kukko, 1991).

2.4.1.2. Effect of Ground Granulated Blast Furnace Slags

BFS particles usually have angular shapes, but they are hard and have smooth surfaces. These particles absorb much less water than portland cement particles so decreases the water demand (ACI 233, 1995; Wainwright, 1986). The reduction in water requirement for a constant workability is influenced by the amount and particle size distribution of BFS and the portland cement used influences the reduction in water demand. Usually maximum water reduction is upto 5% (Wainwright, 1986).

This water reduction is independent on weather slag and cement was ground separately or they were interblended. (Tokyay et al, 2010). The results obtained are illustrated in Figure 2.9.

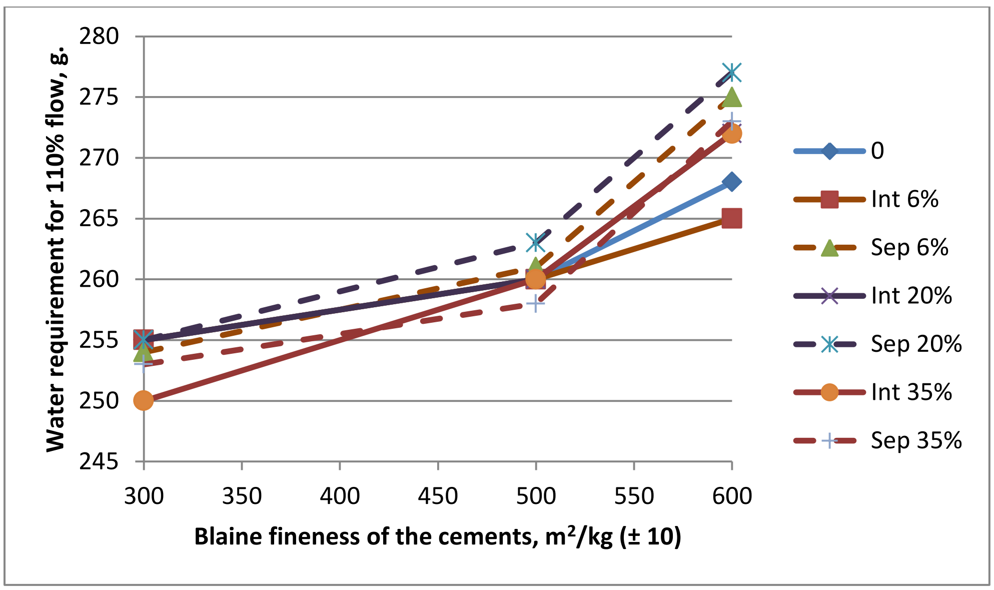

Figure 2.9. Change in water requirement of mortars prepared by using interground and separately ground blended cements with different BFS contents and Blaine specific surface areas (Tokyay et al, 2010).

2.4.1.3. Effect of Silica Fume

The silica fume increases the water demand of concrete as compared to the control concrete without silica fume. The amount of silica fume used directly influences and increases the water demand. (Carette and Malhotra, 1983; Mehta, 1986; Scali et al, 1987). This effect is illustrated in Figure 2.10. The higher specific surface area of silica fume is the basic cause of higher water demand.

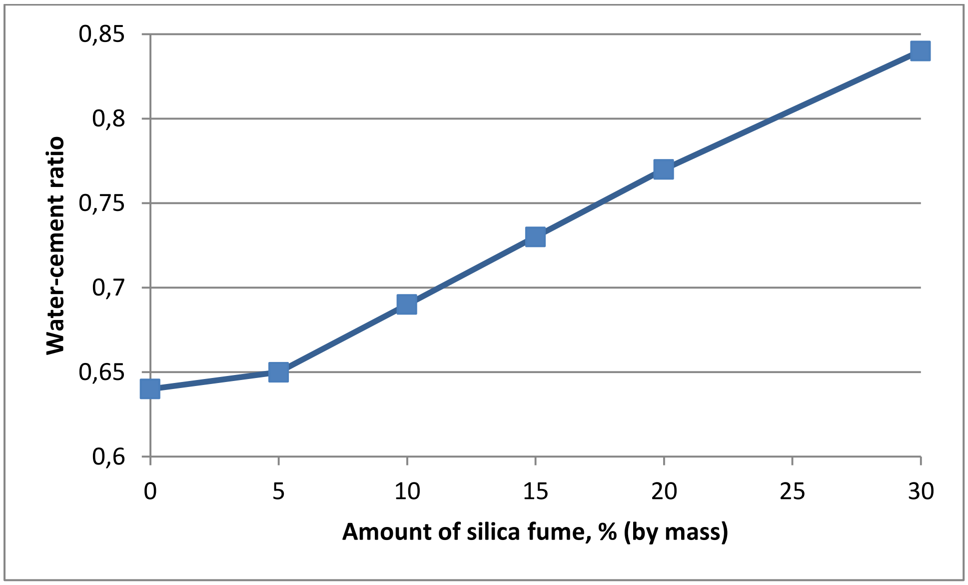

Figure 2. 10. Increase in water cement ratio with increasing silica fume content, to maintain a given slump of concrete (Carette and Malhotra, 1983).

2.4.2. Some of the Reported Results of Different Workability Tests

There is a huge amount of research on the effect of different mineral admixtures on the workability of fresh concretes determined by different test methods. Some of them which are related with the subject of this study are summarized below.

More superplasticizer amount was required for BFS-incorporated mortars beyond 30% replacement, but this requirement was less than superplasticizer requirement for low calcium fly ash. (Wei et al, 2003).

Ternary mix (PC+BFS+fly ash) was found to result in 23.43% decrease in superplasticizer requirement. Quaternary mix (PC+BFS+fly ash+ one of silica fume, metakaolin, or limestone powder) had 0.23%, 13.40%, and 20.47% less superplasticizer requirements, respectively (Meddah et al, 2014).

A high calcium fly ash increased the slump of the concrete for 10, 20, and 30% cement replacement levels (by mass). The increase in slump was proportional to the increase in fly ash content (Nochaiya et al, 2010).

Not only fineness of a mineral admixture affects the workability but particle shape and surface characteristics may be more significant (Şahmaran et al, 2006).

For 10.25% (by mass) BFS replacement level in self-compacting concrete, Filling ability (slump flow, V-funnel, and T50 flow time tests), passing ability (J-ring, U.box tests), and resistance to segregation (modified slump test) were determined. Workability of SCC was improved upto 20% BFS with an optimum content of 15% (Boukendakdji et al, 2012).

In another study with lightweight aggregate, fly ash increased the workability more than the slag and Silica fume. Silica fume controlled the bleeding and upfloating of lightweight aggregates in much better way but workability rapidly decreased with time. Blast furnace slag improved workability but lesser than fly ash (Chen and Liu, 2008).

In a flow table test on mortar, silica fume increased workability upto 15 % and then it decreases workability (Rao, 2003). In study silica fume increased the slump for upto 10 % replacement, but optimum value was 6%. (Shi et al, 2002).

2.4.3. Rheological Properties

Several studies related with the influence of mineral admixtures on yield stress and viscosities of fresh cementitious systems are summarized below.

In a study on the viscosity and yield stress of an ultrafine fly ash (UFFA), a metakaolin (MK), and a silica fume (SF) incorporated cement pastes with constant water-cementitious material ratio and different amounts of high range water reducing agent (HRWRA) replacement of cement by UFFA led to reduced HRWRA amount over the control for a given yield stress and viscosity, whereas SF increased it significantly. MK was found to have almost no effect on the rheological properties. The mineral admixture contents ranged from 0 to 16% of cement, replacing the cement by mass; water-cementitious ratios used were 0.28 to 0.35 and the dosage of a naphthalene sulfonate based HRWRA was 0.45-0.70% of the cementitious material, by mass (Ferraris et al, 2001). In the same study, influence of particle size of mineral admixtures on the yield stress and viscosity was determined by using four fly ashes with mean particle sizes of 18μm (coarse), 10.9μm (medium), 5.7μm (fine), and 3.1μm (ultrafine). All tests were conducted at the mineral admixture content (12%), same water-cementitious material ratio (0.35), and same HRWRA dosage (0.45%). UFFA resulted in the lowest yield stress and viscosity. Highest yield stress was observed in the fine fly ash incorporated paste and highest viscosity was observed in the medium fly ash incorporated paste.

Matrix mortars of concretes were prepared by using a portland cement and two blended cements that contain 30% (by mass of cement) replacement of portland cement by a phosphorus slag and a limestone powder. 3.12% (by mass) silica fume was further used to replace the cements. Equal amounts of phosphorus slag or limestone powder were reduced in blended cements upon silica fume incorporation. Water, HRWRA, and aggregate contents were kept constant in all mixtures. Yield stress and viscosity of blended cement mortars were significantly lowered. Partial replacement of portland cement by silica fume reduced the viscosity as the silica fume amount used increased up to 9%. At 12% replacement, there occurred a large increase in viscosity. A similar trend was observed for the yield stress but the minimum value was obtained at 6% replacement. Yield stress increased at 9% silica fume content, although it was still less than that of the control. At 12 %, it was considerably higher than the control. Neither the viscosities nor the yield stresses of silica fume incorporated blended cement mortars changed much with respect to non silica fume blended cement mortars up to 9% silica fume content. 12% silica fume resulted in increased values of these. The increase in viscosity was higher for the phosphorus slag-blended cement whereas the increase in yield stress was higher for the limestone blended cement (Shi et al, 2002).

In another study on silica fume and fly ash incorporated cement pastes the water-cementitious material ratio of which were kept constant, both the viscosity and the yield stress were determined to increase with increased amount of silica fume and decrease with the increased amount of fly ash (Nathagopalan et al, 2008).

The resistance to flow of silica fume incorporated pastes was found to be depending on the type of plasticizing agent used. Vikan and Justnes (2007) used 0-13.6 % by volume silica fume to partially replace the portland cement to prepare pastes with a constant total solid particle volume fraction. A sodium naphthalene sulfonate-formaldehyde (SNF) and polyacrylate (PA) superplasticizers were used at constant dosages of 1.32% and 0.79% (by mass of total cementitious material) in all mixes. The flow resistance was increased with increasing silica fume content when SNF was used but decreased when PA was used.

Laskar and Talukdar (2008) partially replaced the cement by different amounts of fly ash (FA), silica fume (SF), and rice husk ash (RHA) in three groups of concretes. The mix proportions were held constant within each group. The first and the second had a poly-carboxylic ether based and the third had a sulfonated naphthalene based superplasticizer. Their experimental results are shown in Figure 2.11.

Fly ash resulted in a small decrease in yield stress at around 10 to 20% replacement levels. Beyond those values the change was not significant. There was a slight increase in viscosity for 10% fly ash incorporation however the change was not significant. Viscosity was increased upto 10% replacement by silica fume and then decreased. Yield stress was also decreased largely upto 10% in the mixes with poly-carboxylic ether superplasticizer. At higher replacement levels, its increase was very large. In the concrete with sulfonated naphthalene superplasticizer, yield stress increased at a very low rate with increasing silica fume amount between 5 to 15% replacement levels. Rice husk ash was very effective in reducing the yield stress. On the other hand, it resulted in hug increase in viscosity.

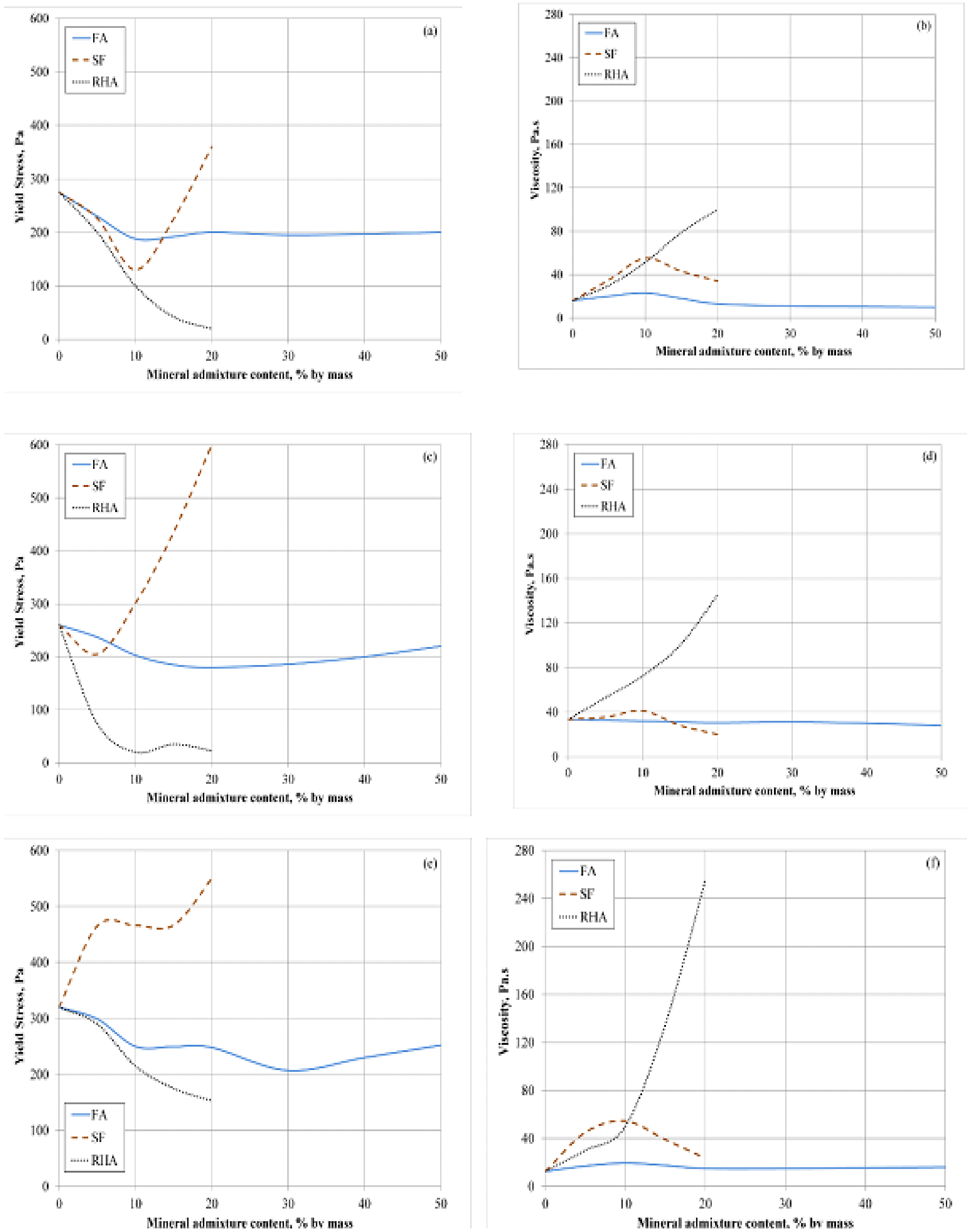

Figure 2. 11. Change in the yield stress and viscosity of three different fresh concretes by mineral admixture use. First two concretes had polycarboxylic ether polymer and the third had sulfonated naphthalene polymer as high range water reducing agents (data from Laskar and Talukdar, 2008).

2.4.4. Bleeding and Segregation

Generally, segregation is defined as the separation of coarse aggregate from the mortar. However, bleeding which may be defined as the appearance of water and some fine particles on the surface of the concrete may be considered as a special form of segregation. It occurs due to the separation of water from the rest of the concrete mix. Usually, these two phenomena are simultaneous.

The factors that increase the possibility of segregation are using (1) large maximum aggregate size (> 25mm), (2) a large proportion of coarse aggregate, (3) coarse aggregate that has much higher density than the fine aggregate, (4) insufficient amount of sand and cementitious materials, (5) irregular and rough surface aggregate, and (6) too wet or too dry mixes (Mindess and Young, 1981).

While the larger aggregate particles settle some of the mixing water moves upwards carrying some fine cement and sand particles together, causing a layer of scum at the top surface which becomes weak both in terms of strength and durability due to its higher water cement ratio and porosity.

Using coarse cementitious materials or high amount of water in the concrete mix are the two basic reasons for bleeding. However, in order to reduce the risk of segregation and bleeding, proper handling, placing, compaction, and finishing methods for fresh concrete which are described in most standards and specifications are as important as or even more important than the factors mentioned.

Properly proportioned concretes that contain carefully selected mineral admixtures generally show less segregation and bleeding. Mineral admixtures which are finer than the portland cement used are preferable. Although use of such materials result in greater plasticity and higher cohesiveness, it is necessary to note several points related with some of the individual mineral admixtures.

When the ratio of surface area of solid particles to volume of water is low, the rate of bleeding increases. For example, coarsely ground pumicite (a natural pozzolan) may increase the water requirement of concrete for a given slump and this may lead to increased bleeding and segregation (ACI 232, 2001). On the other hand, for a proper workability, the amount of solid particles must be maximized and the amount of water should be minimized in the paste which means that the mineral admixture used should not be extremely fine unless a high range water reducing agent is used. Silica fume-incorporated concretes do not segregate appreciably both due to the high fineness of the material and the use of high range water reducing agents. High specific surface area of silica fume results in significantly reduced bleeding because there remains very little free water in the mixture. Furthermore, bleeding channels and pores are blocked physically by silica fume particles (ACI 234, 2000). This blocking effect is also true for other mineral admixtures that are finer than the Portland cement.

Since silica fume concretes show much less bleeding, they have the tendency of plastic shrinkage. Therefore, necessary precautions should be taken to prevent the evaporation of moisture from concrete at early ages especially under conditions such as high fresh concrete temperature, low humidity, and high wind (ACI 234, 2000).

The spherical shape and the hydrophilic nature of the low lime fly ash particles result in a very thin layer of water adsorbed on their surfaces which leads to an even distribution of the mixing water throughout the fresh concrete. Besides providing a greater surface area of solid particles and requiring lower water contents, low lime fly ashes reduce bleeding further due to this physicochemical effect, also (Dhir, 1986).

Bleeding capacity and rate of ground granulated blast furnace slag-incorporated concretes depend on the fineness of the slag as compared to that of the portland cement together which it is used with. Finer slag, when it replaces the portland cement on equal mass basis, results in reduced bleeding whereas coarser slag will cause more bleeding at a higher rate (ACI 233, 2003).

CHAPTER 3

EXPERIMENTAL INVESTIGATION

As it was stated in Chapter 1, the objective of this experimental investigation is to determine (1) the effects of mineral admixture type and amount on the rheological properties of mortars and (2) suitability of various flow curve equations proposed previously by other researchers and (3) propose a new flow curve equation by using the experimental data obtained.

For this purpose, control portland cement mortars and mineral admixture incorporated mortars were prepared and their flow properties were determined by using a rheometer. The details of the experimental study are given in the following sections.

3.1. Properties of the Materials Used

In preparing the fresh mortars portland cement (PC), fly ash (FA), ground granulated blast furnace slag (BFS) and silica fume (SF) were used as the cementitious materials. The sand used was natural sand, the particle size distribution of which was brought to that of a standard sand described in EN 196.1 (2005). All mortar mixtures contained a polycarboxylate based high range water reducing agent (HRWRA).

PC which was obtained from Votorantim Ankara Cement Factory was CEM I 42.5 R. Its properties were in accordance with EN 197.1 (2012). Its chemical composition and physical properties are given in Table 3.1. FA was a low lime fly ash obtained from Tunçbilek Thermal Power Plant. BFS and SF were obtained from Ereğli Steel plant and Antalya Ferrochromium Plant, respectively. The properties of the mineral admixtures are also given in Table 3.1. Particle size distributions of the cementitious materials used were determined by laser particle size (Malvern Mastersizer 2000) and given in Figure 3.1.

Table 3.1 . Properties of the Cementitious Materials Used.

Chemical Composition				
Oxide (%)	PC	FA	BFS	SF
SiO_2	20.27	53.2	42.96	84.14
Al_2O_3	5.09	22.89	11.28	0.17
Fe_2O_3	3.16	6.15	0.87	0.31
CaO	60.98	6.28	33.01	0.58
MgO	1.59	2.22	6.16	5.24
SO_3	2.7	1.15	1.45	1.33
Na_2O	0.39	0.92	0.33	0.4
K_2O	0.53	1.41	0.66	2.88
TiO_2	nd	1.09	0.6	0.01
Loss on Ignition	4.65	2.98	0.33	3.62
Physical Properties				
Blaine Sp. Sur. Area (m^2/kg)	362	421	468	---
Median size (µm)	18.48	17.56	13.00	7.70
Density (g/cm^3)	3.07	2.38	2.85	2.27

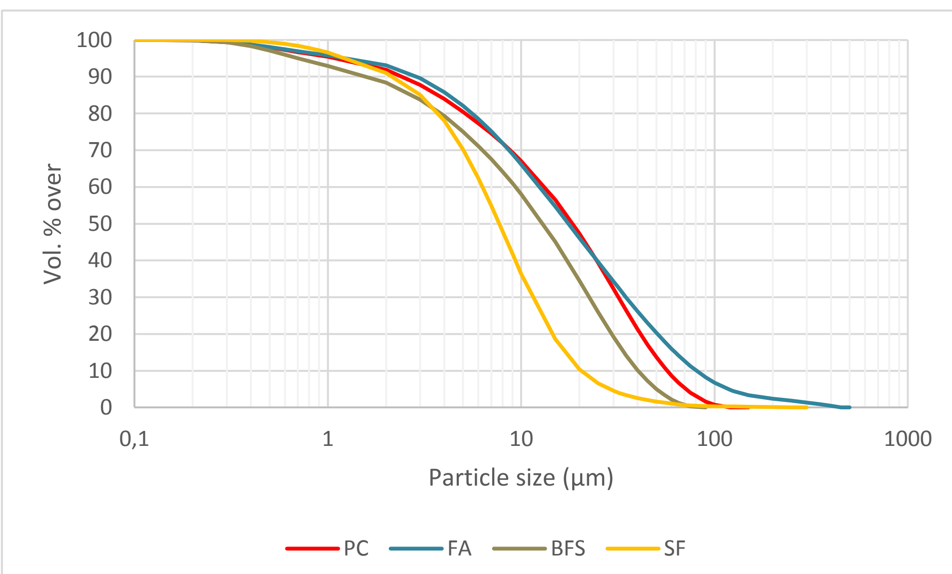

Figure 3. 1. Particle size distributions of the cementitious materials used.

The sand used in the mortars was natural river sand with a bulk specific gravity of 2.65. Its granulometry is shown in Figure 3.2.

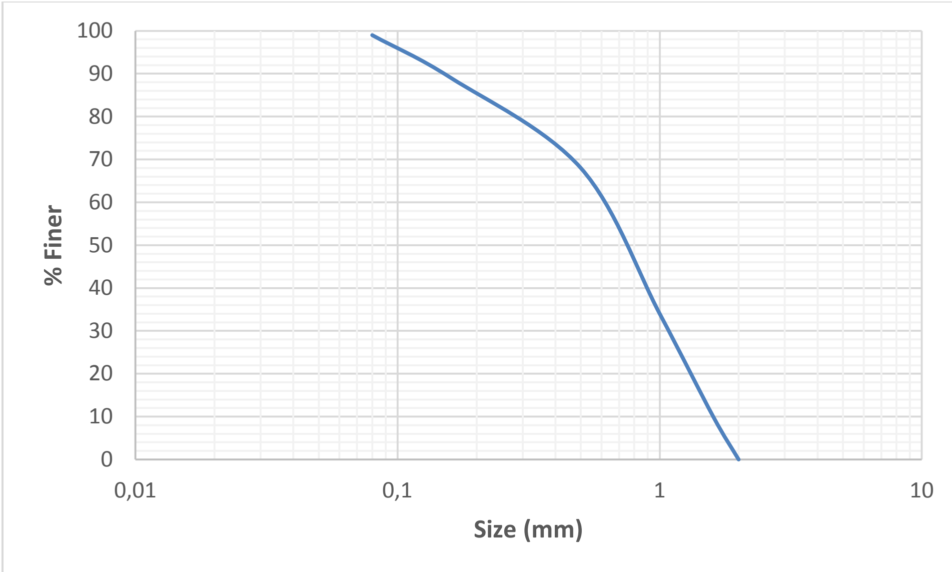

Figure 3.2. Granulometry of the sand used.

3.2. Mortar Mix Proportions

All mortar mixtures used had 1:3 (by mass) cementitious material to sand ratio and a constant HRWRA content of 2% (by mass of cementitious material). Mineral admixture incorporated mortars contained different amounts of FA, BFS, or SF that were used to replace equal amounts of portland cement. Mortar mix designations and relative proportions of the ingredients for each mix are given in Table 3.2. Some other mix were tested but discarded due to being too dry or too wet.

3.3. Apparatus and Test Methods

The mortar mixtures were prepared in batches of 80 to 90 kg, mixed in a pan-type mixer (Figure 3.3). The mixing procedure consisted of adding first the sand into the mixer, and then about half of the mixing water is added and mixed for one minute. Then cement and mineral admixtures are added and mixed for another 2 minutes. HRWRA was introduced into the mix together with the remaining mixing water and mixing continued for two more minutes. Finally, after one minute of rest, the mortar was mixed for two more minutes. Right after mixing is finished, the fresh mortar is transferred into the container of the rheometer to take the initial flow data. Then, while the mortar sample was resting in the container two other data sets were taken at 10 and 20 minutes after the mortar was transferred to the container, to observe the effect of time on flow, also.

Besides these flow table test (ASTM C 230, 2003) was carried out and bleed water amount was measured up to 40 minutes after mixing by a similar method (no vibration was applied) described in ASTM C 232 (2004) for mortars with water-cementitious material ratio of 0.45.

Table 3.2 Mortar Mixes Used.

Mineral Admixture Used	Mix Designation	Relative proportions of the ingredients (by mass)						
		PC	FA	BFS	SF	Sand	Water (net)	HRWRA
None	PC 0.3	1	-	-	-	3	0.30	0.02
	PC 0.4	1	-	-	-	3	0.40	0.02
	PC 0.6	1	-	-	-	3	0.60	0.02
Fly Ash	10FA 0.3	0.9	0.1	-	-	3	0.30	0.02
	10FA 0.35	0.9	0.1	-	-	3	0.35	0.02
	20FA 0.4	0.8	0.2	-	-	3	0.40	0.02
	20FA 0.45	0.8	0.2	-	-	3	0.45	0.02
	40FA 0.55	0.6	0.4	-	-	3	0.55	0.02
	40FA 0.8	0.6	0.4	-	-	3	0.80	0.02
Blast Furnace Slag	10BFS 0.4	0.9	-	0.1	-	3	0.40	0.02
	10BFS 0.5	0.9	-	0.1	-	3	0.50	0.02
	30BFS 0.4	0.7	-	0.3	-	3	0.40	0.02
	60BFS 0.3	0.4	-	0.6	-	3	0.30	0.02
	60BFS 0.4	0.4	-	0.6	-	3	0.40	0.02
	60BFS 0.5	0.4	-	0.6	-	3	0.50	0.02
Silica Fume	5SF 0.4	0.95	-	-	0.05	3	0.40	0.02
	5SF 0.5	0.95	-	-	0.05	3	0.50	0.02
	5SF 0.6	0.95	-	-	0.05	3	0.60	0.02
	10SF 0.4	0.9	-	-	0.1	3	0.40	0.02
	10SF 0.45	0.9	-	-	0.1	3	0.45	0.02
	15SF 0.4	0.85	-	-	0.15	3	0.40	0.02
	15SF 0.45	0.85	-	-	0.15	3	0.45	0.02

Figure 3.3. Mixer and the rheometer used.

The rheometer (Figure 3.3) used in this investigation was e-BT2 which was manufactured by Schleibinger Geräte GH, Germany. The rheometer has built-in sensors for the measurement of the angular velocity and momentum. Nearly 100 data points are obtained from each probe. The data are then used to obtain the flow curves. A typical data plot and a corresponding Bingham flow curve obtained are shown in Figure 3.4

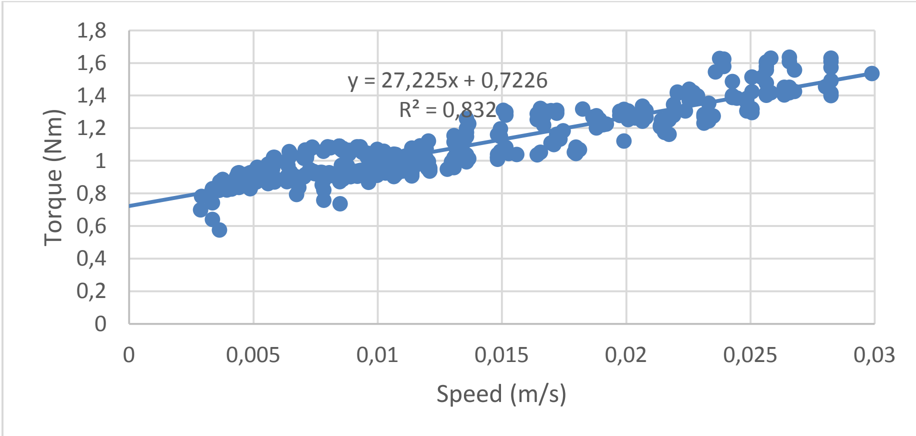

Figure 3.4. Typical data plot obtained from eBT2 rheometer.

CHAPTER 4

TEST RESULTS AND DISCUSSIONS

Cement paste, mortar, or concrete are concentrated suspensions of solid particles. Therefore, particle migration may become an important phenomenon in the rheology of these materials. The solid particles will have the tendency to move to the regions of lower shear rates and due to the differences in the densities of the suspended particles and the liquid medium, vertical segregation is also possible. Furthermore, the time dependent behaviour of these materials may result in changes in the rheological properties due to thixotropy, structural breakdown, or loss of workability (Feys, 2009; Hafid et al, 2010). These would result in measurement artifacts the magnitudes of which depend on the characteristics of the suspension, the working principle of the rheometer, and the shear flow geometry used. Thus, flow curves obtained by means of rheometers may sometimes have various anomalies. Similar problems were also encountered in this experimental work and some of the data obtained were either too much dispersed as shown in Figure 4.1a or a very wide range of torque values were recorded for the same shear rate as shown in Figure 4.1b, or vice versa. For the first case, either the flow was remeasured by using a new batch or (if the problem persists in the new batch, also) the data were discarded. For the second case, the data deviating more than two times the standard deviation of the linear relationship obtained with the original data were eliminated.

4.1. Flow Data Obtained

The torque induced versus the speed of the rheometer probes were obtained as (a) initial data right after mixing as soon as the mortar is placed into the container of the rheometer; (b) 10 minutes and (c) 20 minutes data after 10 and 20 minutes of resting of mortar in the container, respectively.

Since the rheometer used was stated to be designed on the basis that the fresh mortar (or concrete) behaves as a Bingham body, the linear relationship between the torque and speed were determined, also. Figure 4.2 to Figure 4.6 gives the initial flow data for PC and FA. BFS- and SF-incorporated mortars with three different water cement ratios.

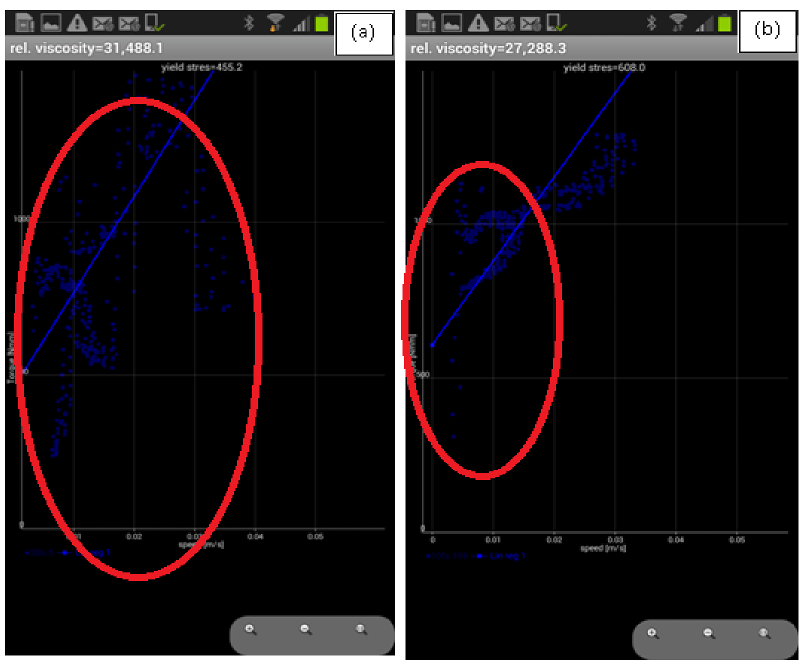

.

Figure 4.1. Examples of flow curves (Snapshots directly obtained from the device). (a) High dispersion of data points and (b) wide variation of data points at the same shear rate.

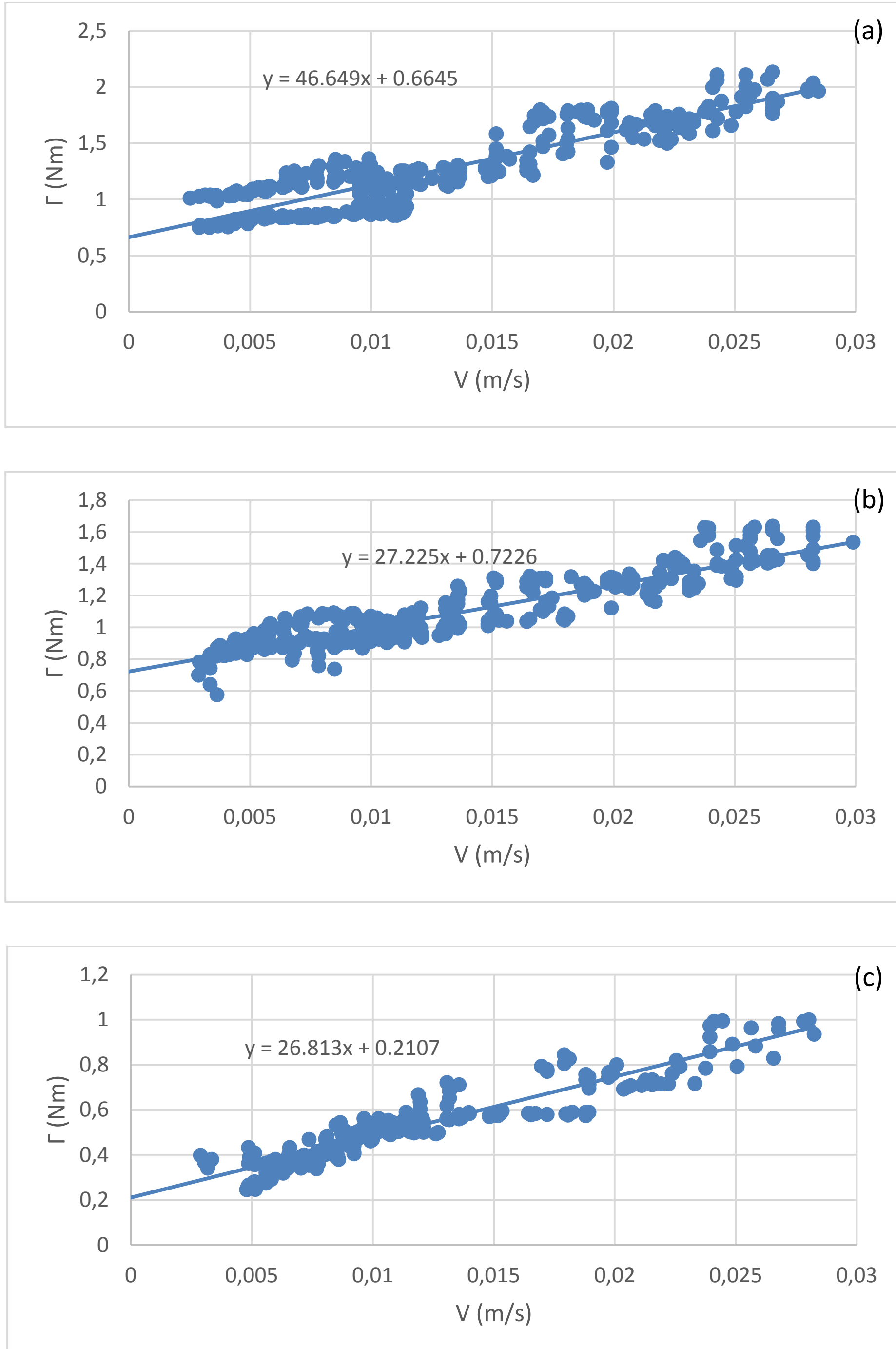

Figure 4.2. Initial torque-speed data and the linear relationships obtained for (a) PC 0.30, (b) PC 0.40, and (c) PC 0.60, assuming Bingham behavior.

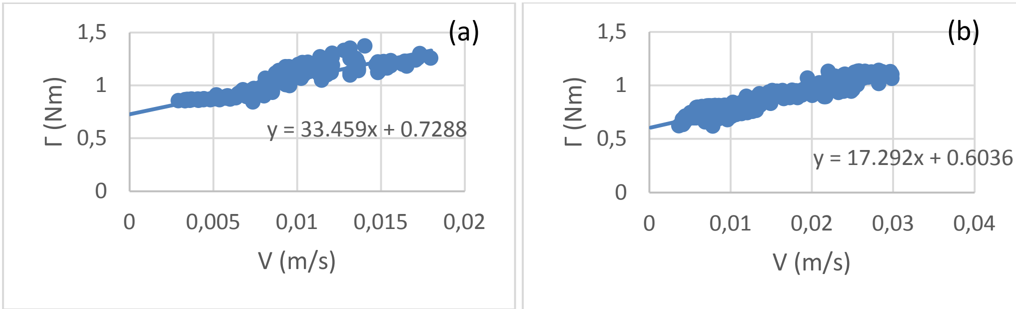

Figure 4.3. Initial torque-speed data and the linear relationships obtained for (a) 10FA 0.30 and (b) 10FA 0.35, assuming Bingham behavior.

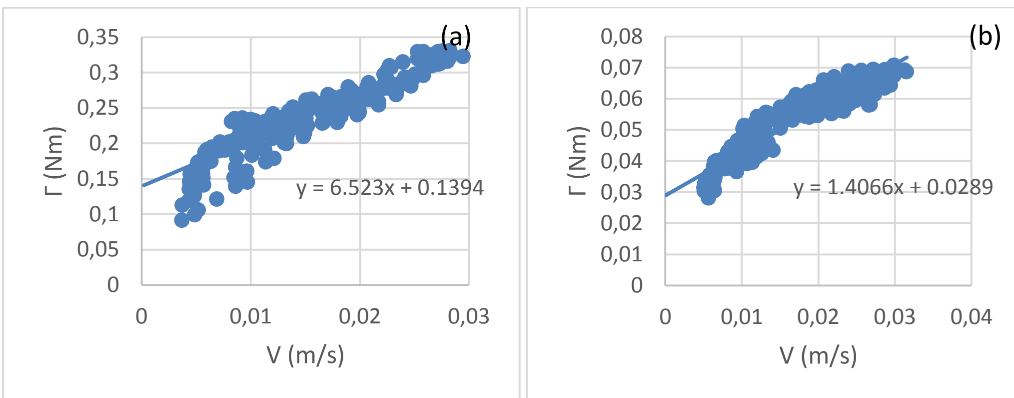

Figure 4.4. Initial torque-speed data and the linear relationships obtained for (a) 20FA 0.40 and (b) 40FA0.55, assuming Bingham behaviour.

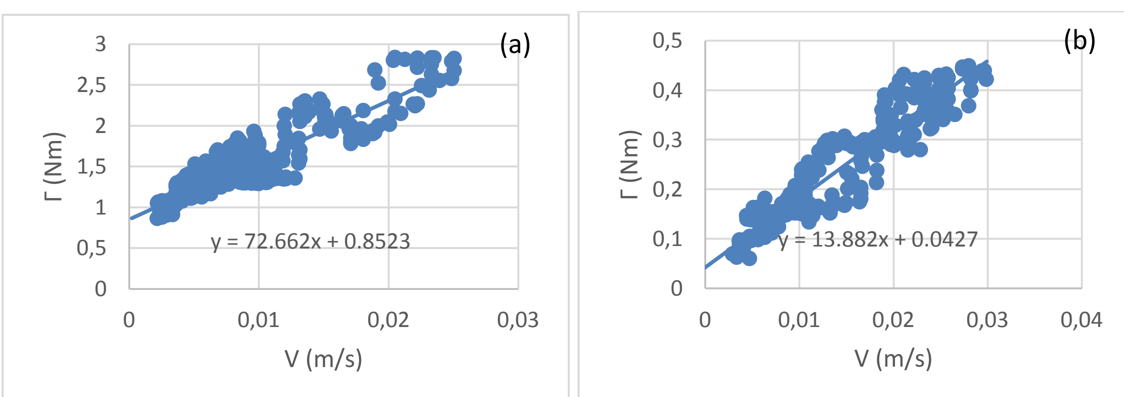

Figure 4.5. Initial torque-speed data and the linear relationships obtained for (a) 10BFS 0.40 and (b) 60BFS 0.40, assuming Bingham behaviour.

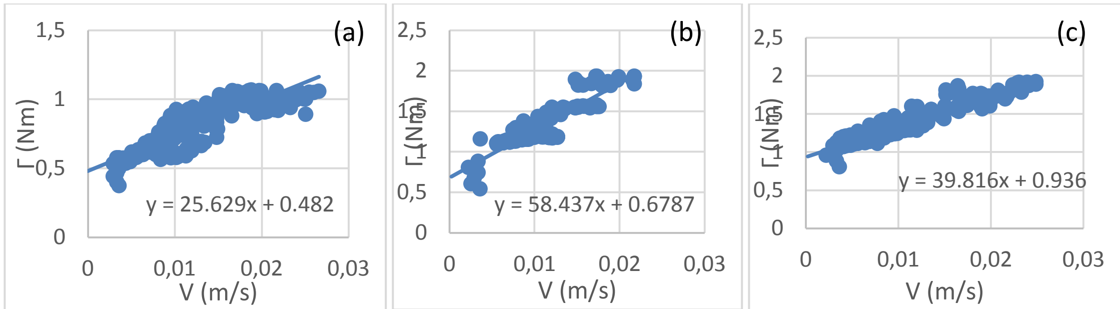

Figure 4.6. Initial torque-speed data and the linear relationships obtained for (a) 5SF0.4, (b) 10SF0.4 and (c)15SF0.4 assuming Bingham behavior.

4.2. Relative Yield Stress and Relative Viscosity Values

As it was previously mentioned, the rheometer used assumes Bingham body behavior for fresh cementitious systems. Therefore, using the data obtained, relative yield stresses and relative plastic viscosities of the mortars were obtained by using the following equation.

$$\Gamma = g + Vh \tag{4.1}$$

Where g (Nm) and h [Nm/(m/sec)] are constants corresponding to relative yield stress and relative plastic viscosity, respectively. Figure 4.7 shows a typical plot of torque (Γ in Nm) versus speed (V in m/sec). Linear regression analysis was performed on the data. The slope of the line defines relative plastic viscosity (h) and the intersection point with the y-axis defines relative yield stress (g). The values obtained for the mortars tested in this investigation are given in Table 4.1.

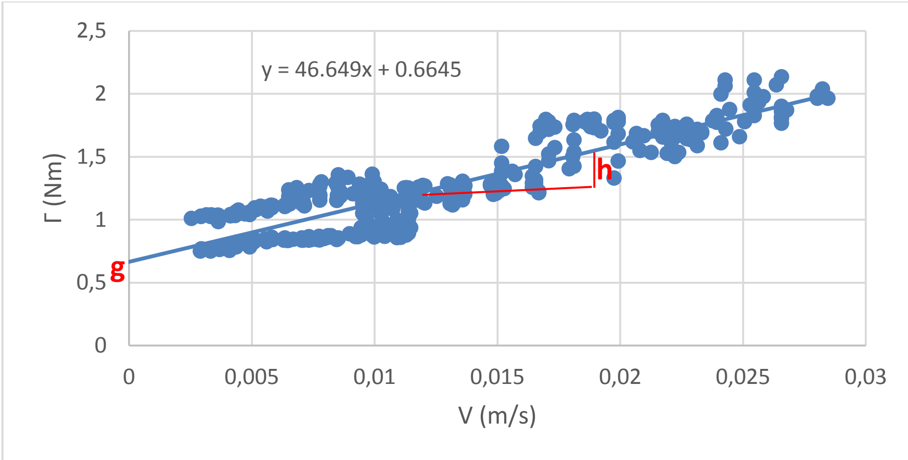

Figure 4.7. Determination of relative yield stress (g) and relative plastic viscosity (h) from torque-speed data obtained from the rheometer.

Flow table tests and bleed water measurements of mortars with water-cementitious material ratio of 0.45 were done because that they may be helpful in interpreting the rheometer test data. The results of these tests are given in Table 4.2.

Table 4.1. Relative Viscosity (h) and Relative Yield Stress (g) Obtained.

Mineral Admixture Used	Mortar Designation		Rel. vis., h [Nm/(m/s)]	Rel. Yield Str., g [Nm]
None	PC 0.30	initial	46.65	0.66
		10.min.	45.99	0.68
	PC 0.40	initial	27.23	0.72
		10.min.	41.46	0.74
		20.min.	46.24	0.47
	PC 0.60	initial	26.81	0.21
Fly Ash	10FA 0.30	initial	33.46	0.73
		10.min.	17.47	0.84
	10FA 0.35	initial	17.29	0.60
		10.min.	14.83	0.81
		20.min.	18.65	1.03
	20FA 0.40	Initial	6.52	0.14
		10.min.	5.46	0.33
	20FA 0.45	Initial	34.78	0.21
		10.min.	34.28	0.36
		20.min.	62.01	0.35
	40FA 0.55	initial	1.41	0.03
		10.min.	2.22	0.06
		20.min.	1.74	0.06
	40FA 0.80	Initial	0.92	0.02
		10.min.	1.55	0.04
		20.min.	1.64	0.04

Table 4.1. (Continued)

Blast Furnace Slag	10BFS 0.40	Initial	72.66	0.85
		20.min.	66.06	0.77
	10BFS 0.50	initial	13.77	0.08
		10.min.	13.94	0.38
		20.min.	54.72	1.02
	30BFS 0.40	Initial	26.03	0.68
	60BFS 0.30	Initial	47.51	1.08
	60BFS 0.40	Initial	13.88	0.04
		20.min.	84.75	0.61
	60BFS 0.50	Initial	108.18	0.20
		10.min.	182.09	0.17
Silica Fume	5SF 0.40	Initial	25.63	0.48
		10.min.	29.55	0.69
	5SF 0.50	Initial	74.83	0.23
	5SF 0.60	Initial	110.46	0.26
	10SF 0.40	Initial	58.44	0.68
	10SF 0.45	Initial	26.49	0.34
		10.min.	24.87	0.80
	15SF 0.40	Initial	39.82	0.94
		10.min.	33.82	1.11
		20.min.	80.17	0.79
	15SF 0.45	Initial	11.22	0.22
		10.min.	30.16	0.46
		20.min.	50.46	1.01

Table 4.2. Flow Table Test Results and Bleed Water Amounts at 40 minutes After Mixing for Mortars with 0.45 Water-cementitious Ratio.

Mortar Designation	Flow (mm)	Bleed water (% volume)
PC 0.45	175	0.60
10FA 0.45	214	0.16
20FA 0.45	200	.
40FA 0.45	133	.
10BFS 0.45	178	>2.0*
30BFS 0.45	187	>2.0
60 BFS 0.45	223	>2.0
5SF 0.45	174	1.6
10SF 0.45	190	1.7
15SF 0.45	193	1.7

*bleeding continued after 40 minutes.

4.3. General Discussion on the Change in Relative Yield Stress

It can be seen from Table 4.1 that water-cementitious ratio, type and amount of mineral admixture incorporated, and time are the three important factors affecting the relative yield stress of the mortars. Assuming Bingham behavior for the mortars, the general tendency in relative yield value is a decrease with increasing water-cementitious material ratio and an increase with increasing time. The effects of mineral admixtures on relative yield value change with the type as shown in Figure 4.8 for mortars with 0.40 water-cementitious material ratio. Use of fly ash reduces the yield value, significantly when compared with portland cement, alone. This effect can be attributed to the spherical shape of low-lime fly ashes which results reduced internal friction. On the other hand, it seems that there are two counteracting effects involved when blast furnace slag is used:

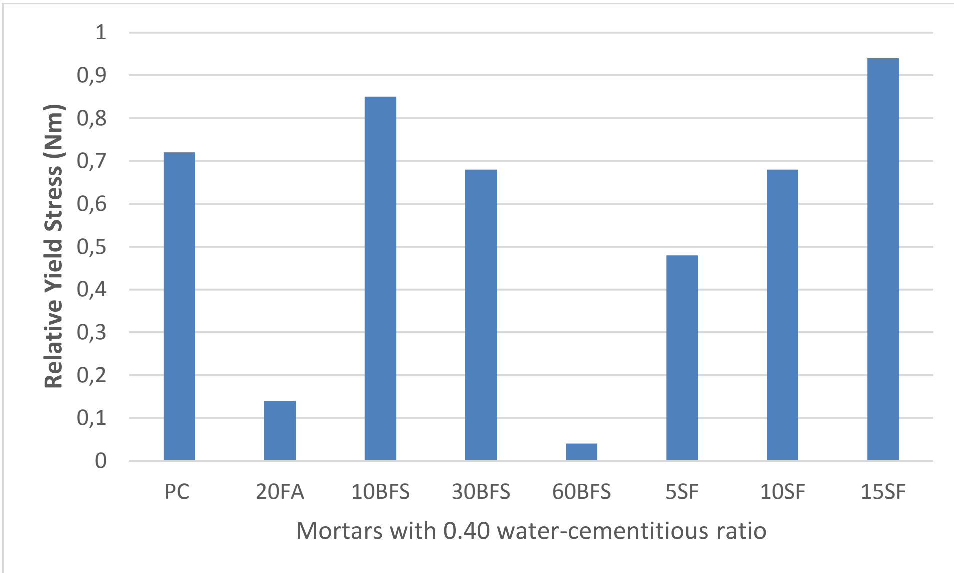

Figure 4.8. Relative yield values of mortars with 0.40 water-cementitious Material ratio.

BFS has angular particle shape which would increase the internal friction. However, the polished surfaces and almost non porous character of these particles result in reduced water requirement. Thus, for a constant water-cementitious material2 ratio, this means higher amount of free water. Therefore, for small amount of BFS, relative yield value may be slightly higher than that of the control but at higher amounts the value decreases considerably. Besides this, when the bleed water contents given in Table 4.2 are compared, BFS-incorporated mortars had much higher bleeding tendency which may be considered as an indication of excess free water in these mortars. This may be another factor in reducing the yield value with increasing BFS content.

Silica fume which is composed of extremely fine particles increases the water requirement for a specified workability. On the other hand, these particles have spherical shapes. Thus, for small amounts of SF, there may be a decrease in yield value when compared with portland cement mortar but it increases with the increasing amount of SF used.

4.4. General Discussion on the Change in Relative Viscosity

Although there are several contradictory values in Table 4.1, the increasing water-cementitious material ratio decreases relative viscosity. Increasing time has an increasing effect on viscosity. The densities of the mineral admixtures were lower than that of the portland cement resulting in higher volume concentration of suspended solids in the mixtures which would lead to higher viscosity. However, the particle shapes, fineness, and surface characteristics may be as effective (or even more) as the concentration. The effects of mineral admixtures on relative viscosity change with the type as shown in Figure 4.9 for mortars with 0.40 water-cementitious material ratio. FA decreases the viscosity whereas small amount of BFS (10%) increases while higher amounts decrease it. Small amount (5%) of SF would not change the viscosity considerably but higher amounts result in increased values.

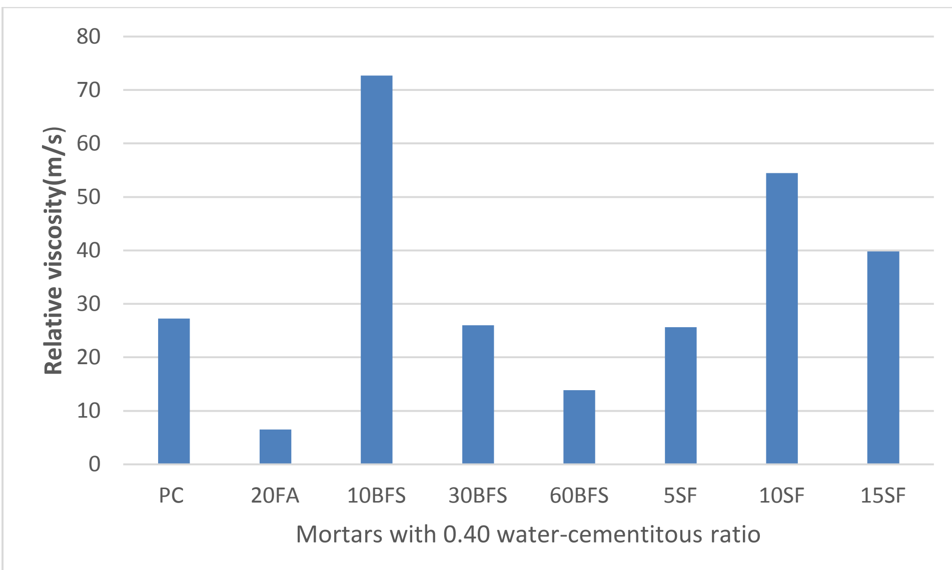

Figure 4.9. Relative viscosities of mortars with 0.40 water-cementitious ratio.

4.5. Effect of Water-cementitious Material Ratio and Time on Portland Cement Mortar Rheology

4.5.1 Effect of w/c Ratio on PC rheology

The behavior of the stiffer mixture (mortar with 0.30 water cement ratio) is different from those of the other two with higher water cement ratios, as shown in Figure 4.10. The former had a steeper slope which indicates a higher viscosity. This can be attributed to the interparticle friction due to low amount of water. Higher water contents in the latter result in a lubricating effect and less interparticle friction leading to milder slopes which indicate lower viscosity. As the water cement ratio increases viscosity decreases.

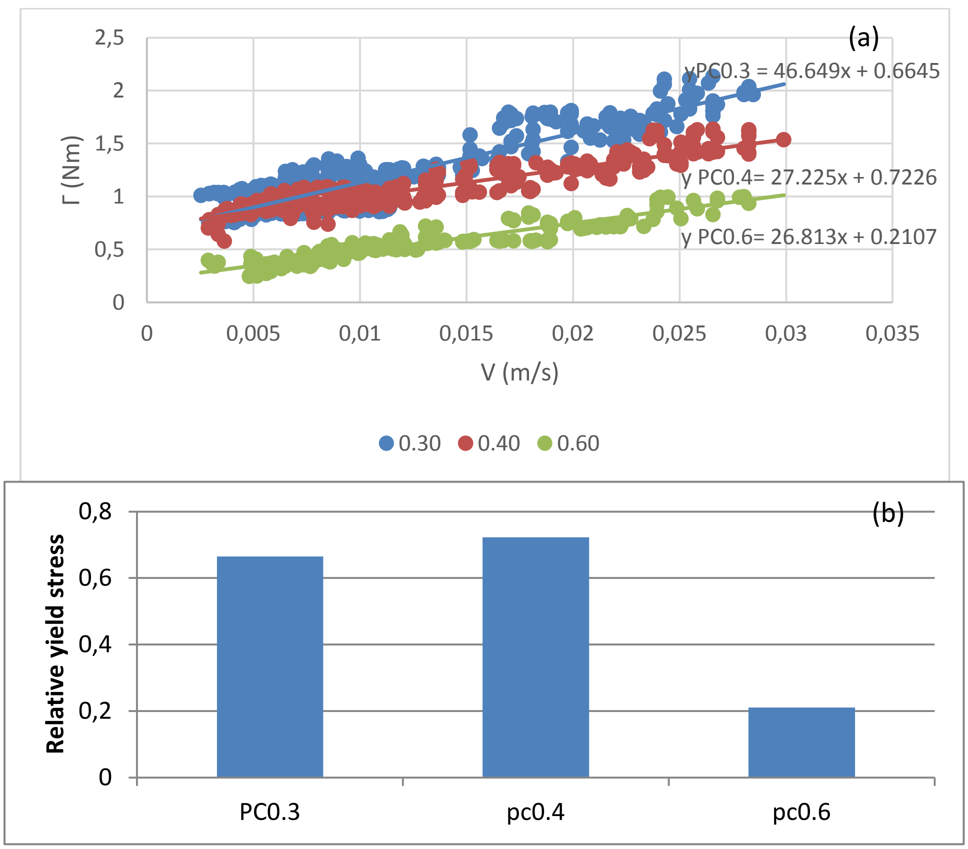

Figure 4. 10. Effect of water cement ratio in PC mix on (a) Torque-velocity relationship (b) relative viscosity (c) relative yield stress.

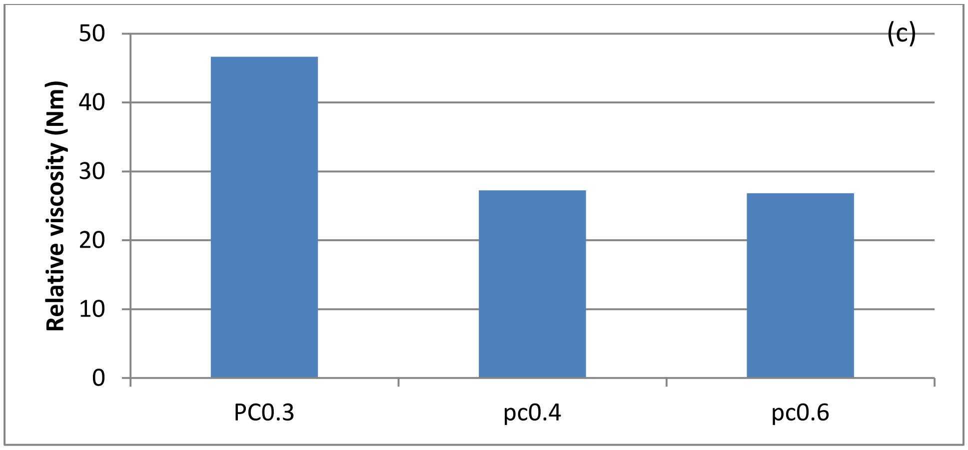

Figure 4.10 (Continued)

Relative yield stress of 0.30 and 0.40 water cement ratio mixtures were similar whereas that of 0.60 water cement ratio mortar was much lower. The relatively high yield value of the stiff mortar (w/c = 0.30) should not be misleading. Most probably, this mortar behaved more like a solid than a plastic suspension at such a low water content. Thus, flocculation of the cement particles and interparticle friction resulted in a high yield value. The effect of w/c ratio on the yield stress is better observed when the other two mortars are compared. Higher water content results in a better dispersion of particles and results in lower yield stress values.

Relative yield stress at w/c 0.3 is 0.67 which increases at w/c 0.4 and becomes 0.73 but at w/c 0.6 it decreases to 0.21. At w/c 0.3, yield stress should be greater but as the water was not enough or water was not able to penetrate evenly hence yield value is little lower. At w/c 0.4, particles are wet and better distributed, so they showed a little higher yield value. At w/c 0.6, particles are far away due to high water content so Van der Waals forces decrease with distance between particles and hence the yield stress.

There is a specific value of w/c for which yield stress is the highest. Mortars with less or more w/c may have lower yield stress values.

Plastic viscosity at w/c 0.3 is 46.64, at w/c 0.4 it becomes 27.23 and at 0.6 it becomes 26.81so there is continuous decline in plastic viscosity value due to higher water content, particles are dispersed and they are not hindering each other’s motion.

4.5.2 Effect of Time on PC Mix.

It can be seen from Figure 4.11 and 4.12 that viscosity increases within the first 10 minutes after mixing. This is probably due to the initial hydration products formed. (It may be due to loss of some water due to evaporation, or absorption and temperature rise due to heat evolution). Yield value does not change significantly within this period, although there is a slight increase. At 20 minutes after mixing however, viscosity remains more or less the same as that of 10 minute measurement whereas the yield value drops considerably. The reduced yield value may be attributed to the tendency of bleeding which results in more free water that may cause the dispersion of particles.

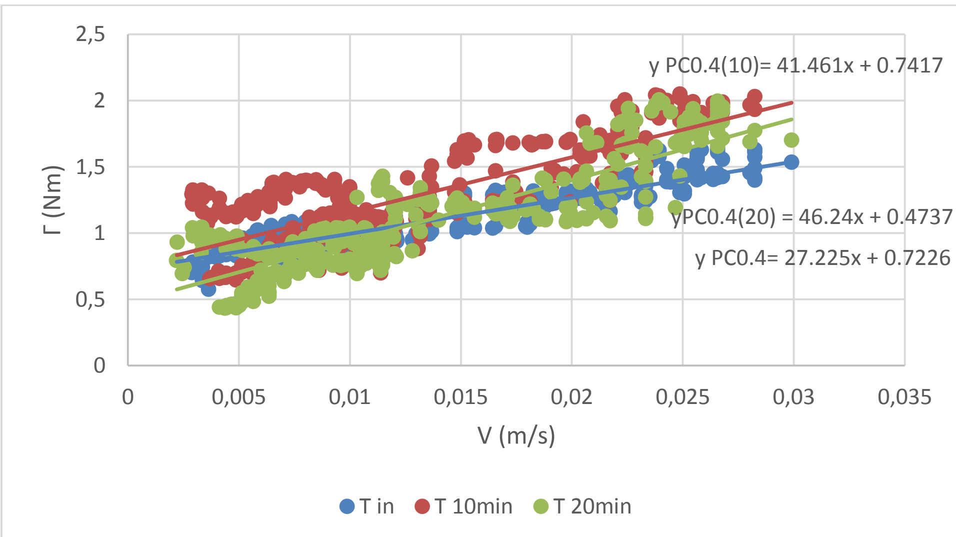

Figure 4.11. Torque-velocity relationship with time for PC mortar

It is observed that after 10 minutes of mixing, yield stress is increased but after 20 minutes, it is decreased. After 20 minutes, as the new products are being formed, particles are losing their shape and hence attraction.

Plastic viscosity increases with time because water is being consumed and so less lubrication is available.

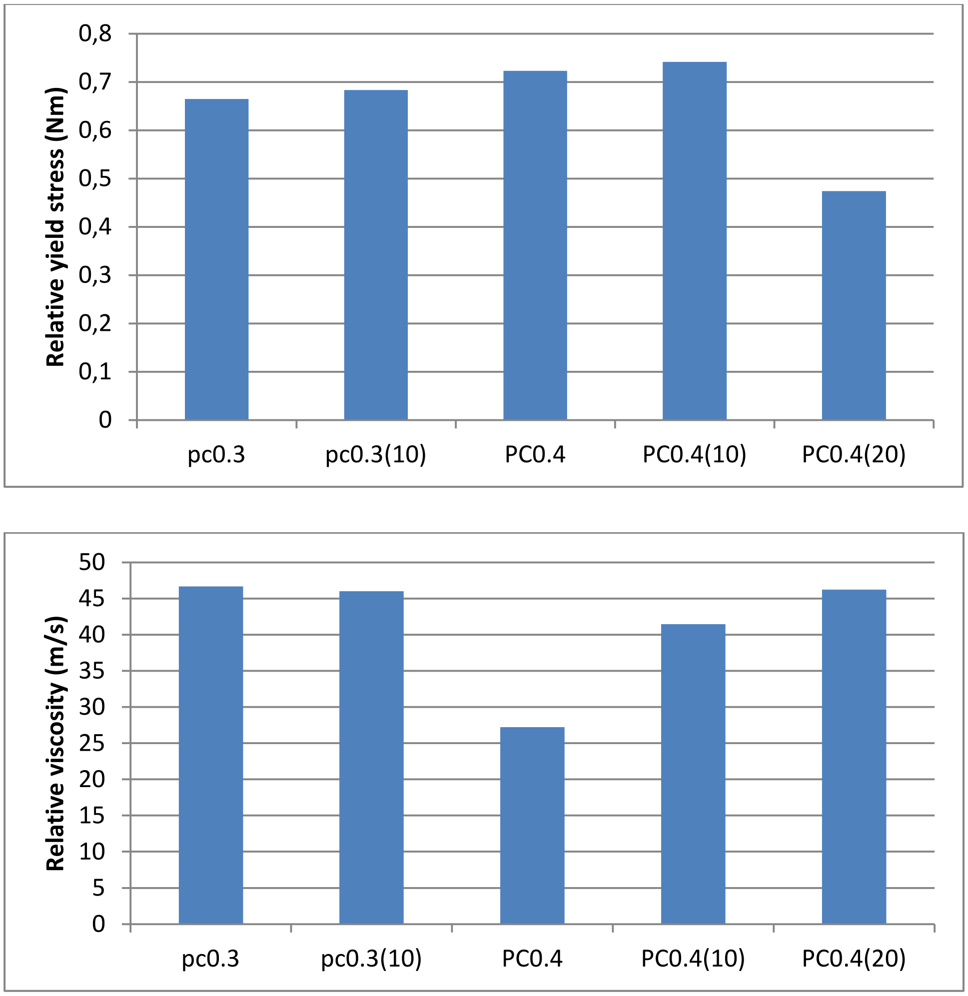

Figure 4.12 Effect of time on the flow behavior of PC 0.4 mortars.

4.6. Effect of Water-cementitious Material Ratio and Time on FA-incorporated Mortars

FA particles are round and smooth usually and have smaller size than PC particles. Round shapes keep particles at a distance (ball bearing effect) and hence cause dispersing effect. Van der Waals forces are less for distantly placed particles. So they have less Van der Waals forces and hence the yield value.

Plastic viscosity largely depends on roughness of surface, charges between particles and is less affected by Van der Waals forces. FA-incorporated mix shows less viscosity as due to smooth and round shape, slipping is easier and interlocking is lesser.

4.6.1 Effect of Amount of FA on Rheology of Mortar

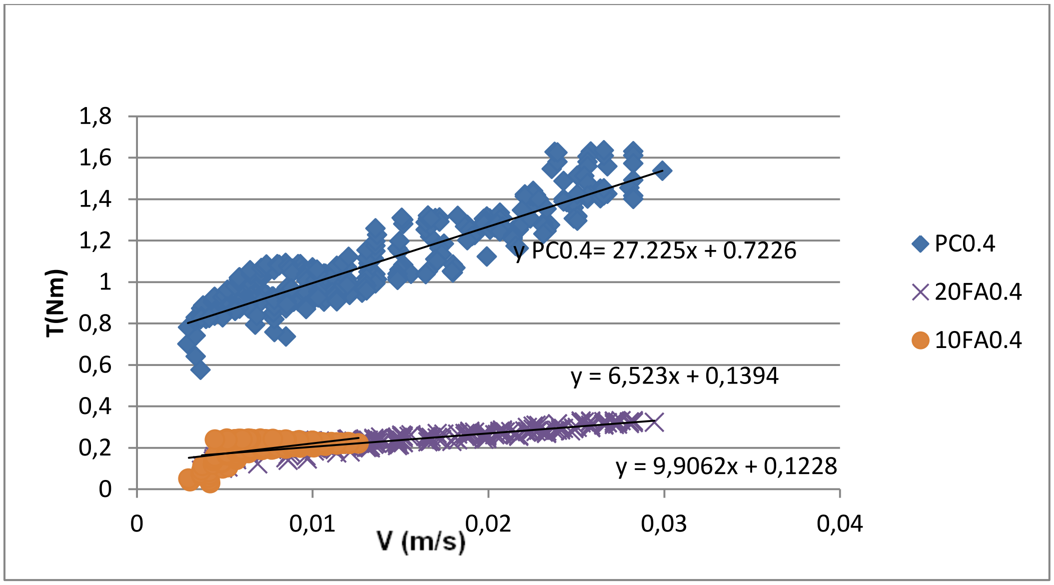

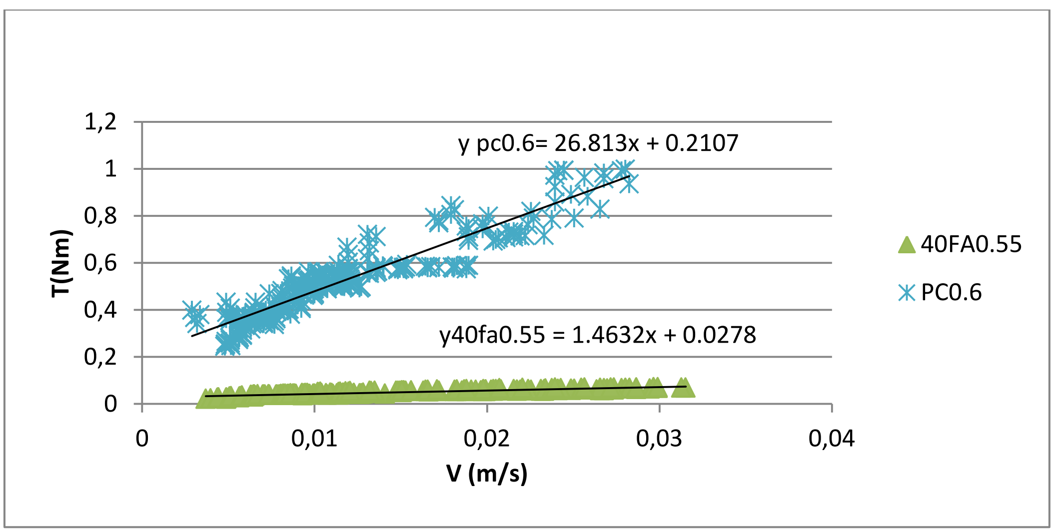

Figure 4. 13 Torque and velocity relationship with respect to amount of FA in mortar

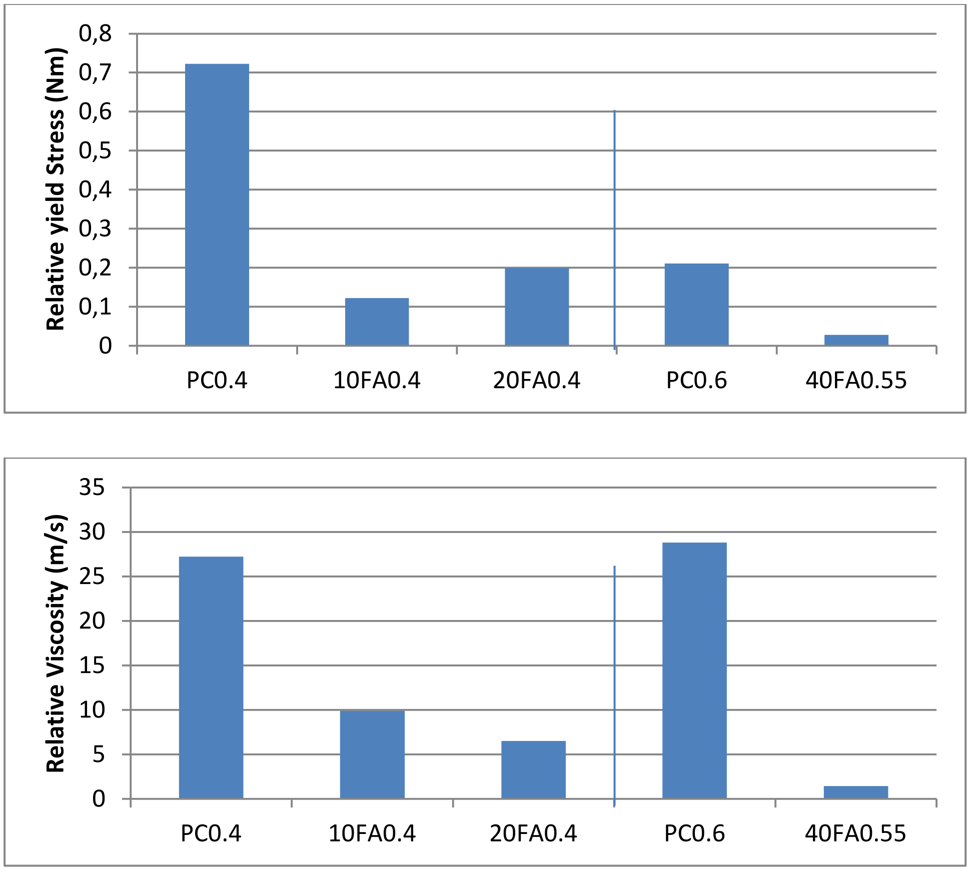

Figure 4.14 Relative yield stress and relative viscosity with respect to amount of FA in mortar

Figure 4.13 and 4.14 show that, fly ash incorporation in mortar decreases yield stress and viscosity considerably.

More fly ash at same w/c slightly increased the yield stress, it may be due to more interpacking than for 10 FA and slightly decreased relative viscosity due to higher amount of smooth and spherical particles helping in slipping away.

By observing PC 0.6 and 40 FA 0.55, it is obvious that both yield stress and plastic viscosity are dropped considerably.

Fly ash being smaller and smoother reduce attraction hence yield stress and plastic viscosity of mix.

4.6.2 Effect of w/c on Rheology of Mortar

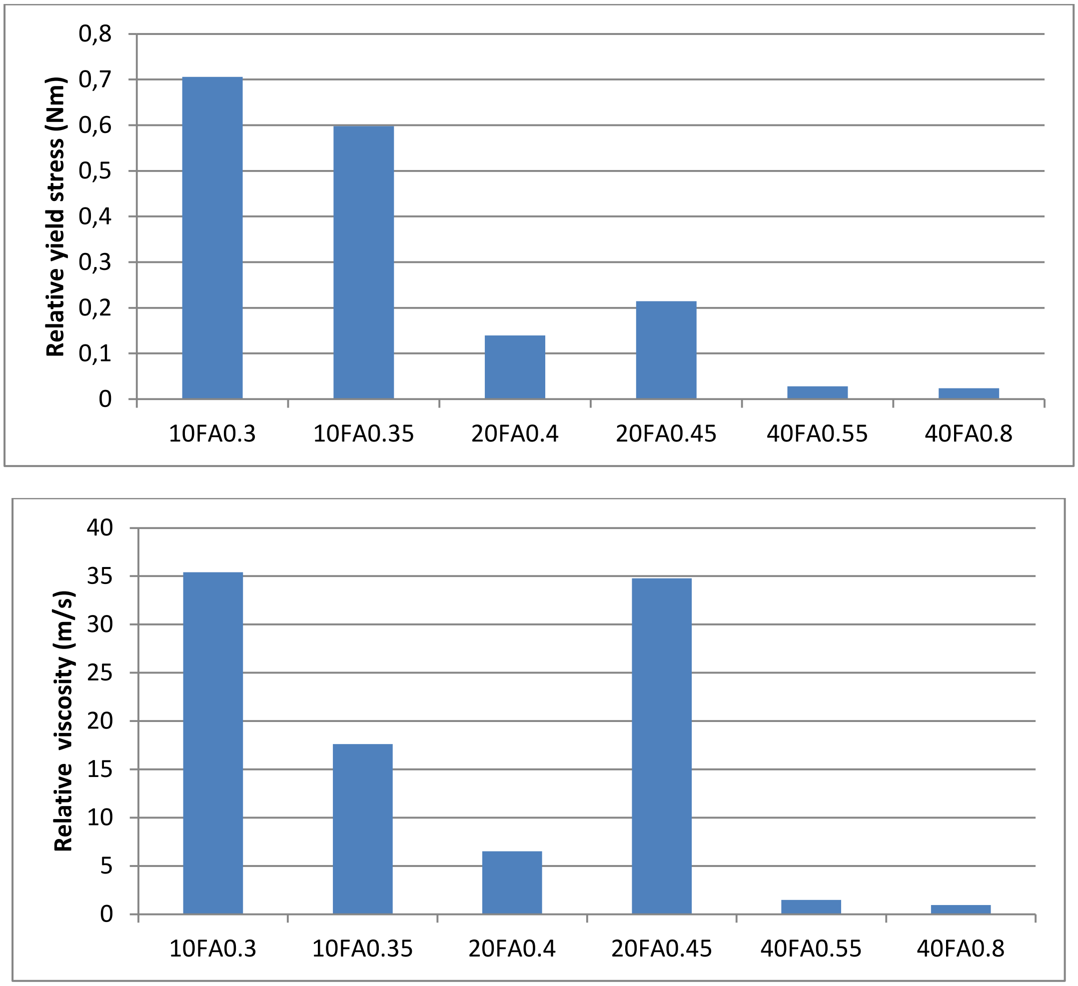

Figure 4.15. Relative yield stress and relative viscosity of FA-incorporated mix with respect to w/c

Figure 4.15 shows that, at 10 FA by increasing w/c from 0.3 to 0.35, yield stress and viscosity both are decreased but for w/c 20FA 0.4 to 0.45 both values increase because water requirement for both amounts of FA-incorporated mix are different. For 40 FA both values are again decreased

It should be noticed that for each amount of mineral admixture, there is an optimum w/c. If water content is insufficient then it will show different yield value and viscosity. If water is excessive, most probably it will show lower values for yield stress and viscosity. By increasing w/c, both yield stress and plastic viscosity is decreased.

4.6.3. Effect of Time on Rheology of FA- incorporated Mortar

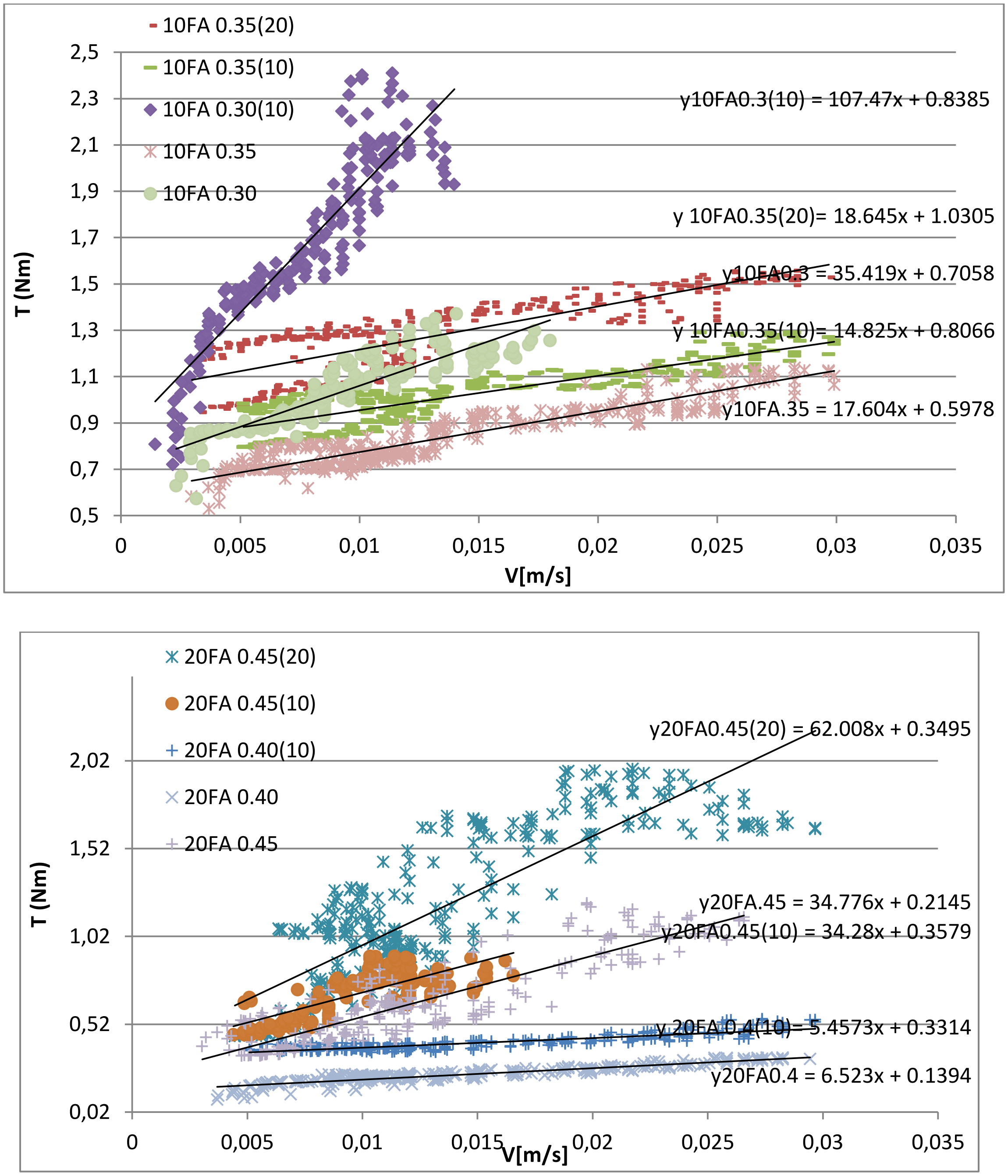

Figure 4.16. Torque-velocity relationship for FA-incorporated mix with respect to time

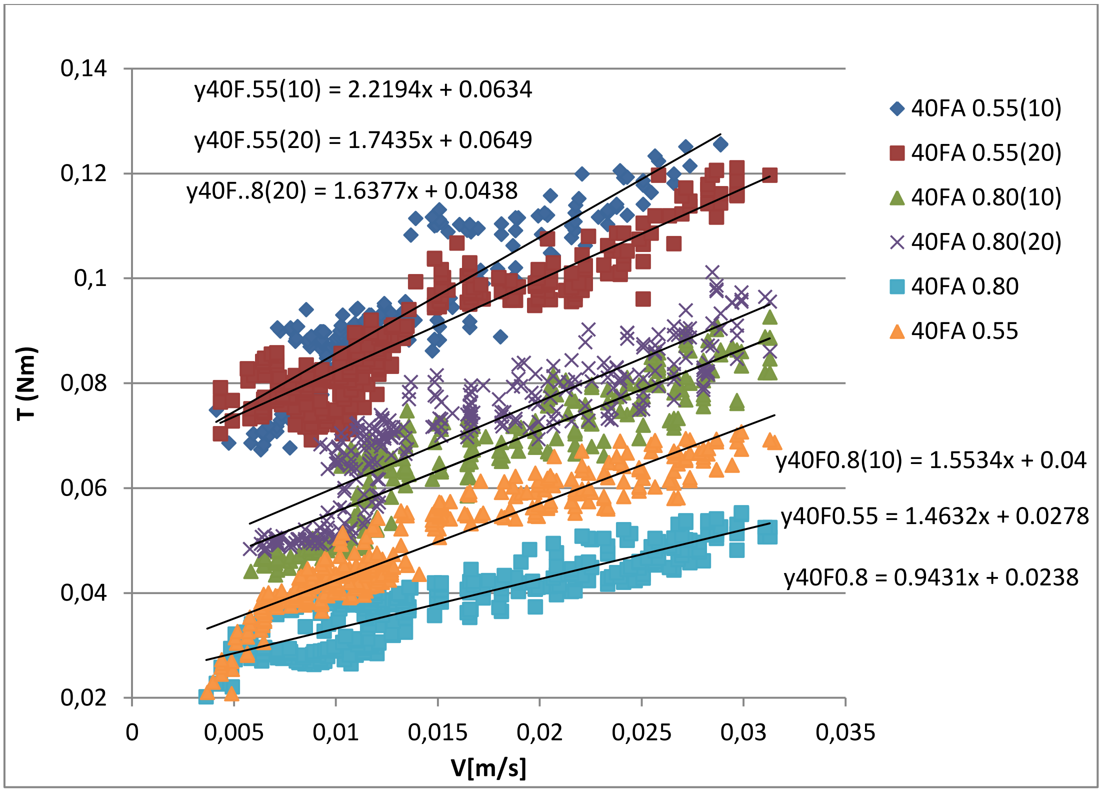

Figure 4.16 (Continued)

Figure 4.16 and 4.17 show that for all cases, yield stress is increased for FA with time.

Relative viscosity is not much changed in most of cases after 10 minutes and is increased after 20 minutes. 10 FA 0.3 is exception because of having very low w/c ratio.

Unlike other cases of admixture incorporated mortars, yield stress increases instead of decreasing at 10 minute because now there is less round shape particle available than in the start. For plain PC yield stress is quite higher than FA. When FA is added, it is smoother and does not show much interlocking and packing. When it lose shape in start of reaction, it should also loose yield value. But in this case yield value is already low and when new product is formed, it increases yield value.

Van der Waals forces are less for distantly placed particle and round FA (in less amount) keeps particle far and allow less interpacking. So they have less Van der Waals forces and hence the yield value.

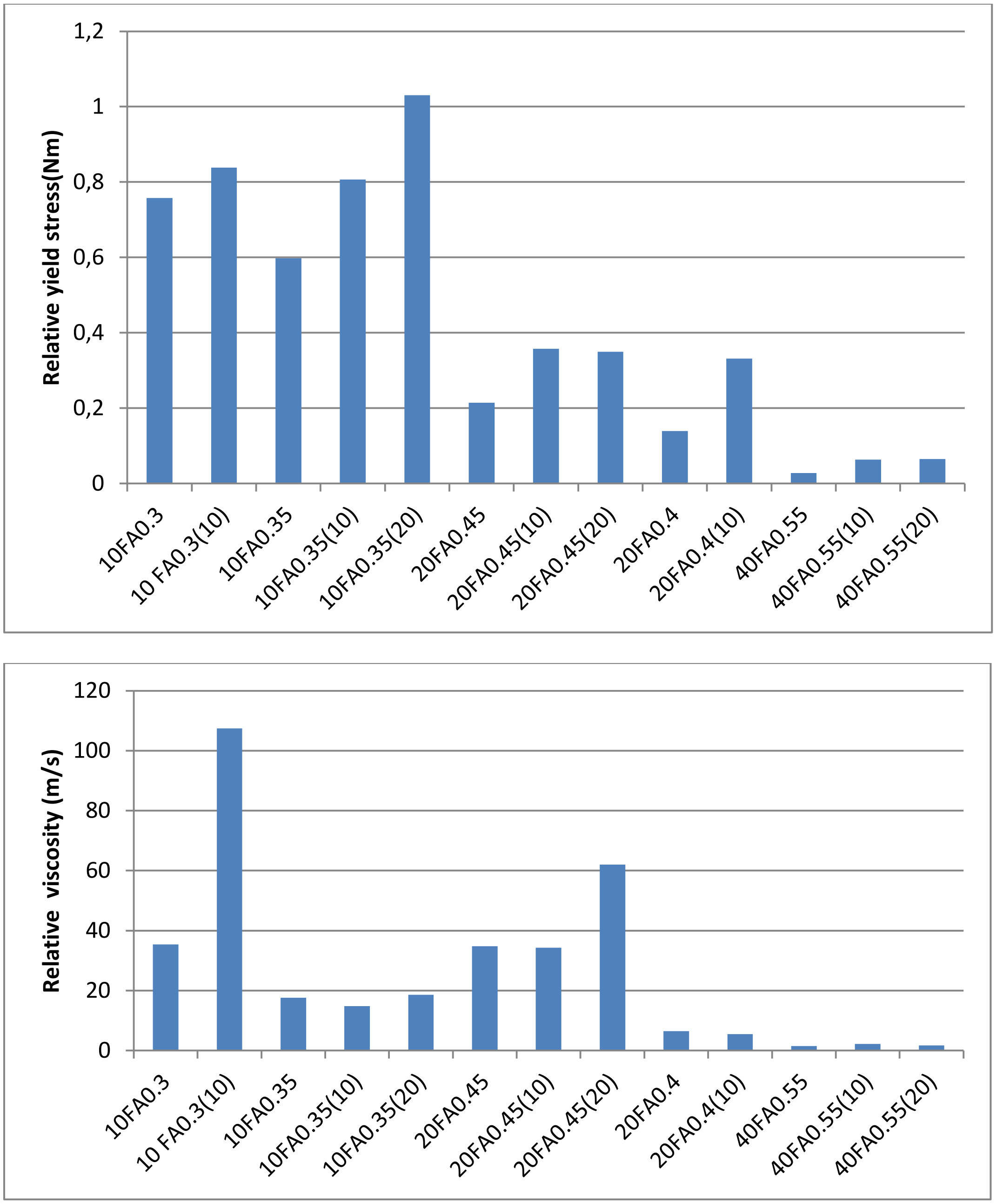

Figure 4.17 Relative yield stress and relative viscosity of FA-incorporated mix with respect to time

4.7. Effect of Water-cementitious Material Ratio and Time on BFS-incorporated Mortars

The flow curves of BFS-incorporated mortars with different water-cementitious ratios are shown in Figure 4.18

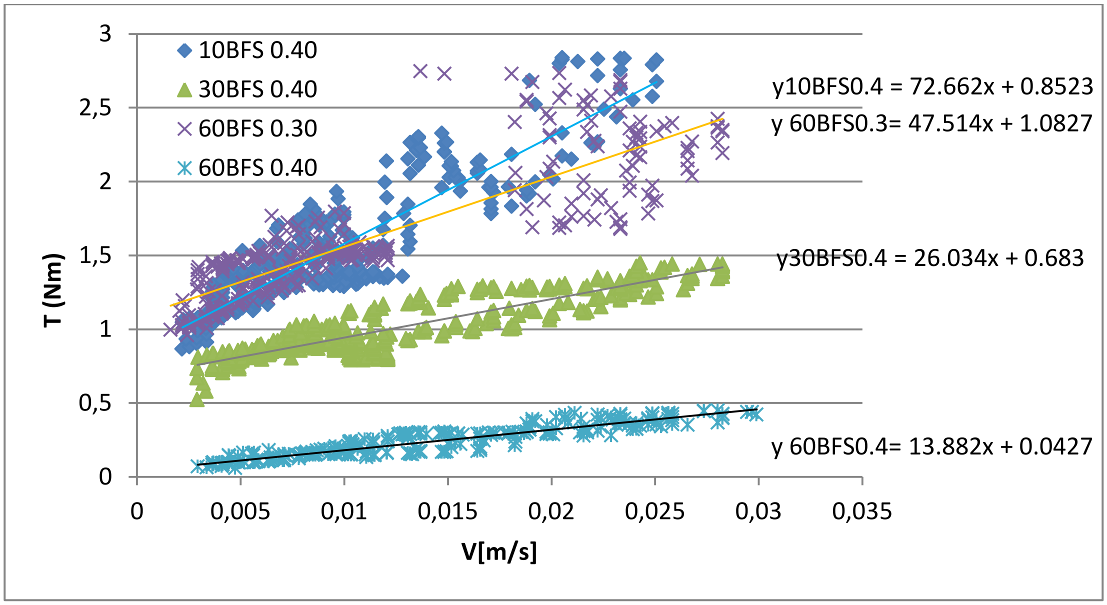

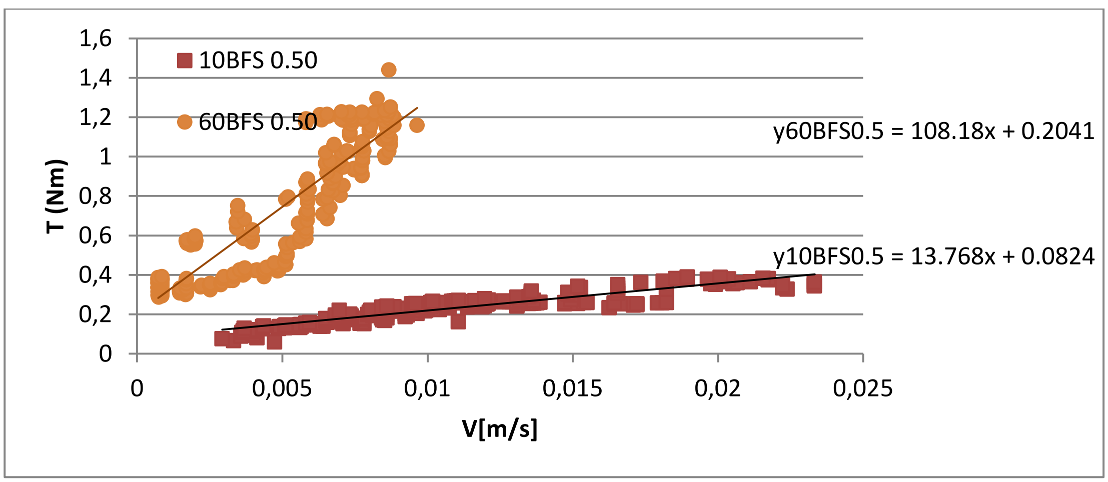

Figure 4.18 Torque-velocity relationship of BFS-incorporated mix at (a) w/c0.3 and 0.4, (b) w/c 0.5

4.7.1 Effect of w/c on Rheology of BFS- incorporated Mortar

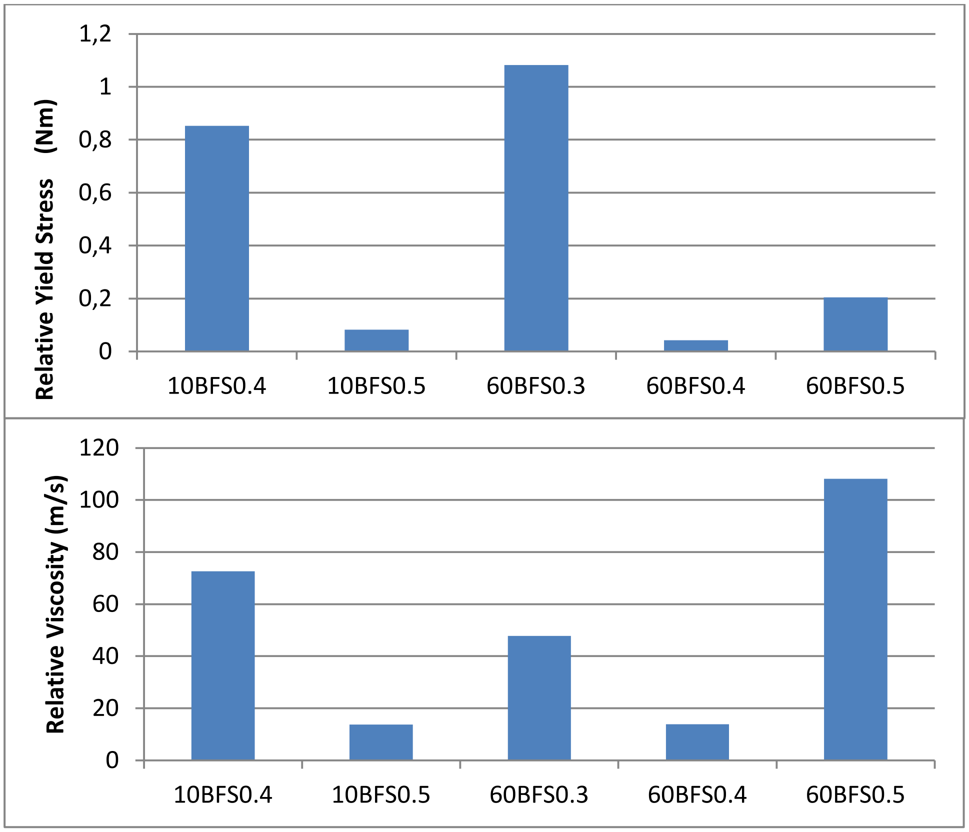

Figure 4.19. Relative yield stress and relative viscosity with respect to w/c in BFS incorporated mortar

Figure 4.19 shows that, both yield stress and viscosity decrease with increasing w/c ratio due to dispersing and lubricating effect of water. Only 60BFS 0.5 is the exception. At 60 BFS0.5 yield value and viscosity decreases by increasing w/c from 0.3 to 0.4 but at 0.5, flocculation causes increase in both values, especially viscosity. At this w/c batch cannot be mixed properly. Flocculation is caused at higher BFS contents and higher w/c.

4.7.2 Effect of Amount of BFS on Rheology of mortar

Figure 4.20 and 4.21 show that, at w/c 0.4, it is obvious that 10 percent replacement increased yield stress and plastic viscosity both. 30% replacement gives almost the same result as plain PC but value is lesser than that of 10S. At 60 % replacement, both plastic viscosity and yield stress are noticeably decreased.BFS used in experiment has polished hard and rough surface with angular shape.

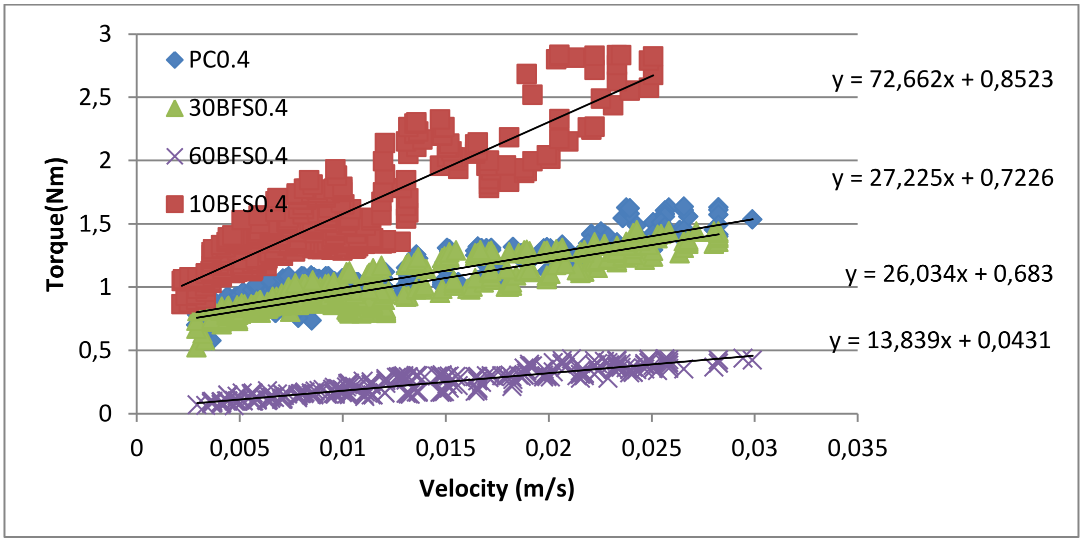

Figure 4.20 Torque and velocity relationship for BFS incorporated mortar with respect to amount at w/c 0.4

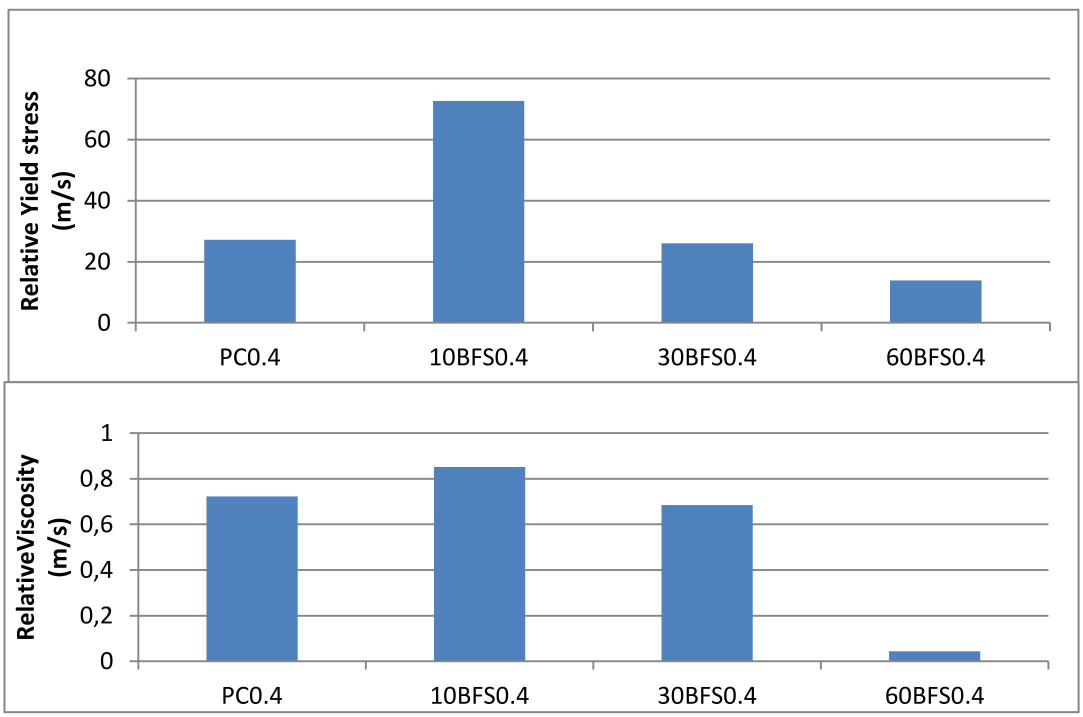

Figure 4.21. Relative yield stress and relative viscosity with respect to amount of BFS in mix at w/c 0.4

The instant increase in yield stress is due to the angular shape which provides mechanical interlocking and does not allow the start of flow easily. But by adding more BFS, PC amount is reduced. As BFS has polished and non-porous surface, free water becomes available in higher amount, reducing yield stress and relative viscosity with increasing BFS amount.

At w/c 0.4, by increasing Slag percentage in the mix, both yield value and plastic viscosity are being decreased.

At water cement 0.5, from 10S0.5 and 60S0.5, both yield and plastic stress is increased. Because water is already sufficient and free water is not playing big role as for w/c 0.4. 60 BFS shows abnormal behavior and higher values because flocculation occurs because for this w/c mix never becomes homogeneous. For example, by adding more water in baby powder, homogeneous mix can never be obtained without grinding. When there exist more powder substance, then they have too much interparticle forces between them and by adding more water, water is not perfectly mix. So flocculation of slag powder increases viscosity many folds.

4.7.3 Effect of Time on Rheology of Mortar

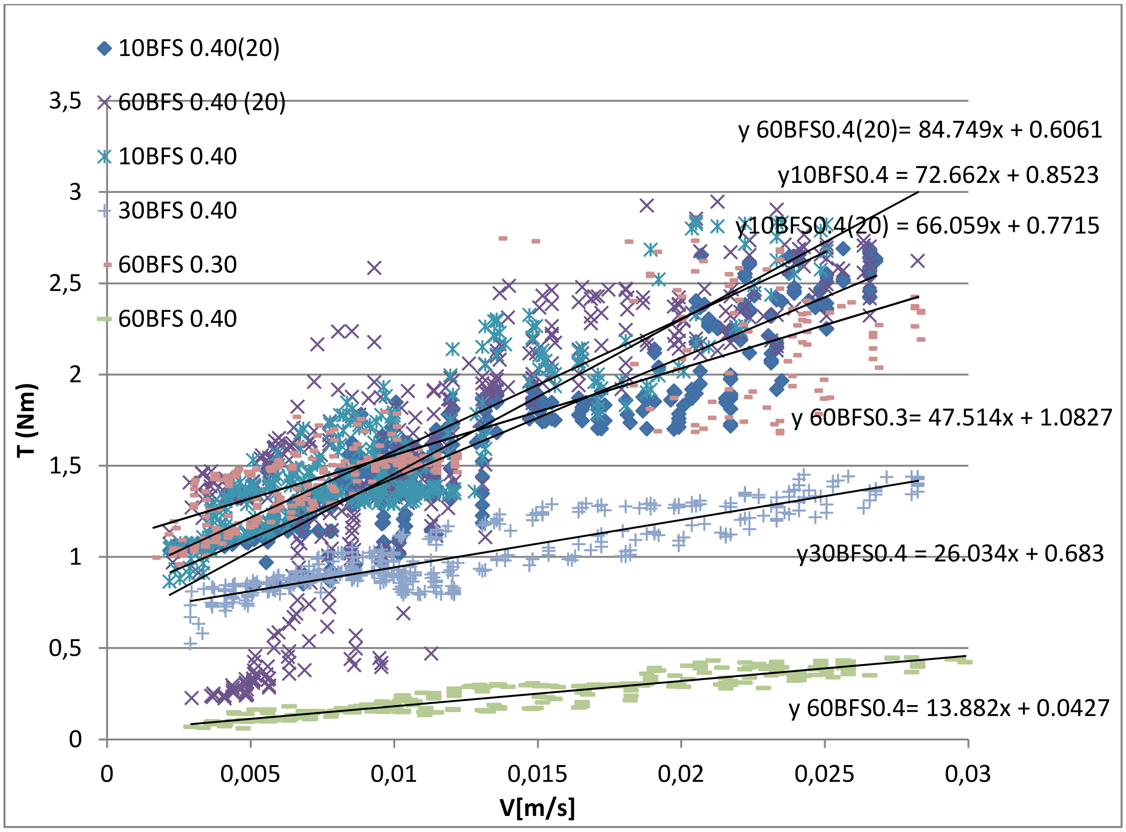

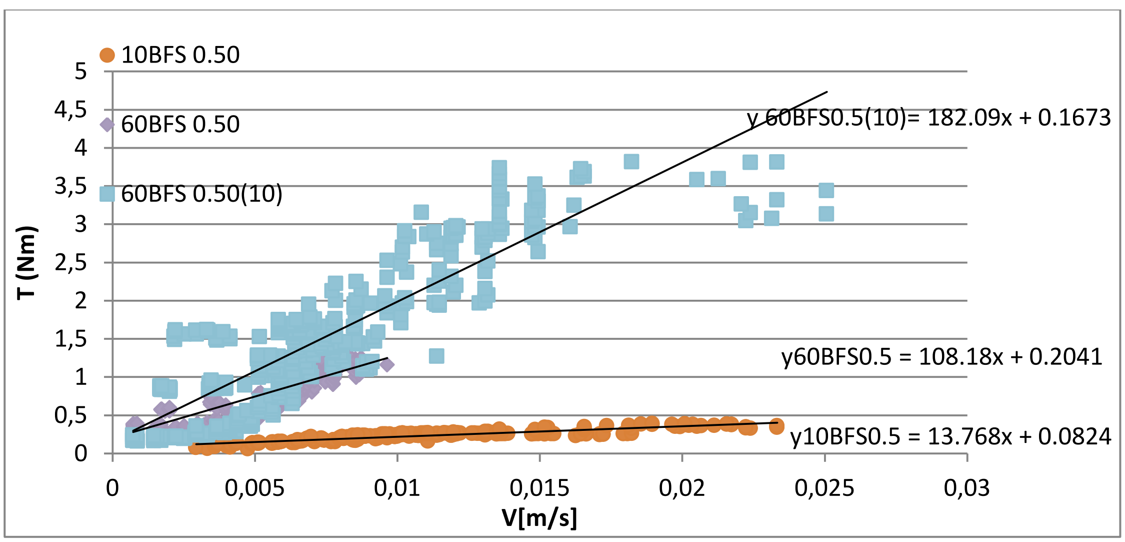

Figure 4.22 Torque and velocity relationship with respect to amount of BFS in mix

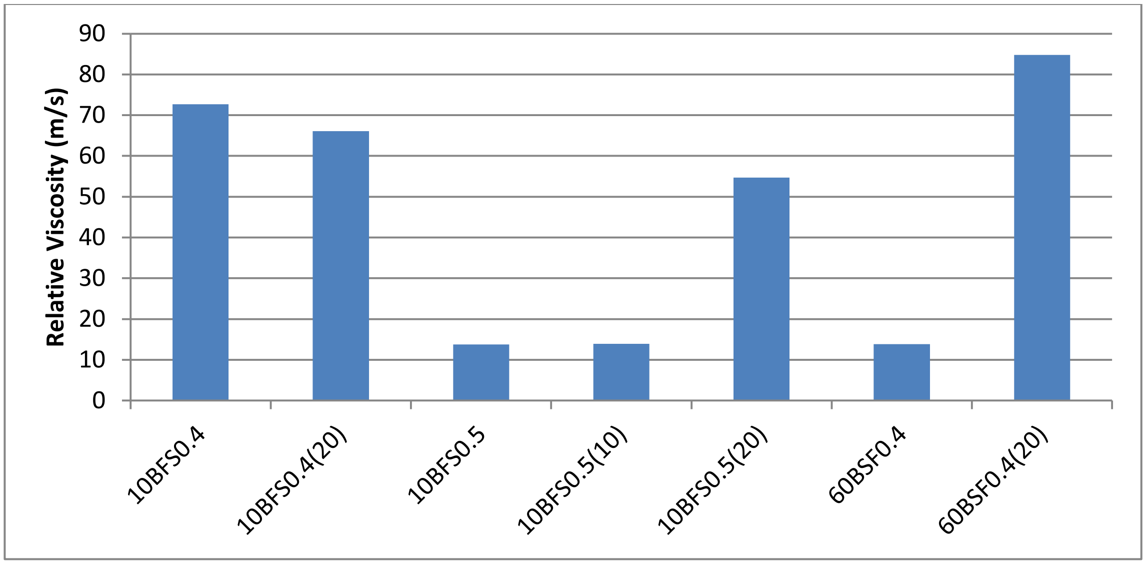

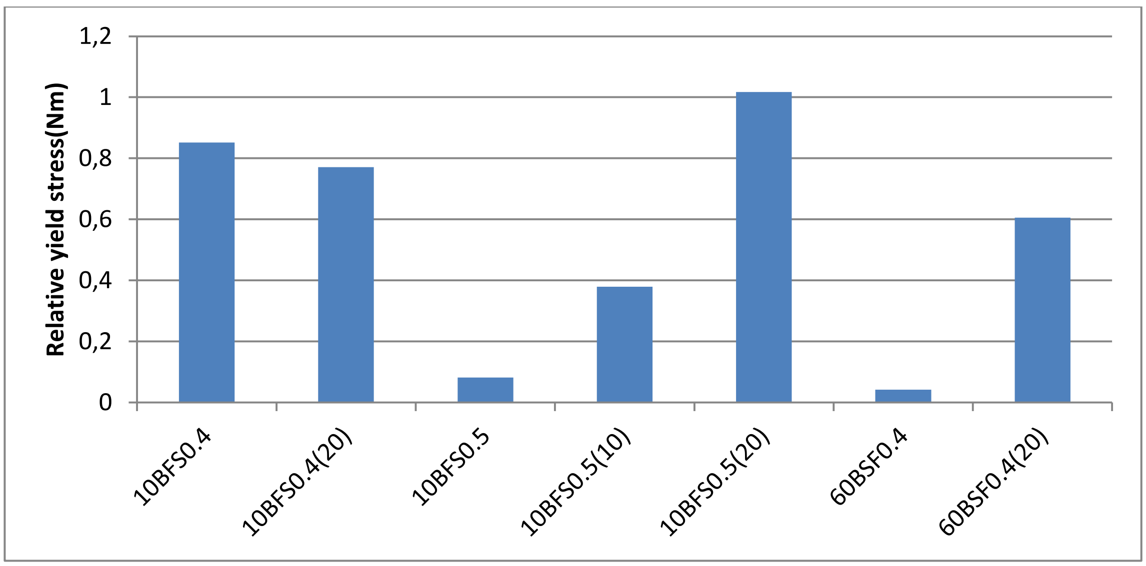

Figure 4. 23 Relative yield stress and relative viscosity for BFS incorporated mortar with respect to time

Figure 4.22 and 4.23 show that generally yield stress and relative viscosity is increased with increasing time. With time, both yield stress and plastic viscosity increases because water is lost due to evaporation and temperature rise.

10BFS0.4 is the only exception, with time both values reduces slightly because w/c is insufficient and it takes time to penetrate dry layers and start reaction. If w/c is less than specific value, then yield value usually decreases first because it takes little time for water to get penetrated everywhere. Hence reactions are slower.

4.8. Effect of Water-cementitious Material Ratio and Time on SF-incorporated Mortars

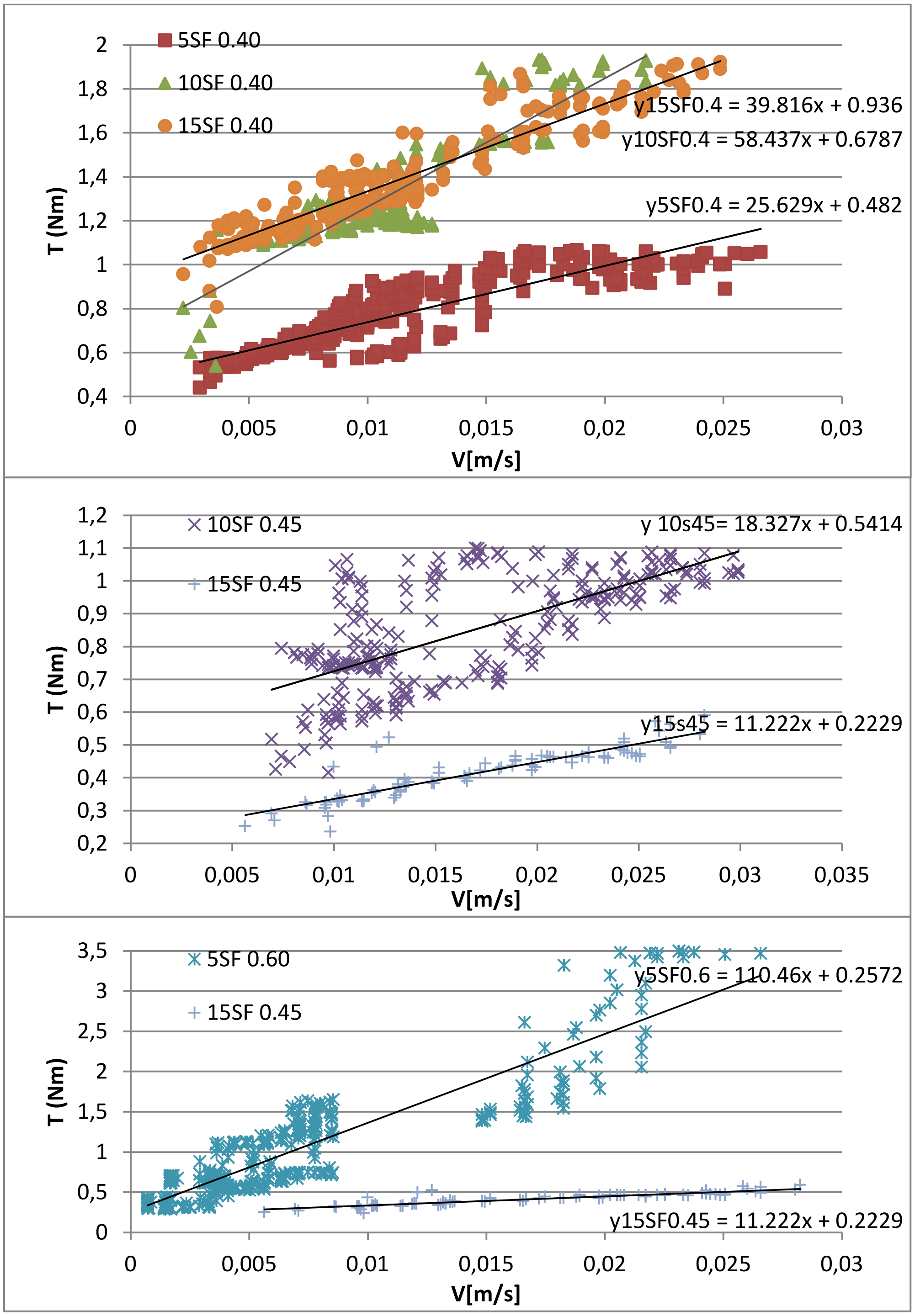

Figure 4.24. Torque –velocity relationship in SF-incorporated mortars

4.8.1 Effect of Amount of SF on Rheology of Mortar

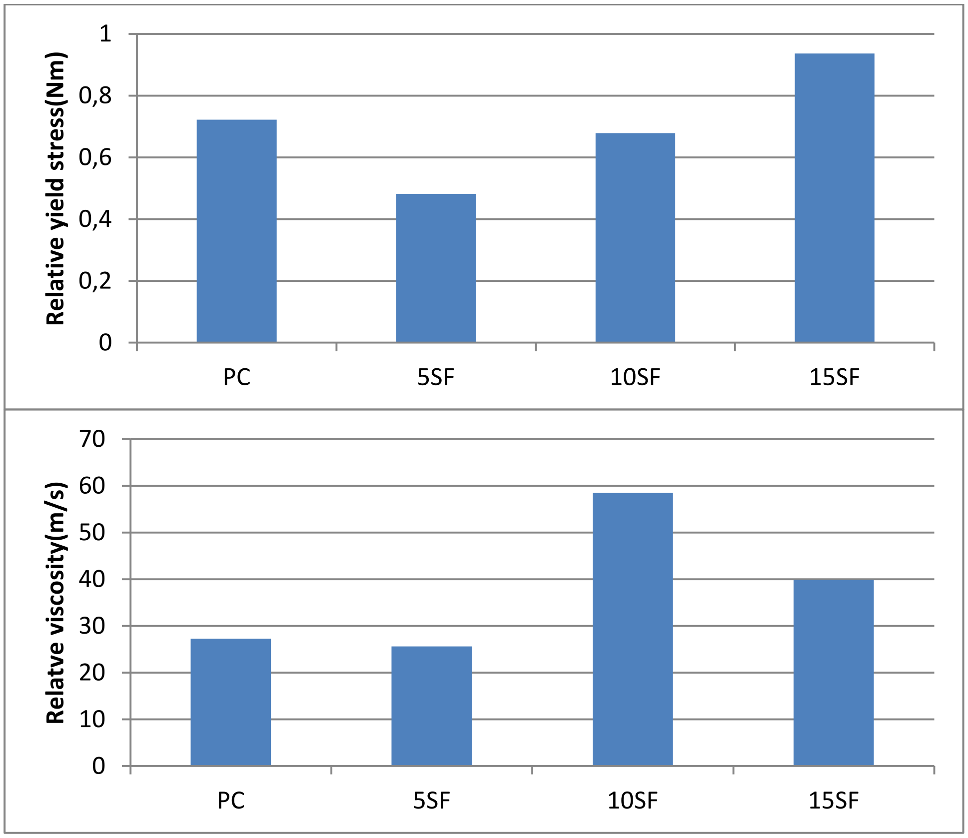

Figure 4.25. Relative yield stress and relative viscosity with respect to amount of SF on mortar

Figure 4.24 and 4.25 show that, at same w/c 0.4, for 0, 5, 10, 15% replacement yield stress decreases for 5SF0.4 and then increases but plastic viscosity first decreases and then increases and then again decreases.

This is all due to balancing of properties e.g. fineness, interpacking (both implies to rubbing surface area), roughness and water available. If rubbing area is more or roughness is high, and water (for lubrication) is low, viscosity will be higher.

At 5 SF, 5% of Cement particles are reduced and small SF molecules, which are not much in amount, comes between cement particles, thus separating them at a distance. This instantly reduces yield stress.

But when SF is increased to 10 %, its amount is increased and starts effecting yield stress and viscosity. Now instead of separating cement particles, they themselves gather in between particles and increases yield value, it becomes similar to PC0.4.

At 15 SF, there is tighter interpacking and Van der Waals forces are increased, hence higher is the yield stress.

Plastic viscosity is decreased at 5 SF as total surface area per unit volume is balancing with lubricating property of very small silica fume. Smaller rounder particle cause easier slipping providing ball bearing effect.

At 10SF, surface area per unit volume is much increased (due to fineness of SF. Actually fineness also contributes to surface area per unit volume). For 10SF, SF particles are enough in number and make tight interpacking and less space.

At 15SF, smaller round particles are very high in number. Hence smallness and roundness of particle contributes in slipping. There is number of big, irregular, and rough cement particles. There is less interlocking. This makes slipping easier than 10SF0.4 but much difficult than PC0.4. Hence viscosity value is lesser than 10 SF but much higher than PC0.4. After balancing of different properties such as roughness, surface area per unit volume, size distribution between 85%cement and 15% SF, interlocking, hence viscosity is reduced from 10 SF viscosity but still v high than simple PC0.4 viscosity.

It is also possible that at 15 % replacement, cement particles are already less in number of silica fume comes between them and nullifies their effect in motion. The major flow resistance is mainly due to silica fume only for 15% SF particle has made the mix smoother.

4.8.2 Effect of w/c on Rheology of SF-incorporated Mortar

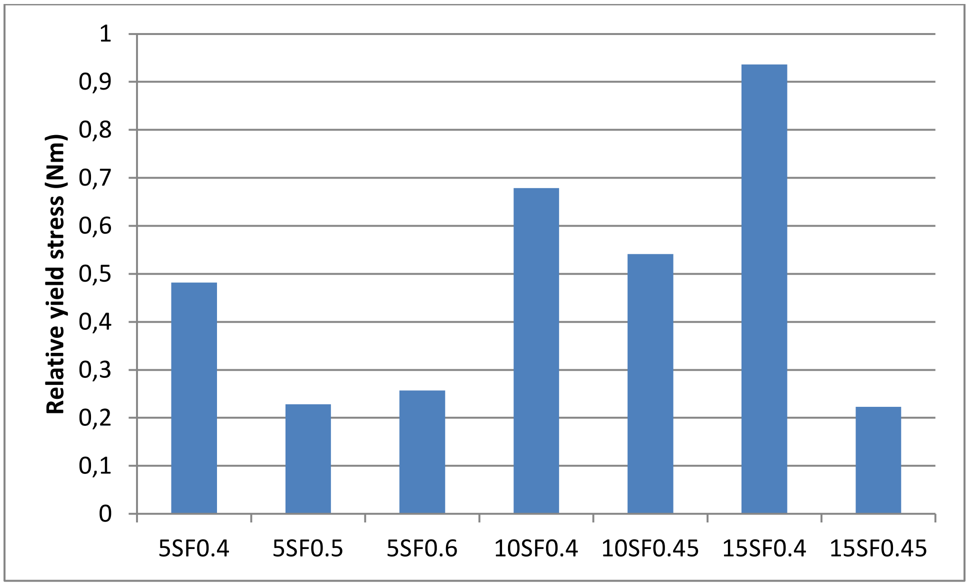

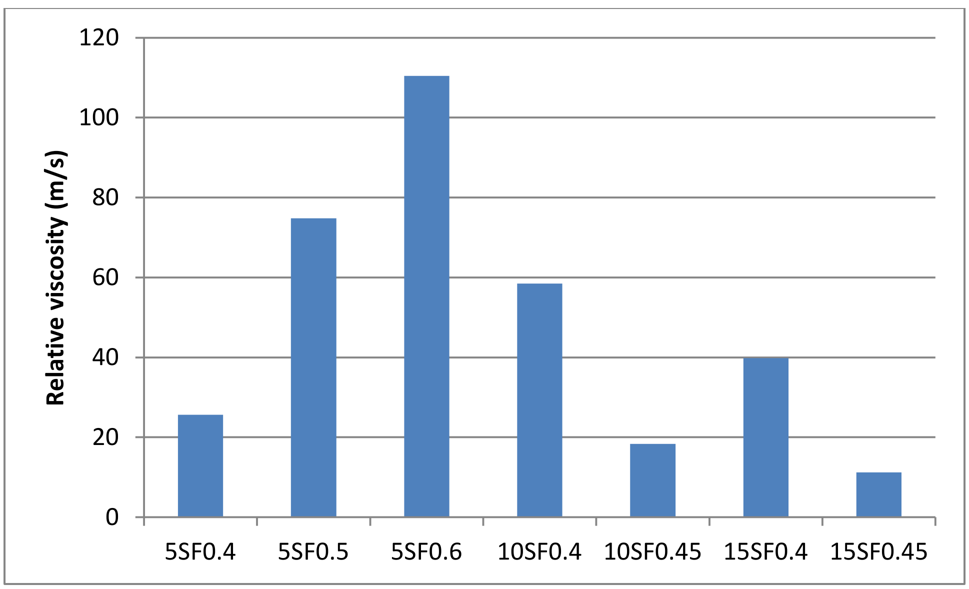

Figure 4.26. Relative yield stress and relative viscosity with respect to amount of SF in mortar

Figure 4.26 shows that yield stress is decreased generally with increasing w/c. while plastic viscosity also decreases with increasing w/c. Small incorporation (5%) is an exception.

At 5SF0.6 yield stress is slightly increased instead of decreasing due to flocculation (improper mixing).

Water causes dispersion and lubrication so decreases both yield stress and viscosity.

Actually this is all due to balancing of properties e.g. fineness, interpacking (both implies to rubbing surface area), roughness and water available. If rubbing area is more or roughness is high, it will and water is low, viscosity will be higher.

4.8.3 Effect of Time on Rheology of SF -incorporated Mortar

Figure 4.27 and 4.28 reveal that, generally yield stress increases at 10 minutes and decreases at 20 minutes while viscosity shows mixed results with time. But generally viscosity is also increased with time.

These values are increasing because rate of reactions are faster and temperature rise is causing an increase in viscosity and sometimes more evaporation. Relative viscosities are showing mixed results because at each time phase the characteristics of mix change. Viscosity depends on available surface area for rubbing, smoothness and water amount for lubrication at that time.

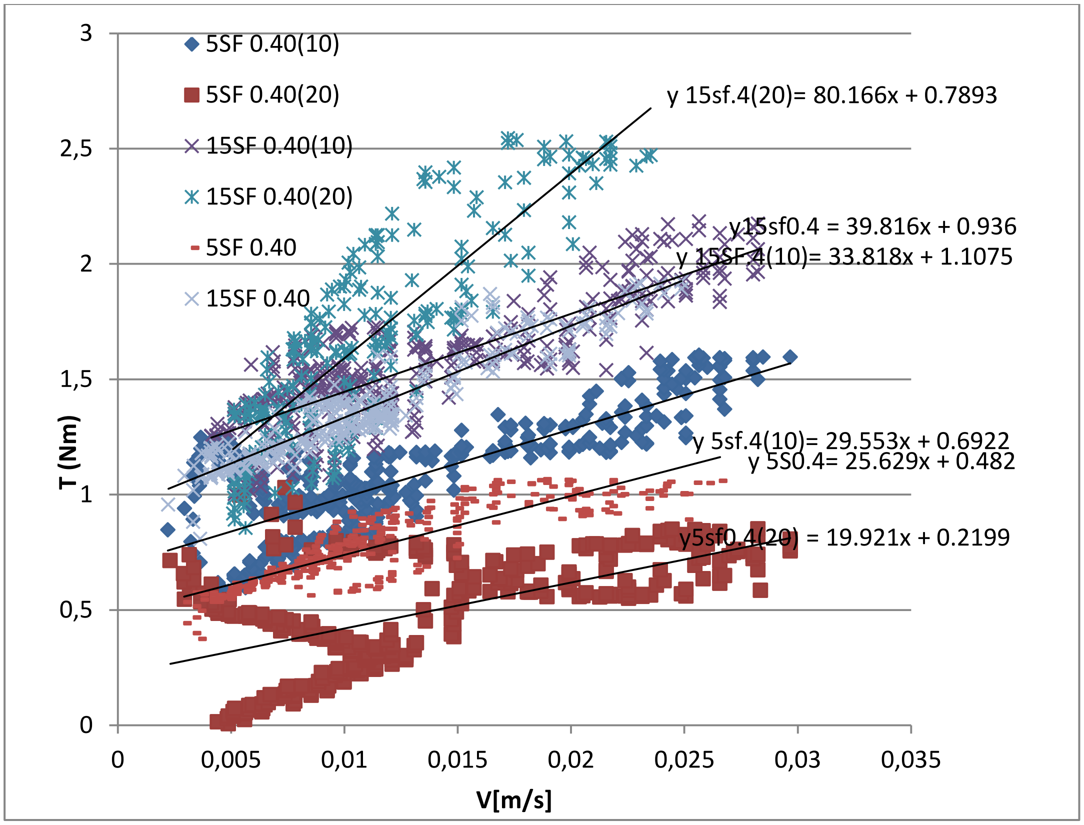

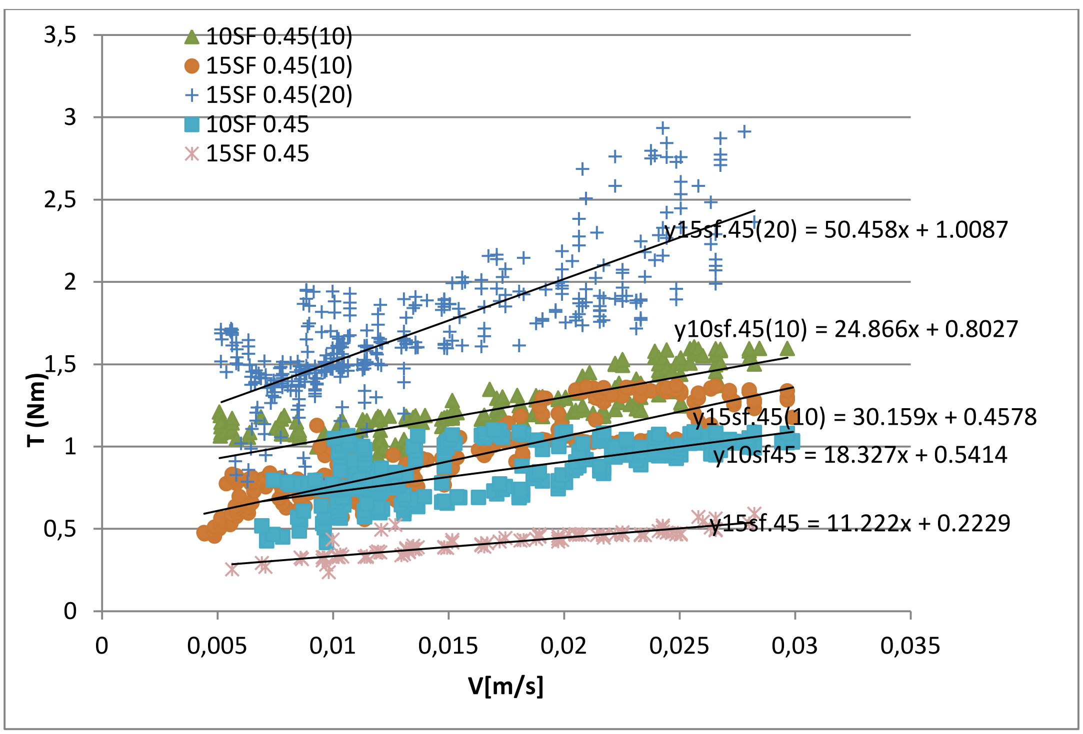

Figure 4.27. Torque – velocity relationship for BFS incorporated mortar with respect to time

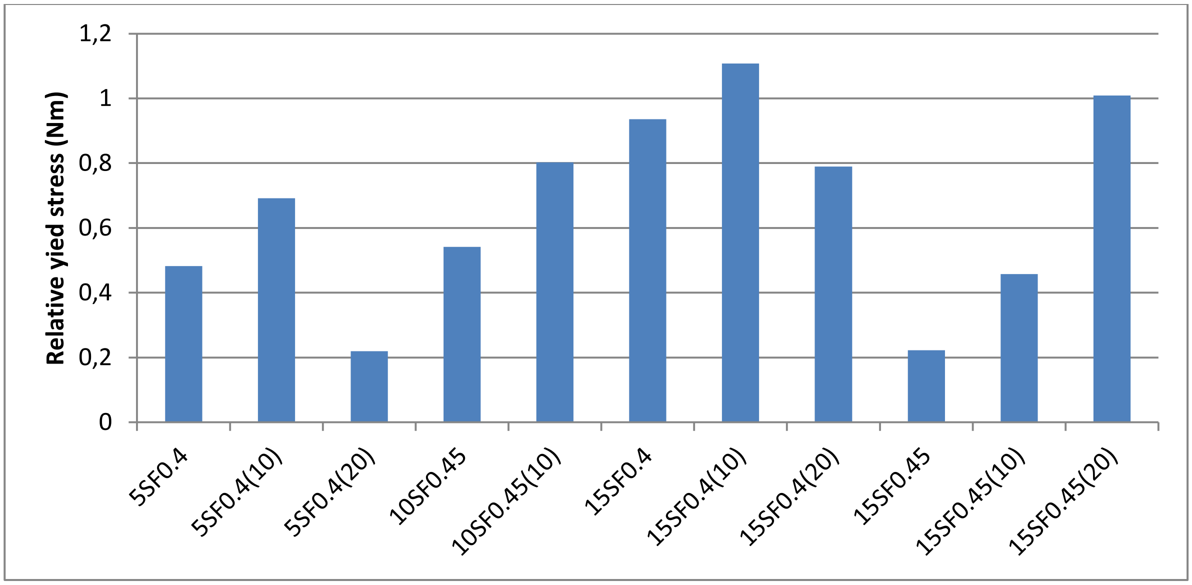

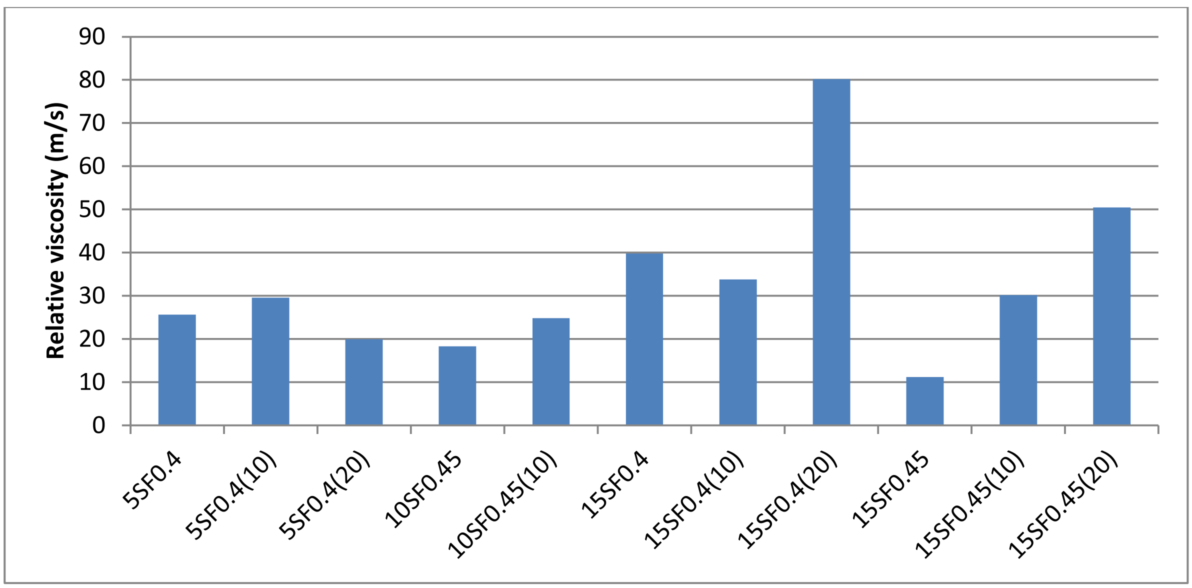

Figure 4.28. Relative yield stress and relative viscosity for SF incorporated mortar with respect to time

4.9 Summary

Experimental results are summarized in the section below.

4.9.1 Yield stress

Basically yield stress, which is the minimum stress required to initiate the flow, is achieved when the force causing the flow increases from the intermolecular forces between the particles.

In mortars, intermolecular forces, mainly Van der Waal forces are the cause of yield stress. If the attractive forces between the particles are higher, then the yield stress is higher.

Van der Waal forces are the attractive or repulsive forces between molecules and atomic groups that are not due to covalent or ionic bonds. Van der Waals forces are not chemical bonds; they are weaker, non directional, depend on closeness of particles and are short range force

Usually there are 3 types of Interparticle/Van der Waal forces,

1. Dipole, existing between positive part of one molecule and negative part of the other molecule,
2. Dispersion force , developed due to temporary induced charges
3. Hydrogen bonds.

One of the general formulas used for assessing the Van der Waals forces in round particles is

$$F = -\frac{AR1R2}{(R1+R2)6r^2} \tag{4.1}$$

Where F is Van der Waals force, R1 and MSE are the radii of particles and r is distance between them, A is a constant.

Van der Waals forces decreases with decreasing size of body. Smaller particles have smaller Van der Waals force but total Van der Waals force per unit volume is the sum of Van der Waals forces in that volume. For particle greater than 250 micrometer, free flow occurs.

Inter particle forces also depend on unevenness of surface. If surface is rough then due to the mechanical interlocking, Van der Waals force is increased.

4.9.2 Viscosity

Viscosity is the resistance developed against the deformation. It is caused by liquid friction. Friction is the force~~,~~ resisting the movement in a mix in a suspension. So, viscosity mainly depends on friction i.e. roughness of a particle and particle packing.

Viscosity depends on surface area per unit volume. As more surface area will cause more interparticle friction and hence hindrance to flow.

It has also been observed that broader size distribution of particles shows more viscosity than narrow size distribution of particles. In this way more particles can be packed in unit volume providing more available surface area for rubbing.

Once particle starts moving, the Van der Waals forces has lesser effect and now roughness and particle packing are to be dealt with.

4.9.3 PC

- There is a specific or optimum water cement ratio for each case of cement plus specific amount of admixture, below which yield stress may be less due to improper mixing. Above this ratio yield stress is again less due to more water causing dispersion and lubrication among particles. So Interparticle forces are less at far placed particles.
- As yield stress and plastic viscosity values are obtained after the balancing of different properties, on one side increase causing factors and on other side

decrease causing factors. So their combined effect will determine whether the value should increase or decrease. These factors are interparticle forces like van der Waals(increase yield stress), particle shape (round decrease viscosity) and roughness (increase viscosity, and has little effect on yield stress due to mechanical interlocking), particle size distribution (increase viscosity and yield stress, good packing), surface area per unit volume (increase viscosity), density (increase yield stress), fineness (increase both), mineral character (lime combining capacity, glassy phase etc), surface charge resulting in the flocculation or dispersion (flocculation increase yield stress, dispersion decrease both), surface hardness and water absorbing quality (porosity), (More free water less yield stress and viscosity), temperature (increase viscosity and decrease slightly the yield stress due to far particles).

- Yield stress increases with time for PC because of loss of water by absorption and evaporation and due to hydration products (chemical bonding).
- Plastic viscosity is decreased with high w/c because more water provides more lubrication and dispersion. Water layer comes between rough particles and allow them to slip easily.

4.9.4 BFS

- By adding little amount of BFS as 10% replacement, rough, polished and hard surface angular BFS increases Yield stress due to mechanical interlocking between angular and rough particles , hindering the flow to start. Plastic viscosity is increased due to same reason.
- By increasing BFS, cement particles are reduced. As BFS surface is polished and hard so free water is available reducing both yield stress and viscosity.
- At 30 % replacement, there is almost no effect on rheology of mortar. It is similar to PC. Even both yield stress and plastic viscosity of the values are less than 10 % incorporation but now they are comparable to ordinary PC values.

- By increasing BFS amount, both of the values are decreased. But if flocculation occurs (at higher replacement and higher w/c) both yield stress and plastic viscosity values usually increases.

4.9.5 FA

- FA instantly reduces both yield stress and plastic viscosity to much lower values due to smooth spherical shape (yield stress decreases due to ball bearing effect and viscosity decreases due to smooth and round particle).
- Van der Waals forces are less for distantly placed particle and round FA keeps particle far and allow less interpacking. So they have less Van der Waals forces and hence the yield value.
- Plastic viscosity increases with time for plain PC but when fly ash is added then it instantly reduces. With the time, plastic viscosity increases as fly ash lose its round shape and irregular products are formed. This provides hindrance in sliding.
- FA yield value increases after 10 and 20 minutes because round particles (main cause of lower yield value) are changing shapes due to deposition of hydration products.
- For higher amount of mineral admixture as 40FA and 60BFS and higher w/c, the both value results are abnormal and usually higher because of flocculation of particles.

4.9.6 SF

- Relative viscosity in SF shows mixed results It is due to balancing of properties e.g. fineness, interpacking (both implies to rubbing surface area), roughness and water available. If rubbing area is more or roughness is high, and water (for lubrication) is low, viscosity will be higher.
- Yield stress decreases at 5 % incorporation and then increases for higher SF incorporation. This is all due to balancing of properties e.g. fineness,

interpacking, roughness and water available. Small amount of SF particles come between cement particles, thus separating them at a distance. This instantly reduces yield stress. But when SF is increased, instead of separating cement particles, SF gathers in between particles and increases yield value

- Plastic viscosity is decreased for small percentage of SF because total surface area per unit volume is balancing with lubricating property of very small silica fume. Small round particle in lesser amount, ball bearing effect and cause easier slipping. However, if SF amount is increased, surface area per unit volume is much increased (due to fineness of SF. Actually fineness also contributes to surface area per unit volume) and makes tight interpacking and less space hence viscosity is increased. At higher SF contents, smaller round particles are very high in amount. Hence smallness and roundness of particle contributes in slipping. There is less number big, irregular, and rough cement particles. There is less interlocking so viscosity may be reduced. After balancing of different properties such as roughness, surface area per unit volume, size distribution, interlocking, hence viscosity is decided
- It is also possible that at high SF incorporation, cement particles are already less in number, SF particles come between them and nullify cement particles effect on motion resistance. The major flow resistance is mainly due to silica fume only.
- In silica fume, yield stress and viscosity values usually increase with time. Relative viscosities show mixed results because at each time phase there are different characteristics of mix. Viscosity depends on available surface area for rubbing, smoothness and water amount for lubrication at that time.

CHAPTER 5

COMPARISON OF MATHEMATICAL FLOW MODELS

5.1 Flow Model

A flow model is considered to be a mathematical equation that describes rheological data such as shear rate and shear stress in a convenient manner (Rao, 1999).

5.1.1 Bingham Model

Bingham model is the simplest and most widely used model till now. It is a 2 parameter model. In this model, graph is drawn between shear stress and shear rate, the intercept gives the yield stress and slope of straight line reveals plastic viscosity. So the graph is drawn between torque applied and velocity to obtain relative yield stress and relative plastic viscosity by eBT2 rheometer.

$$\tau = \tau_0 + \mu\dot{\gamma} \tag{5.1}$$

One of the main discrepancies of Bingham model is its linearity. It does not give any idea about shear thinning and shear thickening behavior.

5.1.2 Herschel Bulkley Model

The main difference of Herschel Bulkley Model from Bingham Model is that, it has three main parameters: the consistency A, the flow index *B*, and the yield shear stress.

Flow index tells the degree to which mortar is shear thinning or shear thickening. If flow index B is less than 1, mortar is shear thinning and vice versa.

$$\tau = \tau_0 + A\dot{\gamma}^B \tag{5.2}$$

The apparent viscosity is calculated as $\eta_{app} = \tau / \dot{\gamma}$. When $\tau_0 = 0$ and B = 1, the model describes a Newtonian fluid; when $\tau_0 > 1$ and B = 1, the model describes a Bingham fluid, and when $\tau_0 = 0$ and B< 1, the model describes a pseudo plastic fluid.
From the experimental graphs obtained by rheometer, it is obvious that relation between torque and velocity is not linear. So Herschel Bulkley has the advantage over Bingham Model. The major discrepancy of Herschel Bulkley model is that the yield stress is to be guessed and if guessed value is inaccurate the whole model is inaccurate. So if any other model suggests yield stress and give shear thinning or shear thickening behavior too, then that model will be much preferable.

5.1.3 Modified Bingham Model

This model is modification of Bingham model. Instead of straight line, 2 degree polynomial is used to describe the model. It has 3 parameters. This model can be regarded as an extension of the Bingham model with a second order term, but also as a second order Taylor development of the Herschel Bulkley equation, which is justified since the parameter *B* in H.B rarely exceeds the value 2. Rearranging all terms and taking the ratio of the second order term to the linear term results in a theoretical relation between B/μ (modified- Bingham) and *B* (Herschel-Bulkley). the parameter B/μ can be applied to describe non linear behavior, indicating shear thinning ($B/\mu < 0$), shear thickening ($B/\mu > 0$) and the Bingham model ($B/\mu = 0$). (Feys, D. 2009)

$$\tau = \tau_0 + \mu\dot{\gamma} + B\dot{\gamma}^2 \tag{5.3}$$

5.1.4 Casson Model

Casson Model is a structural flow model. In Casson model, a straight line results when the square root of shear rate, $V^{0.5}$ and the square root of shear stress, $(T)^{0.5}$ are plotted, with slope $\sqrt{\mu}$ and intercept $\sqrt{To}$.

Till now Casson model has been used for thinner consistency materials.

$$\sqrt{T} = T_{\circ} + \sqrt{\mu V} \tag{5.4}$$

So the graph between square root of T and square root of V is plotted as a straight line. Square of T_0 gives the relative Casson yield stress and square of $\sqrt{\mu}$ gives the Casson Plastic viscosity.

From the following graphs, Casson values are not well fitting for mortars.

5.1.5 Other Models

Hence the research is continued on other models too.

Bingham [14, 98]	$\tau = \tau_o + \mu \dot{\gamma}$;
Herschel-Bulkley [129]	$\tau = \tau_o + A \dot{\gamma}^{B}$;
Robertson-Stiff [130]	$\tau = A(\dot{\gamma} + B)^{C}$;
Modified Bingham [131]	$\tau = \tau_o + \mu \dot{\gamma} + B \dot{\gamma}^{2}$;
Casson [132]	$\sqrt{\tau} = \sqrt{\tau_0} + \sqrt{\mu \dot{\gamma}}$;
De Kee [131]	$\tau = \tau_o + \mu \dot{\gamma} e^{-A \dot{\gamma}}$;
Yahia and Khayat [131]	$\tau = \tau_0 + 2\sqrt{\tau_0 \mu \dot{\gamma} e^{-A\gamma}}$
Quemada [133]	$\tau = \left(\dfrac{1+\sqrt{(A\gamma)}}{B+C\sqrt{(A\gamma)}} \right)^2 \dot{\gamma}$
Vom Berg [134]	$\tau = \tau_o + A \sinh^{-1} (B \dot{\gamma})$

5.2 Model Proposed in This Study

The new model “Maria Idrees Model” has been proposed and is described by equation 5.5.

$$T = T_{\circ} + a\sin bv \tag{5.5}$$

Where, T represents shear stress, a and b are parameters representing relative viscosity and flow coefficients, and To is yield stress. V represents shear strain rate. Sine is used because the graph obtained by rheometer resembles sine wave.

5.3 Methodology Adopted

Experimental values of velocity (V) and Torque (T) are plotted on graph. By applying model equation, T model is plotted against experimental V on the same graph. Parameters are selected by minimizing root mean square error for T model and V experimental.

Some models cannot describe the experimental values, so they are rejected for mortars. The models well describing and most suitable for the data are the successful models for mortar.

A new model is proposed for the mortar.

5.4 Comparison between Different Models

The well suited model is the model which describes the experimental data by applying some parameters. So graphically the best suited model overlaps the experimental data. The average of square of error (difference in experimental and model T values) described by MSE is used to find out the suitability of models. The lower the MSE, the higher is the suitability of that model.

The constant used in models to fit the data to experimental values are the parameters. T_o, μ, A, B are all the parameters. Sometimes they represent some physical meanings e.g. T_O, μ are the yield stress and relative viscosity respectively.

Different Flow Models including proposed model are plotted on graph for PC along the experimental data. The suitability of different models is compared.

Table 5.1. PC0.3, Different Models Parameters

Bingham	T_o	μ		MSE
	0.664	46.649		0.024
Herschel	To	A	B	MSE
	0.826	221.477	1.450	0.023
Robertson	A	B	C	MSE
	9.624	0.927	33.205	0.023
Mod Bingham	To	μ	B	MSE
	0.786	24.479	772.313	0.023
Casson	To	μ		MSE
	0.372	21.358		0.028
De Kee	To	μ	A	MSE
	0.664	46.649	0.000	0.024
Yahya Khayat	To	μ	A	MSE
	0.162	157.126	0.000	0.029
Vom Berg	To	A	B	MSE
	0.664	90.019	0.518	0.024
Proposed	To	a	b	MSE
	0.664	28.294	1.649	0.024

From Appendix Figure A.1 and Table 5.1, it is obvious that for PC 0.3, Herschel-Bulkley and Modified Bingham are showing average mode.

Modified Bingham and Roberstson-Stiff seem to be the best for representing the data while Casson and Yahya and Khayat are least applicable here.

A Robertson-Stiff model seems to be the best suited but the parameters obtained by using these models are not in term of yield stress and viscosity. So these parameters are not well defined physically and since now there is not much research on their physical representation.

Herschel Bulkley is not most suited because it’s To is guessed and is not easily obtained. Here the best value after best analyzing is taken. Normally it is not possible to find out such an accurate value. If the To selected for Herschel Model is not accurate, then whole of the model will be the most inaccurate.

Proposed model also represents the data successfully and better than Bingham Model and due to ease of use, it is better than Herschel Bulkley Model, and due to representing the physical values, it is better than Robertson-Stiff.

Modified Bingham Model and then the model proposed are the best models to describe data efficiently and easily.

Table 5. 2. PC0.3(10), Different Models parameters

Bingham	To	μ		MSE
	0.683081	45.98574		0.056054
Herschel Bulkley	To	A	B	MSE
	0.636179	35.52373	0.920735	0.055998
Robertson-Stiff	A	B	C	MSE
	9.330889	0.923662	30.75023	0.059004
Modified Bingham	To	μ	B	MSE
	0.590799	62.31905	549.854	0.055466
Casson	To	μ		MSE
	0.382948	21.06522		0.056561
De Kee	To	μ	A	MSE
	0.60542	60.16735	8.850339	0.055589
Yahya and Khayat	To	μ	A	MSE
	0.370852	34.19365	19.9163	0.056865
Vom Berg	To	A	B	MSE
	0.62283	1.28572	42.52751	0.055386
Proposed	To	a	B	MSE
	0.59	1.368483	43.08112	0.054846

From Appendix Figure A.2 and Table 5.2, it is obvious that, for PC0.3(10), “Proposed model” is the best fit followed by Vom Berg, Modified Bingham and De Kee. Robertson-Stiff model gives most deviant model

Table 5. 3. PC0.3 (20), Different Models parameters

Bingham	To	μ		MSE
	0.60599	31.67223		0.03758
Herschel Bulkley	To	A	B	MSE
	0.60590	34.35257	1.02024	0.03757
Robertson-Stiff	A	B	C	MSE
	8.87101	0.90898	26.91315	0.03791
Modified Bingham	To	μ	B	MSE
	0.60595	31.67853	(0.20548)	0.03758
Casson	To	μ		MSE
	0.37671	12.55637		0.03854
De Kee	To	μ	A	MSE
	0.62008	29.22907	- (2.68745)	0.03757
Yahya and Khayat	To	μ	A	MSE
	0.50744	5.57537	-(41.64540)	0.03797
Vom Berg	To	A	B	MSE
	0.60498	5.50266	5.78061	0.03758
proposed	To	a	b	MSE
	0.59464	1.77632	18.66363	0.03758

From Appendix Figure A.3 and Table 5.3, it is obvious that, for PC0.3(20) , all of the models are equally applicable except Robertson-Stiff which is most deviant

Table 5. 4 . PC 0.4 Different Models parameters

Bingham	To	μ		MSE
	0.21070	26.81343		0.00310
Herschel Bulkley	To	A	B	MSE
	0.13620	14.81778	0.81512	0.00305
Robertson-Stiff	A	B	C	MSE
	10.75778	0.91549	40.36110	0.00374
Modified Bingham	To	μ	B	MSE
	0.18339	31.42657	158.11	0.00307
Casson	To	μ		MSE
	0.08354	16.53239		0.00305
De Kee	To	μ	A	MSE
	0.18023	32.07966	6.06082	0.00306
Yahya and Khayat	To	μ	A	MSE
	0.07532	40.67876	-(29.81032)	0.00307
Vom Berg	To	A	B	MSE
	0.20995	4.93192	5.45648	0.00310
proposed	To	a	b	MSE
	0.19621	1.21590	23.60771	0.00308

From Appendix Figure A.4 and Table 5.4, it is obvious that, for PC 0.4, all of the models are representing well fit and are applicable. Proposed model also represents the data successfully and better than Bingham Model and due to ease of use, it is better than Herschel Bulkley Model.

Table 5. 5. PC 0.4(10) Different Models parameters

Bingham	To	μ		MSE
	0.742	41.461		0.042
Herschel Bulkley	To	A	B	MSE
	0.920	3.861	0.504	0.076
Robertson-Stiff	A	B	C	MSE
	9.215	0.922	29.781	0.039
Modified Bingham	To	μ	B	MSE
	1.024	- (8.067)	1,682.147	0.037 (-μ)
Casson	To	μ		MSE
	0.453	16.841		0.045
De Kee	To	μ	A	MSE
	0.934	12.021	-(45.264)	0.037
Yahya and Khayat	To	μ	A	MSE
	0.885	0.462	-(126.360)	0.038
Vom Berg	To	A	B	MSE
	0.742	123.776	0.335	0.042
proposed	To	a	b	MSE
	0.742	200.355	0.207	0.042

From Appendix Figure A.5 and Table 5.5, it is obvious that, for PC 0.4 (10), De Kee is the best fit followed by Yahya and Robertson. Proposed model is well suited. Modified Bingham model is failed.

Table 5. 6. PC 0.4(20) Different Models parameters

Bingham	To	μ		MSE
	0.47198	46.63457		0.03419
Herschel Bulkley	To	A	B	MSE
	0.68900	457.92697	1.66146	0.03183
Robertson-Stiff	A	B	C	MSE
	10.23868	0.92907	38.40452	0.03210
Modified Bingham	To	μ	B	MSE
	0.69420	8.18619	1,276.14476	0.03197
Casson	To	μ		MSE
	0.21441	26.24677		0.03655

Table 5.6 (Continued)

De Kee	To	µ	A	MSE
	0.62871	21.83925	-26.45938	0.03205
Yahya and Khayat	To	µ	A	MSE
	0.53997	2.72566	-87.66307	0.03224
Vom Berg	To	A	B	MSE
	0.47196	35.37647	1.31813	0.03419
proposed	To	a	b	MSE
	0.47185	31.60739	1.47553	0.03419

From Appendix Figure A.6 and Table 5.6 , it is obvious that, for PC0.4(20) , Modified Bingham and Herschel Bulkley are best fit and proposed model is well suited.

Table 5. 7. PC0.6, Different Models parameters

Bingham	To	µ		MSE
	0.21070	26.81343		0.00310
Herschel Bulkley	To	A	B	MSE
	0.13620	14.81778	0.81512	0.00305
Robertson-Stiff	A	B	C	MSE
	10.75778	0.91549	40.36110	0.00374
Modified Bingham	To	µ	B	MSE
	0.18339	31.42657	- (158.11000)	0.00307
Casson	To	µ		MSE
	0.08354	16.53239		0.00305
De Kee	To	µ	A	MSE
	0.18023	32.07966	6.06082	0.00306
Yahya and Khayat	To	µ	A	MSE
	0.07532	40.67876	- (29.81032)	0.00307
Vom Berg	To	A	B	MSE
	0.20995	4.93192	5.45648	0.00310
proposed	To	a	b	MSE
	0.19621	1.21590	23.60771	0.00308

From Appendix Figure A.7 and Table 5.7, it is obvious that, for PC0.6 Casson and Herschel Bulkley are the best fits while Proposed model is a well fit.

Table 5. 8. PC0.6 (10), Different Models parameters

Bingham	To	μ		MSE
	0.826	64.832		0.625
Herschel Bulkley	To	A	B	MSE
	0.830	37.652	0.866	0.622
Robertson-Stiff	A	B	C	MSE
	9.422	0.933	31.534	0.646
Modified Bingham	To	μ	B	MSE
	0.037	209.128	-(4,929.130)	0.578
Casson	To	μ		MSE
	0.444	31.520		0.612
De Kee	To	μ	A	MSE
	- (0.143)	274.600	42.707	0.579
Yahya and Khayat	To	μ	A	MSE
	0.005	14,028.950	8.380	0.601
Vom Berg	To	A	B	MSE
	0.066	0.883	266.199	0.593
proposed	To	a	b	MSE
	0.170	2.111	76.249	0.577

From Appendix Figure A.8 and Table 5.8, it is obvious that, for PC0.6(10) ,proposed model is the best fit model ,followed by Modified Bingham and De Kee. Robertson-Stiff, Herschel Bulkley and Bingham are giving deviant results.

Table 5. 9. PC0.6 (20), Different Models parameters

Bingham	To	μ		MSE
	0.337906	16.28494		0.013434
Herschel Bulkley	To	A	B	MSE
	0.2041	4.966121	0.605444	0.012915
Robertson-Stiff	A	B	C	MSE
	8.432034	0.876161	23.36603	0.014096
Modified Bingham	To	μ	B	MSE
	0.2041	38.23089	698.782	0.012434
Casson	To	μ		MSE
	0.21006	6.449938		0.013172
De Kee	To	μ	A	MSE
	0.177861	45.99259	29.89207	0.012448

Table 5.9 (Continued)

Yahya and Khayat	To	µ	A	MSE
	0.05177	11.79332	0.002979	Failed
Vom Berg	To	A	B	MSE
	0.337177	3.689777	4.42553	0.013427
proposed	To	a	b	MSE
	0.232995	0.491283	60.87798	0.012431

From Appendix Figure A.9 and Table 5.9 , it is obvious that, for PC 0.6(20), proposed model is the best fit followed by Modified Bingham and De Kee. Yahya is a failed model for this case.

Table 5. 10. 10FA0.3, Different Models parameters

Bingham	To	µ		MSE
	0.720	34.154		0.006
Herschel Bulkley	To	A	B	MSE
	0.700	26.568	0.932	0.006
Robertson-Stiff	A	B	C	MSE
	10.742	0.914	29.493	0.006
Modified Bingham	To	µ	B	MSE
	0.720	34.154	598,43	0.006
Casson	To	µ		MSE
	0.535	9.213		0.006
De Kee	To	µ	A	MSE
	0.507	122.070	57.774	0.014
Yahya and Khayat	To	µ	A	MSE
	0.068	593.970	41.905	0.010
Vom Berg	To	A	B	MSE
	0.719	5.414	6.322	0.006
proposed	To	a	b	MSE
	0.650	0.616	77.432	0.005

From Appendix Figure A.10 and Table 5.10 , it is obvious that, for 10 FA 0.3 Proposed model is the best suited model. Bingham, Herschel, Modified Bingham and Vom Berg are showing just average results. De Kee and Yahya Model are not well suited.

Table 5. 11. 10FA0.3(10), Different Models parameters

Bingham	To	μ		MSE
	0.838	107.470		0.020
Herschel Bulkley	To	A	B	MSE
	0.590	38.312	0.730	0.019
Robertson-Stiff	A	B	C	MSE
	13.384	0.958	59.942	0.024
Modified Bingham	To	μ	B	MSE
	0.590	184.422	-5,014.553	0.018
Casson	To	μ		MSE
	0.459	50.055		0.023
De Kee	To	μ	A	MSE
	0.559	201.372	38.481	0.018
Yahya and Khayat	To	μ	A	MSE
	0.045	2,140.250	7.780	0.018
Vom Berg	To	A	B	MSE
	0.836	9.021	11.964	0.020
Proposed	To	a	b	MSE
	0.838	33.889	3.172	0.020

From Appendix Figure A.11 and Table 5.11, it is obvious that, for 10FA0.3(10) , Modified Bingham, De Kee and Yahya are best fit and proposed model is acceptable model.

Table 5. 12. 10FA0.3(10) , Different Models parameters

Bingham	To	μ		MSE
	0.597789	17.603651		0.002281
Herschel Bulkley	To	A	B	MSE
	0.757815	62,300.6244	3.343380	0.004525
Robertson-Stiff	A	B	C	MSE
	7.727756	0.867634	17.653006	0.002336
Modified Bingham	To	μ	B	MSE
	0.572052	21.727990	-129.746760	0.002317
Casson	To	μ		MSE
	0.433236	5.081892		0.003603
De Kee	To	μ	A	MSE
	0.598486	17.491917	-0.200399	0.002281
Yahya and Khayat	To	μ	A	MSE
	0.509001	2.581951	30.110687	0.002283
Vom Berg	To	A	B	MSE
	0.597415	4.088786	4.316724	0.002281
Proposed	To	a	b	MSE
	0.597769	17.673664	0.996180	0.002281

From Appendix Figure A.12 and Table 5.12, it is obvious that, for 10 FA0.35, Proposed, Bingham De Kee and Vom Berg are showing the best results. Modified Bingham is not as good for 10FA0.35. Robertson-Stiff and Herschel-Bulkley are not better for representing 10FA0.35

Table 5. 13. 10FA0.35(10) , Different Models parameters

Bingham	To	μ		MSE
	0.80663	14.82517		0.00379
Herschel Bulkley	To	A	B	MSE
	0.77753	10.09062	0.87625	MSE
Robertson-Stiff	A	B	C	MSE
	7.18952	0.83515	12.00314	0.00382
Modified Bingham	To	μ	B	MSE
	0.78305	18.37624	-(107.96693)	0.00380
Casson	To	μ		MSE
	1.17780	-(0.05000)		Failed
De Kee	To	μ	A	MSE
	0.79856	16.05299	2.40287	0.00379
Yahya and Khayat	To	μ	A	MSE
	0.70652	1.75945	- (22.89305)	0.00378
Vom Berg	To	A	B	MSE
	0.80331	1.13209	13.44083	0.00379
Proposed	To	a	b	MSE
	0.80438	1.39396	10.82446	0.00379

From Appendix Figure A.13 and Table 5.13 , it is obvious that, for 10 FA 0.35 (10), Yahya is the best fit model, followed by Proposed, Modified Bingham and other models. Casson is a failed model.

Table 5. 14. 10FA0.35(20) , Different Models parameters

Bingham	To	μ		MSE
	1.030452	18.64477		0.008433
Herschel Bulkley	To	A	B	MSE
	0.975293	10.24601	0.809957	0.008392
Robertson-Stiff	A	B	C	MSE
	7.012071	0.856556	12.23984	0.00856
Modified Bingham	To	μ	B	MSE
	0.955307	31.21599	405.837	0.008437

Table 5.14 (Continued)

Casson	To	μ		MSE
	0.842255	3.614895		0.0108
De Kee	To	μ	A	MSE
	0.993935	24.97139	9.208212	0.008359
Yahya and Khayat	To	μ	A	MSE
	0.879092	2.885952	15.4435	0.008432
Vom Berg	To	A	B	MSE
	1.001185	0.510599	44.42718	0.008348
proposed	To	a	b	MSE
	0.999291	0.611199	37.17879	0.008329

From Appendix Figure A.14 and Table 5.14, it is obvious that, for 10 FA 0.35(20), Proposed model is the best model, followed but Vom Berg and Yahya model.

Table 5. 15. 20FA 0.4, Different Models Parameters

Bingham	To	μ		MSE
	0.139433	6.522990		0.000323
Herschel Bulkley	To	A	B	MSE
	0.121000	3.699612	0.819928	0.000311
Robertson-Stiff	A	B	C	MSE
	8.928877	0.834383	22.315034	0.000350
Modified Bingham	To	μ	B	MSE
	0.120749	9.311614	-(85.754936)	0.000314
Casson	To	μ		MSE
	0.084784	2.639835		0.000302
De Kee	To	μ	A	MSE
	0.112119	10.890065	15.086907	0.000313
Vom Berg	To	A	B	MSE
	0.139333	1.882116	3.471906	0.000322
proposed	To	a	b	MSE
	0.127009	0.220346	36.167387	0.000320

From Appendix Figure A.15 and Table 5.15, it is obvious that, for 20FA0.4, Casson shows the best result. Herschel Bulkley is also showing the best result but its To is guessed. It is not easy to guess it accurately and with ease. So Casson, De Kee, Modified Bingham and Proposed model represents the data successfully. Yahya-Khayat model fails to give any parameter and representing the data.

Table 5. 16. 20FA 0.4 (10), Different Models parameters

Bingham	To	μ		MSE
	0.3314	5.4573		0.0004
Herschel Bulkley	To	A	B	MSE
	0.3775	2,455.7156	2.7534	0.0003
Robertson-Stiff	A	B	C	MSE
	6.6973	0.7416	9.9980	0.0004
Modified Bingham	To	μ	B	MSE
	0.3887	-(2.9655)	253.7253	0.0003(-μ)
Casson	To	μ		MSE
	0.2707	1.0442		0.0009
De Kee	To	μ	A	MSE
	0.3626	1.4401	-(44.4402)	0.0003
Yahya and Khayat	To	μ	A	MSE
	0.0264	181.2749	37.3240	0.0010
Vom Berg	To	A	B	
	0.3313	1.5983	3.4199	0.0004
proposed	To	a	b	MSE
	0.3314	3.2688	1.6702	0.0004

From Appendix Figure A.16 and Table 5.16, it is obvious that, for 20 FA 0.4 (10), De Kee models are followed by proposed and other models.

Table 5. 17. 20FA 0.45, Different Models parameters

Bingham	To	μ		MSE
	0.214	34.776		0.011
Herschel Bulkley	To	A	B	MSE
	0.313	98.540	1.306	0.011
Robertson-Stiff	A	B	C	MSE
	11.198	0.925	44.954	0.011
Modified Bingham	To	μ	B	MSE
	0.279	23.963	369.761	0.011
Casson	To	μ		MSE
	.	16.369		0.225
De Kee	To	μ	A	MSE
	0.270	25.874	-(10.345)	0.011

Table 5.17 (Continued)

Yahya and Khayat	To	µ	A	MSE
	0.135	20.359	-(49.389)	0.011
Vom Berg	To	A	B	MSE
	0.214	- (8.779)	- (3.967)	0.011
proposed	To	a	b	MSE
	0.214	7.369	4.729	0.011

From Appendix Figure A.17 and Table 5.17, it is obvious that, for 20FA 0.45, Modified Bingham and Yahya are the best data describing model. Proposed, Bingham and Vom Berg are also good models. Casson model does not describe data successfully.

Table 5. 18. 20FA 0.45 Different Models parameters

Bingham	To	µ		MSE
	0.358	34.280		0.007
Herschel Bulkley	To	A	B	MSE
	0.592	145,792.480	3.116	0.010
Robertson-Stiff	A	B	C	MSE
	14.157	0.922	42.924	0.007
Modified Bingham	To	µ	B	MSE
	- (0.017)	118.174	- (4,283.914)	0.005(–To)
Casson	To	µ		MSE
	0.192	16.095		0.007
De Kee	To	µ	A	MSE
	0.847	- (469.538)	368.357	0.005(- µ)
Yahya and Khayat	To	µ	A	MSE
	0.009	1,444.455	10.223	0.006
Vom Berg	To	A	B	MSE
	0.357	5.884	5.838	0.007
proposed	To	a	b	MSE
	0.357	4.354	7.896	0.007

From Appendix Figure A.18 and Table 5.18, it is obvious that, for 20FA0.45(10), Yahya-Khayat model and Proposed model are best suited model. Modified Bingham showed negative yield stress and De Kee model showed negative viscosity.

Table 5. 19. 20FA0.45(20), Different Models

Bingham	To	μ		MSE
	0.356433	61.58067		0.05684
Herschel Bulkley	To	A	B	MSE
	0.356	49.25131	0.944646	0.05639
Robertson-Stiff	A	B	C	MSE
	10.50002	0.932748	40.01892	0.070921
Modified Bingham	To	μ	B	MSE
	0.19741	146.8328	2701.93	0.045213
Casson	To	μ		MSE
	0.115737	42.41017		0.055768
De Kee	To	μ	A	MSE
	0.22163	161.3188	27.58855	0.047021
Yahya and Khayat	To	μ	A	MSE
	0.001767	11511.42	20.4472	0.057315
Vom Berg	To	A	B	MSE
	0.07494	1.050743	120.3404	0.048956
proposed	To	a	b	MSE
	1.333382	0.53418	214.7681	0.053351

From Appendix Figure A.19 and Table 5.19, it is obvious that, for 20FA0.45(20), De Kee model followed by Vom Berg and proposed models are the best models. Robertson-Stiff is deviant model.

Table 5. 20. 40FA0.55, Different Models parameters

Bingham	To	μ		MSE
	0.027793	1.463216		1.47E.05
Herschel Bulkley	To	A	B	MSE
	0.0276	58.08437	1.973984	7.79E.05
Robertson-Stiff	A	B	C	MSE
	8.306183	0.770086	21.2262	1.89E.05
Modified Bingham	To	μ	B	MSE
	0.015041	3.354947	56.2501	1.06E.05
Casson	To	μ		MSE
	0.05	59.36014		Failed
De Kee	To	μ	A	MSE
	0.014864	3.598111	24.45004	1.02E.05

Table 5.20 (Continued)

Yahya and Khayat	To	µ	A	MSE
	0.05	17727.44	2.13821	Failed
Vom Berg	To	A	B	MSE
	0.013172	0.024334	156.9582	1.02E.05
proposed	To	a	b	MSE
	0.018452	0.046054	55.77056	1.09E.05

From Appendix Figure A.20 and Table 5.20, it is obvious that, for 40 FA0.55 Casson and Yahya-Khayat model fails completely. De Kee, Vom Berg and then Modified Bingham and Proposed Models are the best to describe data. Bingham, Robertson-Stiff and Herschel Bulkley are not good representative of data.

Table 5. 21. 40FA0.55(10), Different Models parameters

Bingham	To	µ		MSE
	0.063427	2.219432		3.51E.05
Herschel Bulkley	To	A	B	MSE
	0.068269	4.13172	1.189506	3.67E.05
Robertson-Stiff	A	B	C	MSE
	8.212526	0.754432	16.97995	3.78E.05
Modified Bingham	To	µ	B	MSE
	0.065749	1.878388	10.70371	3.62E.05
Casson	To	µ		MSE
	0.042668	0.747645		5.49E.05
De Kee	To	µ	A	MSE
	0.119208	23.8594	194.7709	3.5E.05
Yahya and Khayat	To	µ	A	MSE
	0.00148	238.74	43.38202	Failed
Vom Berg	To	A	B	MSE
	0.06341	0.93199	2.383328	3.51E.05
proposed	To	a	b	MSE
	0.063078	0.205961	10.96374	3.49E.05

From Appendix Figure A.21 and Table 5.21, it is obvious that, for 40 FA 0.55 (10), proposed model is the best model followed by De Kee and Vom Berg models. Yahya-Khayat model is failed.

Table 5. 22. 40FA 0.55(20) Different Models parameters

Bingham	To	μ		MSE
	0.064893	1.743549		2.24E.05
Herschel Bulkley	To	A	B	MSE
	0.07639	34.20612	1.88588	2.6E.05
Robertson-Stiff	A	B	C	MSE
	7.137428	0.706573	13.39038	2.27E.05
Modified Bingham	To	μ	B	MSE
	0.054616	3.247786	44.9787	2.64E.05
Casson	To	μ		MSE
	.0.05	10.74271		Failed
De Kee	To	μ	A	MSE
	0.065277	1.687541	.0.97888	2.23E.05
Yahya and Khayat	To	μ	A	MSE
	0.035165	1.733799	6.355624	2.59E.05
Vom Berg	To	A	B	MSE
	0.064887	1.067274	1.634311	2.24E.05
proposed	To	A	B	MSE
	0.062363	0.065049	31.29025	2.29E.05

From Appendix Figure A.22 and Table 5.22 , it is obvious that, for 40 FA0.55(20), Vom Berg and proposed models are the best fit. Bingham is also showing minimum error. Casson models is failed.

Table 5. 23. 40FA0.8, Different Models parameters

Bingham	To	μ		MSE
	0.023778	0.943137		1.2E.05
Herschel Bulkley	To	A	B	MSE
	0.019085	0.440664	0.74536	1.19E.05
Robertson-Stiff	A	B	C	MSE
	8.122777	0.714822	17.08164	1.26E.05
Modified Bingham	To	μ	B	MSE
	0.004636	3.693028	79.7742	2.36E.05
Casson	To	μ		MSE
	.0.05	8.900707		Failed
De Kee	To	μ	A	MSE
	0.038058	7.771221	567.3011	6.59E.05

Table 5.23 (Continued)

Yahya and Khayat	To	μ	A	MSE
	2.5E.05	631.6975	38.28236	Failed
Vom Berg	To	A	B	MSE
	0.023759	0.260675	3.626167	1.2E.05
Proposed	To	a	b	MSE
	0.014921	0.030938	67.5337	2E.05

From Appendix Figure A.23 and Table 5.23, it is obvious that, for 40FA0.8, Casson and Yahya-Khayat model fails. De Kee is not good. Bingham, Robertson-Stiff and Vom Berg are good models. Proposed model and H bar showing good results.

Table 5. 24. 40FA0.8(10), Different Models parameters

Bingham	To	μ		MSE
	0.039975	1.553429		3.05E.05
Herschel Bulkley	To	A	B	MSE
	0.059726	189030.8	4.448125	6.63E.05
Robertson-Stiff	A	B	C	MSE
	9.774206	0.719128	16.33292	3.36E.05
Modified Bingham	To	μ	B	MSE
	0.051373	0.082267	39.98606	4.01E.05
Casson	To	μ		MSE
	0.00504	0.170478		Failed
De Kee	To	μ	A	MSE
	0.095708	13.6855	121.4336	3.75E.05
Yahya and Khayat	To	μ	A	MSE
	0.02002	1.315706	24.63542	Failed
Vom Berg	To	A	B	MSE
	0.039965	0.904759	1.717922	3.05E.05
proposed	To	a	b	MSE
	0.039771	0.195074	8.063803	3.04E.05

From Appendix Figure A.24 and Table 5.24, it is obvious that, for 40FA0.8(10), Proposed model is the best model followed by Vom Berg and Bingham. Yahya and Casson models are failed. Modified Bingham and Herschel Bulkley are not as good representative models for this case. It is obvious from graphs too

Table 5. 25. 40FA0.8(20), Different Models parameters

Bingham	To	μ		MSE
	0.043769	1.637746		3.7E.05
Herschel Bulkley	To	A	B	MSE
	0.060997	897.6268	2.884676	5.97E.05
Robertson-Stiff	A	B	C	MSE
	7.490408	0.735119	16.36359	4.06E.05
Modified Bingham	To	μ	B	MSE
	0.0282	3.666	55.646	3.17E.05
Casson	To	μ		MSE
	0.05	6.815398		Failed
De Kee	To	μ	A	MSE
	0.021407	4.969328	26.87169	3.08E.05
Yahya and Khayat	To	μ	A	MSE
	0.03738	4.767104	.0.44127	Failed
Vom Berg	To	A	B	MSE
	0.043769	10.49885	0.155994	3.7E.05
proposed	To	a	b	MSE
	0.043682	0.316839	5.195622	3.7E.05

From Appendix Figure A.25 and Table 5.25, it is obvious that, for 40FA0.8(20),De Kee and Modified Bingham models followed by Proposed , Vom Berg and Bingham models are the best suited models. Yahya and Casson models are failed.

Table 5. 26. 10BFS0.4, Different Models parameters

Bingham	To	μ		MSE
	0.8523	72.6616		0.0382
Herschel Bulkley	To	A	B	MSE
	0.9761	157.9820	1.2172	0.0376
Robertson-Stiff	A	B	C	MSE
	10.5980	0.9425	39.6947	0.0381
Modified Bingham	To	μ	B	MSE
	0.9370	54.5398	743.7200	0.0375
Casson	To	μ		MSE
	0.4722	33.6712		0.0434
De Kee	To	μ	A	MSE
	0.8523	72.6616	85.34	0.0382

Table 5.26 (Continued)

Yahya and Khayat	To	μ	A	MSE
	0.1888	274.8616		0.0439
Vom Berg	To	A	B	MSE
	0.8519	21.5746	3.3695	0.0382
Proposed	To	a	b	MSE
	0.8521	19.7373	3.6845	0.0382

From Appendix Figure A.26 and Table 5.26, it is obvious that, for 10 BFS 0.4, Modified Bingham model is the best representing model. Herschel Bulkley also represents data well but it depends on the guessed To value. Vom Berg, Proposed all models are describing data v successfully.

It is obvious from the graph that proposed is very successful model to describe the data.

Table 5. 27. 10BFS 0.40(20), Different Models Parameters

Bingham	To	μ		MSE
	0.7794	65.6155		0.0334
Herschel Bulkley	To	A	B	MSE
	0.9101	128.4419	1.2005	0.0329
Robertson-Stiff	A	B	C	MSE
	10.0345	0.9364	35.5873	0.0337
Modified Bingham	To	μ	B	MSE
	0.8649	50.8797	492.4293	0.0330
Casson	To	μ		MSE
	0.3901	33.9580		0.0364
De Kee	To	μ	A	MSE
	0.8618	51.8271	-(8.0227)	0.0330
Yahya and Khayat	To	μ	A	MSE
	0.5940	18.8624	-(44.6912)	0.0338
Vom Berg	To	A	B	MSE
	0.7793	57.8046	1.1352	0.0334
proposed	To	a	b	MSE
	0.7791	33.8405	1.9398	0.0334

From Appendix Figure A.27 and Table 5.27, it is obvious that, for 10BFS0.4(20), Herschel Bulkley . Modified Bingham, De Kee have least errors. Proposed is suitably fit model.

Table 5. 28. 10BFS 0.5, Different Models Parameters

Bingham	To	μ		MSE
	0.0824	13.7681		0.0007
Herschel Bulkley	To	A	B	MSE
	0.1920	62,300.6200	3.2901	0.0018
Robertson-Stiff	A	B	C	MSE
	11.5009	0.9074	46.1174	0.0010
Modified Bingham	To	μ	B	MSE
	0.0164	26.1515	- (491.7000)	0.0005
Casson	To	μ		MSE
	0.0305	8.8295		0.0006
De Kee	To	μ	A	MSE
	0.0005	30.8185	29.6173	0.0005
Yahya and Khayat	To	μ	A	MSE
	0.0164	48.9614	- (27.7790)	0.0007
Vom Berg	To	A	B	MSE
	0.0823	3.5984	3.8318	0.0007
Proposed	To	a	b	MSE
	0.0824	17.6550	0.7799	0.0007

From Appendix Figure A.28 and Table 5.28, it is obvious that, for 10 S0.5, Modified Bingham and De Kee are the best models followed by Casson and proposed Model. Note: Both Herschel Bulkley and Modified Bingham models are showing opposite behaviour of shear thinning and shear thickening.

Table 5. 29. 10BFS 0.50(10), Different Models Parameters

Bingham	To	μ		MSE
	0.3790	13.9423		0.0043
Herschel Bulkley	To	A	B	MSE
	0.2600	8.8728	0.7937	0.0048
Robertson-Stiff	A	B	C	MSE
	8.1104	0.8579	19.3784	0.0046
Modified Bingham	To	μ	B	MSE
	0.2583	31.4882	- (525.4309)	0.0039
Casson	To	μ		MSE
	0.2479	4.9967		0.0045

Table 5.29 (Continued)

De Kee	To	μ	A	MSE
	0.1997	43.7950	30.2818	0.0038
Yahya and Khayat	To	μ	A	MSE
	0.0555	115.1642	15.2213	0.0038
Vom Berg	To	A	B	MSE
	0.1587	0.2207	251.5378	0.0038
proposed	To	a	b	MSE
	0.2952	0.4331	54.3413	0.0040

From Appendix Figure A.29 and Table 5.29, it is obvious that, for 10S0.5(10), De Kee, Yahya and Vom Berg are giving the best results, followed by Modified Bingham and proposed models.

Table 5. 30. 10BFS 0.50(20), Different Models Parameters

Bingham	To	μ		MSE
	1.017	54.718		0.048
Herschel Bulkley	To	A	B	MSE
	1.353	1,158.155	1.886	0.044
Robertson-Stiff	A	B	C	MSE
	9.098	0.929	27.995	0.046
Modified Bingham	To	μ	B	MSE
	1.351	3.656	1,623.632	0.045
Casson	To	μ		MSE
	0.594	23.411		0.056
De Kee	To	μ	A	MSE
	1.213	26.997	-(23.806)	0.046
Yahya and Khayat	To	μ	A	MSE
	1.090	2.271	- (79.690)	0.046
Vom Berg	To	A	B	MSE
	1.017	37.045	1.478	0.048
proposed	To	a	b	MSE
	1.017	35.912	1.524	0.048

From Appendix Figure A.30 and Table 5.30, it is obvious that, for 10S0.5(20), all models including proposed model shows good fit. But Modified Bingham and Herschel Bulkley show least errors.

Table 5. 31. 30BFS 0.40, Different Models Parameters

Bingham	To	µ		MSE
	0.68301	26.03356		0.00761
Herschel Bulkley	To	A	B	MSE
	0.66896	22.62735	0.95703	0.00761
Robertson-Stiff	A	B	C	MSE
	8.79378	0.89294	21.93103	0.00781
Modified Bingham	To	µ	B	MSE
	0.64827	32.06989	-201.89	0.00766
Casson	To	µ		MSE
	0.46999	8.52747		0.00912
De Kee	To	µ	A	MSE
	0.64417	32.60604	7.68349	0.00769
Yahya and Khayat	To	µ	A	MSE
	0.54920	5.36118	-29.3869	0.00759
Vom Berg	To	A	B	MSE
	0.68223	4.65347	5.61689	0.00761
Proposed	To	a	b	MSE
	0.67913	2.13116	12.46073	0.00761

From Appendix Figure A.31 and Table 5.31, it is obvious that, for 30S0.4, Yahya-Khayat, Proposed, Vom Berg, Herschel Bulkley and Bingham are the best mode. Modified Bingham is not as good in this case. Casson is not well describing model although it is usable too.

Table 5. 32. 30BFS 0.40(10), Different Models Parameters

Bingham	To	μ		MSE
	0.683009	26.033583		0.007609
Herschel Bulkley	To	A	B	MSE
	0.799898	207.561990	1.604650	0.008240
Robertson-Stiff	A	B	C	MSE
	8.354896	0.894823	21.877119	0.007836
Modified Bingham	To	μ	B	MSE
	0.675455	27.470583	-(55.343613)	0.007612
Casson	To	μ		MSE
	- (0.207084)	20.941775		Failed
De Kee	To	μ	A	MSE
	0.675404	27.492104	2.093965	0.007612
Yahya and Khayat	To	μ	A	MSE
	-(0.1553)	182.223440	6.665037	Failed
Vom Berg	To	A	B	MSE
	0.684049	4.566290	5.680045	0.007616
proposed	To	a	b	MSE
	0.678973	1.716465	15.512029	0.007611

From Appendix Figure A.32 and Table 5.32, it is obvious that, for 30S0.4(10), Proposed and Herschel Bulkley models shows the least error, followed by Modified Bingham and De Kee. Casson and Yahya models fail.

Table 5. 33. 30BFS 0.40(20), Different Models Parameters

Bingham	To	μ		MSE
	0.716	41.031		0.034
Herschel Bulkley	To	A	B	MSE
	0.927	822.827	1.852	0.032
Robertson-Stiff	A	B	C	MSE
	9.301	0.922	30.078	0.032
Modified Bingham	To	μ	B	MSE
	0.919	4.666	1,253.166	0.032
Casson	To	μ		MSE
	0.436	16.785		0.038
De Kee	To	μ	A	MSE
	0.848	18.589	-(29.153)	0.033
Yahya and Khayat	To	μ	A	MSE
	0.755	1.650	-(87.497)	0.033

Table 5.33 (Continued)

Vom Berg	To	A	B	MSE
	-1.963	-(0.263)	-(8,611,579.624)	0.065(-ve To)
proposed	To	a	b	MSE
	0.709	8.119	5.117	0.035

From Appendix Figure A.33 and Table 5.33 , it is obvious that, for 30S0.4(20), Herschel Bulkley, Robertson-Stiff and Modified Bingham are showing the best results. Vom Berg model is failed due to negative value. Proposed model is a suitable model.

Table 5. 34. 30BFS 0.45, Different Models Parameters

Bingham	To	μ		MSE
	1.065	40.890		0.510
Herschel Bulkley	To	A	B	MSE
	1.486	145,792.480	3.446	0.564
Robertson-Stiff	A	B	C	MSE
	10.494	0.896	19.939	0.518
Modified Bingham	To	μ	B	MSE
	0.505	132.626	-(2,865.775)	0.488
Casson	To	μ		MSE
	0.713	14.229		0.507
De Kee	To	μ	A	MSE
	2.207	-620.874)	210.565	0.472 (-μ)
Yahya and Khayat	To	μ	A	MSE
	0.325	124.503	12.213	0.504
Vom Berg	To	A	B	MSE
	1.059	6.100	6.745	0.510
proposed	To	a	b	MSE
	0.571	1.492	70.383	0.482

From Appendix Figure A.34 and Table 5.34, it is obvious that, for 30BFS0.45, De Kee shows negative viscosity. Proposed model are the best models to describe the experimental data with the least error. After these 2 models, Modified Bingham is showing better result.

Table 5. 35. 30BFS 0.45 , Different Models Parameters

Bingham	To	μ		MSE
	0.967413	64.93549		0.300117
Herschel Bulkley	To	A	B	MSE
	1.017776	81.33145	1.068379	0.299961
Robertson-Stiff	A	B	C	MSE
	9.238779	0.933092	29.91271	0.309521
Modified Bingham	To	μ	B	MSE
	0.775655	97.52313	1062.97	0.297454
Casson	To	μ		MSE
	0.542999	29.724		0.304167
De Kee	To	μ	A	MSE
	0.844234	86.51515	9.111662	0.298533
Yahya and Khayat	To	μ	A	MSE
	0.51233	50.58677	19.4588	0.307984
Vom Berg	To	A	B	MSE
	0.830488	1.717667	48.02583	0.297313
proposed	To	a	b	MSE
	2.029844	0.77073	220.5919	0.207104

From Appendix Figure A.35 and Table 5.35 , it is obvious that, for 30S 0.45 (10), Proposed model is the best suited model. Other models are not showing good results.

Table 5. 36. 30BFS 0.45(20), Different Models Parameters

Bingham	To	μ		MSE
	0.661039	80.64036		0.24378
Herschel Bulkley	To	A	B	MSE
	0.6	59.61886	0.913832	0.242533
Robertson-Stiff	A	B	C	MSE
	10.42155	0.9406	38.85749	0.264634
Modified Bingham	To	μ	B	MSE
	0.2534	152.24	2419	0.228342
Casson	To	μ		MSE
	0.274959	48.54822		0.241841
De Kee	To	μ	A	MSE
	0.28819	151.1055	20.04848	0.23506

Table 5.36 (Continued)

Yahya and Khayat	To	μ	A	MSE
	0.033266	1432.473	13.193	0.243369
Vom Berg	To	A	B	MSE
	0.412436	1.589643	74.5726	0.235626
proposed	To	a	b	MSE
	0.306339	2.24051	57.84091	0.228944

From Appendix Figure A.36 and Table 5.36 , it is obvious that, for 30BFS0.45(20) , Proposed and Modified Bingham models are the best models. Robertson-Stiff is deviant model.

Table 5.37. 60BFS 0.30, Different Models Parameters

Bingham	To	μ		MSE
	1.082719	47.51444		0.046021
Herschel Bulkley	To	A	B	MSE
	0.756114	13.80649	0.605435	0.044376
Robertson-Stiff	A	B	C	MSE
	8.88952	0.921853	24.9246	0.049298
Modified Bingham	To	μ	B	MSE
	0.946102	77.02031	1037.2	0.043887
Casson	To	μ		MSE
	0.746533	16.03389		0.044443
De Kee	To	μ	A	MSE
	0.942447	79.54722	17.46365	0.04404
Yahya and Khayat	To	μ	A	MSE
	.0.04316	17727.43	35.09296	Failed
Vom Berg	To	A	B	MSE
	0.013346	0.506819	1346.18	0.049478
proposed	To	a	b	MSE
	0.973166	1.301199	51.20778	0.043614

From Appendix Figure A.37 and Table 5.37, it is obvious that, for 60BFS0.3, best suited model is Proposed model. Yahya-Khayat model is failed. Then Modified Bingham, followed by De Kee and Herschel Bulkley are better models.

Table 5. 38. 60BFS 0.4, Different Models Parameters

Bingham	To	μ		MSE
	0.042689	13.88215		0.001512
Herschel Bulkley	To	A	B	MSE
	0.00899	8.302136	0.837883	0.001497
Robertson-Stiff	A	B	C	MSE
	11.39604	0.906854	47.70416	0.001936
Modified Bingham	To	μ	B	MSE
	0.0258	16.681	90.673	0.001494
Casson	To	μ		MSE
	0.00172	6.068761		Failed
De Kee	To	μ	A	MSE
	0.025423	16.81831	6.127437	0.001495
Yahya and Khayat	To	μ	A	MSE
	0.010241	47.85711	43.0664	0.001576
Vom Berg	To	A	B	MSE
	0.042444	3.499698	3.975361	0.001512
proposed	To	a	b	MSE
	0.029959	0.548497	28.27748	0.001493

From Appendix Figure A.38 and Table 5.38, it is obvious that, for 60 S0.4, again the best suited model is proposed model with the least error, followed by Modified Bingham, De Kee then Herschel Bulkley. Casson model is failed completely.

Table 5. 39. 60BFS0.40(10), Different Models Parameters

Bingham	To	μ		MSE
	0.211	43.972		0.031
Herschel Bulkley	To	A	B	MSE
	0.200	34.995	0.941	0.031
Robertson-Stiff	A	B	C	MSE
	13.593	0.927	47.311	0.035
Modified Bingham	To	μ	B	MSE
	0.041	73.753	-1050.064	0.030
Casson	To	μ		MSE
	- (0.185)	56.339		Failed
De Kee	To	μ	A	MSE
	-0.011	86.311	22.386	0.029
Yahya and Khayat	To	μ	A	MSE
	-0.165	238.754	43.328	Failed

Table 5.39 (Continued)

Vom Berg	To	A	B	MSE
	0.209	6.227	7.096	0.031
proposed	To	a	b	MSE
	0.209	6.022	7.337	0.031

From Appendix Figure A.39 and Table 5.39, it is obvious that, for 60 S0.4 (10), Casson and Yahya-Khayat model is failed. De Kee is showing negative value, hence is failed. Proposed model is well fit.

Table 5. 40. 60BFS0.40(20), Different Models Parameters

Bingham	To	μ		MSE
	0.606144	84.74879		0.164658
Herschel Bulkley	To	A	B	MSE
	0.230558	34.22193	0.717039	0.162697
Robertson-Stiff	A	B	C	MSE
	11.23928	0.943118	43.08682	0.180958
Modified Bingham	To	μ	B	MSE
	0.370462	129.1507	1587.44	0.160541
Casson	To	μ		MSE
	0.242001	52.48303		0.163183
De Kee	To	μ	A	MSE
	0.375228	130.5945	14.93148	0.160989
Yahya and Khayat	To	μ	A	MSE
	0.020802	2180.686	17.2205	0.164063
Vom Berg	To	A	B	MSE
	0.430828	1.773012	63.61539	0.160849
Proposed	To	A	B	MSE
	0.410132	2.308896	49.23265	0.15941

From Appendix Figure A.40 and Table 5.40, it is obvious that, for 60BFS0.4 (20), Proposed model is the best fit. Modified Bingham and other models are suitable too.

Table 5. 41. 60BFS0.5, Different Models Parameters

Bingham	To	µ		MSE
	0.2041	108.1794		0.0256
Herschel Bulkley	To	A	B	MSE
	0.3074	897.6272	1.4575	0.0210
Robertson-Stiff	A	B	C	MSE
	24.7868	0.9723	156.1501	0.0211
Modified Bingham	To	µ	B	MSE
	0.2188	98.5493	1045.54	0.0229
Casson	To	µ		MSE
	0.0702	73.2661		0.0256
De Kee	To	µ	A	MSE
	0.3019	49.7455	- (87.7442)	0.0210
Yahya and Khayat	To	µ	A	MSE
	0.2406	10.1550	281.67	0.0213
Vom Berg	To	A	B	MSE
	0.2040	31.1970	3.4687	0.0235
proposed	To	a	b	MSE
	0.2043	33.4057	3.2377	0.0235

From Appendix Figure A.41 and Table 5.41, it is obvious that, for 60 BFS 0.5, De Kee, Herschel Bulkley, Robertson-Stiff and Yahya are showing best results.

By looking at graph, proposed model is also approximating the averages. Casson though comparatively less accurate is also applicable.

Table 5. 42. 60BFS0.50(10), Different Models Parameters

Bingham	To	µ		MSE
	0.188612	180.0851		0.189787
Herschel Bulkley	To	A	B	MSE
	1.088936	189030.8	2.838902	0.503748
Robertson-Stiff	A	B	C	MSE
	22.9109	0.956216	75.02795	0.319797
Modified Bingham	To	µ	B	MSE
	0.151	201.48	4498.3	0.315021
Casson	To	µ		MSE
	0.027617	156.1533		0.190577
De Kee	To	µ	A	MSE
	0.147299	205.9687	30.10296	0.123473

Table 5.42 (Continued)

Yahya and Khayat	To	μ	A	MSE
	0.03347	3513.375	52.0655	Failed
Vom Berg	To	A	B	MSE
	0.083933	3.549407	58.29134	0.181314
proposed	To	a	b	MSE
	0.044966	3.881272	55.32936	0.176251

From Appendix Figure A.42 and Table 5.42, it is obvious that, for 60BFS 0.50(10**),** De Kee and proposed are the best fit models. Modified Bingham is showing large error. Yahya gave negative reading so it fails

Table 5. 43. 5SF0.4 Different Models Parameters

Bingham	To	μ		MSE
	0.4820	25.6293		0.0059
Herschel Bulkley	To	A	B	MSE
	0.4820	19.6522	0.9361	0.0058
Robertson-Stiff	A	B	C	MSE
	9.0245	0.9008	26.8628	0.0070
Modified Bingham	To	μ	B	MSE
	0.4820	25.6293	.	0.0059
Casson	To	μ		MSE
	0.3015	9.9874		0.0052
De Kee	To	μ	A	MSE
	0.2935	64.6535	31.1695	0.0046
Yahya and Khayat	To	μ	A	MSE
	0.0132	1,298.3327	18.9425	0.0047
Vom Berg	To	A	B	MSE
	0.2819	0.3413	193.3837	0.0047
proposed	To	a	b	MSE
	0.3559	0.6576	66.7839	0.0044

From Appendix Figure A.43 and Table 5.43, it is obvious that, 5SF0.4 is best described by the proposed model. Then Vom Berg and Yahya models are better models. Modified Bingham, Bingham and Herschel Bulkley models are not comparatively good. Models are showing pseudoplastic (Shear thinning) behaviour of 5SF0.5.

Table 5. 44. 5SF0.4(10)Different Models Parameters

Bingham	To	μ		MSE
	0.6922	29.5534		0.0227
Herschel Bulkley	To	A	B	MSE
	0.8316	298.9100	1.6703	0.0216
Robertson-Stiff	A	B	C	MSE
	8.5748	0.9045	24.3042	0.0220
Modified Bingham	To	μ	B	MSE
	0.8230	7.1097	741.8900	0.0217
Casson	To	μ		MSE
	0.4628	10.2870		0.0251
De Kee	To	μ	A	MSE
	0.7902	14.0943	-(25.6910)	0.0218
Yahya and Khayat	To	μ	A	MSE
	0.7109	1.1033	-(78.2744)	0.0220
Vom Berg	To	A	B	MSE
	0.6912	5.6891	5.2078	0.0227
proposed	To	a	b	MSE
	0.6922	33.8089	0.8742	0.0227

From Appendix Figure A.44 and Table 5.44 , it is obvious that, for 5SF0.4(10), Modified Bingham, De Kee n Yahya are best fit but proposed model is also shows good fit and highly acceptable. Casson is showing most deviant result.

Table 5. 45 . 5SF0.4(20)Different Models Parameters

Bingham	To	μ		MSE
	0.220	19.921		0.037
Herschel Bulkley	To	A	B	MSE
	0.394	62,300.624	3.299	0.039
Robertson-Stiff	A	B	C	MSE
	9.805	0.902	34.502	0.036
Modified Bingham	To	μ	B	MSE
	0.289	8.510	361.864	0.036
Casson	To	μ		MSE
	0.102	11.032		0.037
De Kee	To	μ	A	MSE
	0.264	12.990	-(14.012)	0.036

Table 5.45 (Continued)

Yahya and Khayat	To	μ	A	MSE
	0.219	2.275	- (65.263)	0.037
Vom Berg	To	A	B	MSE
	0.219	4.367	4.575	0.037
proposed	To	a	b	MSE
	0.220	17.681	1.127	0.037

From Appendix Figure A.45 and Table 5.45, it is obvious that, for 5SF0.4(20), Modified Bingham, De Kee and Robertson-Stiff are giving best fit. Proposed is highly acceptable.

5SF 0.5 is a special case in which most of the models are giving negative values Herschel Bulkley, Modified Bingham, De Kee all gives negative values.

Table 5. 46. 5SF0.5 Different Models Parameters

Bingham	To	μ		MSE
	0.228139	74.82824		0.05257
Herschel Bulkley	To	A	B	MSE
	.0.26063	22.68995	0.624048	0.048379
Robertson-Stiff	A	B	C	MSE
	11.55961	0.941848	50.54032	0.077736
Modified Bingham	To	μ	B	MSE
	0.0774	133.1657	2124.68	0.043795
Casson	To	μ		MSE
	0.056963	57.44082		0.051156
De Kee	To	μ	A	MSE
	0.06194	134.4911	20.39495	0.045203
Yahya and Khayat	To	μ	A	MSE
	0.001377	13118.66	32.9258	0.055408
Vom Berg	To	A	B	MSE
	0.017765	1.35797	80.95412	0.045849
proposed	To	A	b	MSE
	0	1.927316	56.93589	0.041545

From Appendix Figure A.46 and Table 5.46, it is obvious that, for 5SF0.5, proposed model has least error.

Table 5. 47. 5SF0.5(10) Different Models Parameters

Bingham	To	μ		MSE
	0.550899	32.34214		0.090188
Herschel Bulkley	To	A	B	MSE
	0.327758	10.45682	0.633973	0.089347
Robertson-Stiff	A	B	C	MSE
	8.912425	0.908094	27.23554	0.093363
Modified Bingham	To	μ	B	MSE
	0.327422	72.40925	1361.86	0.08651
Casson	To	μ		MSE
	0.331152	13.54387		0.08933
De Kee	To	μ	A	MSE
	0.365626	68.43585	23.71869	0.087656
Yahya and Khayat	To	μ	A	MSE
	0.127523	123.1663	4.245506	0.089435
Vom Berg	To	A	B	MSE
	0.446729	0.628451	77.12097	0.088125
proposed	To	a	b	MSE
	0.351988	0.927679	65.19149	0.085004

From Appendix Figure A.47 and Table 5.47, it is obvious that, for 5SF0.5(10), Proposed model is the best fit, followed by Modified Bingham which is average fit only.

Table 5. 48. 5SF0.6 Different Models Parameters

Bingham	To	μ		MSE
	0.257	110.460		0.089
Herschel Bulkley	To	A	B	MSE
	0.372	213.632	1.178	0.088
Robertson-Stiff	A	B	C	MSE
	15.206	0.956	74.801	0.091
Modified Bingham	To	μ	B	MSE
	0.362	78.006	1462.08	0.087
Casson	To	μ		MSE
	-(0.099)	57.662		Failed
De Kee	To	μ	A	MSE
	0.377	74.897	- (17.676)	0.086

Table 5.48 (Continued)

Yahya and Khayat	To	µ	A	MSE
	0.178	71.762	- (82.955)	0.084
Vom Berg	To	A	B	MSE
	0.256	22.308	4.954	0.089
proposed	To	a	b	MSE
	0.257	348.793	0.317	0.089

From Appendix Figure A.48 and Table 5.48, it is obvious that, for 5SF.6, Yahya-Khayat, De Kee and Modified Bingham give the best results. All models are applicable but Casson model fails completely.

Table 5. 49. 5SF0.6(10) , Different Models Parameters

Bingham	To	µ		MSE
	0.257201	110.46		0.089143
Herschel Bulkley	To	A	B	MSE
	0.372385	213.8322	1.178431	0.087839
Robertson-Stiff	A	B	C	MSE
	14.07694	0.957131	74.89074	0.090796
Modified Bingham	To	µ	B	MSE
	0.3615	78.006	1462.1	0.086524
Casson	To	µ		MSE
	0.062936	86.22877		0.091853
De Kee	To	µ	A	MSE
	0.376926	74.88587	17.682	0.08598
Yahya and Khayat	To	µ	A	MSE
	0.001355	17727.44	58.8124	0.085652
Vom Berg	To	A	B	MSE
	0.256282	35.531	3.110802	0.089172
proposed	To	a	b	MSE
	0.257083	39.82442	2.773295	0.089166

From Appendix Figure A.49 and Table 5.49, it is obvious that, for 5SF0.6(10),Best result is given by Yahya-Khayat and De Kee then Modified Bingham. Proposed model is giving good acceptable result.

Table 5. 50. 10SF0.4, Different Models Parameters

Bingham	To	μ		MSE
	0.679	58.437		0.014
Herschel Bulkley	To	A	B	MSE
	0.796	132.747	1.231	0.014
Robertson-Stiff	A	B	C	MSE
	12.372	0.934	39.550	0.014
Modified Bingham	To	μ	B	MSE
	0.769	41.625	693.787	0.014
Casson	To	μ		MSE
	0.357	28.172		0.015
De Kee	To	μ	A	MSE
	0.766	42.818	(13.158)	0.014
Yahya and Khayat	To	μ	A	MSE
	- (0.008)	1883.19	48.706	Failed
Vom Berg	To	A	B	MSE
	0.677	7.738	7.587	0.014
proposed	To	a	b	MSE
	0.676	7.151	8.211	0.014

From Appendix Figure A.50 and Table 5.50, it is obvious that, for 10SF0.4, all of the models are applicable except Yahya model, which fails to describe data.

Table 5. 51. 10SF0.4(20), Different Models Parameters

Bingham	To	μ		MSE
	0.6988	56.5539		0.0130
Herschel Bulkley	To	A	B	MSE
	0.6381	46.2622	0.9337	0.0141
Robertson-Stiff	A	B	C	MSE
	8.7406	0.9208	25.7865	0.0286
Modified Bingham	To	μ	B	MSE
	0.6787	58.4249	0.5340	0.0140
Casson	To	μ		MSE
	0.3554	28.2874		0.0206
De Kee	To	μ	A	MSE
	0.7663	42.8162	-(13.1595)	0.0138
Yahya and Khayat	To	μ	A	MSE
	0.5854	10.3396	- (62.1563)	0.0137
Vom Berg	To	A	B	MSE
	- (5.4496)	- (0.5605)	- (8,611,579)	failed
proposed	To	a	b	MSE
	0.6782	8.8868	6.5890	0.0140

From Appendix Figure A.51 and Table 5.51, it is obvious that, for 10SF0.4(20), Bingham , Yahya , De Kee are best fit. Vom Berg shows negative value of yield stress and is failed. Proposed and Modified Bingham are good fit. Robertson-Stiff is deviant.

Table 5. 52. 10SF0.45, Different Models Parameters

Bingham	To	μ		MSE
	0.5414	18.3269		0.0151
Herschel Bulkley	To	A	B	MSE
	0 .7566	145,792.4798	3.6289	0.0176
Robertson-Stiff	A	B	C	MSE
	0.0573	0.8552	18.1108	0.0153
Modified Bingham	To	μ	B	MSE
	4154	34.3579	-445.243	0.0149
Casson	To	μ		MSE
	0.3512	6.5978		.0161
De Kee	To	μ	A	MSE
	1.0659	-187.6537	166.5996	0.0151
Yahya and Khayat	To	μ	A	MSE
	2882	15.3146	-4.9225	0.0149
Vom Berg	To	A	B	MSE
	0.5407	4.2215	4.3564	0.0151
proposed	To	a	b	MSE
	5392	2.4788	7.4628	0.0150

From Appendix Figure A.52 and Table 5.52, it is obvious that, for 10SF 0.45, Modified Bingham and Yahya-Khayat model followed but proposed mode are the best fit models. Casson and Herschel Bulkley models are deviant one.

Table 5. 53. 10SF0.45(10), Different Models Parameters

Bingham	To	μ		MSE
	0.802682	24.86565		0.011099
Herschel Bulkley	To	A	B	MSE
	0.951991	296.4175	1.736588	0.009367
Robertson-Stiff	A	B	C	MSE
	7.921932	0.8891	19.01567	0.010271
Modified Bingham	To	μ	B	MSE
	1.135851	.21.0978	1357.571	0.008525
Casson	To	μ		MSE
	0.558779	7.796384		0.012461
De Kee	To	μ	A	MSE
	0.986114	4.144775	59.864	0.00901

Table 5.53 (Continued)

Yahya and Khayat	To	μ	A	MSE
	0.9659	0.051717	153.637	0.009061
Vom Berg	To	A	B	MSE
	0.802426	15.09184	1.648609	0.011101
proposed	To	a	b	MSE
	1.306211	0.25868	152.1787	0.008156

From Appendix Figure A.53 and Table 5.53, it is obvious that, for 10SF0.45(10) , Proposed model is the best fit followed by Modified Bingham, De Kee and Herschel Bulkley model.

Table 5. 54. 10SF0.45(20),Different Models Parameters

Bingham	To	μ		MSE
	0.2199	19.9209		0.0366
Herschel Bulkley	To	A	B	MSE
	0.2890	82.6671	1.4190	0.0361
Robertson-Stiff	A	B	C	MSE
	9.8068	0.9023	34.5178	0.0364
Modified Bingham	To	μ	B	MSE
	0.2894	8.5103	361.8633	0.0363
Casson	To	μ		MSE
	0.1035	10.8972		0.0371
De Kee	To	μ	A	MSE
	0.2641	12.9971	- (13.9969)	0.0364
Yahya and Khayat	To	μ	A	MSE
	-(0.0518)	11.7934	0.0029	Failed
Vom Berg	To	A	B	MSE
	0.2195	4.2685	4.6806	0.0366
proposed	To	a	b	MSE
	0.2148	1.1100	18.5960	0.0366

From Appendix Figure A.54 and Table 5.54, it is obvious that, for 10SF0.45(20), Modified Bingham, Robertson-Stiff and De Kee are the best fit, while proposed model is well acceptable. Yahya-Khayat model fails.

Table 5. 55. 15SF0.4, Different Models Parameters

Bingham	To	μ		MSE
	0.93600	39.81651		0.00582
Herschel Bulkley	To	A	B	MSE
	0.91256	33.36553	0.94801	0.00581
Robertson-Stiff	A	B	C	MSE
	9.30704	0.91554	25.20298	0.00623
Modified Bingham	To	μ	B	MSE
	0.91992	42.88175	-118.46	0.00581
Casson	To	μ		MSE
	0.64653	12.80975		0.01042
De Kee	To	μ	A	MSE
	0.92014	42.86791	2.83766	0.00581
Yahya and Khayat	To	μ	A	MSE
	0.74430	8.65814	-31.46	0.00586
Vom Berg	To	A	B	MSE
	0.93484	6.02953	6.63144	0.00582
proposed	To	a	b	MSE
	0.92117	1.78996	23.45361	0.00580

From Appendix Figure A.55 and Table 5.55, it is obvious that, for 15SF0.4, Best suited model is the Casson and then the proposed model. All models are qualifying for this case.

Table 5. 56. 15SF0.4(10),Different Models Parameters

Bingham	To	μ		MSE
	1.1213	32.9788		0.0199
Herschel Bulkley	To	A	B	MSE
	1.2494	151.8702	1.4510	0.0193
Robertson-Stiff	A	B	C	MSE
	7.8870	0.9035	18.7561	0.0195
Modified Bingham	To	μ	B	MSE
	1.2247	16.1761	544.6483	0.0194
Casson	To	μ		MSE
	0.8339	8.8721		0.0225
De Kee	To	μ	A	MSE
	1.2080	19.7319	- (17.2851)	0.0194

Table 5.56 (Continued)

Yahya and Khayat	To	μ	A	MSE
	1.1579	0.8030	- (78.4500)	0.0198
Vom Berg	To	A	B	MSE
	1.1212	22.3152	1.4782	0.0199
proposed	To	A	B	MSE
	1.1215	19.3649	1.7027	0.0199

From Appendix Figure A.56 and Table 5.56, it is obvious that, for 15SF0.4(10),Herschel Bulkley, Modified Bingham and De Kee are best fit. Proposed is an average acceptable model

Table 5. 57. .15SF0.4(20),Different Models Parameters

Bingham	To	μ		MSE
	0.9413	68.6880		0.0645
Herschel Bulkley	To	A	B	MSE
	1.1536	454.2815	1.5105	0.0586
Robertson-Stiff	A	B	C	MSE
	10.8676	0.9403	37.6429	0.0612
Modified Bingham	To	μ	B	MSE
	1.1570	23.4621	1,907.4482	0.0600
Casson	To	μ		MSE
	0.6559	23.0067		0.0870
De Kee	To	μ	A	MSE
	1.0952	38.8150	- (24.9445)	0.0610
Yahya and Khayat	To	μ	A	MSE
	0.5394	-(7.7849)	-(77.6753)	Failed
Vom Berg	To	A	B	MSE
	0.9417	16.2336	4.2314	0.0645
proposed	To	a	b	MSE
	0.9403	18.3318	3.7534	0.0645

From Appendix Figure A.57 and Table 5.57 , it is obvious that, for 15SF0.4(20),Modified Bingham, De Kee and Robertson-Stiff are the best suited model. Proposed model is good acceptable model. Yahya-Khayat model fails.

Table 5. 58. 15SF0.45, Different Models Parameters

Bingham	To	μ		MSE
	0.222922	11.22157		0.001084
Herschel Bulkley	To	A	B	MSE
	0.356029	189030.8	3.808256	0.001786
Robertson-Stiff	A	B	C	MSE
	10.20268	0.852593	23.02041	0.001144
Modified Bingham	To	μ	B	MSE
	0.181463	16.6101	154.651	0.00106
Casson	To	μ		MSE
	0.433666	0.05		Failed
De Kee	To	μ	A	MSE
	0.538366	10.245	165.4342	0.001135
Yahya and Khayat	To	μ	A	MSE
	0.086718	16.2521	7.83716	0.001051
Vom Berg	To	A	B	MSE
	0.222681	3.183094	3.532712	0.001084
proposed	To	a	b	MSE
	0.221654	1.391031	8.156409	0.001082

From Appendix Figure A.58 and Table 5.58, it is obvious that, for 15 SF 0.45, Yahya-Khayat, Modified Bingham and proposed models are most suited. Bingham does not show thixotropic character so can be excluded from the best list. So Yahya-Khayat, Modified Bingham and then the proposed model are the best.

Casson Model fails completely.

Table 5. 59 15SF0.45(10), Different Models Parameters

Bingham	To	μ		MSE
	0.457783	30.15881		0.014556
Herschel Bulkley	To	A	B	MSE
	0.661689	897.6271	1.997895	0.016173
Robertson-Stiff	A	B	C	MSE
	9.270061	0.907586	29.10102	0.015086
Modified Bingham	To	μ	B	MSE
	0.450121	31.3264	35.9501	0.014554
Casson	To	μ		MSE
	0.242183	14.63561		0.014807

Table 5.59 (Continued)

De Kee	To	μ	A	MSE
	0.451238	31.16012	1.002896	0.014554
Yahya and Khayat	To	μ	A	MSE
	0.253334	20.33327	22.7598	0.014736
Vom Berg	To	A	B	MSE
	0.457484	10.95846	2.755254	0.014555
proposed	To	a	b	MSE
	0.437086	1.432522	22.75359	0.014521

From Appendix Figure A.60 and Table 5.60, it is obvious that, for 15SF0.45(10), Proposed model is the best fit model, followed by Modified Bingham , De Kee and Vom Berg Models.

Table 5. 60. 15SF0.45(20), Different Models Parameters

Bingham	To	μ		MSE
	1.0087	50.4580		0.0611
Herschel Bulkley	To	A	B	MSE
	1.3025	829.6986	1.8148	0.0591
Robertson-Stiff	A	B	C	MSE
	8.9287	0.9259	26.8849	0.0596
Modified Bingham	To	μ	B	MSE
	1.2860	7.4370	1,374.8629	0.0591
Casson	To	μ		MSE
	0.6064	20.7345		0.0632
De Kee	To	μ	A	MSE
	1.2279	19.8860	-(31.8741)	0.0591
Yahya and Khayat	To	μ	A	MSE
	1.1347	1.1445	-(96.0462)	0.0592
Vom Berg	To	A	B	MSE
	1.0086	34.1228	1.4791	0.0611
proposed	To	a	b	MSE
	1.0088	32.8866	1.5340	0.0611

From Appendix Figure A.60 and Table 5.60, it is obvious that, for 15SF0.45(20), Modified Bingham , Herschel Bulkley and Robertson-Stiff are the best fit models while Proposed model is average and acceptable.

5. 5 Discussions

Different models are being developed to represent cement based material rheological data. Till now Bingham models is the most commonly used model. It has some discrepancies. As graph obtained by cement based material may not necessarily be linear and Bingham model is linear one, so it is not the best suited model.

Recently Herschel Bulkley model is used in new applications. It has an advantage over Bingham model, this graph is not linear and most of the people believe that it defines the shear thinning or shear thickening behavior of mortar.

While interpreting graphs, Modified Bingham model seems to be most suited in majority of cases but it shows negative values of yield stress and viscosities in a few mix. So far it is not being much used for cement based material. The Modified Bingham model is also associated with Herschel Bulkley by using ratio of coefficients. Hence it also defines shear thinning and shear thickening behavior of cement based mix.

An important observation is that “not all of the time, Herschel Bulkley Model and Modified Bingham Model show the same results about shear thinning and shear thickening behaviour of mix. Hence Herschel Bulkley model is not very reliable for deciding whether material is shear thinning or shear thickening and more research is needed to prove it.”

The Proposed model is proved to be a very good model, more accurate than Bingham, more easily used than Herschel Bulkley and one of the best models to represent admixture mixed mortars. It never fails, never shows negative results, never have larger errors and easily fit up to 20 minutes after mixing.

5.6 Observations

The observations made related with the suitability of the models studied in this investigation are given below.

5.6.1 Observations for PC

5.6.1.1 Rheology of PC Right After Mixing

For plain PC with no mineral admixture, “Proposed model” is a much suitable for use in simple PC. Modified Bingham is good model but it sometimes shows negative viscosity. Casson is suitable for high w/c. Robertson-Stiff is good fit for low w/c and not good for high w/c. Bingham being linear, and Herschel Bulkley for inaccurate To are not one of the best models. Robertson-Stiff, if shows the good result, is not good for use because it does not show any To.

- For PC 0.3, Herschel Bulkley and Modified Bingham are showing average graph lines.

  Modified Bingham and Roberstson-Stiff seem to be the best for representing the data while Casson and Yahya-Khayat are least applicable here.

  Robertson-Stiff model seems to be the best suited but the parameter obtained by using the model is not in the terms of yield stress and viscosity. So these parameters are not well defined physically and since now there is not much research on their physical representation.

  Herschel Bulkley is not most suited because it’s To is guessed and is not easily obtained. Here the best value after best analyzing is taken. Normally it is not possible to find out such an accurate value. If the To selected for Herschel Bulkley Model is not accurate, then whole of the model will be the most inaccurate.

  “Proposed model” also represents the data successfully and better than Bingham Model and due to ease of use, it is better than Herschel Bulkley

Model , and due to representing the physical values , it is better than Robertson-stiff.

The “Proposed model” is the best models to describe data efficiently and easily.

- For PC 0.4, all of the models are representing data and are applicable. “Proposed model” also represents the data successfully and better than Bingham Model and due to ease of use, it is better than Herschel Bulkley Model.
- For PC 0.6, Casson, De Kee, Yahya and “Proposed model” are the top representing models for the data. Robertson-Stiff is the least suited.

Proposed model” is suitable for all cases including plain PC and admixture containing mortars. It is never failed in any case. It proved to be the best describing model in some cases. So it is a reliable model.

Modified Bingham model is also suitable but could not give good data description for a few cases.

Casson and Yahya-Khayat model have failed many times. Robertson-Stiff model does not show yield stress value. Bingham is linear so deficient one. Herschel Bulkley is not much reliable due to guessed value of yield stress. Vom Berg Model is just average. De Kee Model is a successful model for some of the mineral admixture incorporated models cases only.

5.6.1.2. Rheology of PC at 10 minutes

“Proposed model” is the best fit model at 10 minutes for PC 0.3 and PC 0.6. Modified Bingham and De Kee are good fits. Robertson-Stiff model is not fit at 10 minutes for simple PC.

- For PC0.3(10), “Proposed model” is the best fit followed by Vom Berg, Modified Bingham and De Kee. Robertson-Stiff model gives most deviant model.

- For PC 0.4 (10), Modified Bingham showed negative viscosity. De Kee is the best fit followed by Yahya and Robertson. Proposed model is well suited.
- For PC0.6(10) , “Proposed model” is the best fit model , followed by Modified Bingham and De Kee. Robertson-Stiff, Herschel Bulkley and Bingham are giving deviant results.

5.6.1.3. Rheology of PC at 20 minutes

“Proposed model” is suitable model at 20 minutes for simple PC. Robertson-Stiff and Yahya models should not be used at 20 minutes because they may fail.

- For PC0.3(20) , all of the models are equally applicable except Robertson-Stiff which is most deviant.
- For PC0.4(20) , Modified Bingham and Herschel Bulkley are best fit and proposed model is well suited.
- For PC 0.6(20), “Proposed model” is the best fit followed by Modified Bingham and De Kee. Yahya is a failed model for this case.

5.6.2 Observation for BFS

For BFS “Proposed model” is a very suitable and among one of the best models. It best describes 60BFS0.3, 60BFS0.4, 30BFS0.4, 30 BFS0.45. In all cases of BFS, it is a suitable model and is very successfully describing the data.

Modified Bingham model is a good approximate model but for 30BFS0.4, it does not show good result.

De Kee is also a good model for describing BFS mortars. Bingham model due to its linearity and Herschel Bulkley model due to its error-able To value are not good models.

- For 10 BFS 0.4, Modified Bingham model is the best representing model. Herschel Bulkley also represents data well but it depends on the guessed To value. Vom Berg, “Proposed model” and all the models are describing data successfully.

“Proposed model” is a very successful model to describe the data.

- For 10 BFS0.5, Modified Bingham and De Kee are the best models followed by Casson and proposed model.

Note: Both Herschel Bulkley and Modified Bingham are showing different results in terms of shear thinning and shear thickening.

- For 30BFS0.4, Yahya , “Proposed model” Vom Berg, Herschel Bulkley and Bingham are the best models. Modified Bingham is not as good in this case. Casson is not much suitable model.
- For 30BFS0.45, De Kee and “Proposed model” are the best models to describe the experimental data with the least error. After these 2 models, Modified Bingham is showing better result.
- For 60BFS0.3, Best suited model is “Proposed model” .Yahya-Khayat model is failed. Then Modified Bingham , followed by De Kee and Herschel Bulkley are good models.
- For 60 BFS0.4, Again the best suited model is “Proposed model” with the least error , followed by Modified Bingham, De Kee then Herschel Bulkley. Casson model is failed completely. De Kee, Herschel Bulkley, Robertson-Stiff and Yahya are showing best results. By looking at graph, “Proposed model” is also approximating the averages. Casson though comparatively less accurate is also applicable.
- For 60 BFS 0.5, De Kee, Herschel Bulkley, Robertson-Stiff and Yahya are showing best results. By looking at graph, “Proposed model” is also approximating the averages. Casson though comparatively less accurate is also applicable.

5.6.2.1. Rheology of BFS at 10 minutes

For 30BFS0.4(10) , 30BFS 0.45 (10)and 60BFS 0.50(10**)** "**Proposed model"** is the best fit model. It is suitable for all cases at 10 minute rheological interpretation in all cases. Casson and Yahya-Khayat model fails. De Kee is showing good results at 10 minutes for Slag.

- For 10BFS0.5(10), De Kee , Yahya and Vom Berg are giving the best results , followed by Modified Bingham and proposed models.
- For 30BFS0.4(10), Proposed and Herschel Bulkley models shows the least error , followed by Modified Bingham and De Kee. Casson And Yahya models fail.
- For 30BFS 0.45 (10), Proposed model is the best suited model. Other models are not showing good results.
- For 60 BFS0.4 (10), Casson and Yahya-Khayat model is failed. De Kee is the best fit. Proposed model is well fit.
- For 60BFS 0.50(10**),** De Kee and proposed are the best fit models. Modified Bingham is showing large error. Yahya gave negative reading so it fails.

5.6.2.3 Rheology of BFS at 20 minute

For 30BFS0.45(20) and 60BFS0.4 (20) **"Proposed model"** is the best fit model. It is suitable for all cases at 20 minute rheological interpretation in all cases. Modified Bingham is showing good results in all cases.

- For 10BFS0.4(20), Herschel Bulkley . Modified Bingham, De Kee have least errors. Proposed is suitably fit model.
- For 10BFS0.5(20), all models including proposed model shows good fit. But Modified Bingham and Herschel Bulkley shows least errors.
- For 30BFS0.4(20), Herschel Bulkley, Robertson-Stiff and Modified Bingham are showing the best results. Vom Berg model is failed due to negative value. Proposed model is a suitable model.
- For 30BFS0.45(20) , Proposed and Modified Bingham models are the best models. Robertson-Stiff is deviant model.

- For 60BFS0.4 (20), Proposed model is the best fit. Modified Bingham and other models are suitable too.

5.6.3 Observation for FA

5.6.3.1 Rheology of FA Mortars Right After Mixing

Proposed model is one of the best models for FA incorporated mortars. It shows best results in many cases. Proposed model proved the best for 10FA, better for 20 FA and 40 FA.

Modified Bingham model also proved to be suited in most of the cases but it showed negative vaues of yield stress and viscosity for 20 FA..

- For 10 FA 0.3 Proposed model is the best suited model. Bingham, Herschel, Modified Bingham and Vom Berg are showing just average results. De Kee and Yahya Model are not well suited.
- For 10 FA0.35, Proposed, Bingham De Kee and Vom Berg are showing the best results. Modified Bingham is not as good for 10FA0.35. Robertson-Stiff and Herschel are not better for representing 10FA0.35
- For 20FA0.4, Casson shows the best result. Herschel Bulkley is also showing the best result but its To is guessed. It is not easy to guess it accurately and with ease. So Casson, Dekee and Proposed model represents the data successfully. Yahya-Khayat model fails to give any parameter and representing the data.
- For 20FA 0.45,Yahya are the best data describing model. Proposed , Bingham and Vom Berg are also good models. Casson model does not describe data successfully.
- For 10 FA 0.4, all of the models are best describing models. By looking at the graph proposed models and Modified Bingham seems to be the most suited models.
- For 40 FA0.55 Casson and Yahya-Khayat model fails completely. De Kee, Vom Berg and then Modified Bingham and Proposed Models are the best to describe

data. Bingham Robertson-Stiff and Herschel Bulkley are not good representative of data.

- For 40FA0.8, Casson and Yahya-Khayat model fails. De Kee is not good. Bingham, Robertson-Stiff and Vom Berg are good models. Proposed model and Herschel Bulkley models are showing good results.

5.6.3.2. Rheology of FA at 10 minutes

For 40 FA 0.55 (10) and 40FA0.8(10), **"Proposed model"** is the best fit model. It is suitable for all cases at 10 minute rheological interpretation in all cases.

Modified Bingham and De Kee are providing best result for 10 FA and 20 FA (low amount of admixture). Yahya is one of the best for 10 FA (min amount of FA). But fails at high amount of FA i.e. 40 FA. Casson model is not suitable because it may fail at low and high both amount of FA.

- For 10FA0.3(10) , Modified Bingham, De Kee and Yahya are best fit and proposed model is acceptable model.
- For 10 FA 0.35 (10), Yahya is the best fit model , followed by Proposed , Modified Bingham and other models. Casson is a failed model.
- For20 FA 0.4 (10), Modified Bingham and De Kee models are followed by proposed and other models.
- For 20FA0.45(10), Modified Bingham showed negative yield stress . De Kee are best models followed by Yahya model. Proposed model is also well suited model.
- For 40 FA 0.55 (10) , proposed model is the best model followed by De Kee and Vom Berg models. Yahya-Khayat model is failed.
- For40FA0.8(10), Proposed model is the best model followed by Vom Berg and Bingham. Yahya and Casson models are failed. Modified Bingham and Herschel Bulkley are not as good representative models for this case. It is obvious from graphs too

5.6.3.3. Rheology of FA at 20 minutes

At 20 minutes FA , **“Proposed model”** is the one of the best fit model. Yahya and casson fails at 40 FA. Vom Berg is showing good results for FA at 20 minutes.

- For 10 FA 0.35(20), Proposed model is the best model, followed but Vom Berg and Yahya model.
- For 20FA0.45(20), Modified Bingham, De Kee model followed by Vom Berg and proposed models are the best models. Robertson-Stiff is deviant model.
- For 40 FA0.55(20),Vom Berg and proposed models are the best fit. Bingham is also showing minimum error.
- For 40 FA (high amount of admixture) Proposed model is better applicable for 40FA0.55 and 40 FA 0.8.Casson and Yahya models fail for 40 FA.

5.6.4 Observation for SF

5.6.4.1. Rheology of SF Mortars Right After Mixing

Mortars having silica fume as mineral ~~admixtures~~ are very well modeled by the “Proposed model”. Yahya-Khayat model is also well suited for Silica fume mortar cases. But due to the complexity of models, Casson and Yahya-Khayat model fails in some cases.

- 5SF0.4 is best described by the “Proposed model”. Then Vom Berg and Yahya models are better models. Modified Bingham, Bingham and Herschel Bulkley models are not comparatively good.
- For 5SF 0.5, “Proposed model” is a good model.
- For 5SF0.6,Yahya , De Kee and Modified Bingham gives the best results. All models are applicable but Casson model fails completely.
- For 10SF0.4, All of the models are applicable except Yahya model, which fails to describe values.

- For 15SF0.4 , Best suited model is the Casson and then the "Proposed model". All models are qualifying for this case.
- For 15 SF 0.45, Yahya ,Modified Bingham and "Proposed model" are most suited. Bingham does not show thixotropic character so can be excluded from the best list. So Yahya ,Modified Bingham and then the "Proposed model", are the best. Casson Model fails completely.
-

5.6.4.2. Rheology of SF at 10 minutes

For 5SF0.5(10), 10SF0.45(10) and 15SF0.45(10), **"Proposed model"** is the best fit model. At 10 minute and w/c 0.45 **"Proposed model"** proved to be the best fit model. Modified Bingham and De Kee models are showing good results at 20 minutes. Yahya-Khayat model is good for low SF only. Casson is failed many times.

- For 5SF0.4(10), Modified Bingham, De Kee and Yahya are best fit but proposed model is also shows good fit and highly acceptable. Casson is showing most deviant result.
- For 5SF0.5(10), Proposed model is the best fit, followed by Modified Bingham which is average fit only.
- For 5SF0.6(10),Best result is given by Yahya and De Kee then Modified Bingham. Proposed model is giving good acceptable result.
- For 10SF0.4(10), Best result is shown by Modified Bingham and Herschel Bulkley model. Proposed model is acceptable. Casson is failed model here.
- For 10SF0.45(10) , Proposed model is the best fit followed by Modified Bingham, De Kee and Herschel Bulkley model.
- 15SF0.4(10),Herschel Bulkley, Modified Bingham and De Kee are best fit. Proposed is an average acceptable model.
- For 15SF0.45(10), Proposed model is the best fit model, followed by Modified Bingham , De Kee and Vom Berg Models.

5.6.4.3. Rheology of SF at 20 minutes

Modified Bingham is the goodt fit but and proposed is suitable model for all cases. Yahya is failed many times.

- For 5SF0.4(20), Modified Bingham, De Kee and Robertson-Stiff are giving best fit. Proposed is highly acceptable.
- For 10SF0.4(20), Bingham , Yahya , De Kee are best fit. Proposed and Modified Bingham are good fit. Robertson-Stiff is deviant.
- For 10SF0.45(20), Modified Bingham, Robertson-Stiff and De Kee are the best fit, while proposed model is well acceptable. Yahya-Khayat model fails.
- For 15SF0.4(20),Modified Bingham, De Kee and Robertson-Stiff are the best suited model. Proposed model is good acceptable model. Yahya-Khayat model fails.
- For 15SF0.45(20), Modified Bingham , Herschel Bulkley and Robertson-Stiff are the best fit models while Proposed model is average and acceptable.

  Finally

  "Proposed model" is one of the best fit models, when used instantly, after 10 minutes of mixing or even after 20 minutes of mixing. In many cases, it was the best fit and in other cases, it was very well suited model. It never failed and never gives negative values.

CHAPTER 6

CONCLUSIONS AND RECOMMENDATIONS FOR FUTURE RESEARCH

6.1 Conclusions

6.1.1 Rheological behaviour of admixtures

- Yield stress is the minimum force per unit area required to start the flow. It mainly depends on Van der Waals forces (Inter particle forces). When applied force just overcomes these attractive forces then it is yield force (corresponding to yield stress). Torque which is product of this applied force and distance is used to determine these Van der Waals forces per unit area (yield stress).
- Yield stress is dependent on size, number of particles and distance between them.
- Plastic viscosity shows resistance to flow which depends on the roughness of surface and the particle packing. Particle packing provide more resistance to flow due to more rubbing between large surface areas. So this will be determined by the effect on velocity of rheometer by applying force (i.e. torque equal to force into distance)
- There is a specific or optimum water cement ratio for each case of cement plus specific amount of admixture, below which yield stress may be less due to improper mixing. Above this ratio yield stress is again less due to more water causing dispersion and lubrication among particles.
- As yield stress and plastic viscosity values are obtained after the balancing of different factors causing increase or decrease in these values. So their combined

effect will determine whether the value should increase or decrease. These factors are interparticle forces e.g. van der Waals(increase yield stress), particle shape (round shape decrease viscosity) and roughness (increase viscosity, and has a little effect on yield stress due to mechanical interlocking), particle size distribution (increase viscosity and yield stress, good packing) , Surface area per unit volume (increase viscosity) , density (increase yield stress) , fineness, (increases both values), mineral character (lime combining capacity, glassy phase etc), surface charge resulting in the flocculation or dispersion (flocculation increase yield stress, dispersion decrease both), surface hardness and water absorbing quality (porosity, more free water less yield stress and viscosity), temperature (increase viscosity and decrease slightly the yield stress due to far particles), radioactivity

- Yield stress increases with time for PC because of loss of water by absorption and evaporation and due to hydration products (chemical bonding).
- Plastic viscosity is decreased with high w/c because more water provides more lubrication and dispersion. Water layer comes between rough particles and allow them to slip easily.
- By adding little amount of BFS as 10% replacement, rough, polished and hard surface angular BFS increases Yield stress due to mechanical interlocking between angular and rough particles , hindering the flow to start. plastic viscosity is increased due to same reason.
- By increasing BFS, cement particles are reduced. As BFS surface is polished and hard so free water is available reducing both yield stress and viscosity.
- At 30 % replacement, there is almost no effect on rheology of mortar. It is similar to PC. Even both yield stress and plastic viscosity of the values are less than 10 % incorporation but now they are comparable to ordinary PC values.
- By increasing BFS amount, both of the values are decreased. But if flocculation occurs (at higher replacement and higher w/c) both yield stress and plastic viscosity values usually increases.

- FA instantly reduces both yield stress and plastic viscosity to much lower values due to smooth spherical shape (yield stress decreases due to ball bearing effect and viscosity decreases due to smooth and round particle).
- Van der waal forces are less for distantly placed particle and round FA keeps particle far and allow less interpacking. So they have less Van der Waals forces and hence the yield value.
- Plastic viscosity increases with time for plain PC but when Fly ash is added then it instantly reduces. With the time, plastic viscosity increases as Fly ash lose its round shape and irregular products are formed. This provides hindrance in sliding.
- FA yield value increases after 10 and 20 minutes because round particles (main cause of lower yield value) are changing shapes due to deposition of hydration products.
- For higher amount of mineral admixture as 40FA and 60BFS and higher w/c, the both value results are abnormal and usually higher because of flocculation of particles.
- Relative viscosity in SF shows mixed results It is due to balancing of properties e.g. fineness, interpacking (both implies to rubbing surface area), roughness and water available. If rubbing area is more or roughness is high, and water (for lubrication) is low, viscosity will be higher.
- Yield stress decreases at 5 % incorporation and then increased continuously. This is all due to balancing of properties e.g. fineness, interpacking, roughness and water available. Small amount of SF particles come between cement particles, thus separating them at a distance. This instantly reduces yield stress. But when SF is increased, instead of separating cement particles, SF gathers in between particles and increases yield value
- Plastic viscosity is decreased for small percentage of SF incorporation because total surface area per unit volume is balancing with lubricating property of very small silica fume. Smaller rounder particle, less in number, provide ball bearing effect, cause easier slipping. But if SF amount is increased, surface area per unit volume is much increased (due to fineness of SF, Actually fineness also

contributes to surface area per unit volume) and make tight interpacking and less space hence viscosity is increased. At higher SF, smaller round particles are v high in number. Hence smallness and roundness of particle contributes in slipping. There is less number of big cement irregular rough particles. There is less interlocking so viscosity may be reduced. After balancing of different properties such as roughness, surface area per unit volume, size distribution, interlocking, hence viscosity is decided

- It is also possible that at high replacement, cement particles are already less in number and silica fume comes between them and nullify their effect in motion resistance. The major flow resistance is mainly due to silica fume only.
- In silica fume, yield stress and viscosity values usually increases with time.. Relative viscosities are showing mixed results because at each time phase there are different properties of mix and viscosity depends on available surface area for rubbing, smoothness and water amount for lubrication at that time.

6.1.2 Suitability of different models

- Bingham models is the most widely used but a linear model.
- Herschel Bulkley model is not linear and defines the shear thinning or thickening but Yield stress is to be guessed so it is not much accurate and easy to use.
- Modified Bingham model seems to be most suited in many cases but it shows negative viscosities and yield stress in some cases. So it is not much reliable model
- Herschel Bulkley model and Modified Bingham model are correlated but they may show opposite result about shear thinning and shear thickening. Yahya Model and Casson models are failed many times. De Kee model shows both good and bad fits for data. Vom Berg may fail too.
- “Proposed model” is one of best fit model, more accurate than Bingham, more easily used than Herschel Bulkley model and one of the best models to represent

admixture mixed mortars. It never fails, never shows negative results, never have larger errors and easily fit upto 20 minutes after mixing..

6.1.3 Suitability of proposed model

"Proposed" model is the best fit models especially when admixtures are added in mortar, when used instantly, after 10 minutes of mixing or even after 20 minutes of mixing. In many cases, it was the best fit and in other cases, it was very well suited model. It never failed and never showed negative values. **"Maria Idrees Model**" is the best fit model at 10 minutes for PC 0.3 and PC 0.6, 20 minutes for plain PC , 60BFS0.3, 60BFS0.4 , 30BFS0.4, 30BFS0.45, 30BFS0.4(10) , 30BFS 0.45 (10)and 60BFS 0.50(10), 10FA, better for 20 FA and 40 FA., 40 FA 0.55 (10), 40FA0.8(10), , 5SF0.5(10), 10SF0.45(10) and 15SF0.45(10).

Proposed model is showing the best result hence it can be easily and efficiently used for cement based materials.

6.2 Future Recommendations

- More research work is needed to find out the optimum results for desired efficiencies. (30BFS0.4 has same rheological results to the simple PC0.4 so is just useless in terms of rheology.)
- The w/c for max. yield stress for each mix should be found out. A formula, if possible should be developed by considering basic parameters.
- A study can also be conducted to know the replacement percent of admixture on which highest yield stress value can be obtained.
- In other words new mix design methods should be developed considering the rheology of mix. Much research is needed to propose mix design with mineral admixture and chemical admixtures. Formulae should be developed so that, by

varying constituent amount of mix, desired yield stress and viscosity can be obtained.

- The relation between mortar and concrete should be developed to co-relate their rheological properties.
- Some studies show that slump is related to yield stress only. Yield stress may reduce/increase with time but slump value is always decreased with time. So slump value is not only dependent on yield stress. A new model for slump correlating to rheological parameters should be developed.
- Different models show contradiction in shear thinning and shear thickening behavior of mortar. More investigation should be done.

REFERENCES

ACI 232.1R. 2001. Use of Raw or Processed Natural Pozzolans in Concrete, ACI Committee 232 Report, ACI 232.1R-00, American Concrete Institute, Farmington Hills, MI.

ACI 233. 2003. Slag Cement in Concrete and Mortar. ACI Committee 233 Report, ACI 233R-03, American Concrete Institute, Farmington Hills, MI.

ACI 234. 2000. Guide for the Use Of Silica Fume in Concrete. ACI Committe 234 Report, ACI 234R-96, American Concrete Institute, Farmington Hills, MI.

ASTM C 230. 2003. Standard Specification for Flow Table for Use in Tests of Hydraulic Cement. ASTM International, PA, USA.

ASTM C 232. 2004. Standard Test Methods for Bleeding of Concrete. ASTM International, PA, USA.

Banfill, P.F.G. 2006. Rheology of Fresh Cement and Concrete, Rheology Reviews, The British Society of Rheology, 61-130.

Boukendakdji, O., Kadri, E-H., Kenai, S. 2012. Effects of Granulated Blast Furnace Slag and Superplasticizer Type on the Fresh Properties and Compressive Strength of Self-compacting Concrete, Cement and Concrete Composites, 34, pp. 583-590.

Braun, H., Gebauer, J. 1983. Possibilities and Limits of Using Fly-ash in Cement, Zement-Kalk-Gips, 36 (5), 254-258.

Carette, G.G., Malhotra, V.M. 1983. Early-age Strength Development of Concrete Incorporating Fly Ash and Condensed Silica Fume, 1st Int Conf Use of Fly Ash, Silica Fume, Slag, and Other Mineral By-products in Concrete, ACI SP-79, V.2, pp. 765-784.

Chen, B., Liu, J. 2008. Experimental Application of Mineral Admixtures in Lightweight Concrete with High Strength and Workability, Construction and Building Materials, 22, pp. 655-659.

Davis R.E., Carlson, R.W., Kelly, J.W., Davis, H.E. 1937. Properties of Cements and Concretes Containing Fly Ash, ACI J Proceedings, 33(5), 577- 612.

Dhir, R.K. 1986. Pulverized-fuel Ash. In Cement Replacement Materials (Ed. R.N. Swamy), pp. 197-256, Surrey University Press.

EN 196-1. 2005. Methods of Testing Cement – Part 1: Determination of Strength. CEN, Brussels.

EN 197-1. 2012. Cement-Part 1: Composition, specification and conformity criteria. CEN, Brussels.

Ferraris, C.F. 1999. Measurement of the Rheological Properties of High Performance Concrete: State of the Art Report, J. Res. Natl. Stand. Technol., 104(5), 461-478

Ferraris, C.F., Obla, K.H., Hill, R. 2001. The Influence of Mineral Admixtures on the Rheology of Cement Paste and Concrete, Cement and Concrete Research, 31, pp. 245-255.

Feys, D. 2009. Interactions Between Rheological Properties and Pumping of Self-Compacting Concrete, PhD Thesis, Gent University, Belgium, 398 pp.

Fidjestøl, P. Lewis, R. 1988. Microsilica as an Addition. In Lea's Chemistry of Cement and Concrete (Ed. P.C Hewlett), Elsevier, London.

Hafid, F., Ovarlez, G., Toussaint, F., Jezequel, P.H., Roussel, N. 2010. Estimating Measurement Artifacts in Concrete Rheometers from MRI Measurement on Model Materials in Design, Production and Placement of Self-Consolidating Concrete (Eds. K.H. Khayat and D. Feys), pp. 127-137, RILEM.

Helmuth, R.A. 1986. Water-Reducing Properties of Fly Ash Cement Pastes, Mortars, and Concretes: Causes and Test Methods, ACI SP-91,pp. 723-740.

Hočevar, A., Kavčič, F., Bokan-Bosiljkov, V. 2013. Rheological Parameters of Fresh Concrete – Comparison of Rheometers, Gradevinar, 65 (2), 99-109.

Hu, J. 2005. A Study of Effects of Aggregate on Concrete Rheology, PhD Thesis, Iowa State University, Ames, 192 pp.

Koehler, E.P. and Fowler, D.W. 2004. Development of a Portable Rheometer for Fresh Portland Cement Concrete, Research Report ICAR-105-3F, Int. Center for Aggregates Res. The University of Texas at Austin, 306pp.

Laskar, A.I., Talukdar, S. 2008. Rheological Behavior of High Performance Concrete with Mineral Admixtures and Their Blending, Construction and Building Materials, 22, pp. 2345-2354.

Meddah, M.S., Lachiya, M. C., Dhir, R.K. 2014. Potential Use of Binary and Composite Limestone Cements in Concrete Production, Construction and Building Materials, 58, 193-205.

Mehta, P.K. 1986. Condensed Silica Fume. In Cement Replacement Materials (Ed. R.N. Swamy), Surrey University Press.

Mindess, S., Young, J.F. 1981. Concrete, Prentice-Hall, Englewood Cliffs, NJ.

Nanthagopalan, P., Haist, M., Santhanam, M., Müller, H.S. 2008. Investigation on the Influence of Granular Packing on the Flow Properties of Cementitious Suspensions, Cement and Concrete Composites, 30, pp. 763-768.

Nochaiya, T., Wongkeo, W., Chaipanich, A. 2010. Utilization of Fly Ash with Silica Fume and Properties of Portland Cement-Fly Ash-Silica Fume Concrete, Fuel, 89, pp. 768-774.

Ochoa, M.V. 2006. Analysis of Drilling Fluid Rheology and Tool Joint Effect to Reduce Errors in Hydraulics Calculations, PhD Thesis, Texas A&M University, Texas, 177 pp.

Parsegian, V. A. (2006). Van der Waals Forces: A Handbook for Biologists, Chemists, Engineers, and Physicists. Cambridge University Press. ISBN 978-0-521-83906-8.

Rao, G.A. 2003. Investigations on the Performance of Silica Fume-Incorporated Cement Pastes and Mortars, Cement and Concrete Research, 33 (11), pp. 1765-1770.

Roy, D.M. and Idorn, G.M. 1993. Concrete Microstructure, SHRP-C-340, pp. 6-16, Strategic Highway Research Program, National Research Council, Washington, DC.

Şahmaran, M., Christianto, H.A., Yaman, İ.Ö. 2006. The Effect of Chemical admixtures and Mineral Additives on the properties of Self-Compacting Mortars, Cement and Concrete Composites, 28, 432-440.

Sakai, E., Hoshimo, S., Ohba, Y., Daimon, M. 1997. The fluidity of Cement Paste with Various Types of Inorganic Powders, Proc. 10th Int Cong on Chemistry of Cement, p. 2ii002-010, Stockholm.

Scali, M.J., Chin, D., Berke, N.S. 1987. Effect of Microsilica and Fly Ash Upon the Microstructure and Permeability of Concrete, Proc. 9th Int Conf Cement Microscopy, Reno, pp. 375-387.

Shi, Y., Matsui, I., Feng, N. 2002. Effects of Compound Mineral Powders on Workability and Rheological Property of HPC, Cement and Concrete Research, 32, pp. 71-78.

Tokyay, M., Delibaş, T., Aslan, Ö. 2010. Effects of Mineral Admixture Type, Grinding Process, and Cement Fineness on the Physical and Mechanical Properties of BFS-, Natural Pozzolan-, and Limestone-incorporated Cements, Working Paper AR-GE 2010/01-B, Turkish Cement Manufacturers' Association (TÇMB), 45p. (in Turkish)

Vikan, H., Justnes, H. 2007. Rheology of Cementitious Paste with Silica Fume or Limestone, Cement and Concrete Research, 37, pp. 1512-1517.

von Berg, W. Kukko, H. 1991. Fresh Mortar and Concrete With Fly Ash, Fly Ash in Concrete – Properties and Performance, Rept. Tech. Comm. 67-FAB RILEM (Ed. K. Wesche), E & FN Spon, London.

Wallevik, O.H. 1983. Description of Fresh Concrete Properties by Use of Two-Point Workability Test Instrument, M.Sc. Thesis, The Norwegian Institute of Technology.

Wallevik, O.H. and Wallevik, J.E. 2011. Rheology as a Tool in Concrete Science: The Use of Rheographs and Workability Boxes, Cement and Concrete Research, 41, 1279-1288.

Wallevik, O.H., Feys, D., Wallevik, J.E., Khayat, K.H. 2015. Avoiding Inaccurate Interpretations of Rheological Measurements for Cement-Based Materials, Cement and Concrete Research, 78, 100-109.

Wei, S., Handong, Y., Binggen, Z. 2003. Analysis of Mechanism on Water-reducing Effect of Fine Ground Slag, High-calcium Fly Ash, and Low-calcium Fly Ash, Cement and Concrete Research, 33, pp. 1119-1125.

Yen, T., Tang, C-W., Chang, C-S., Chen, K-H. 1999. Flow Behavior of High Strength High Performance Concrete, Cement and Concrete Research, 21, 413-424.

APPENDIX

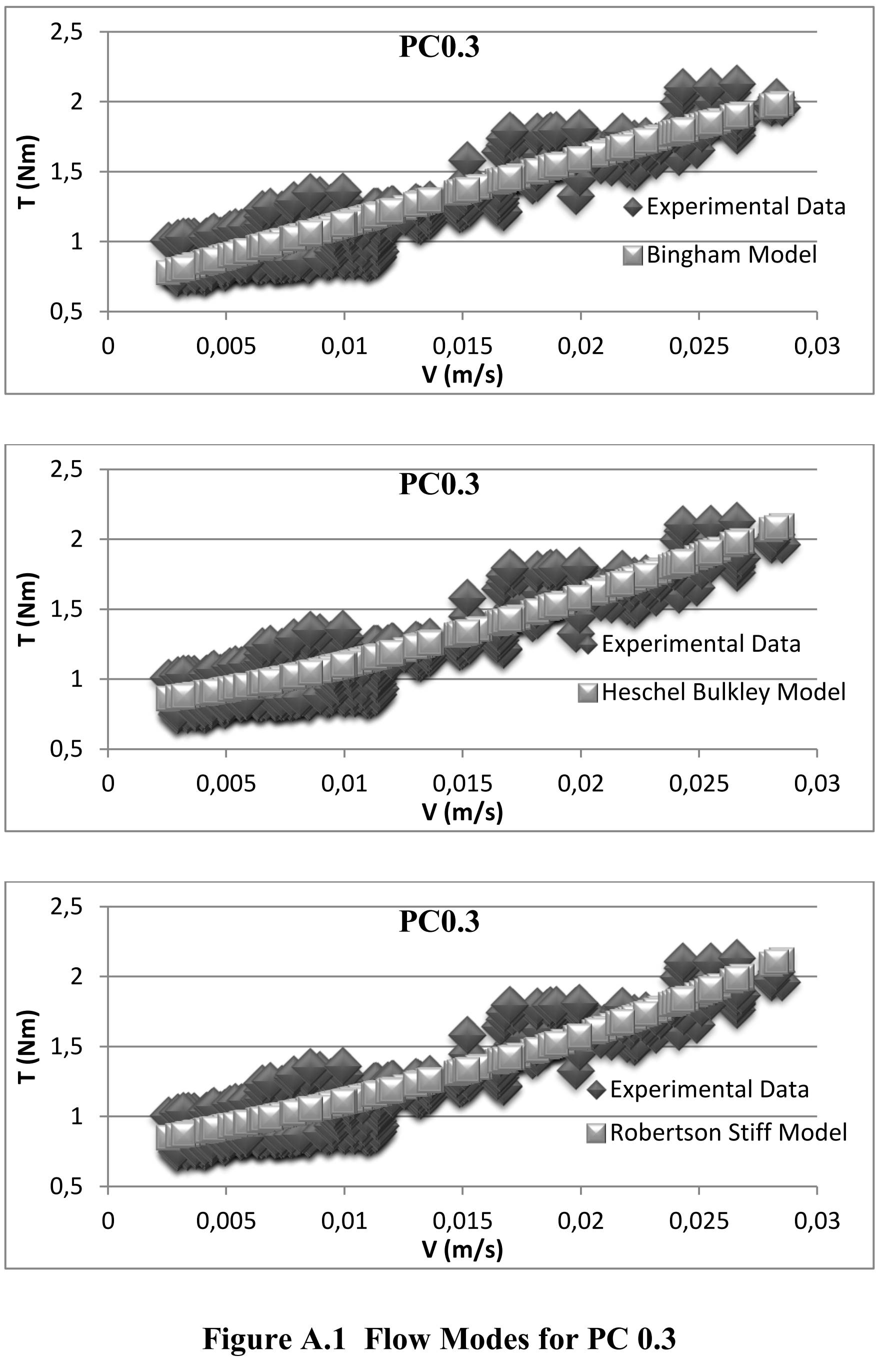

Figure A.1 Flow Modes for PC 0.3

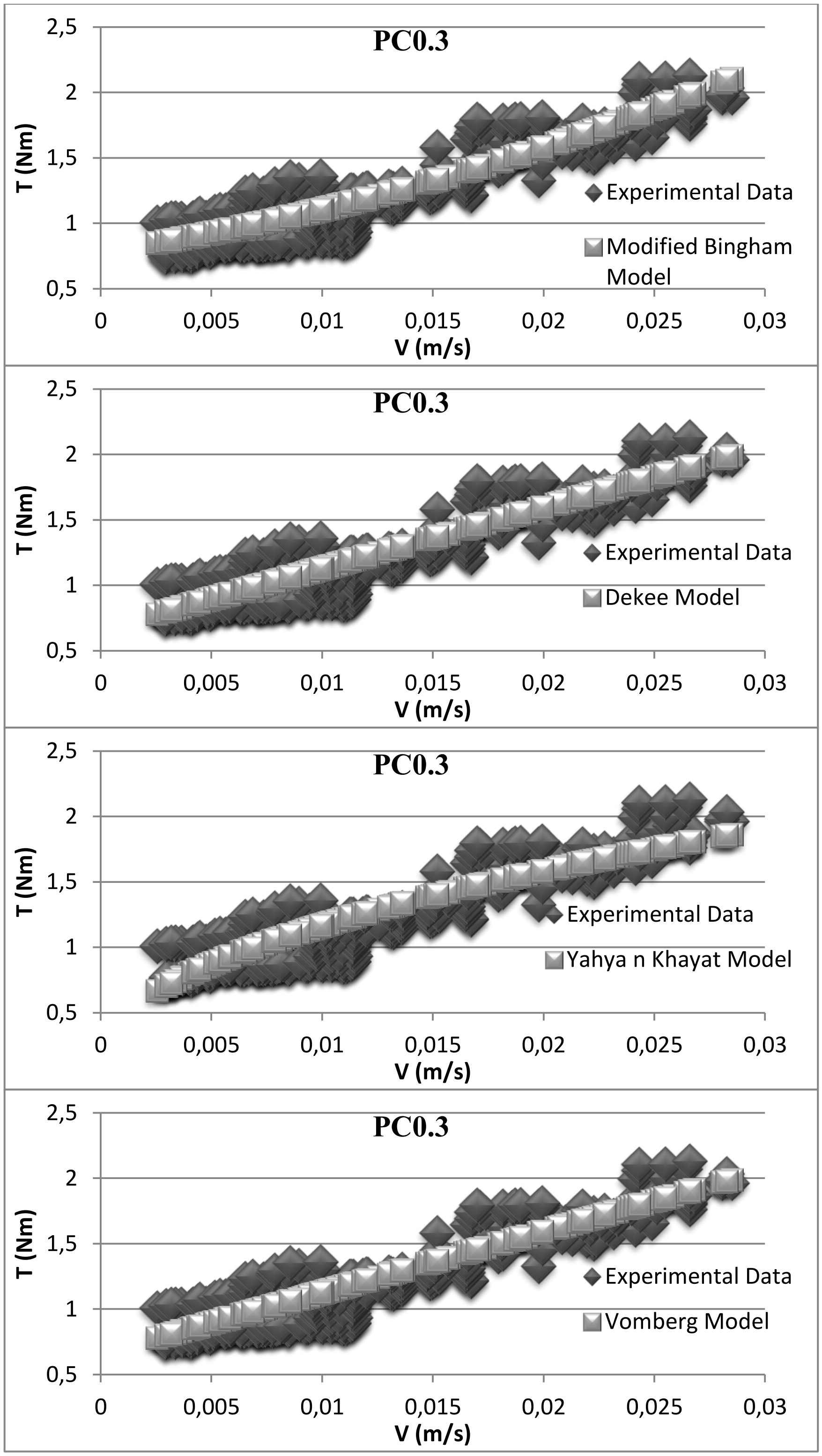

Figure A.1 (Continued)

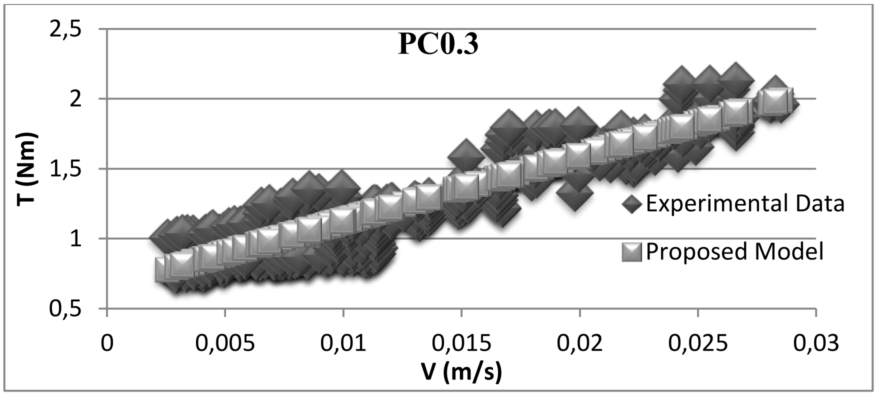

Figure A.1 (Continued)

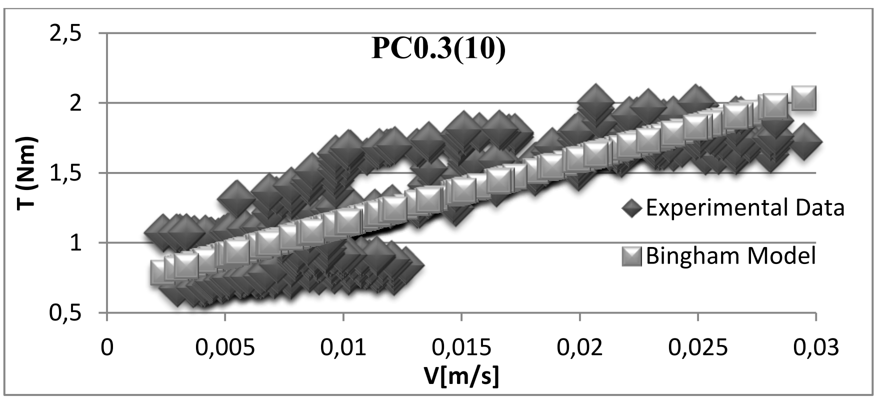

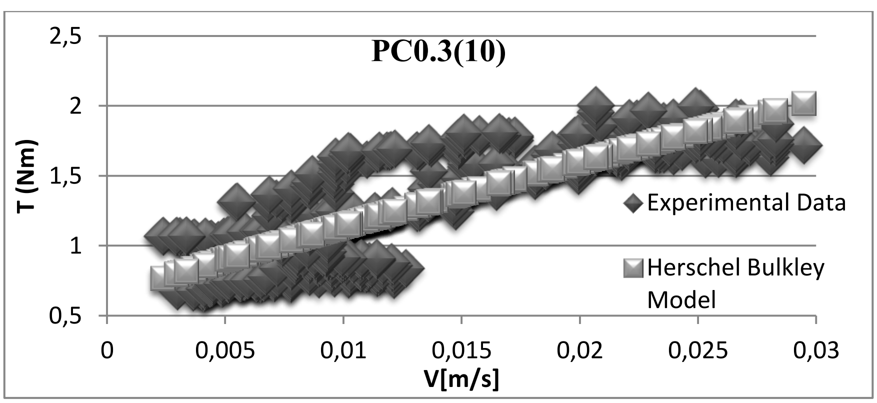

Figure A.2 Flow Modes for PC 0.3

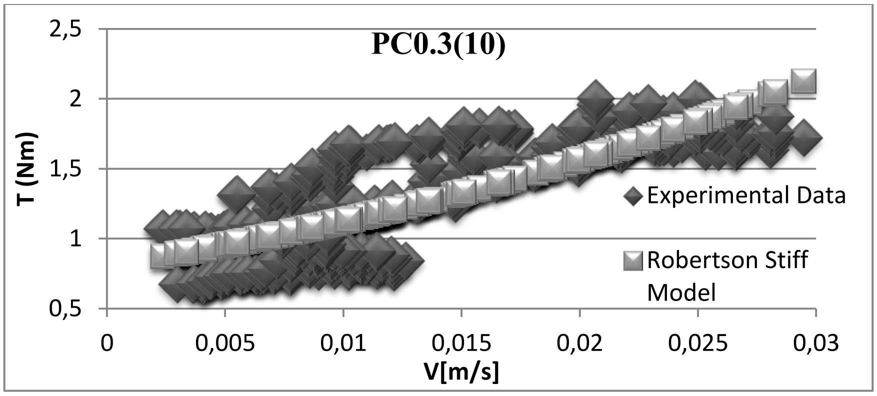

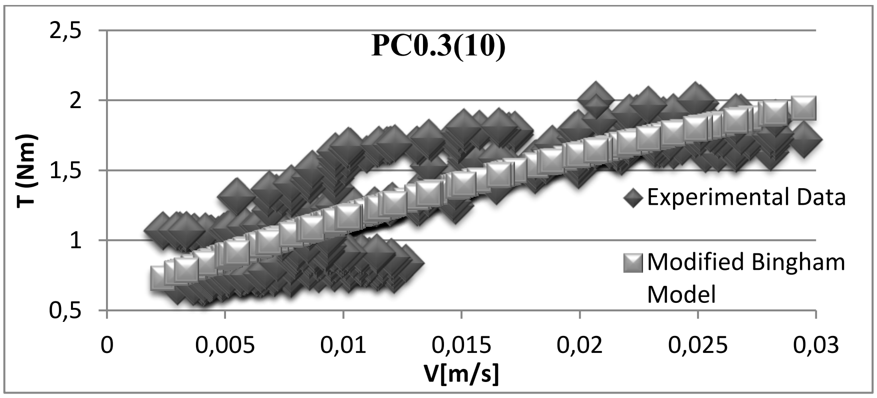

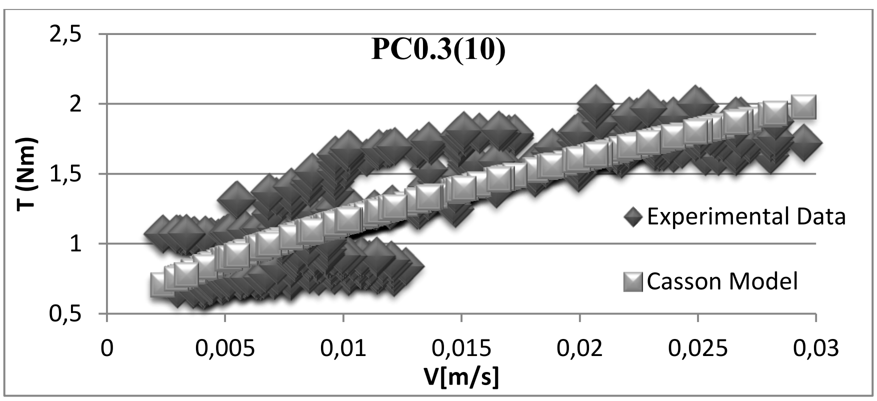

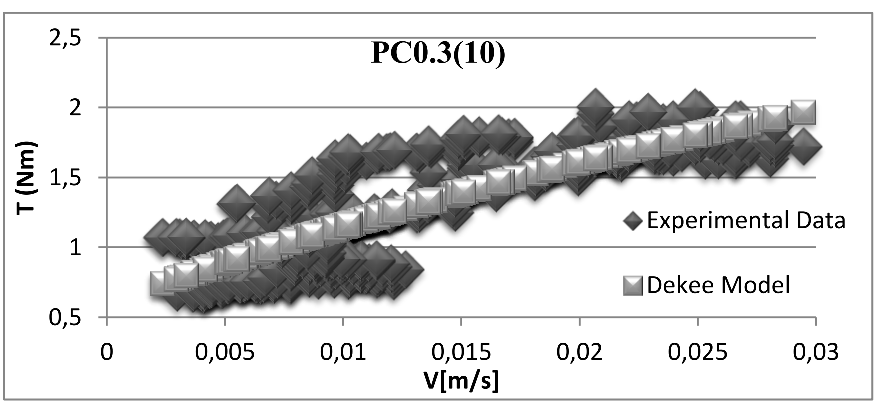

Figure A.2 (Continued)

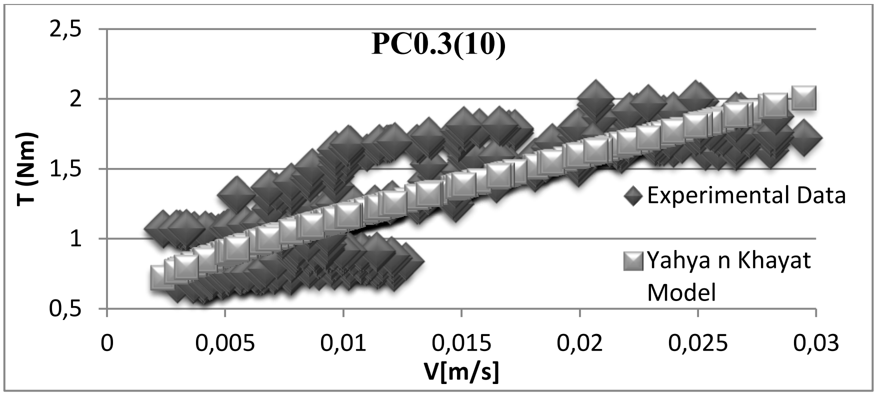

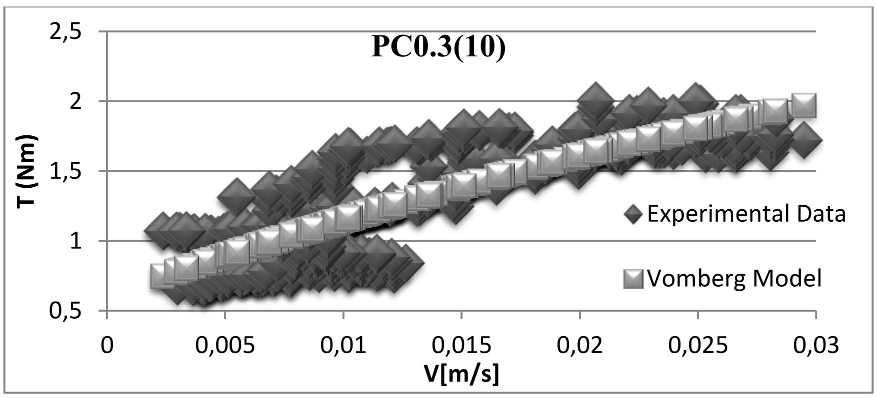

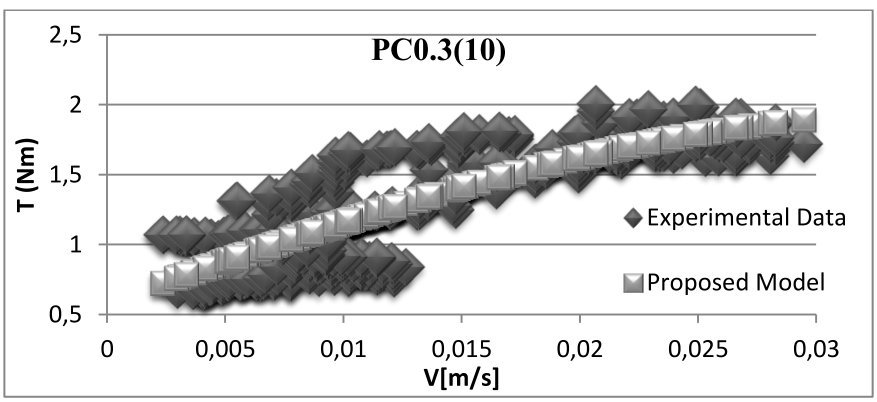

Figure A.2 (Continued)

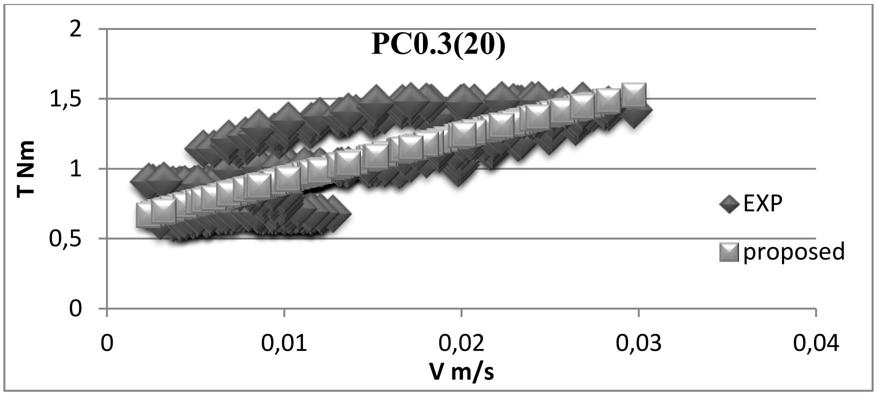

Figure A.3 Flow Model for PC0.3(20)

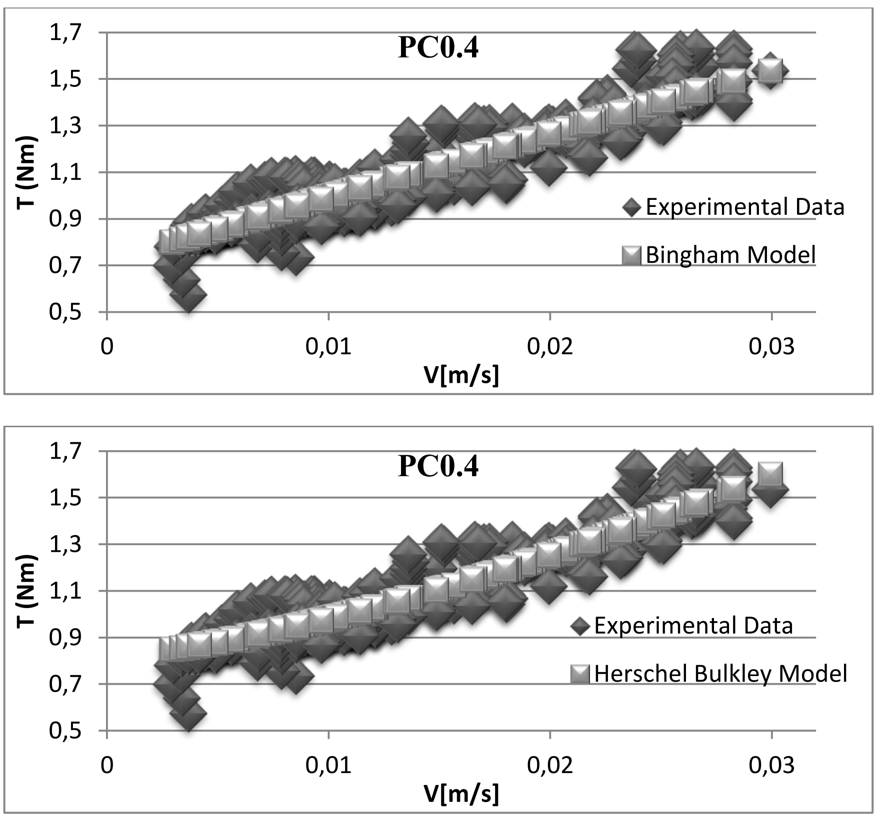

Figure A.4 Flow Models for PC0.4

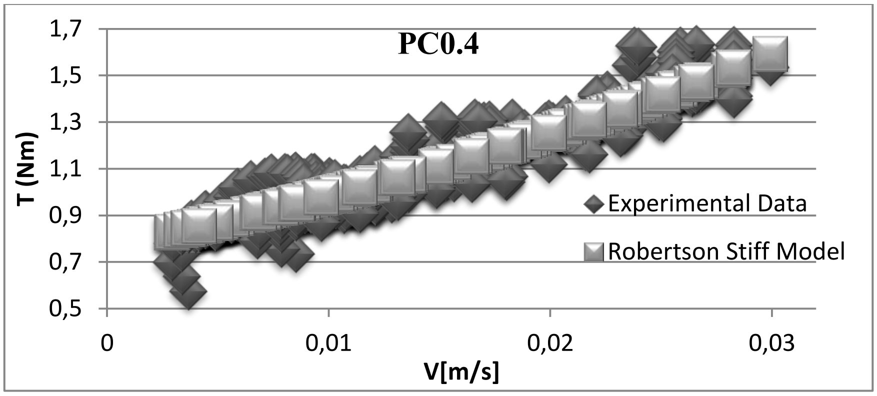

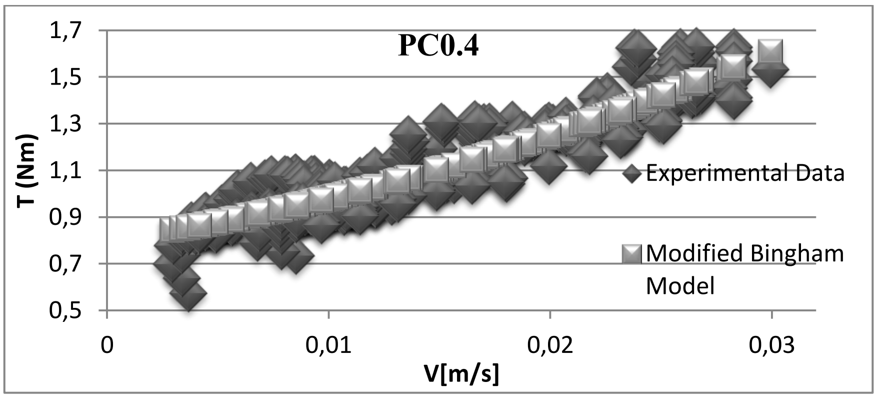

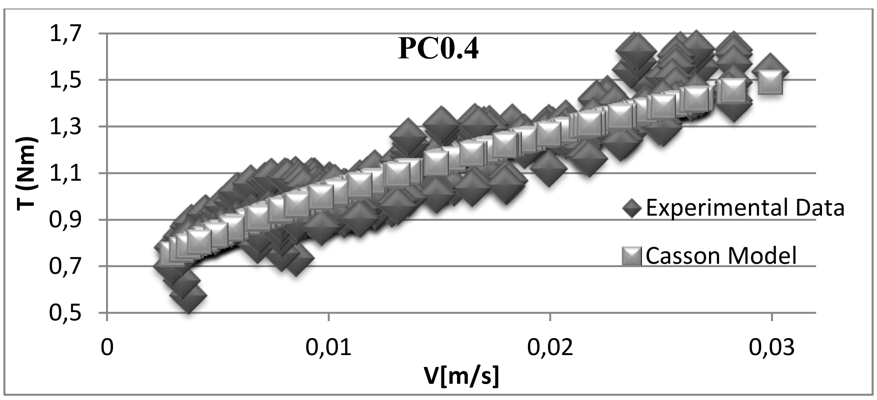

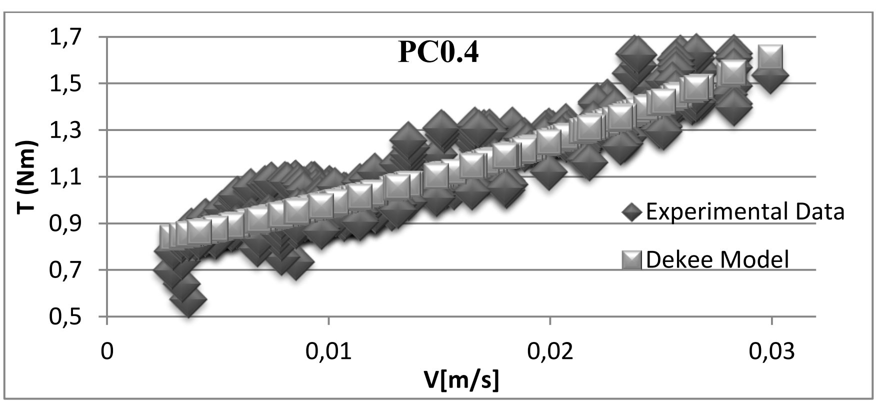

Figure A. 4 (Continued)

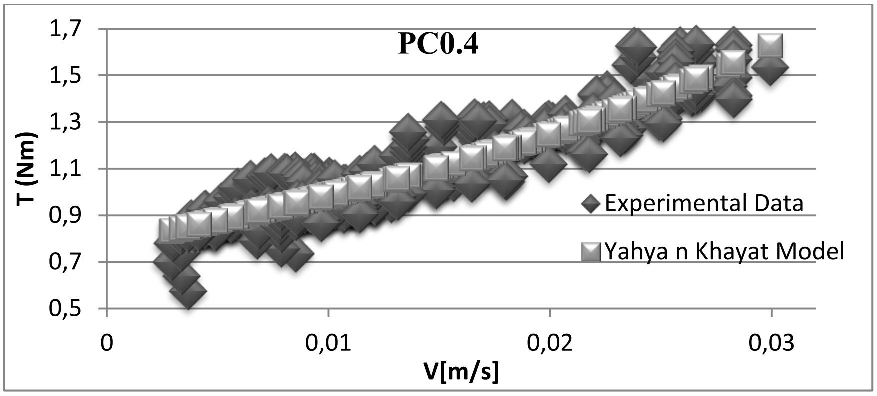

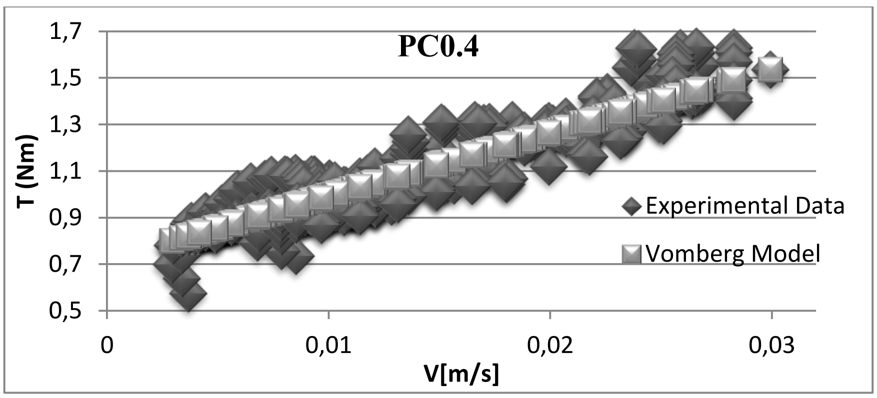

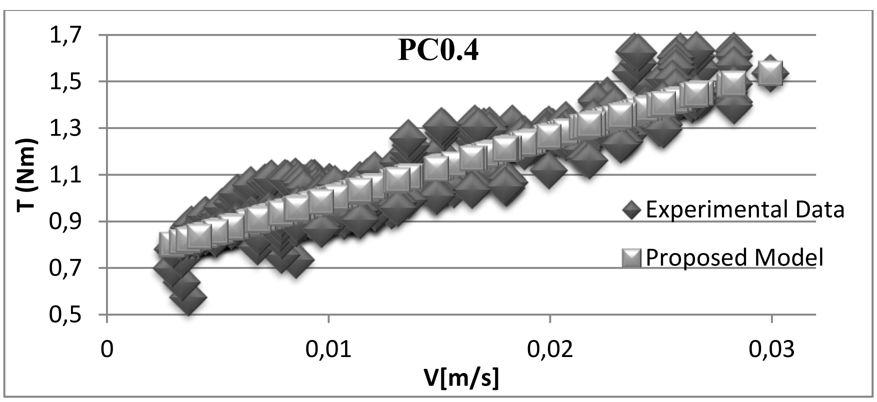

Figure A.4 (Continued)

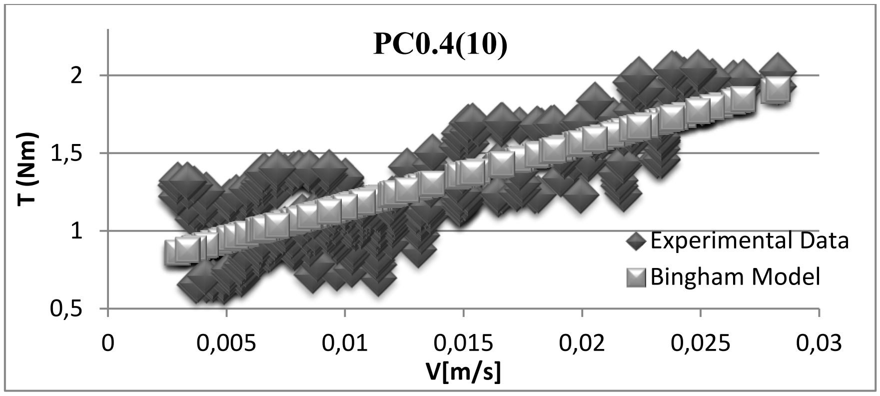

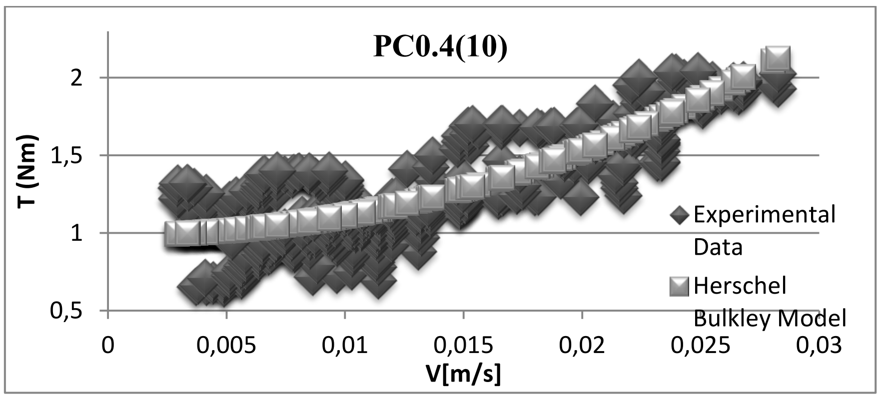

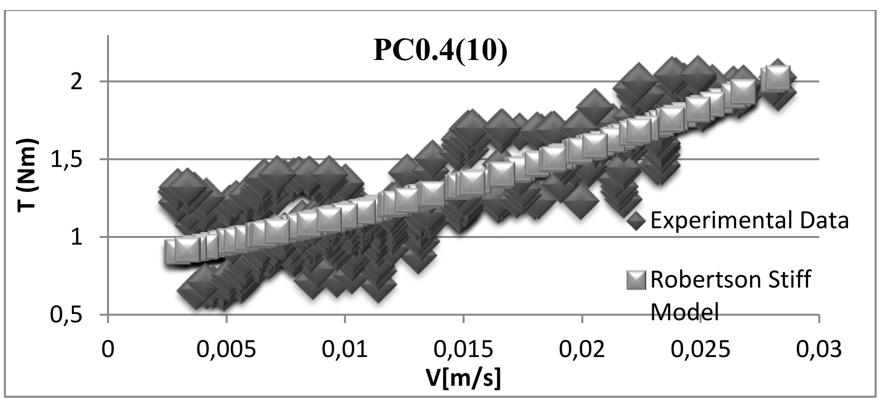

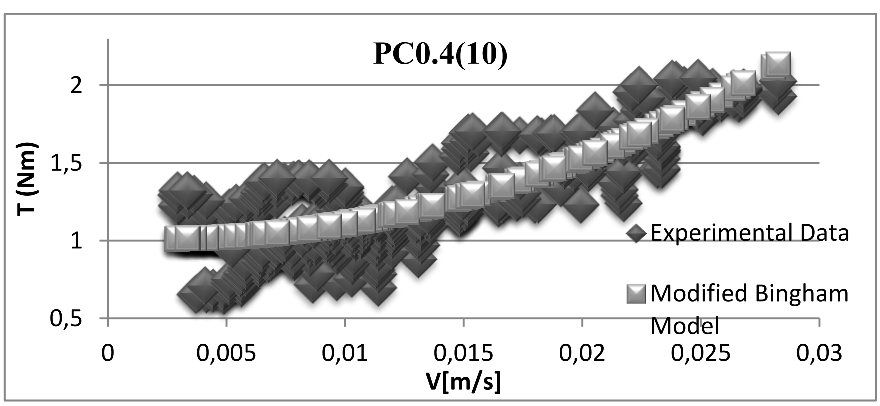

Figure A.5 Flow Model for PC 0.4(10)

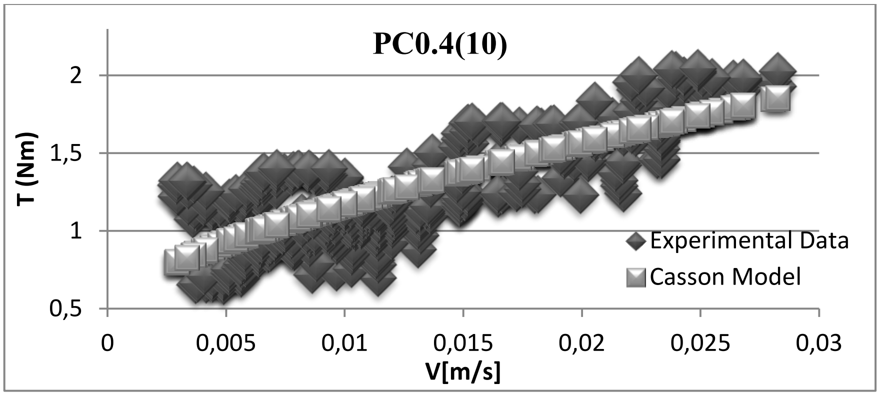

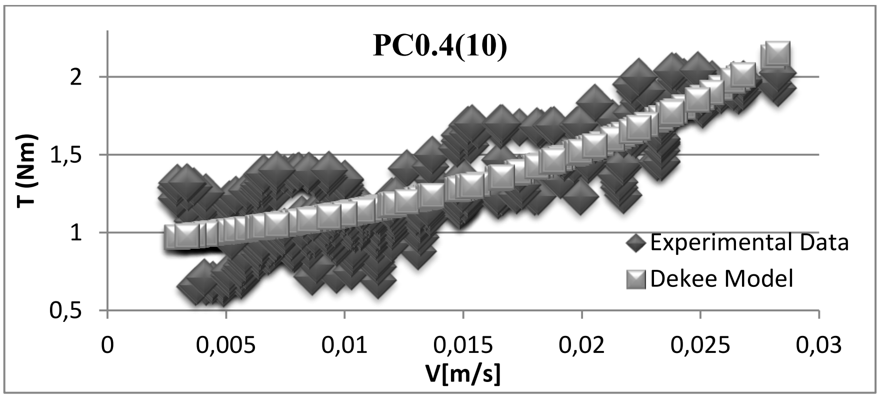

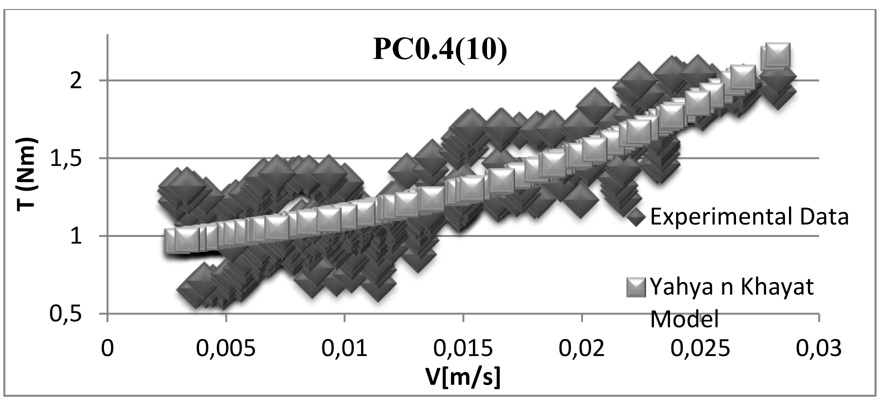

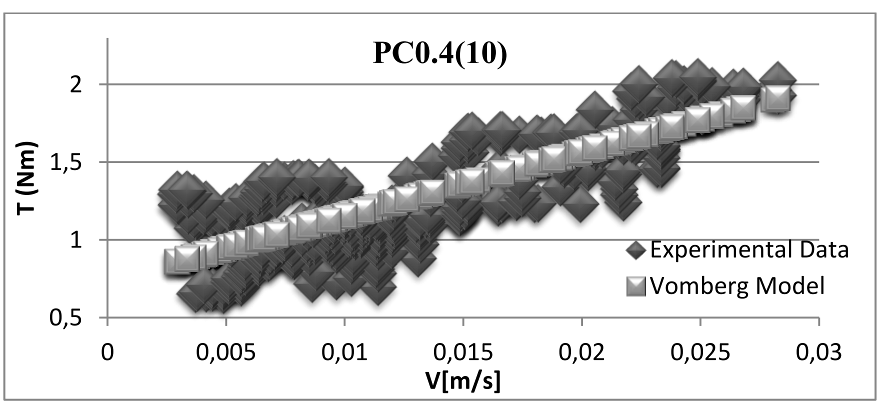

Figure A.5 (Continued)

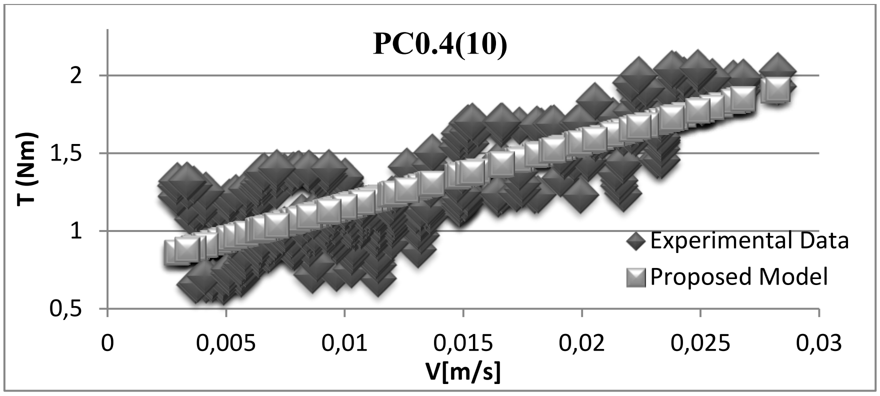

Figure A.5 (Continued)

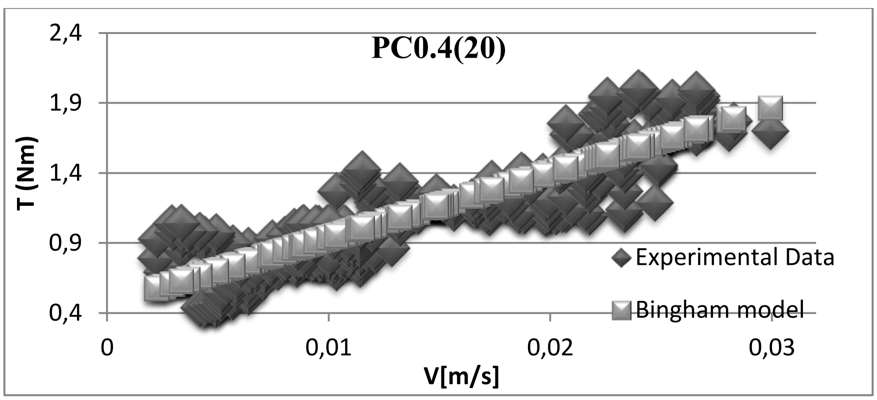

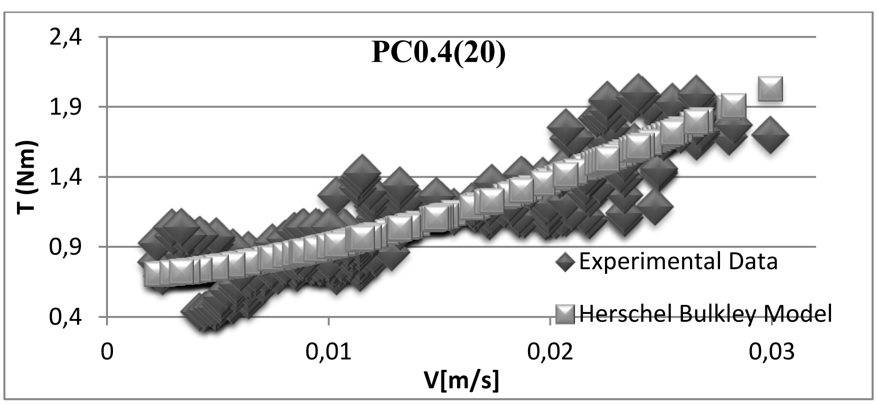

Figure A.6 Flow Models for PC 0.4 (20)

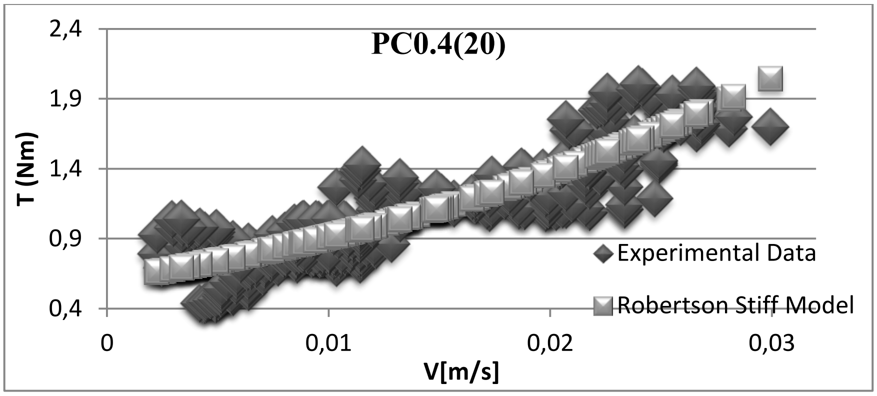

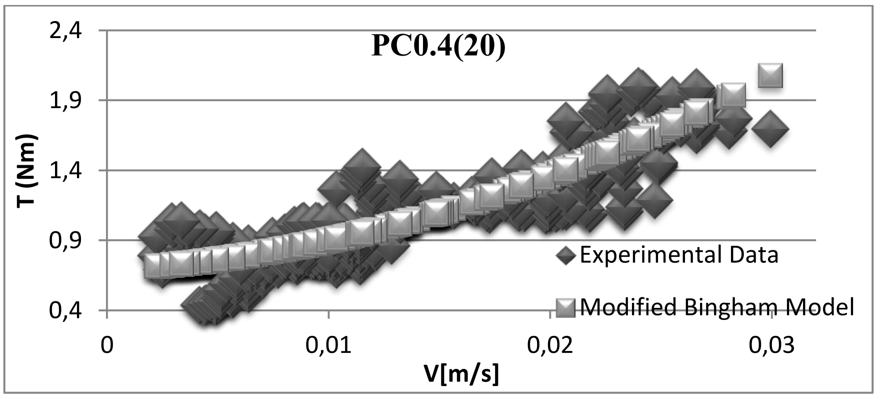

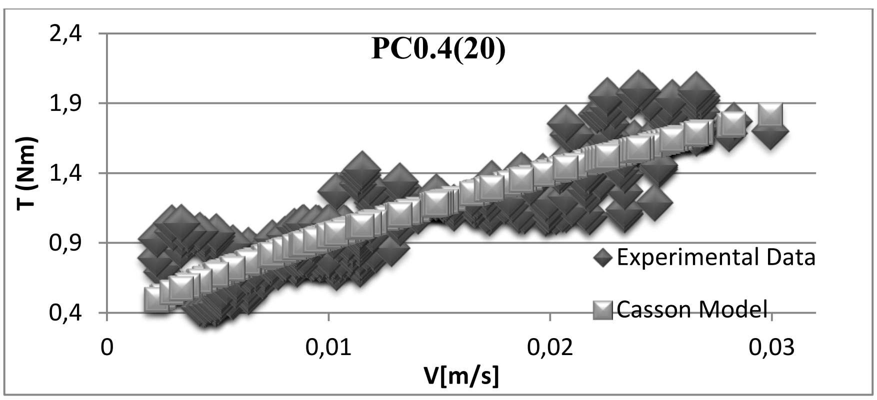

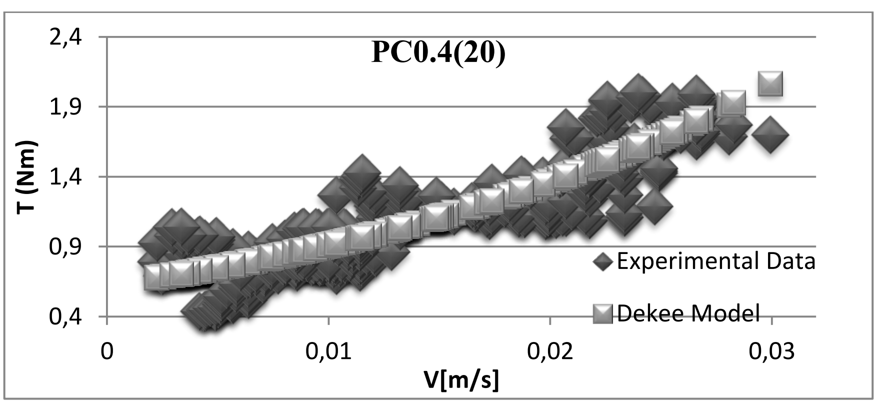

Figure A.6 (Continued)

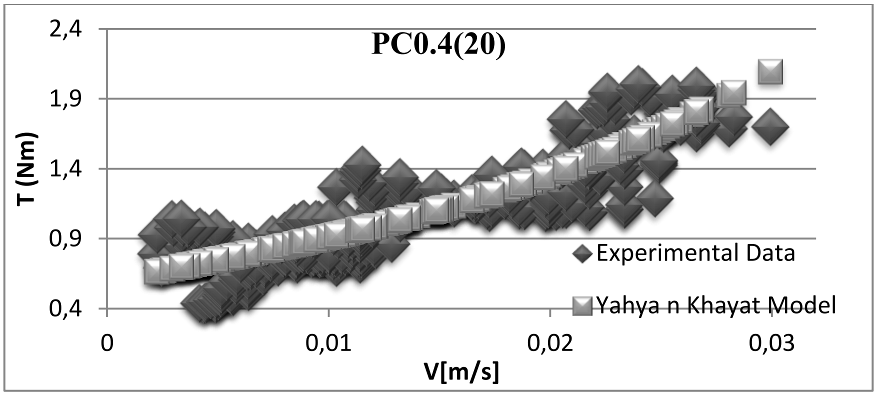

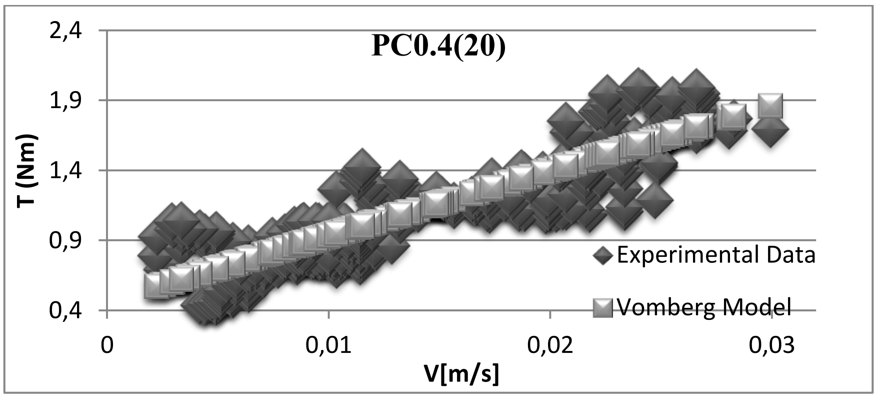

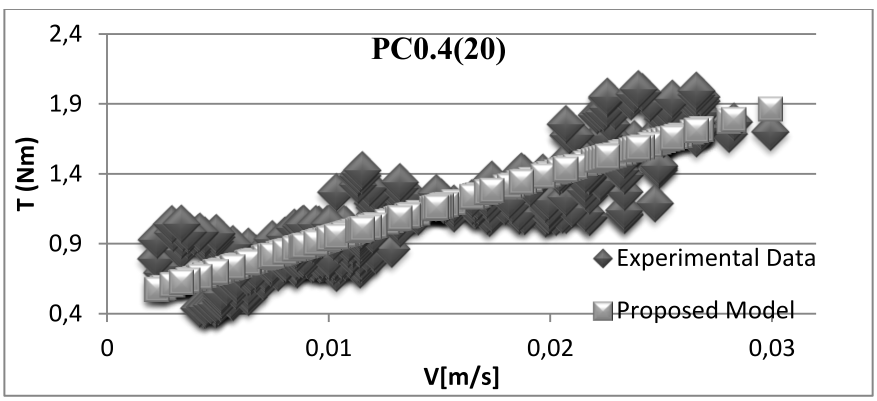

Figure A.6 (Continued)

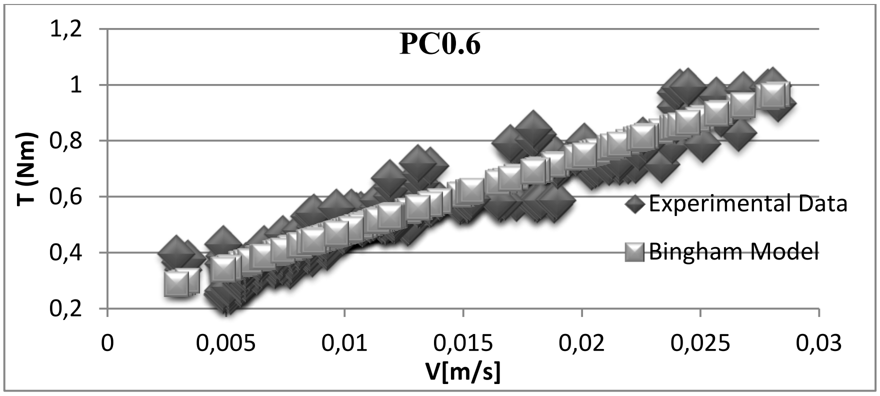

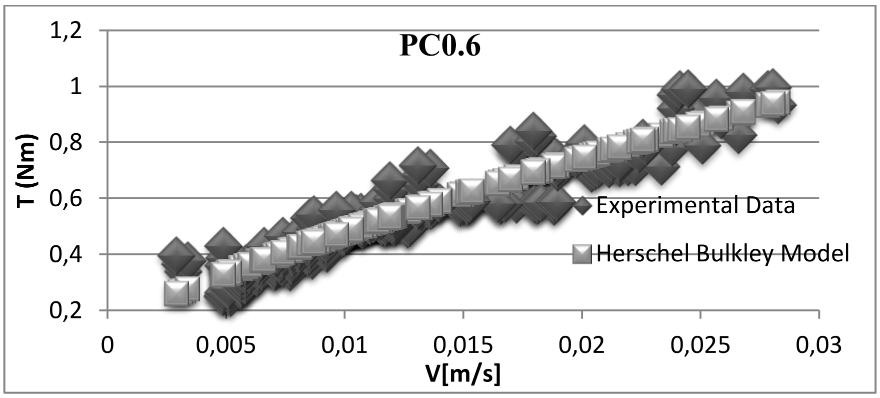

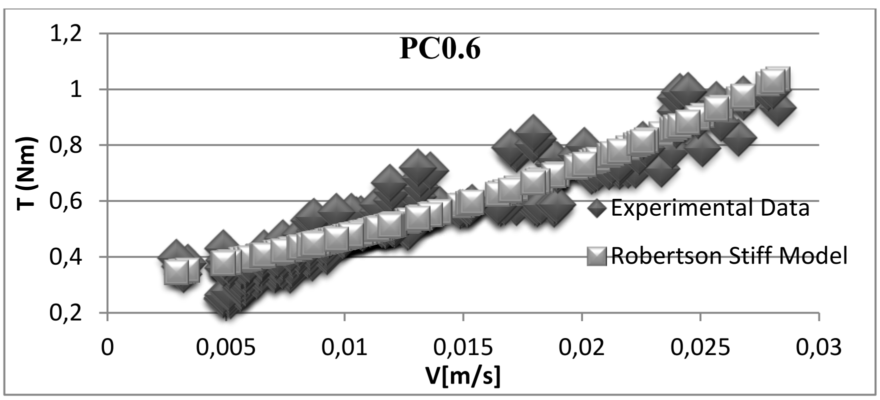

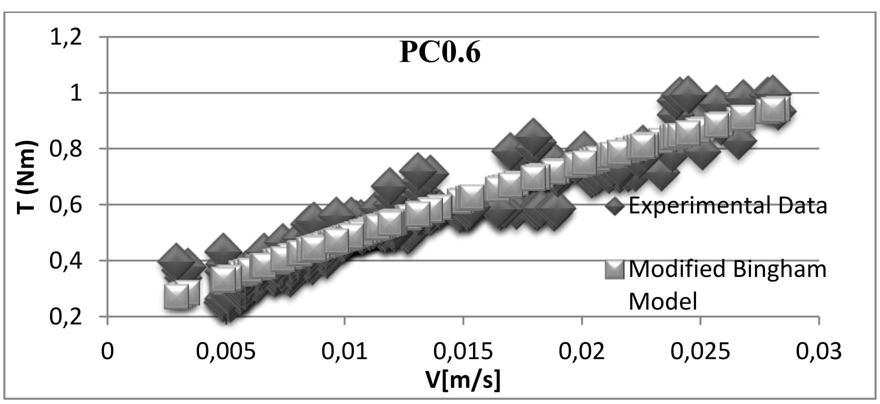

Figure A.7 Flow Models for PC 0.6

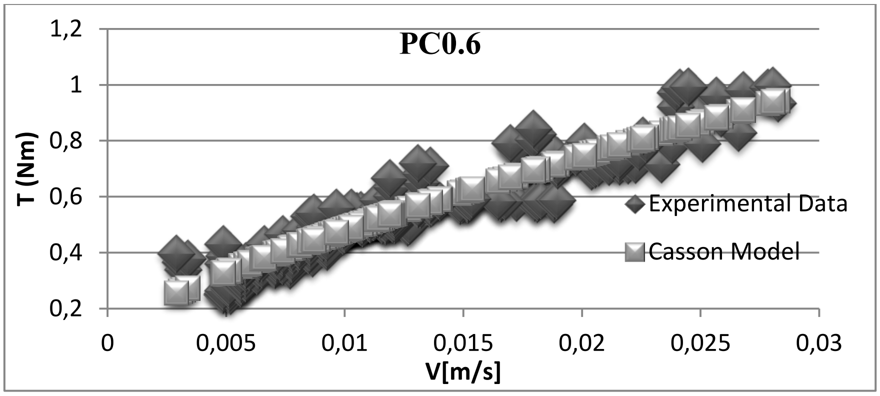

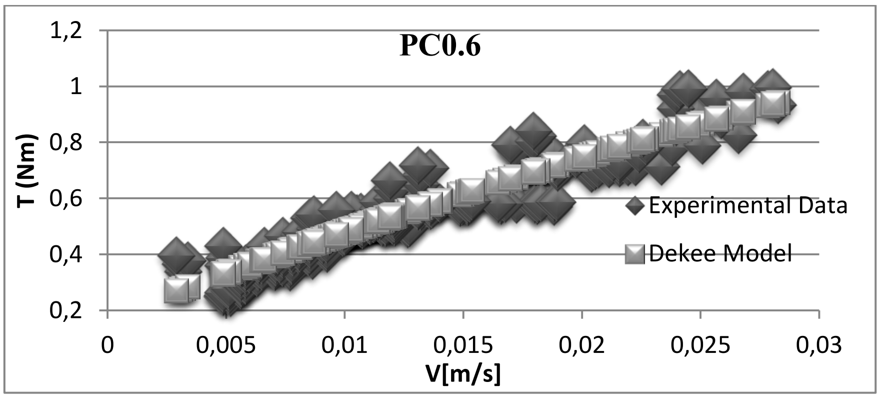

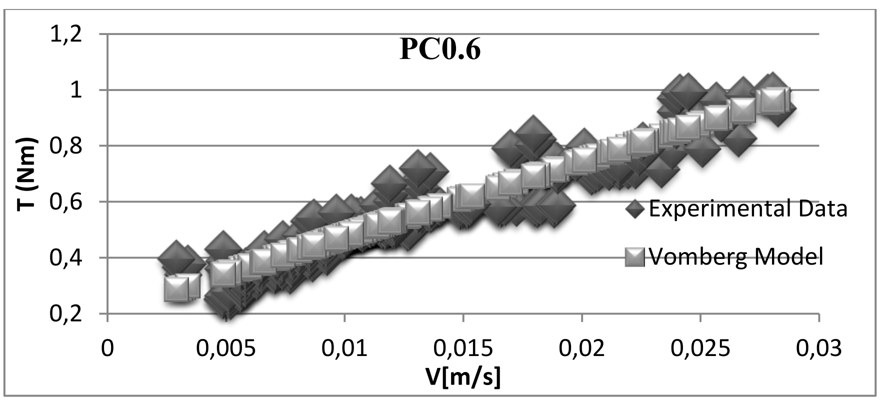

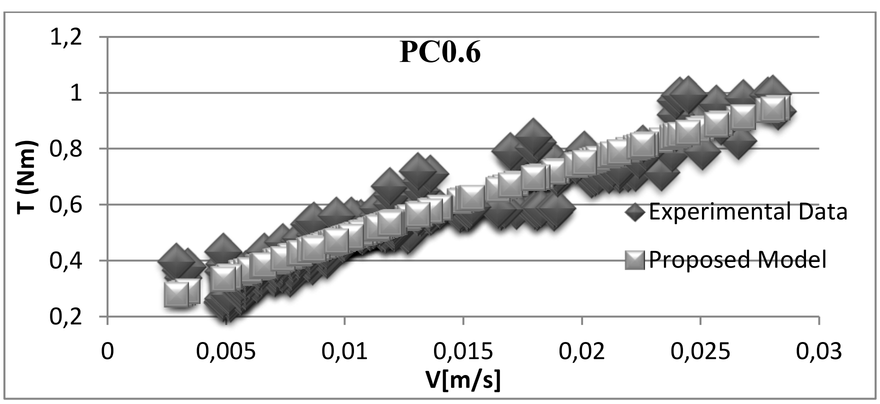

Figure A.7 (Continued)

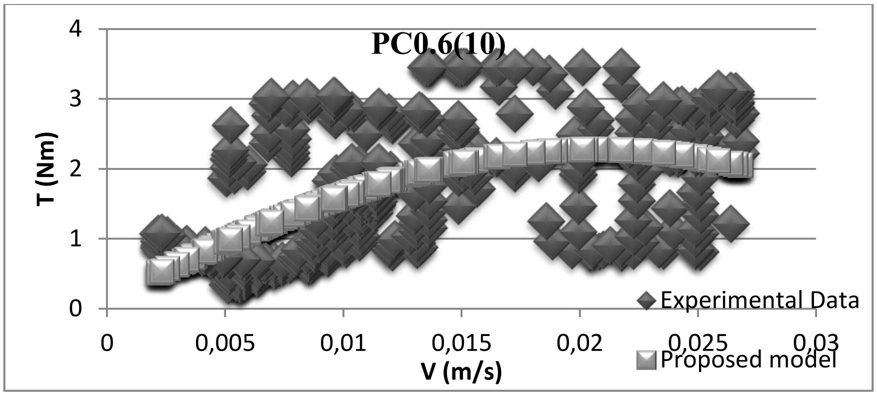

Figure A.8 Flow Model for PC0.6(10)

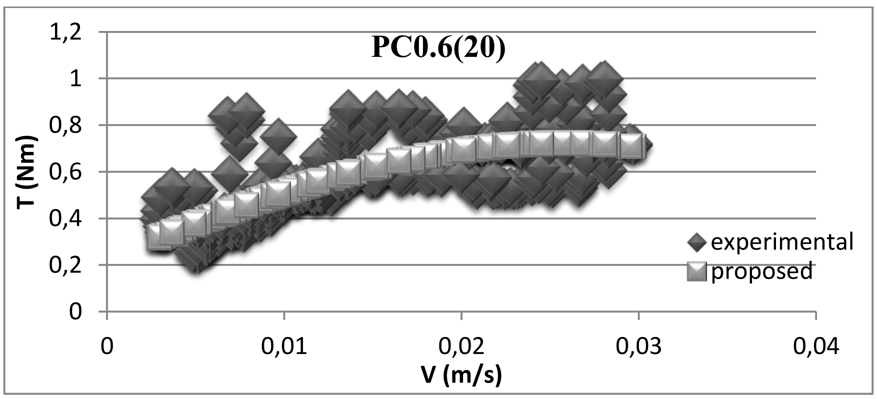

Figure A.9 Flow Model for PC0.6(20)

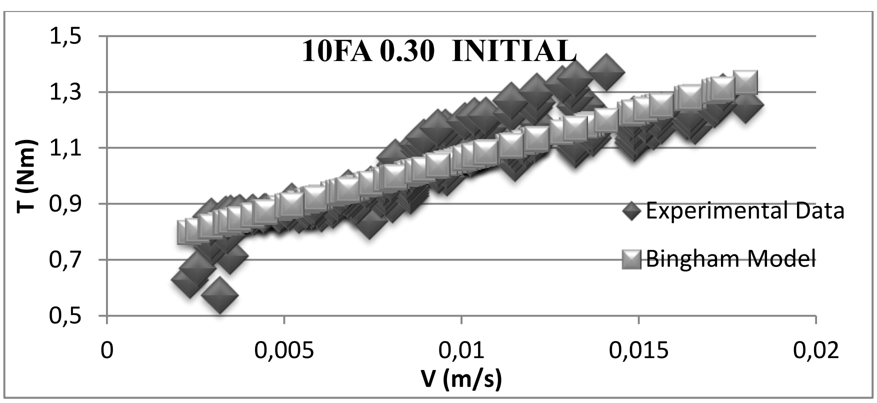

Figure A.10 Flow Models for 10FA0.3

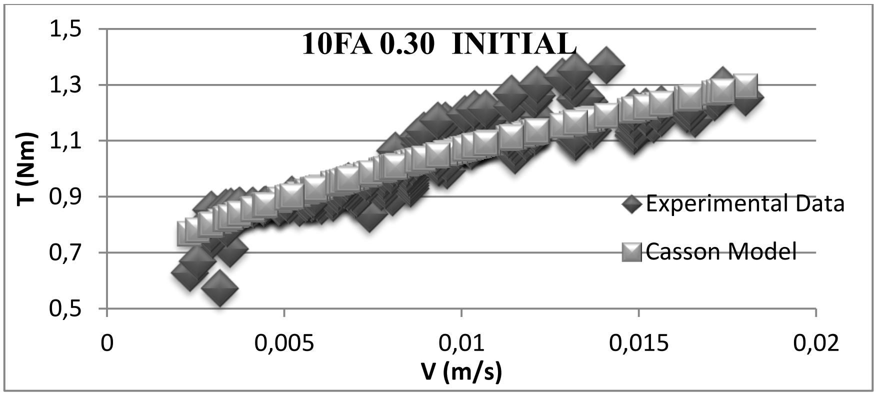

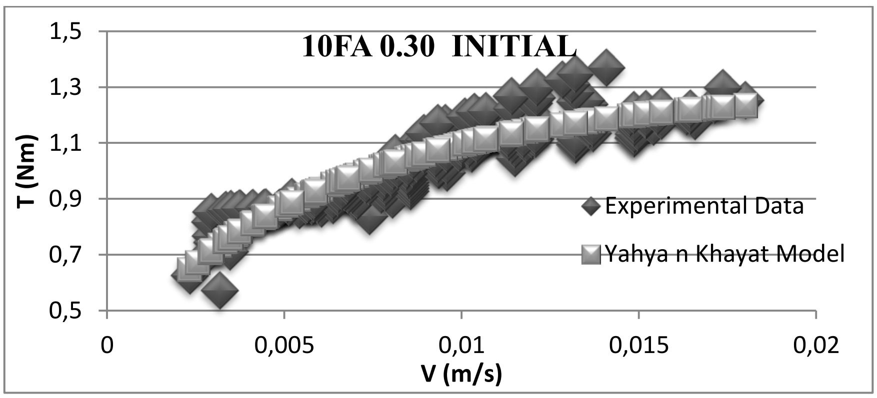

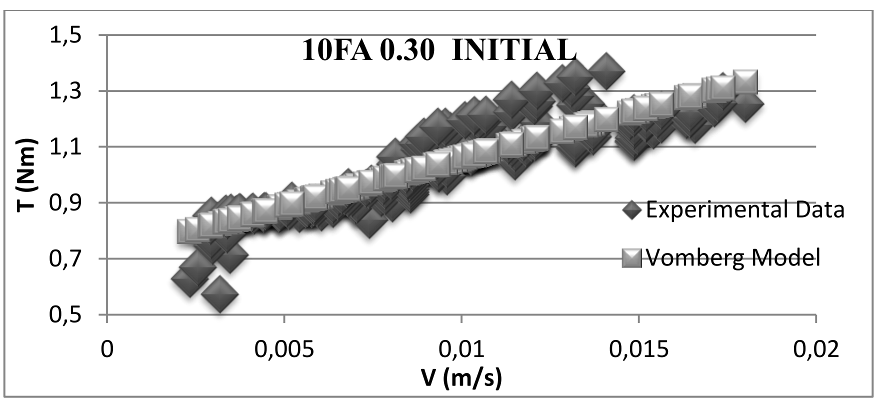

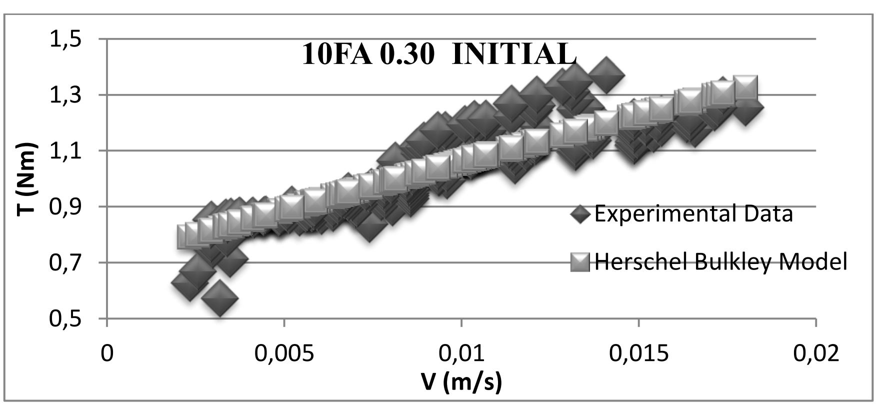

Figure A.10. (Continued)

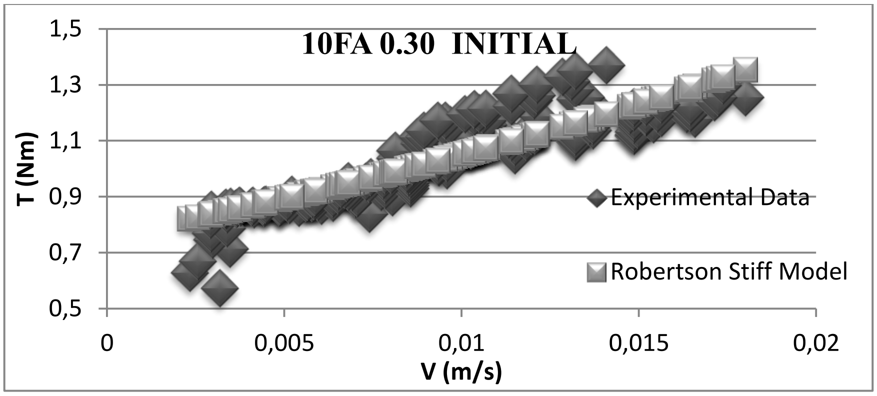

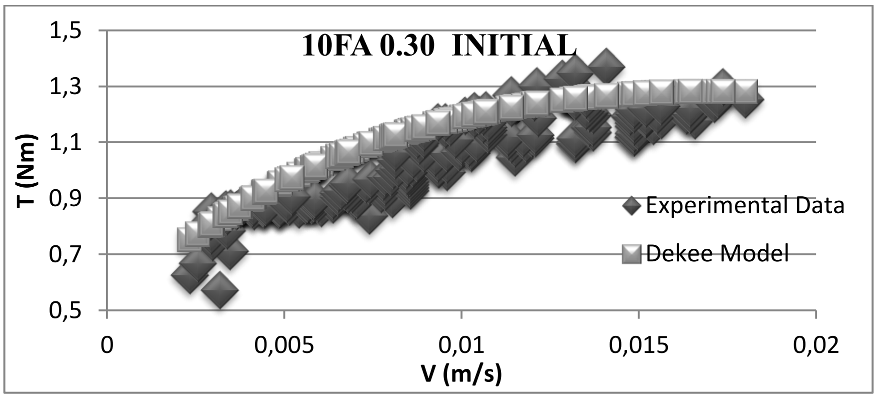

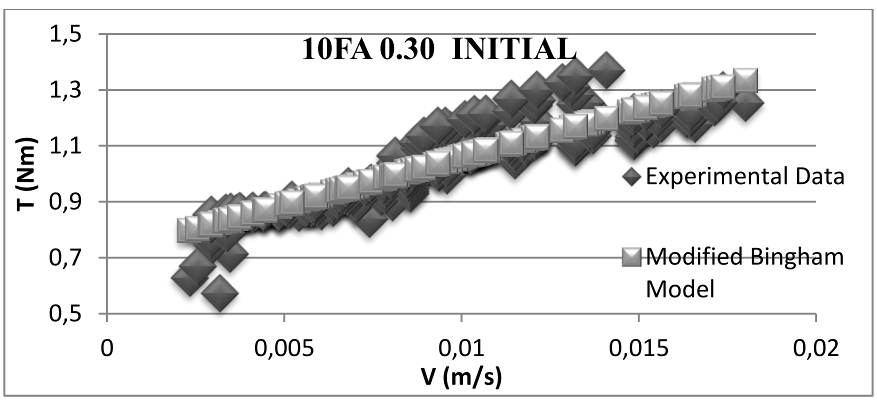

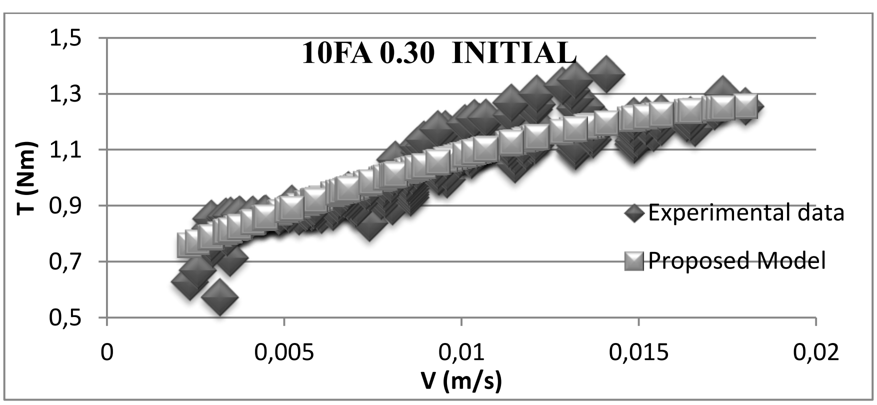

Figure A.10. (Continued)

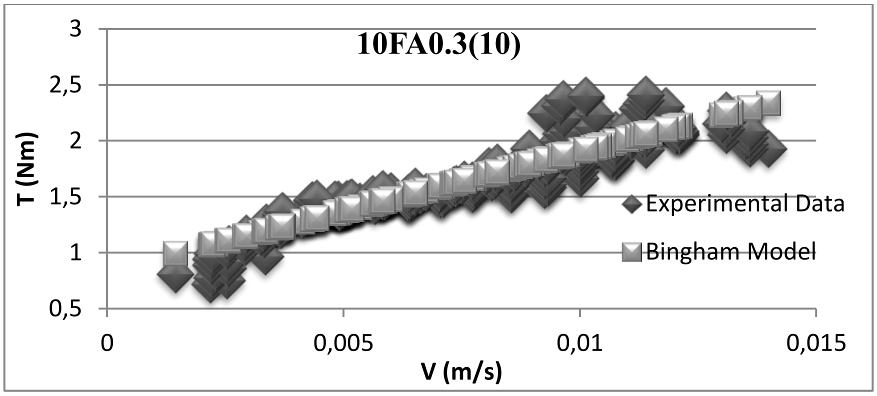

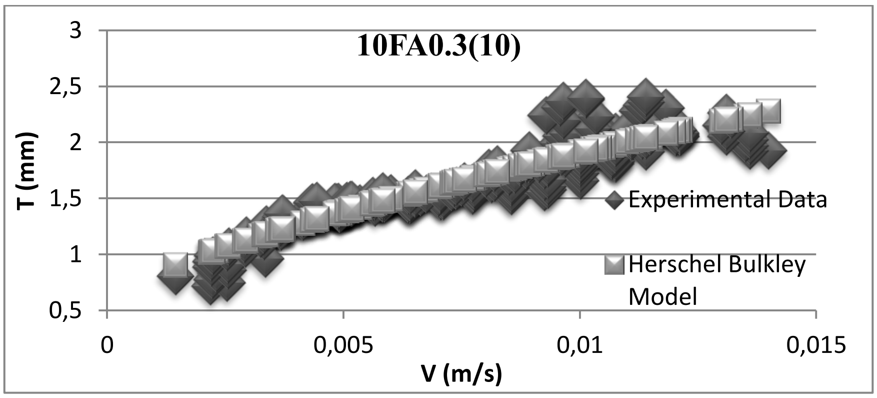

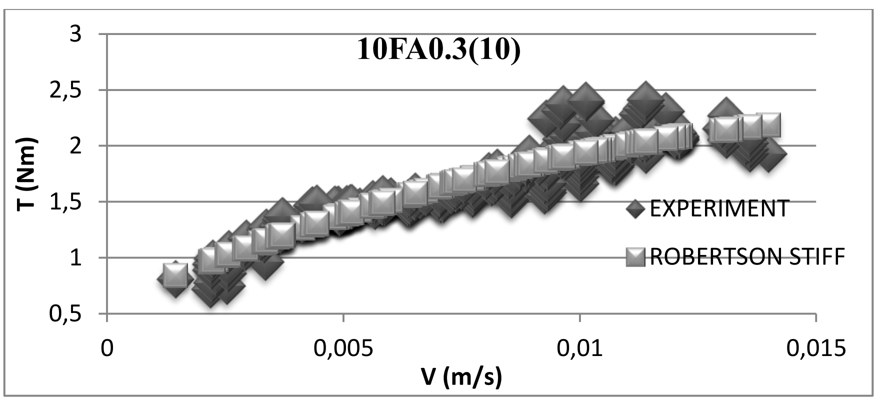

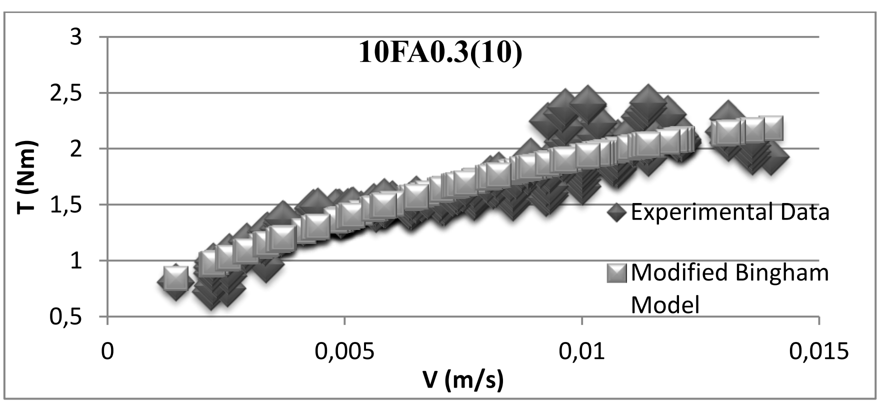

Figure A.11 Flow Models for 10FA 0.3 (10)

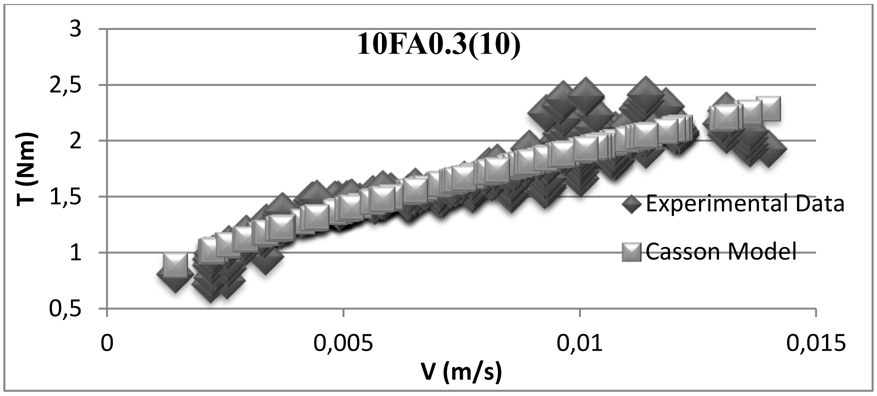

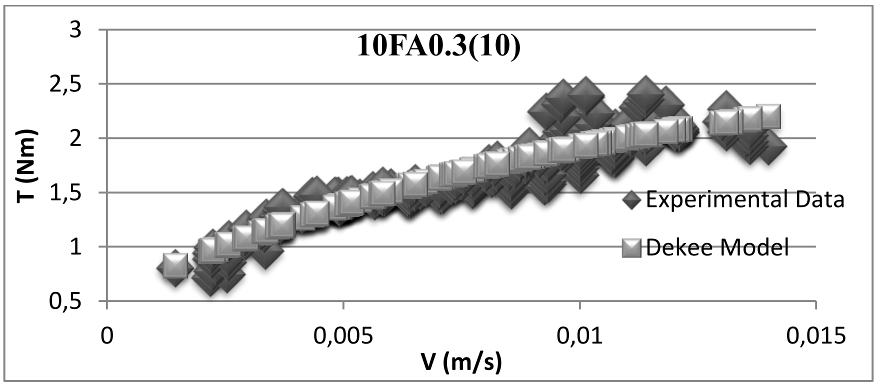

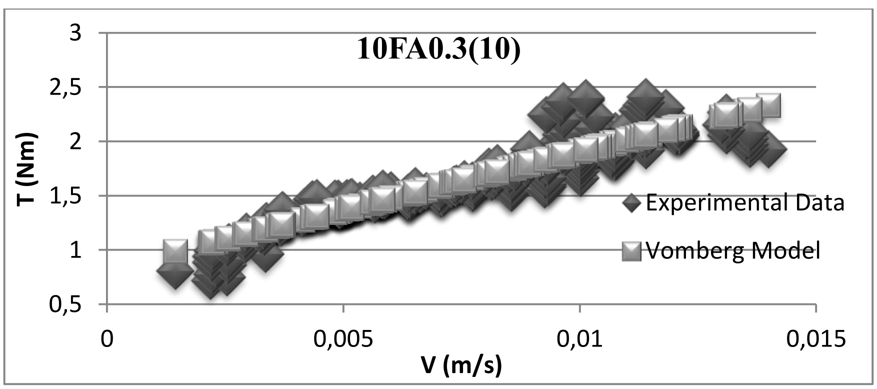

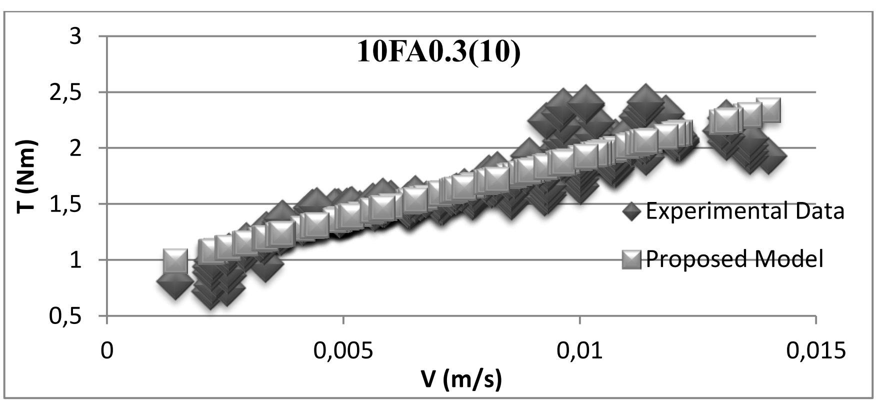

Figure A.11. (Continued)

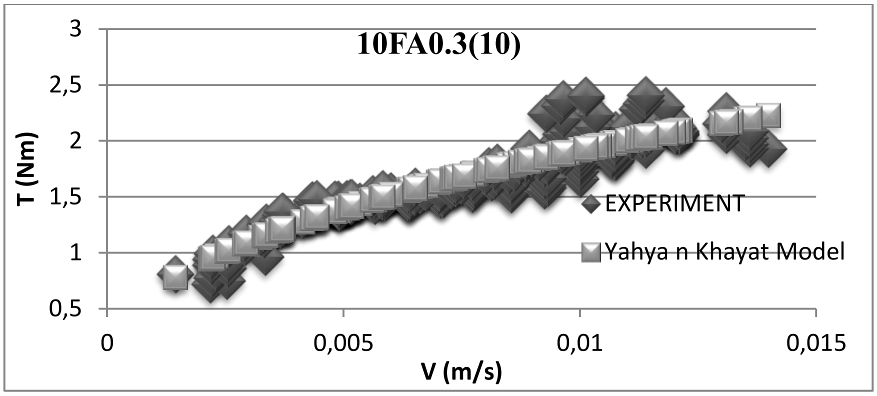

Figure A.11. (Continued)

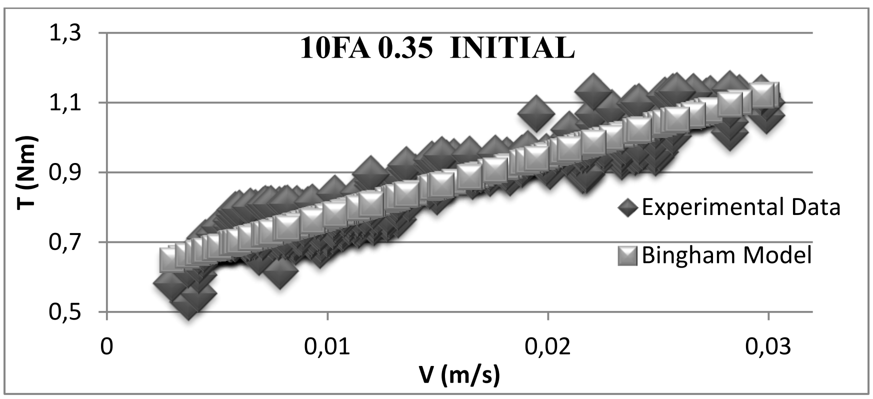

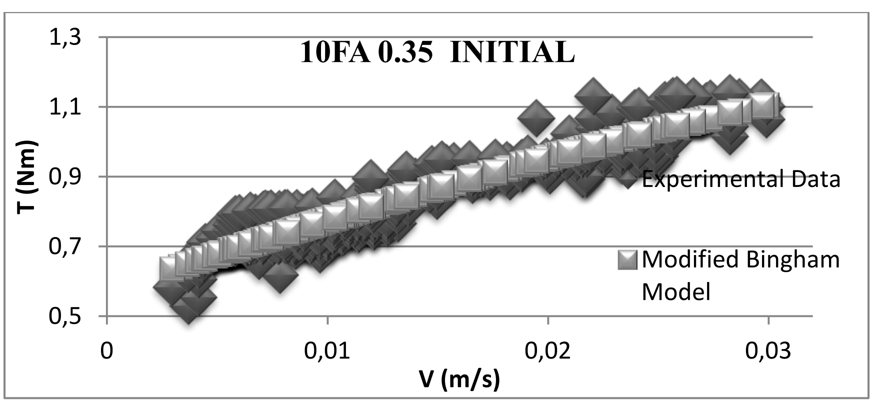

Figure A.12 Flow Models for 10FA0.35

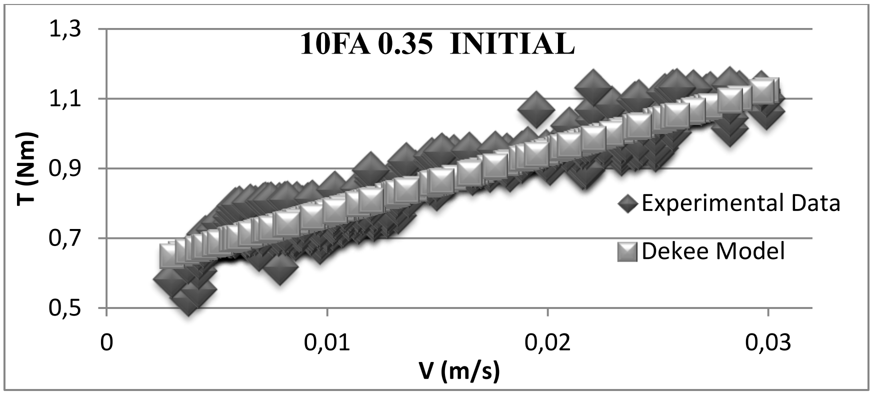

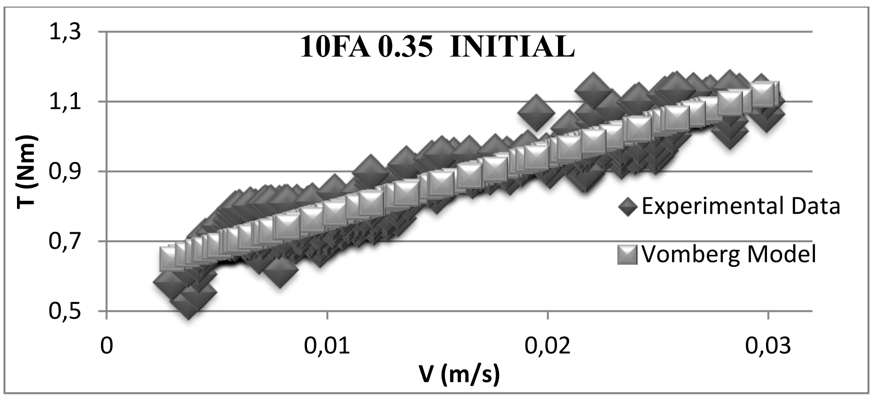

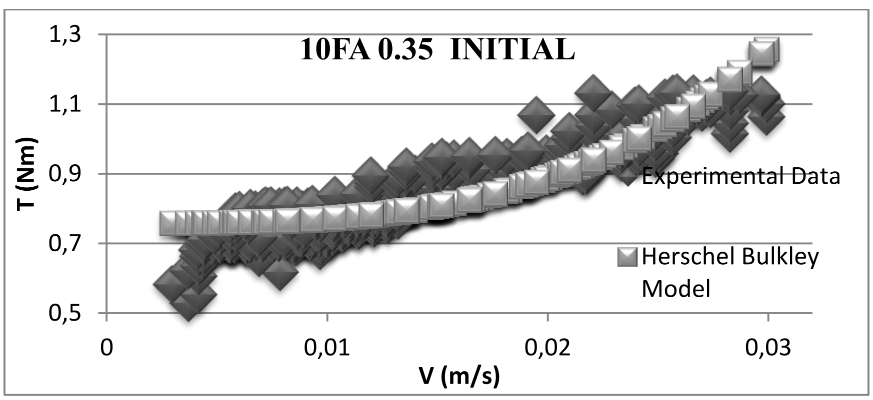

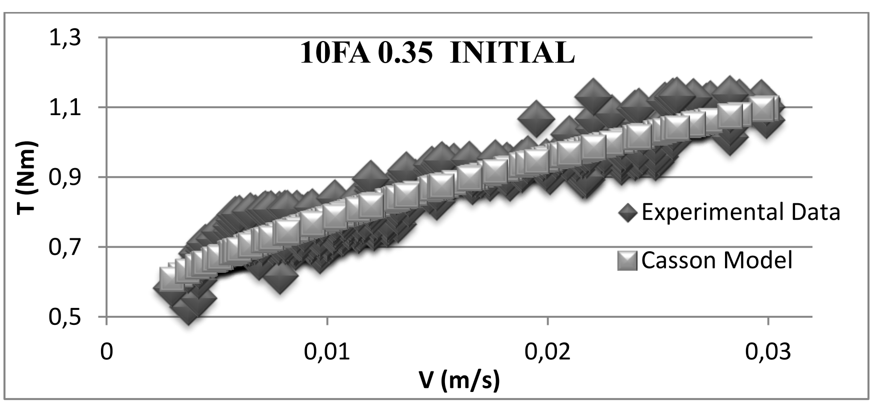

Figure A.12. (Continued)

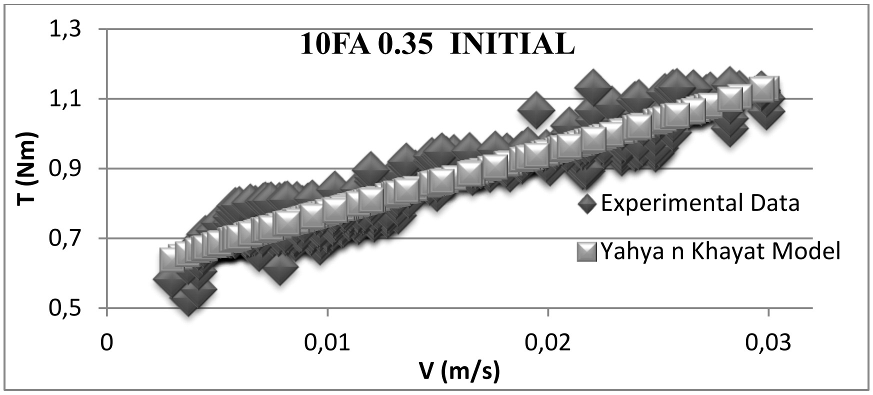

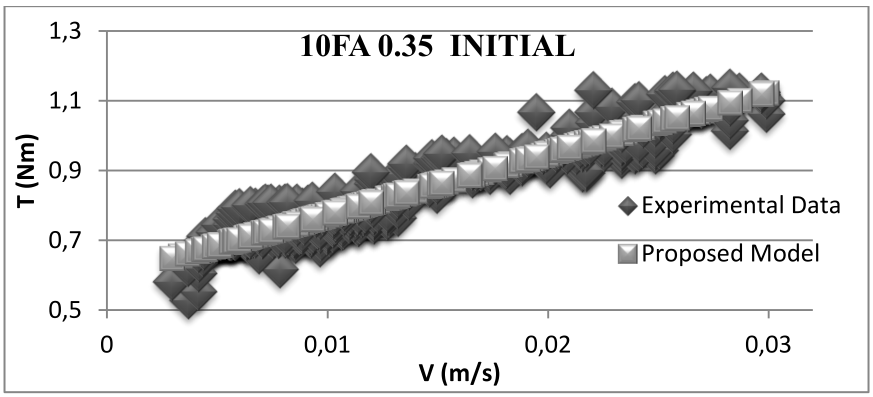

x

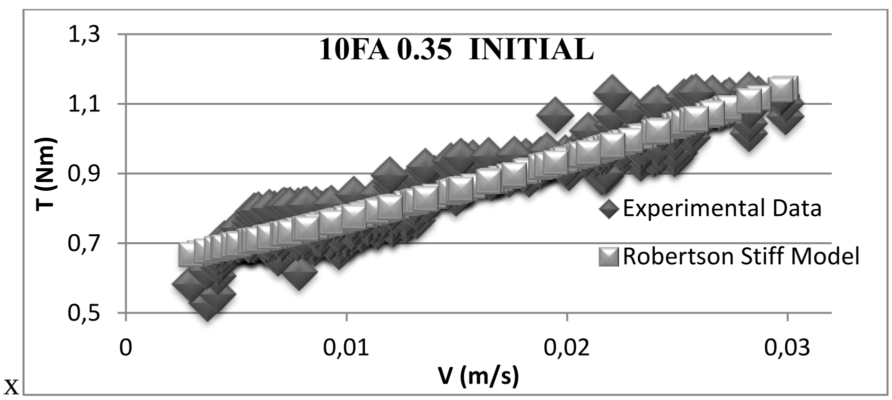

Figure A.12. (Continued)

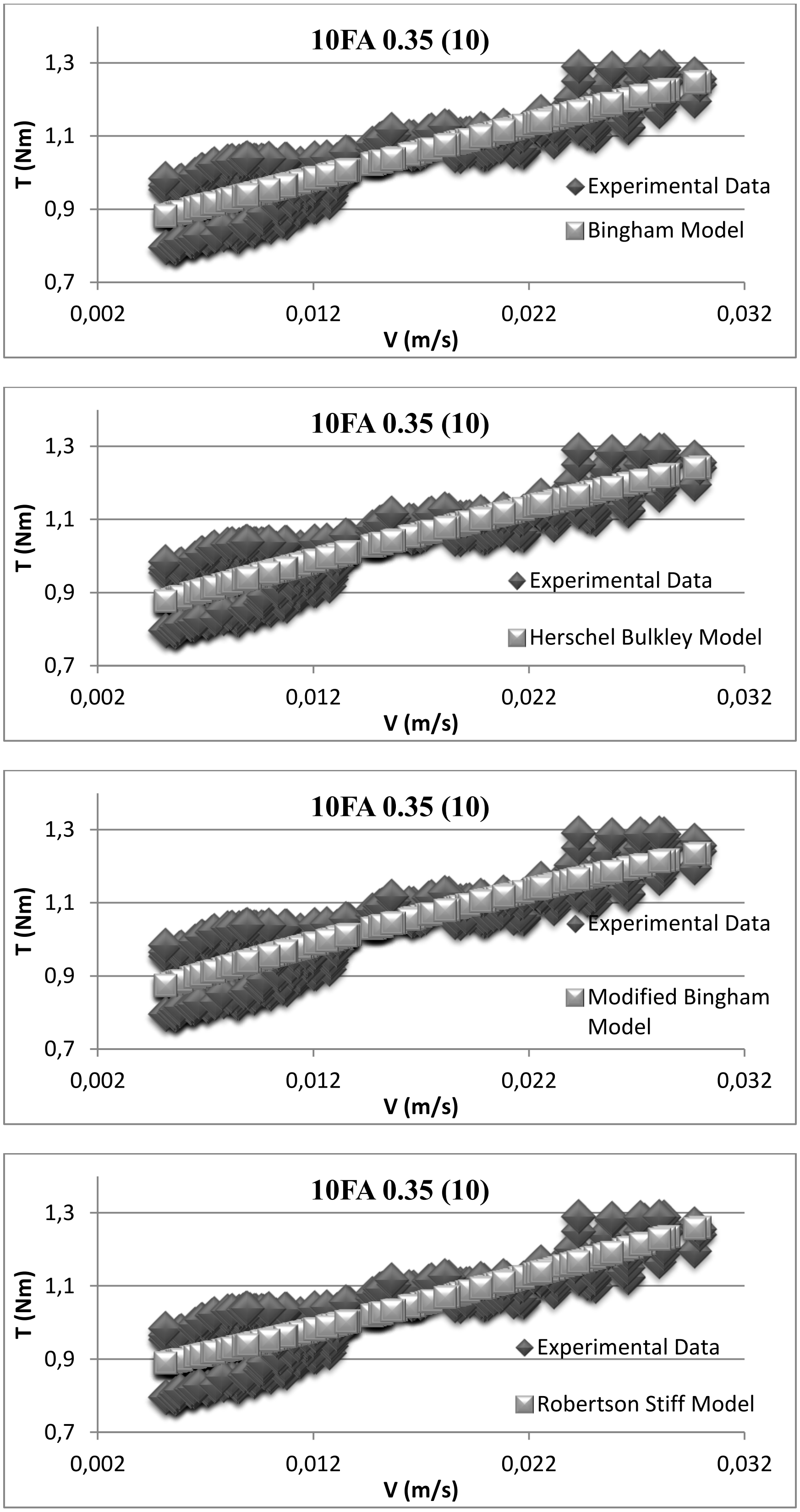

Figure A.13 Flow Models for 10FA0.35(10)

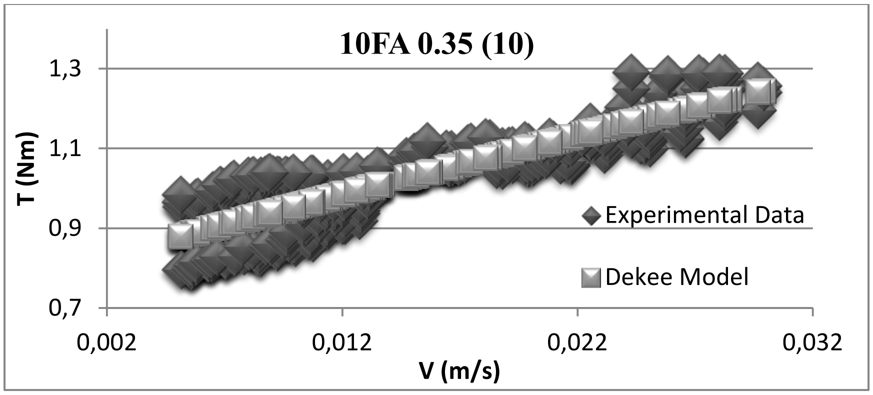

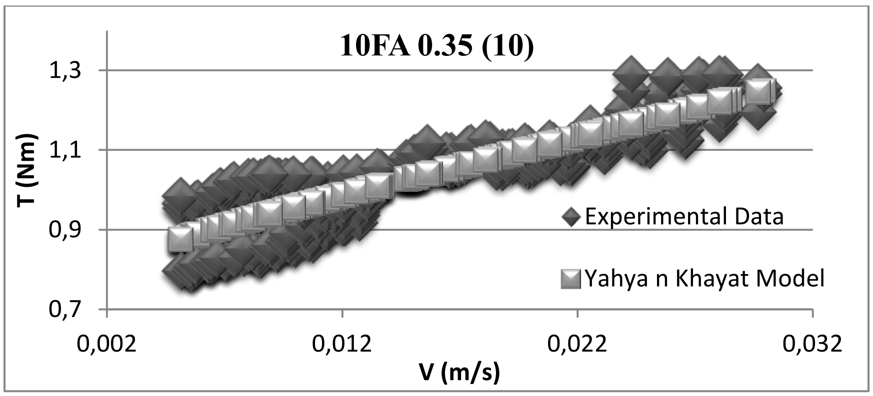

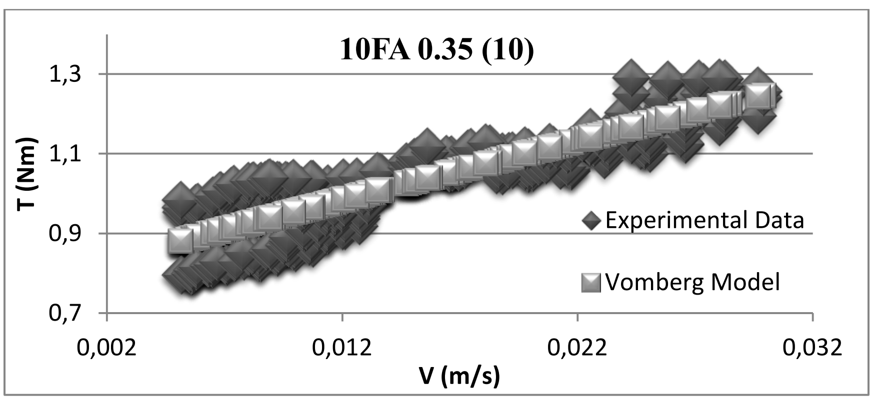

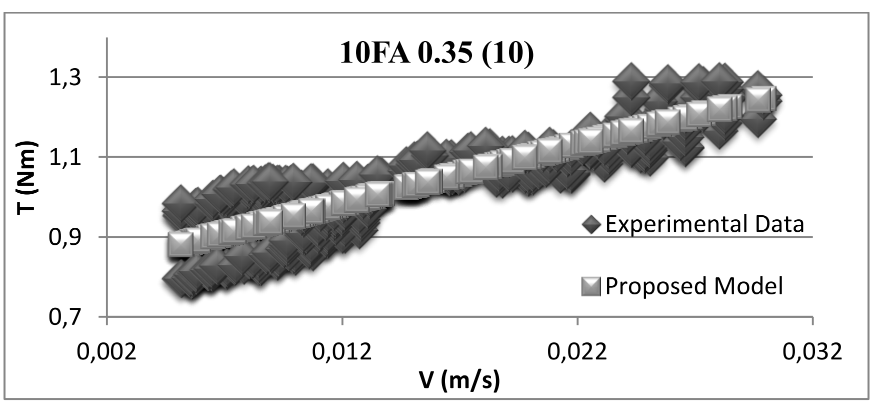

Figure A.13 (Continued)

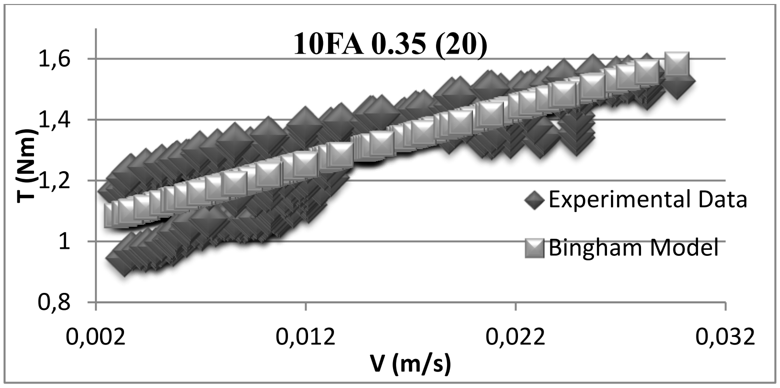

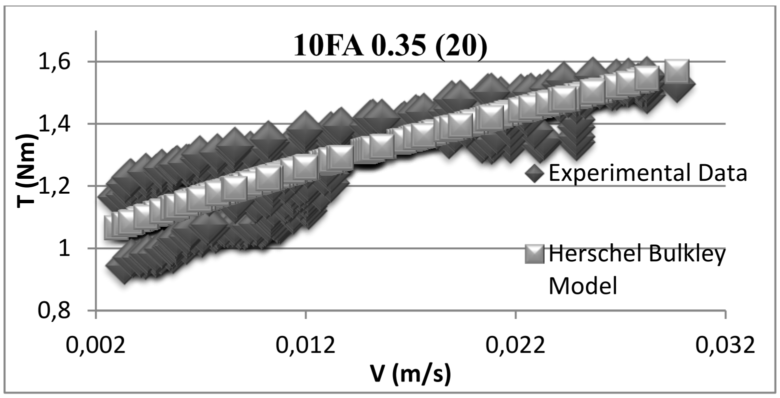

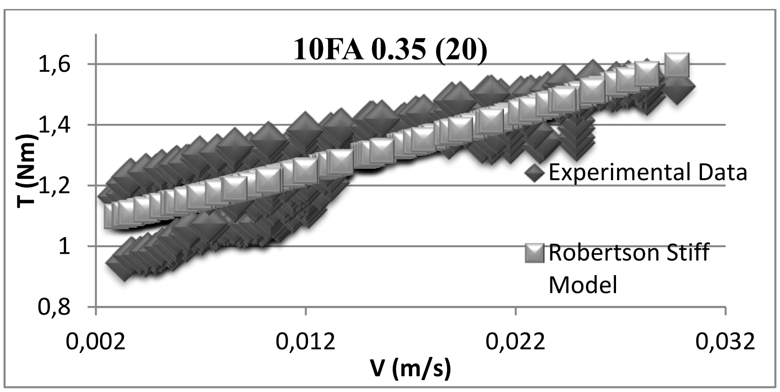

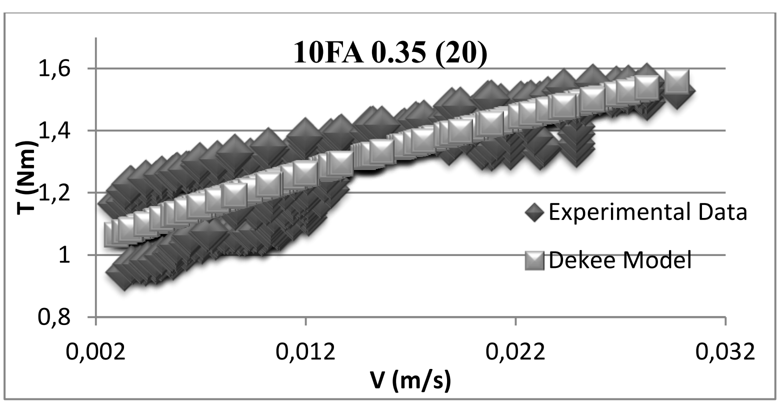

Figure A.14 Flow Models for 10 FA0.35(20)

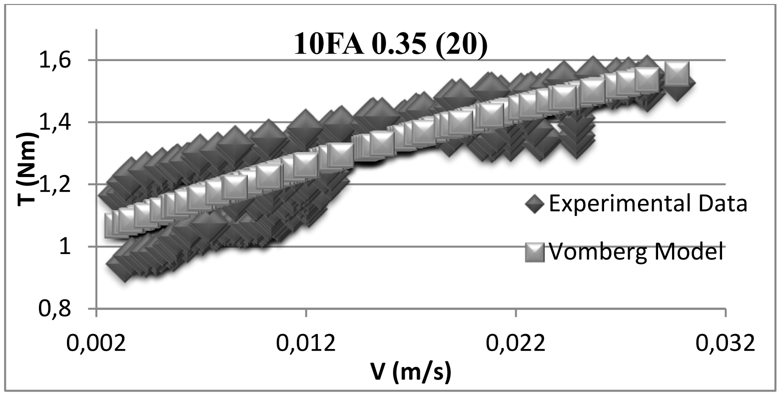

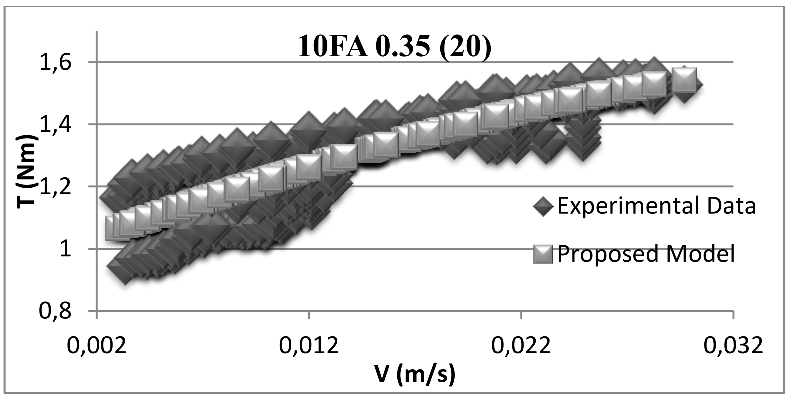

Figure A.14 (Continued)

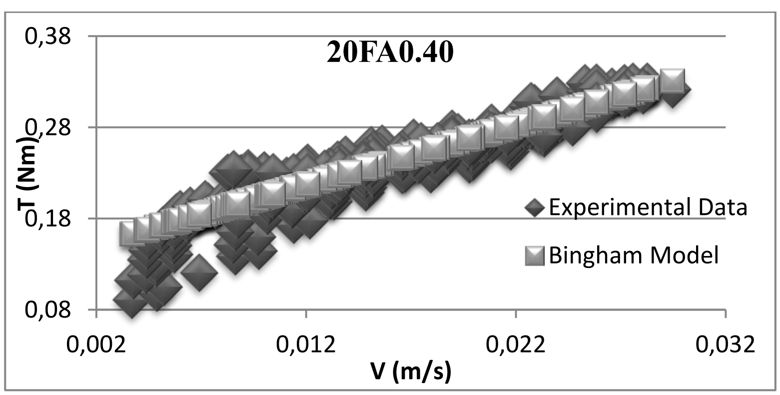

Figure A.15 Flow Models for 20FA 0.4

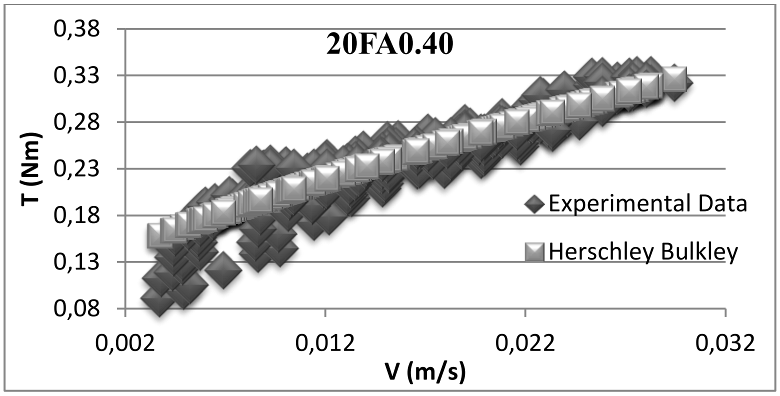

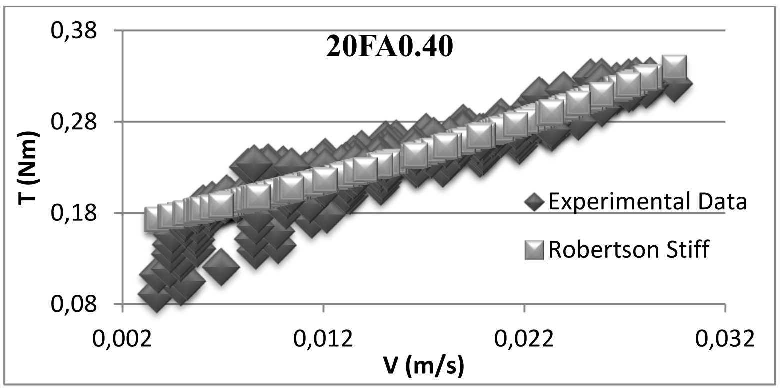

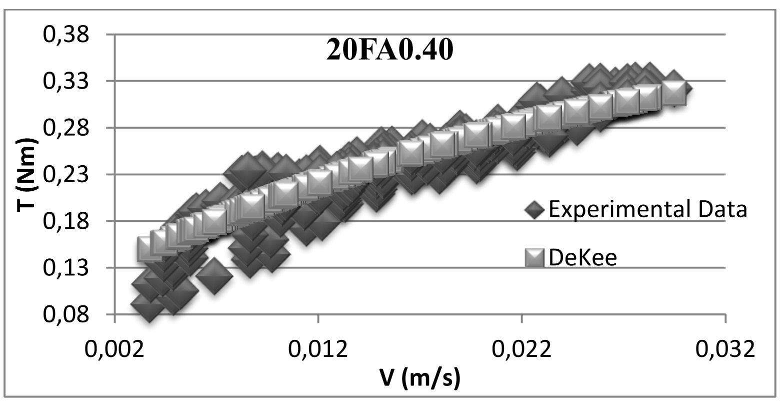

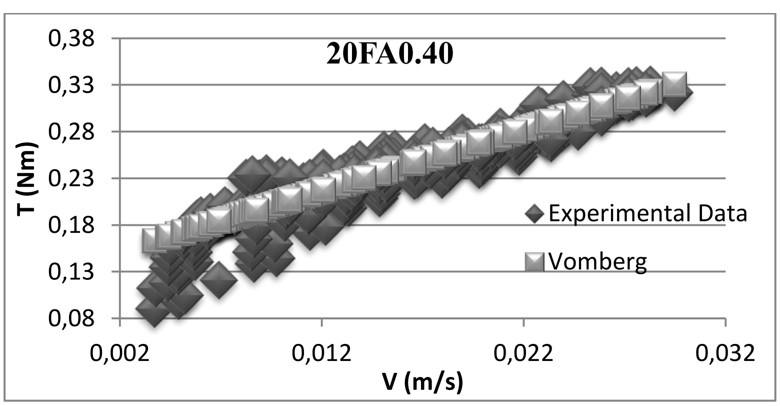

Figure A.15 (Continued)

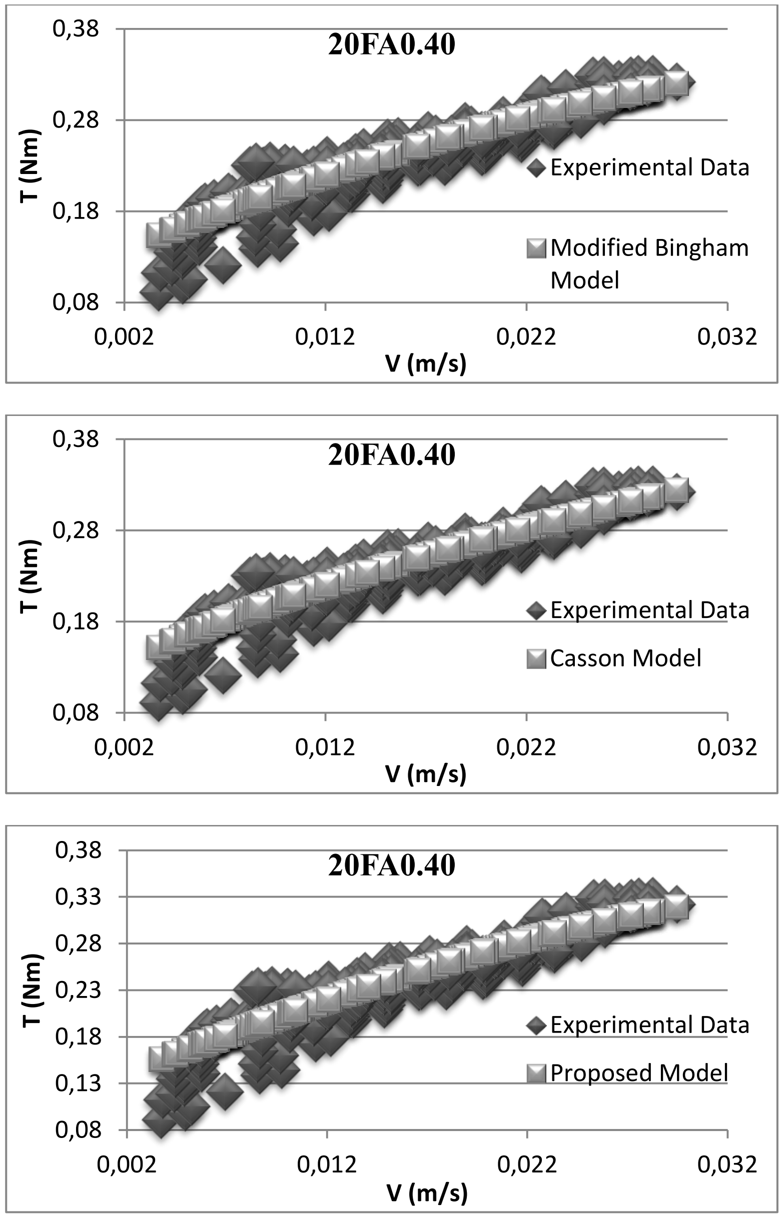

Figure A.15 (Continued)

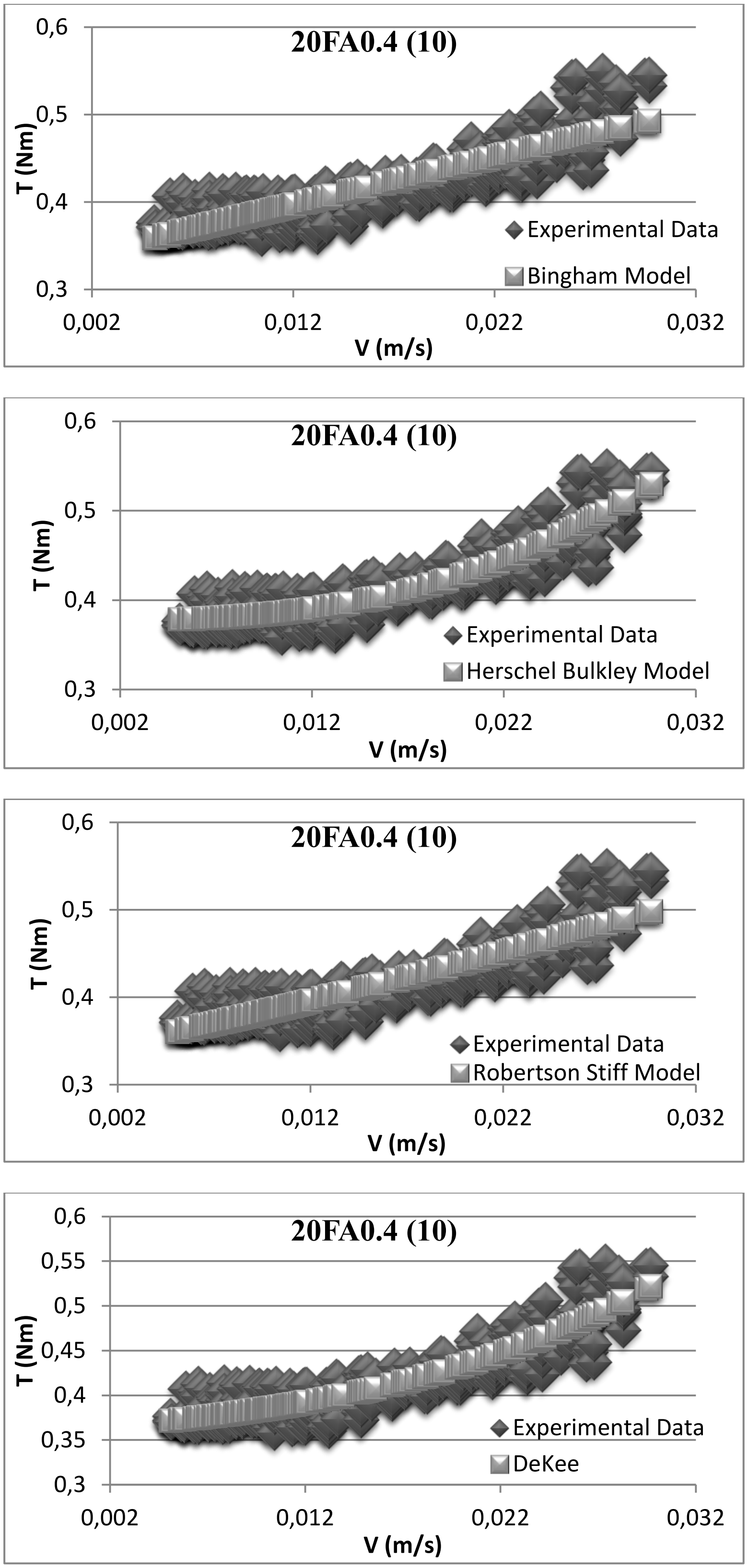

Figure A.16. Flow Models for 20FA 0.4(10)

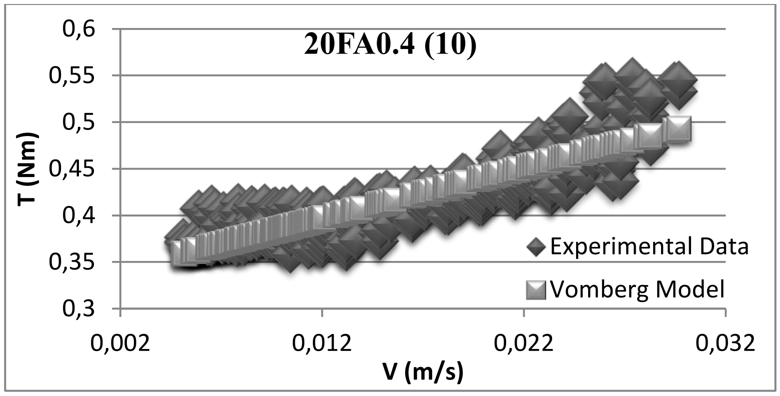

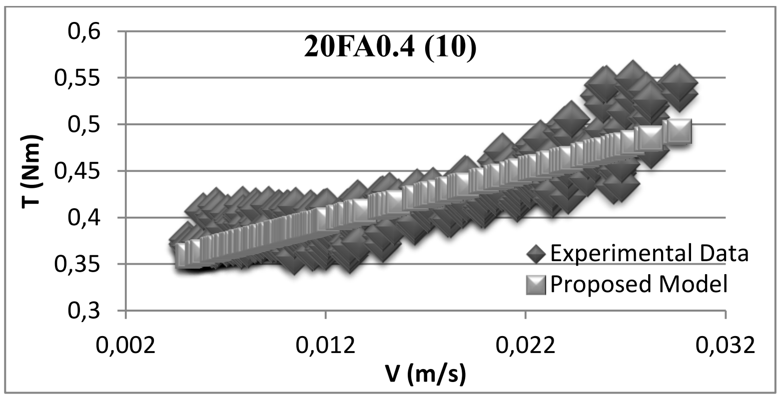

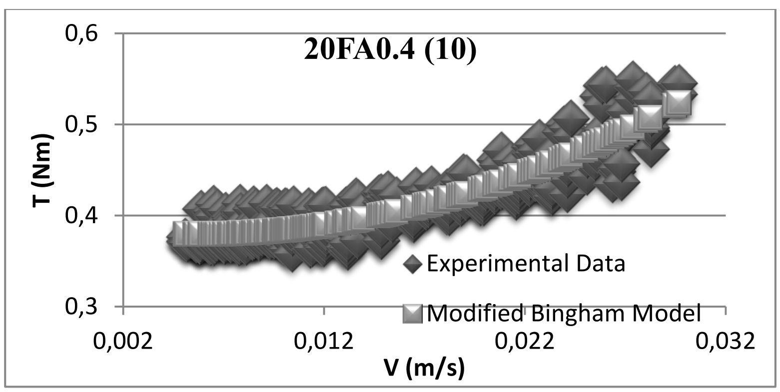

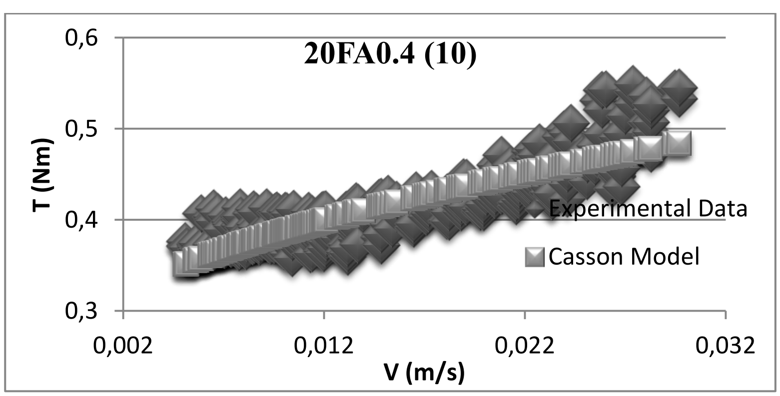

Figure A.16 (Continued)

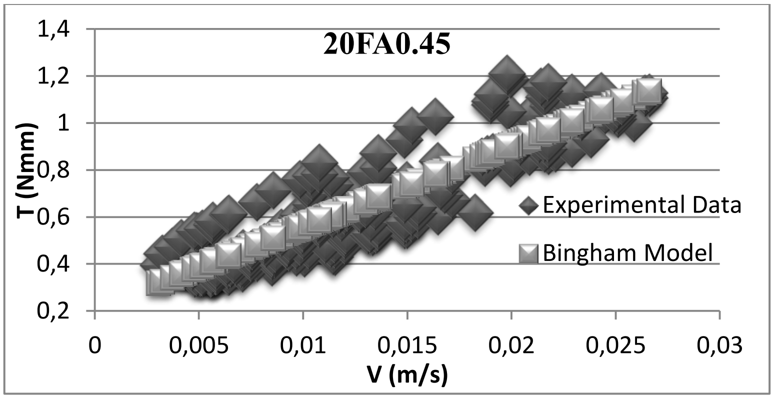

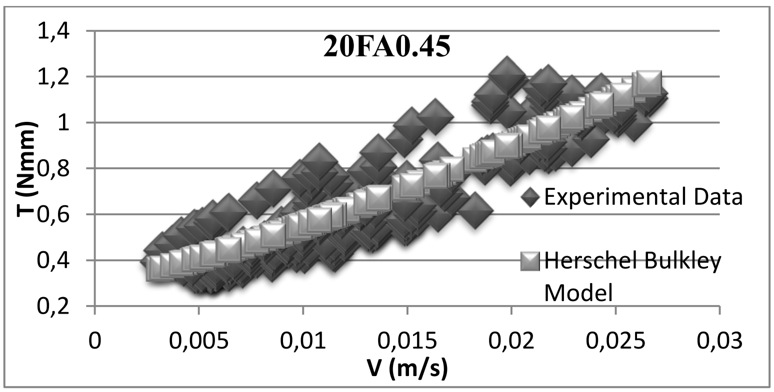

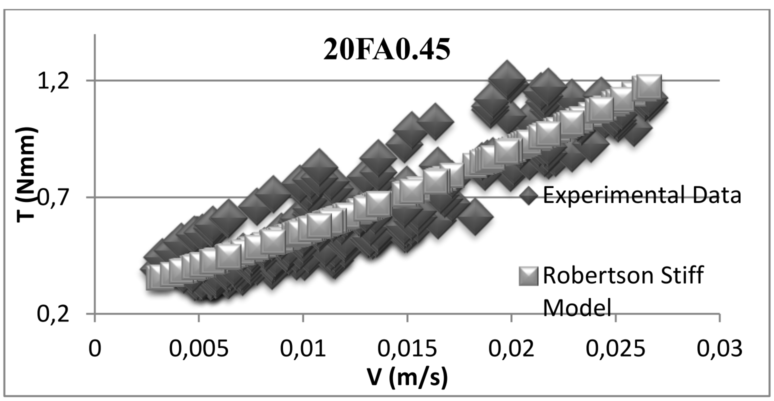

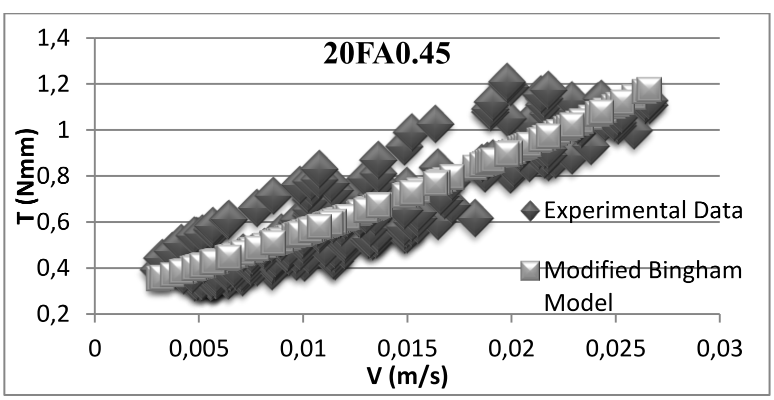

Figure A.17 Flow Models for 20FA 0.45

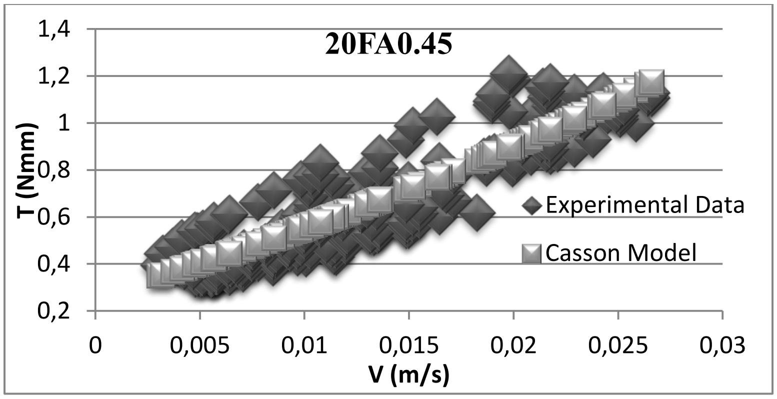

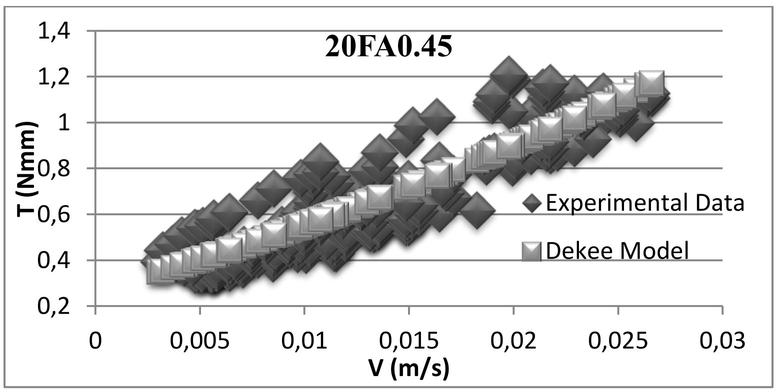

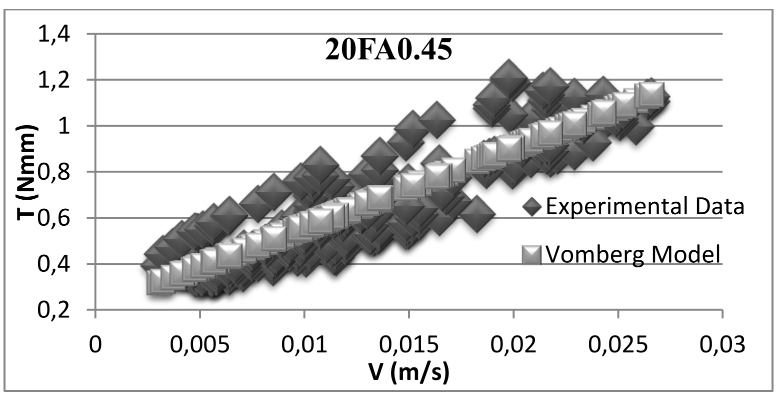

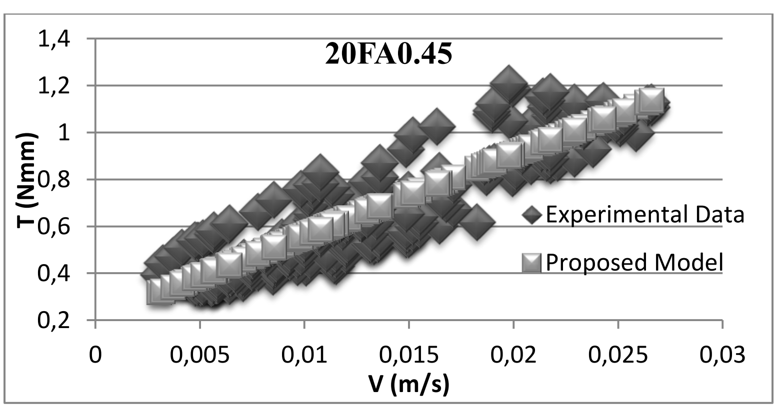

Figure A.17 (Continued)

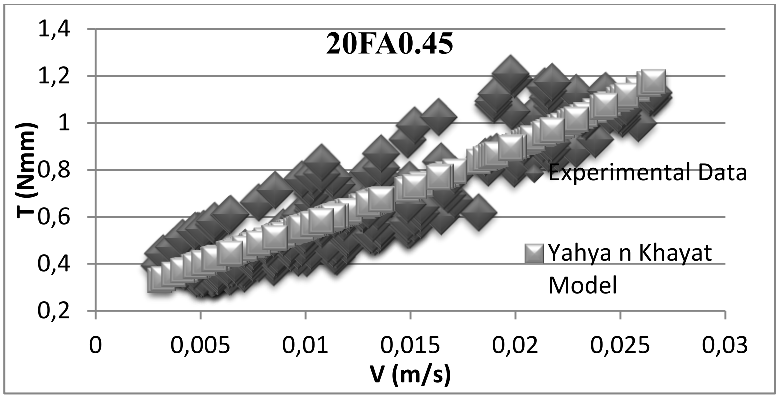

Figure A.17 (Continued)

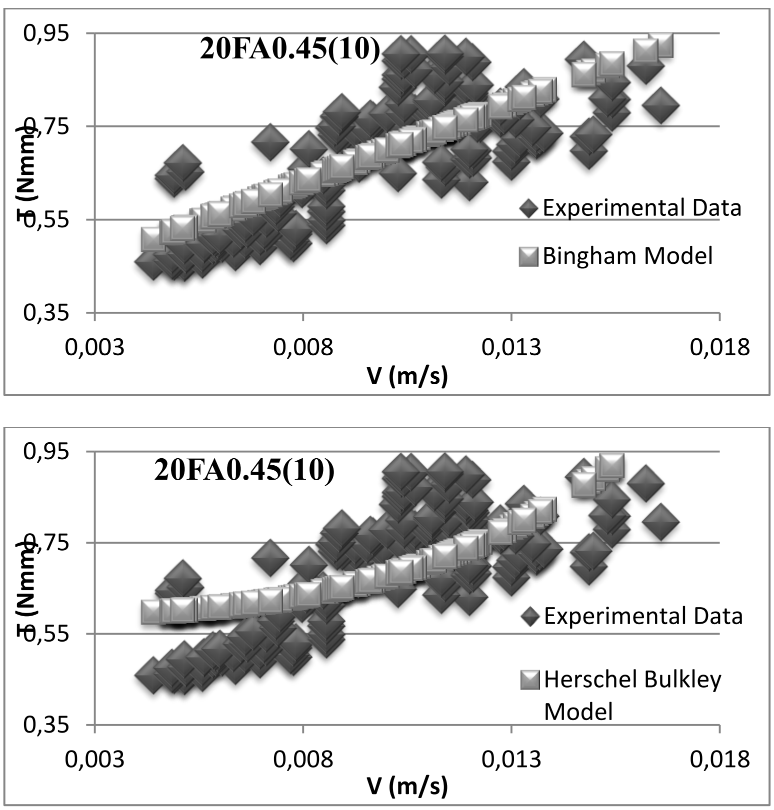

Figure A.18 Flow Models for 20FA 0.45(10)

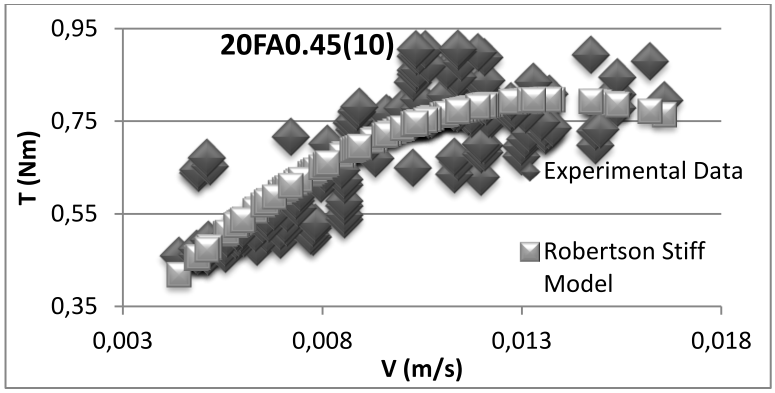

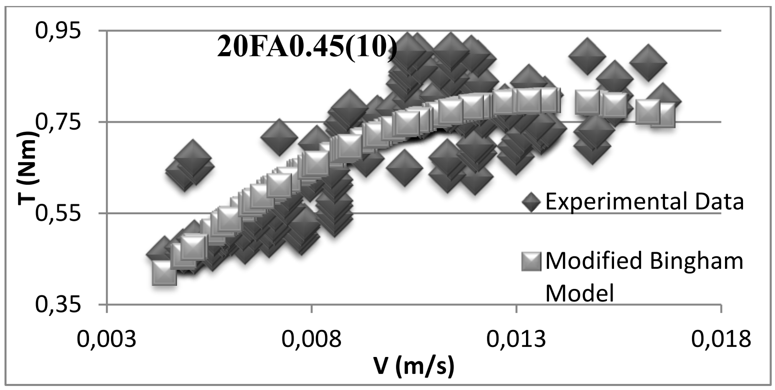

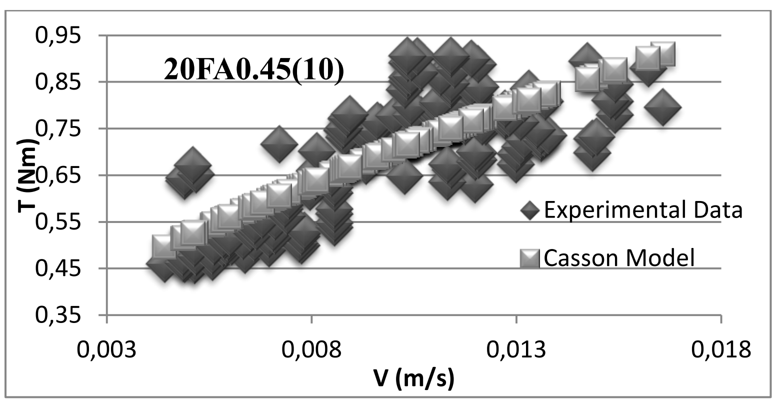

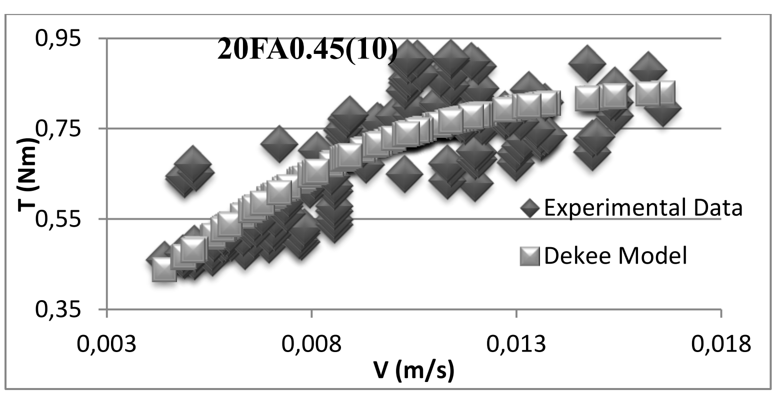

Figure A.18. (Continued)

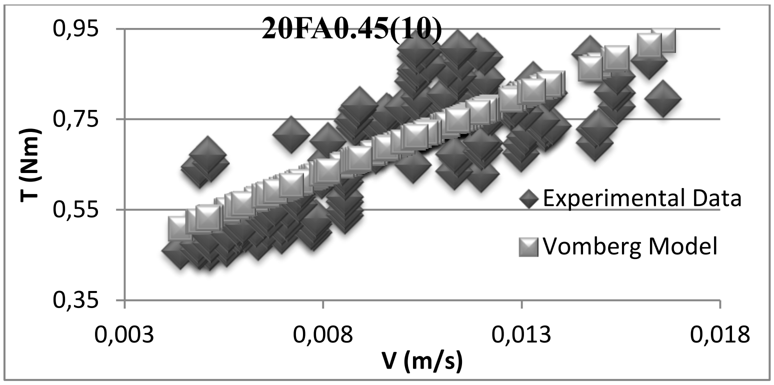

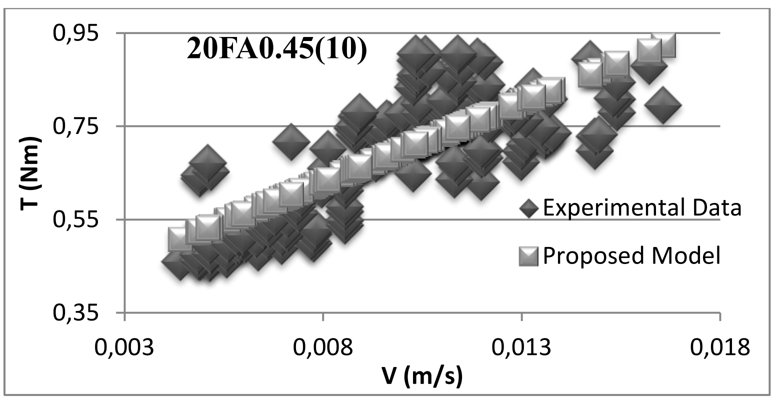

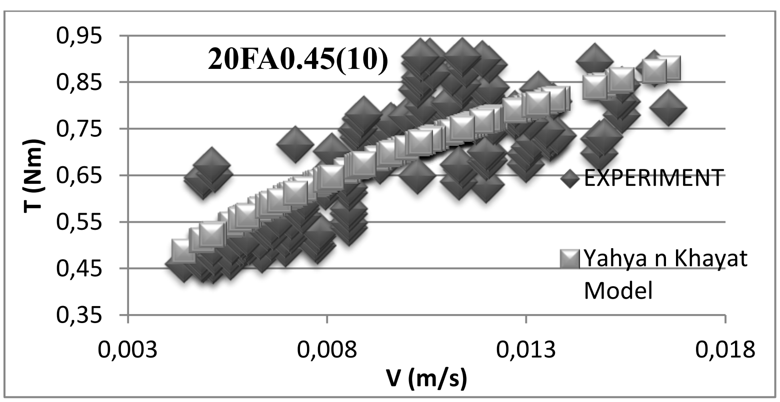

Figure A.18. (Continued)

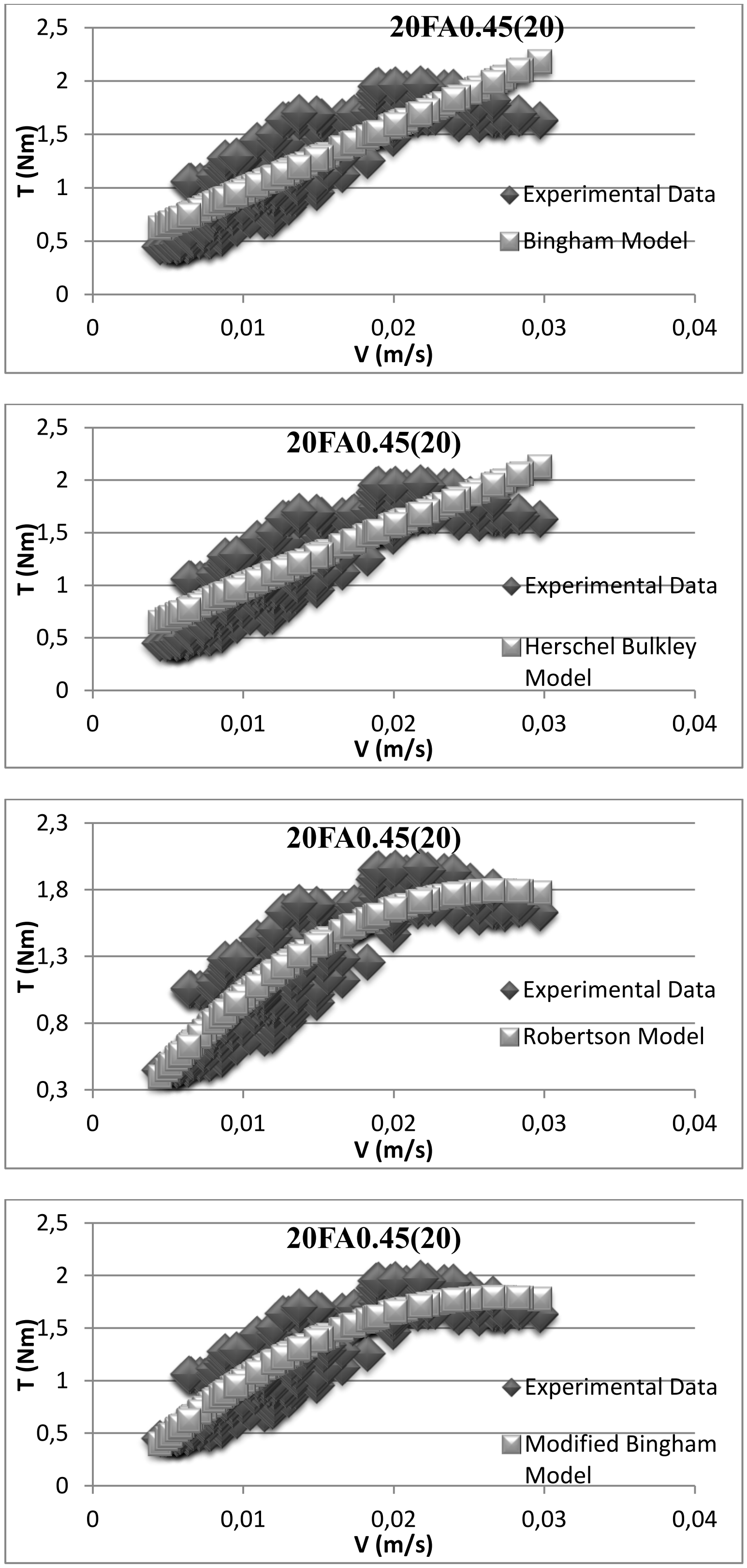

Figure A.19 Flow Models for 20FA 0.45(20)

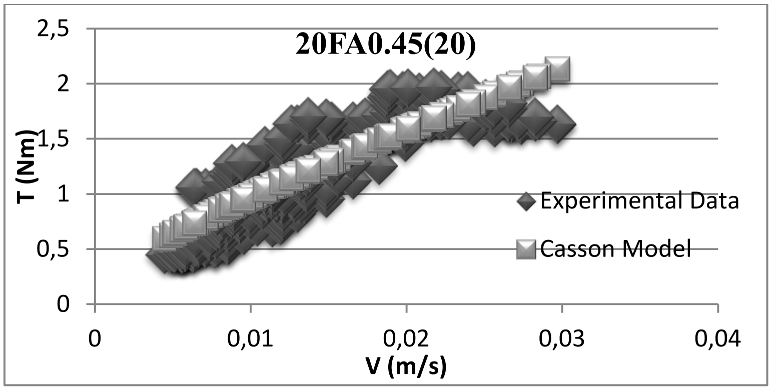

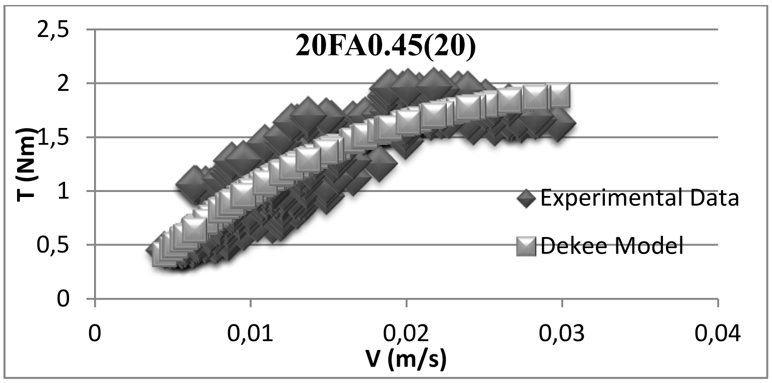

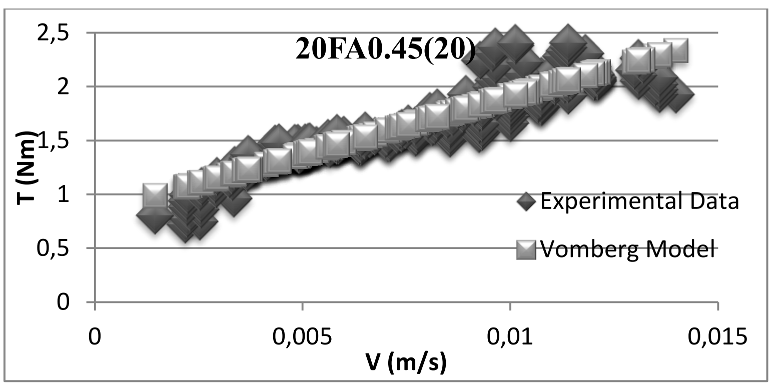

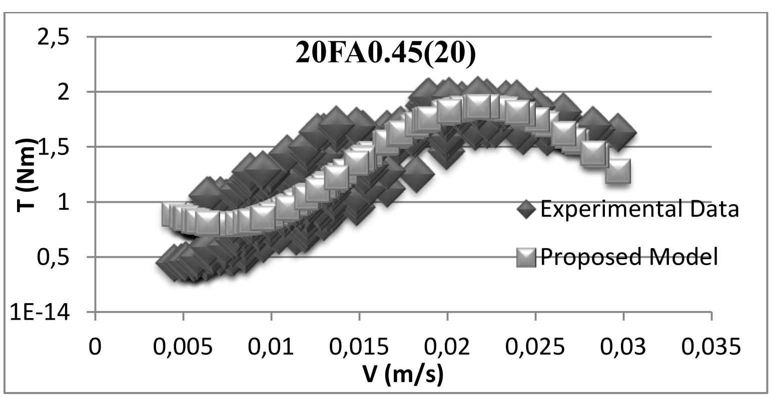

Figure A.19. (Continued)

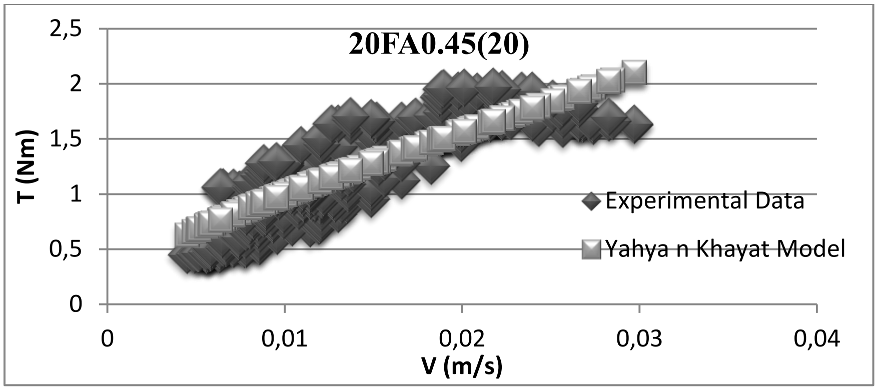

Figure A.19. (Continued)

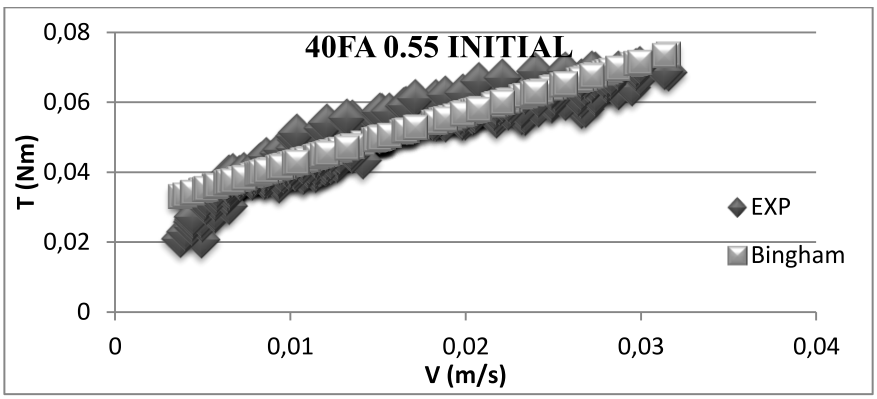

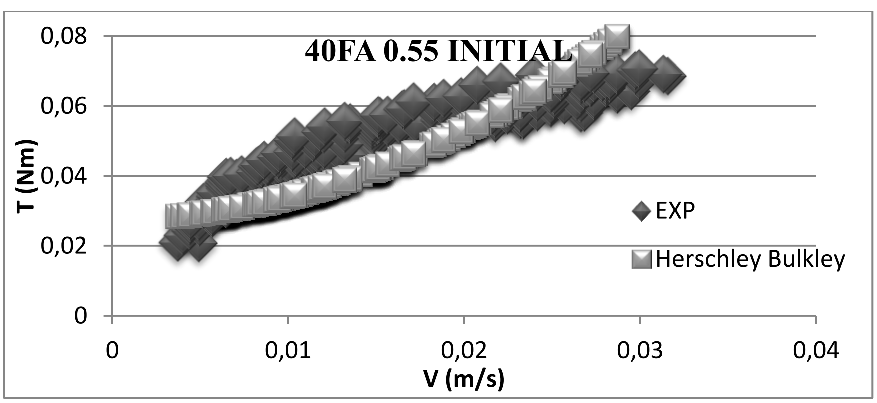

Figure A.20 Flow Models for 40FA0.55,

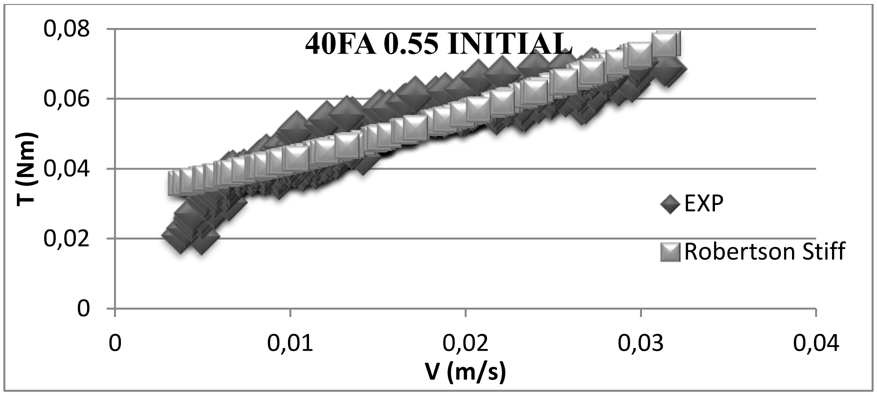

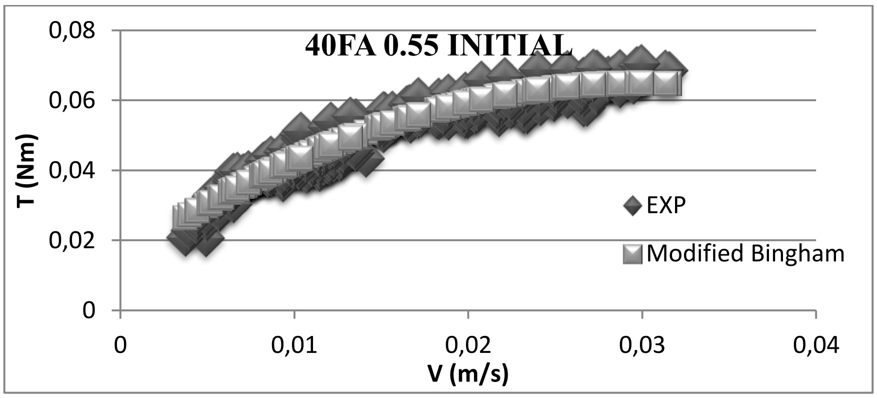

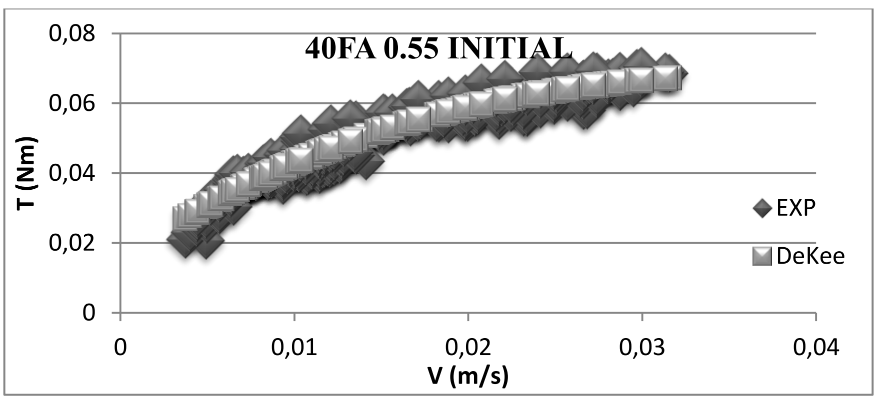

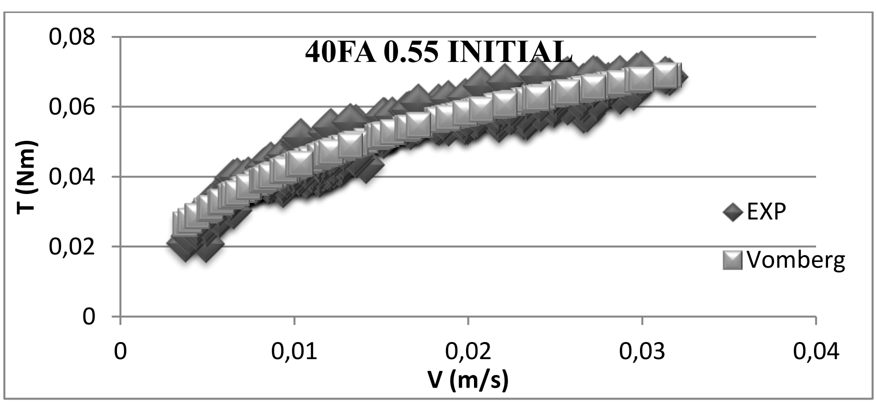

Figure A.20 (Continued)

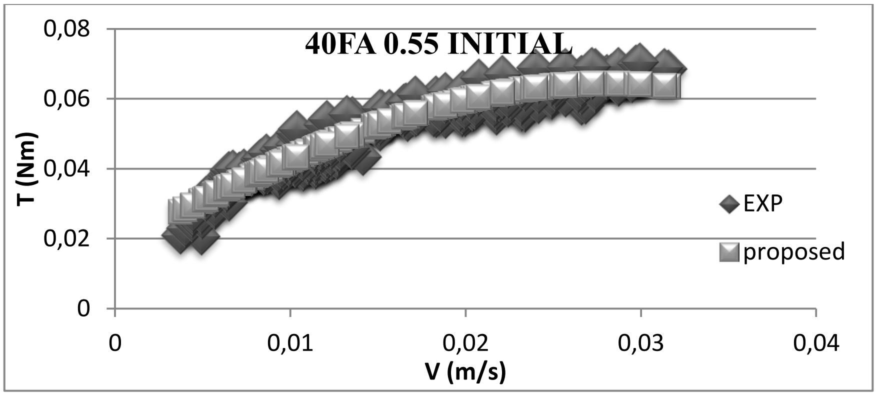

Figure A.20 (Continued)

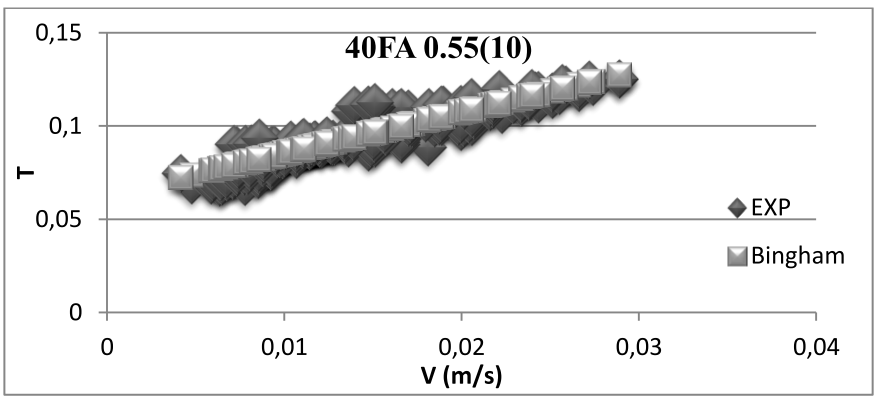

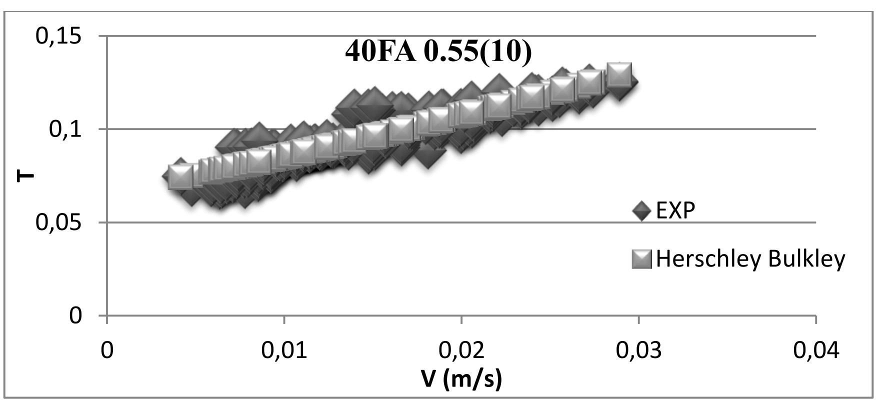

Figure A.21 Flow Models for 40FA0.55(10)

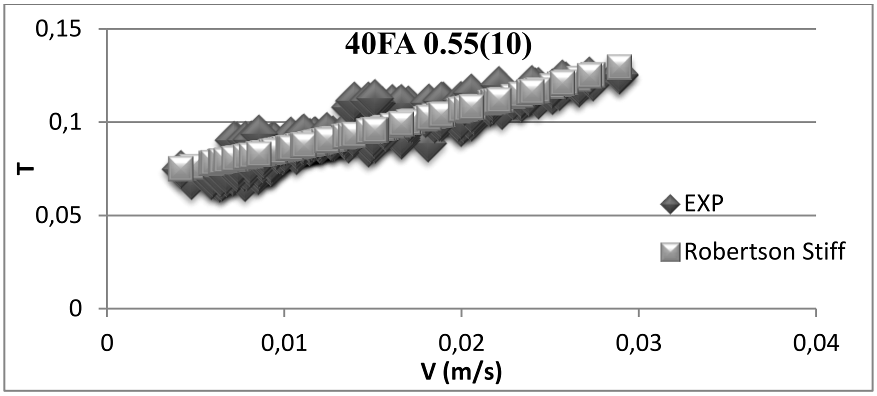

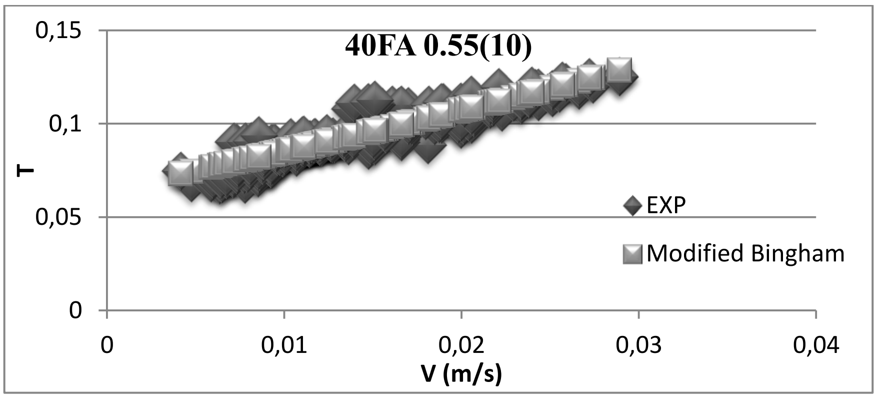

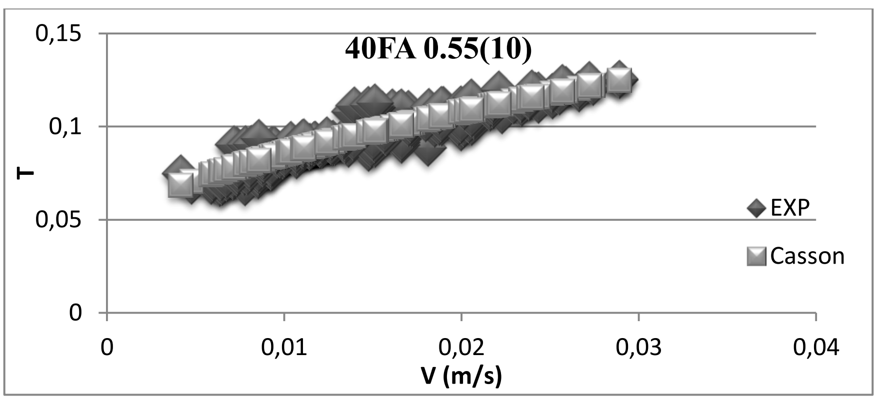

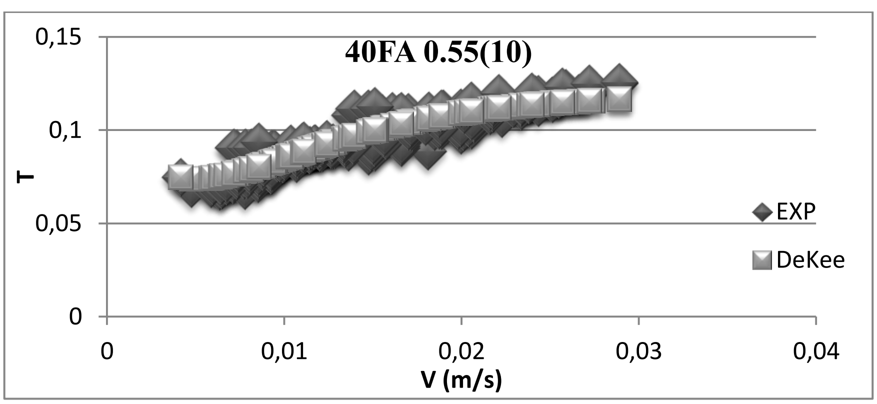

Figure A.21 (Continued)

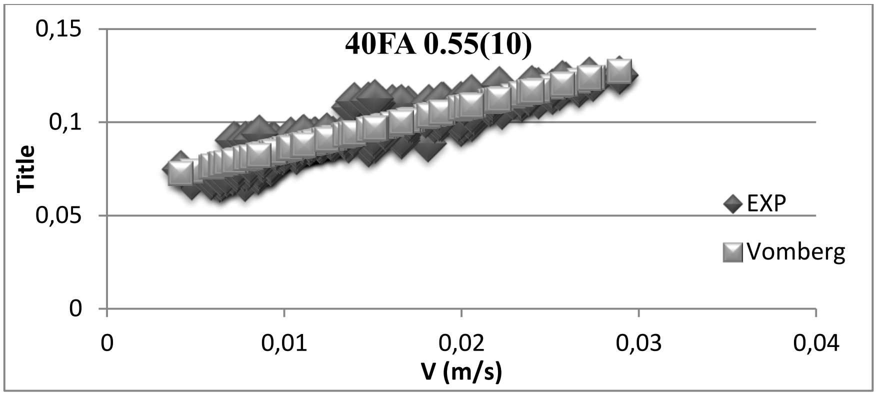

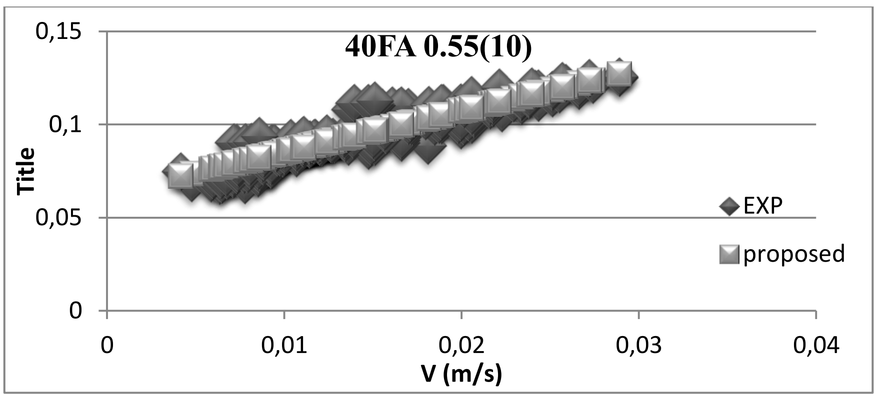

Figure A.21 (Continued)

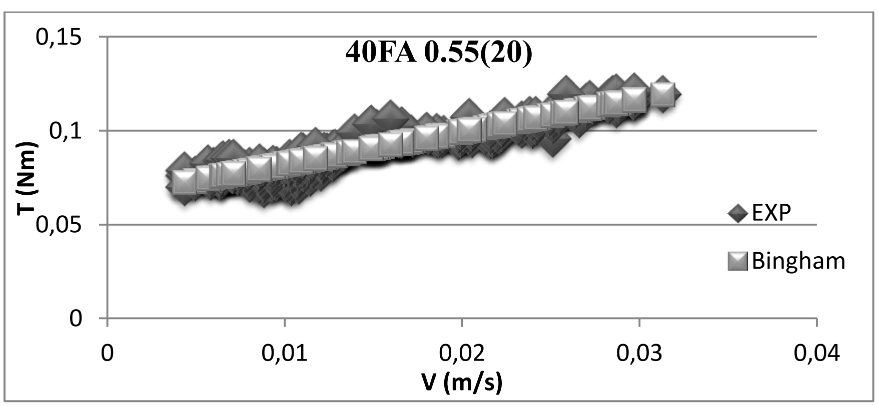

Figure A.22 FA0.55(20) , Different Models

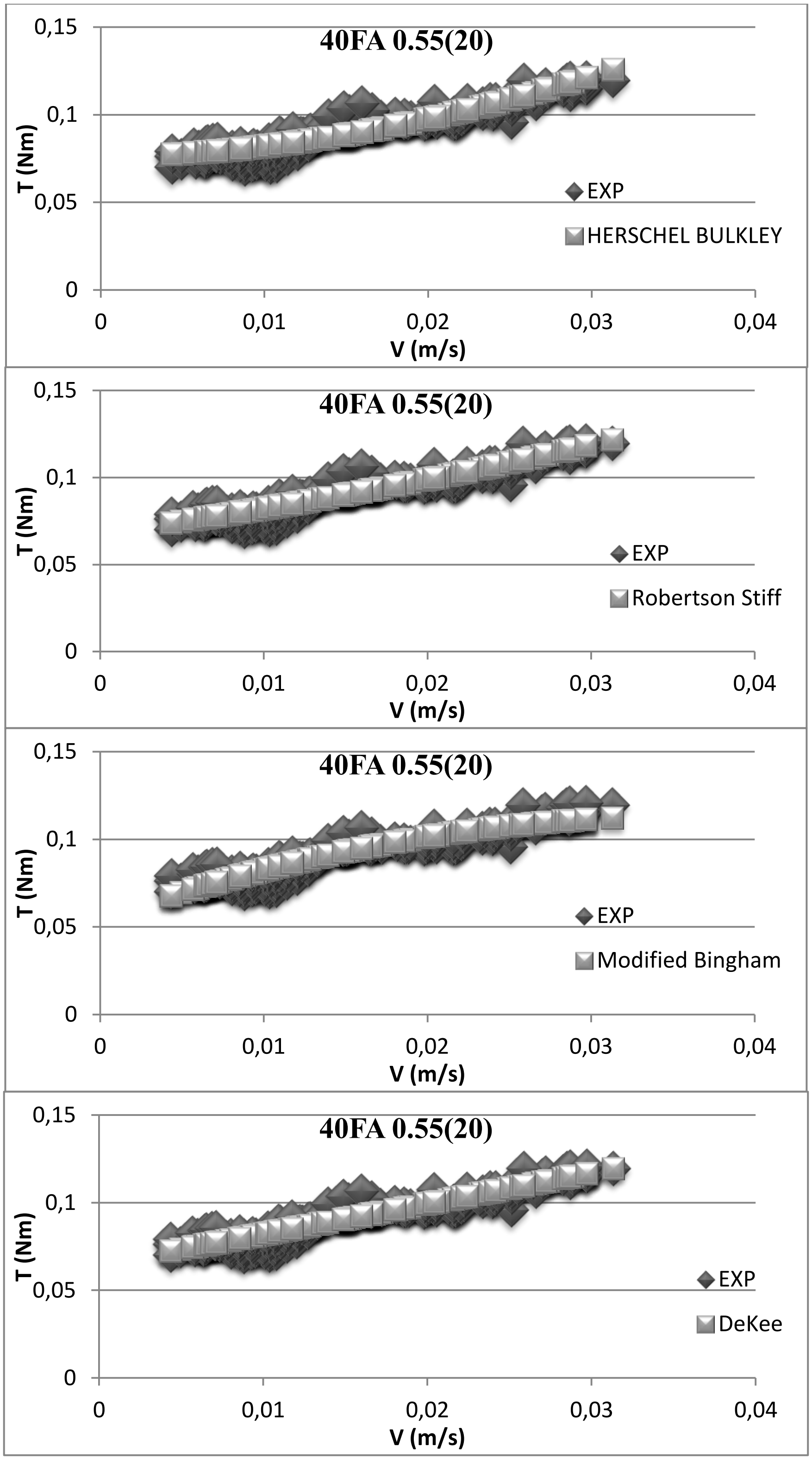

Figure A.22 (Continued)

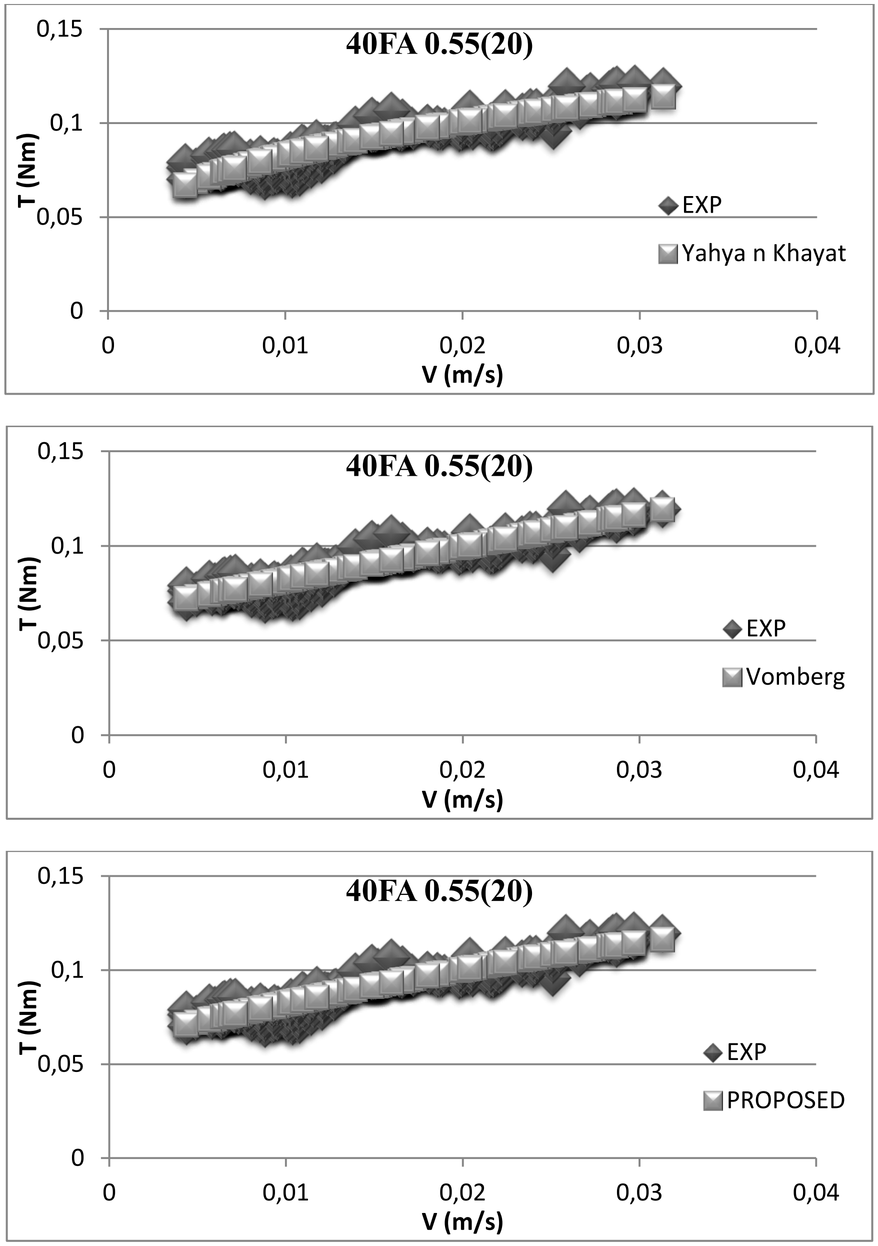

Figure A.22 (Continued)

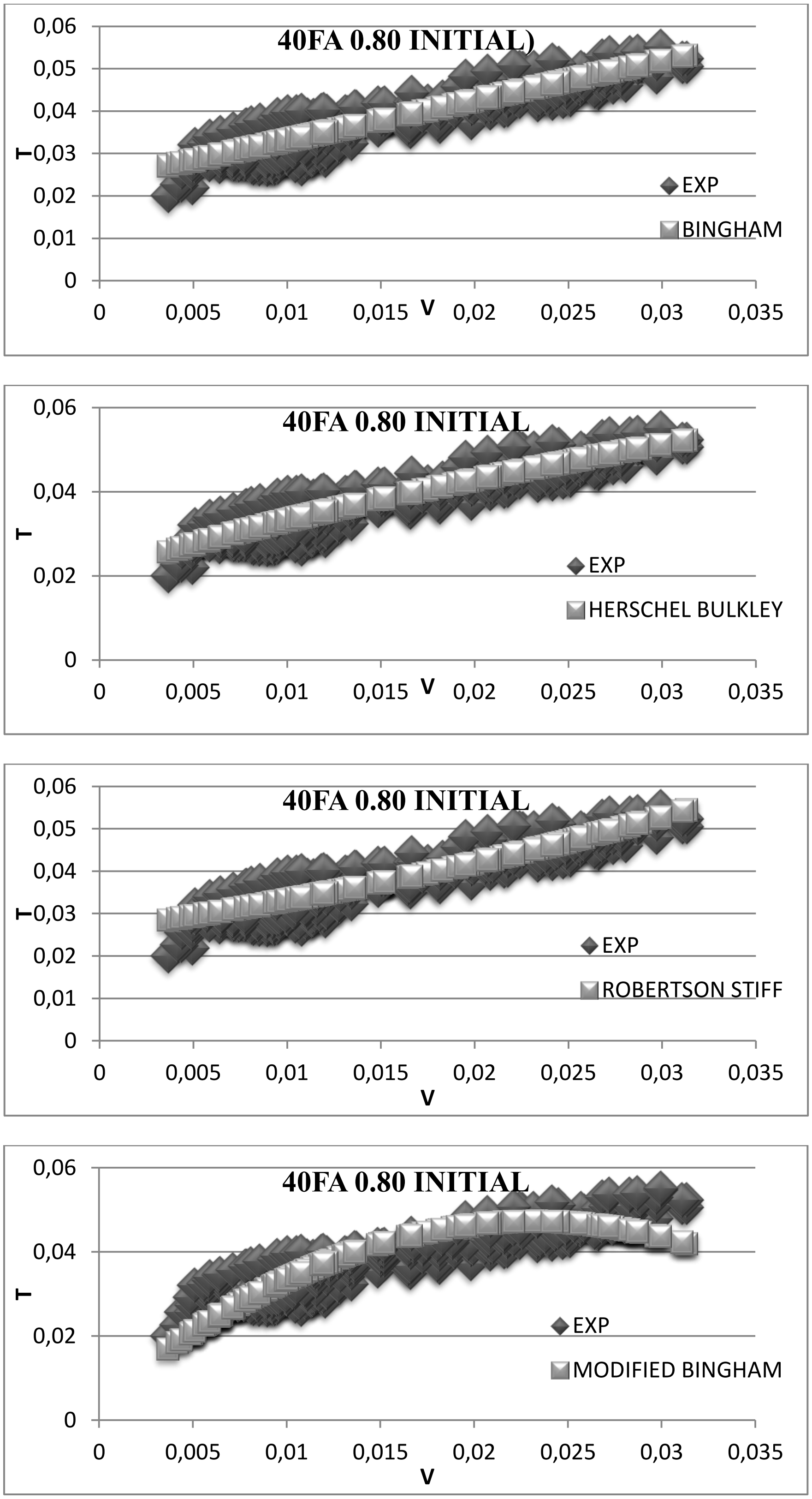

Figure A.23 Flow Models for 40FA0.8

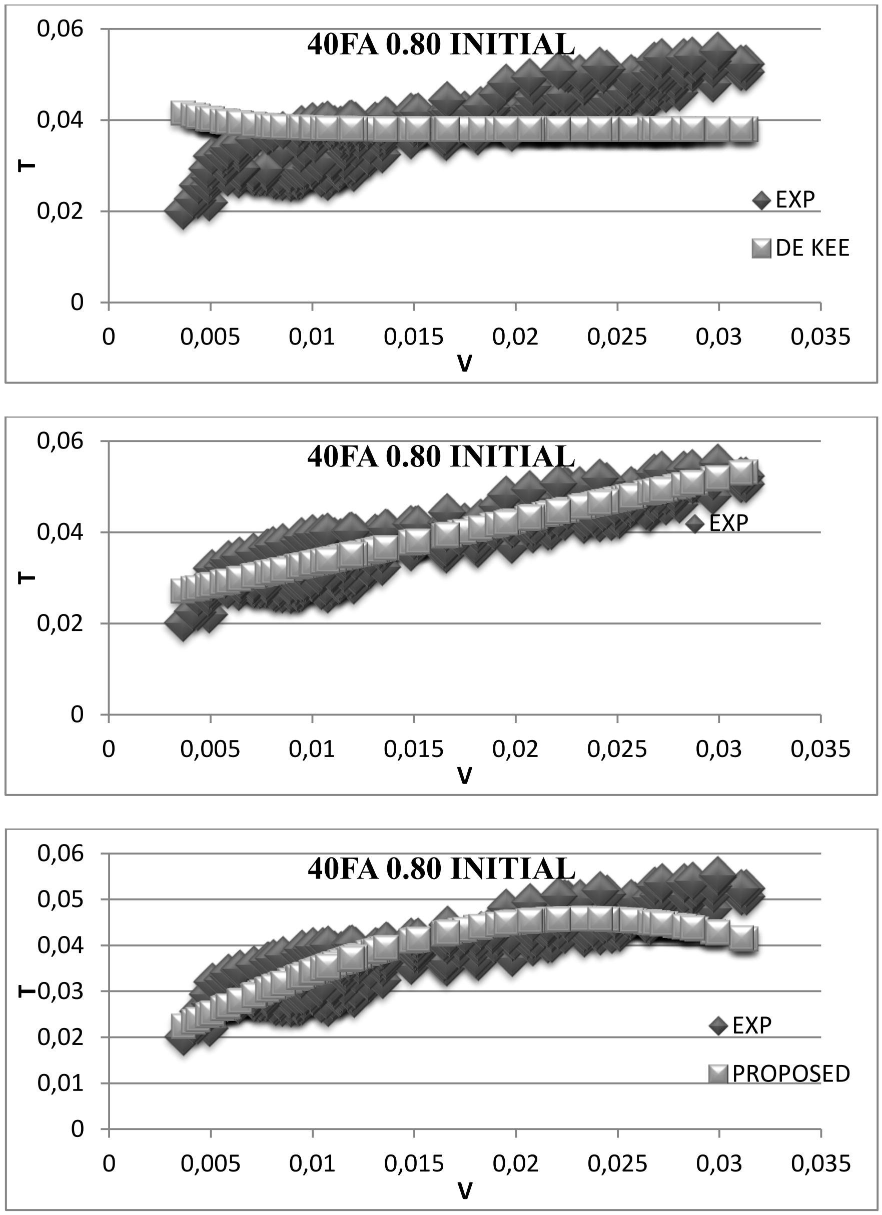

Figure A.23 (Continued)

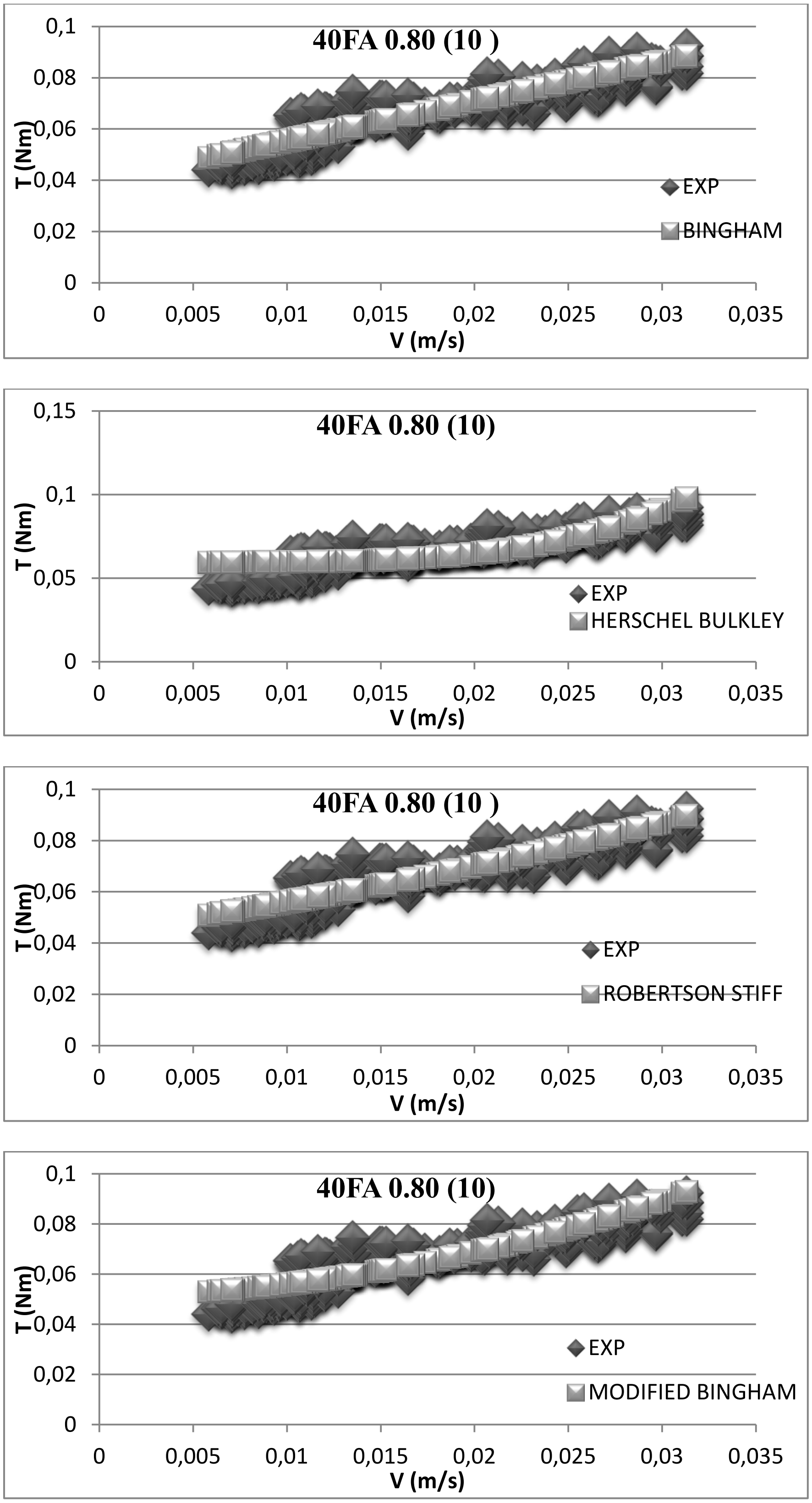

Figure A.24 Flow Models for 40FA0.8(10)

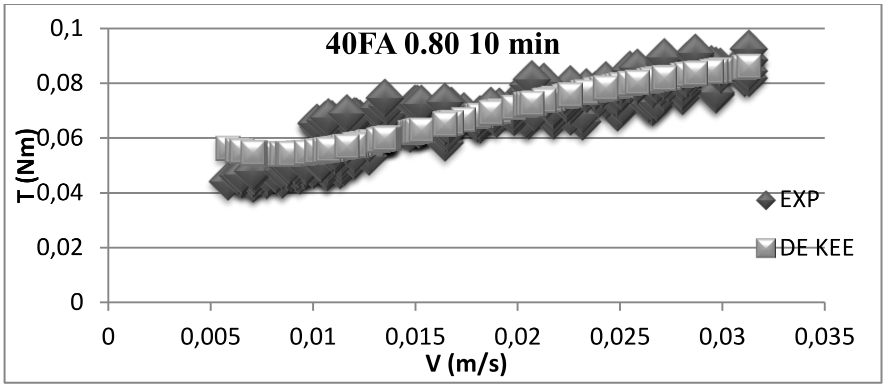

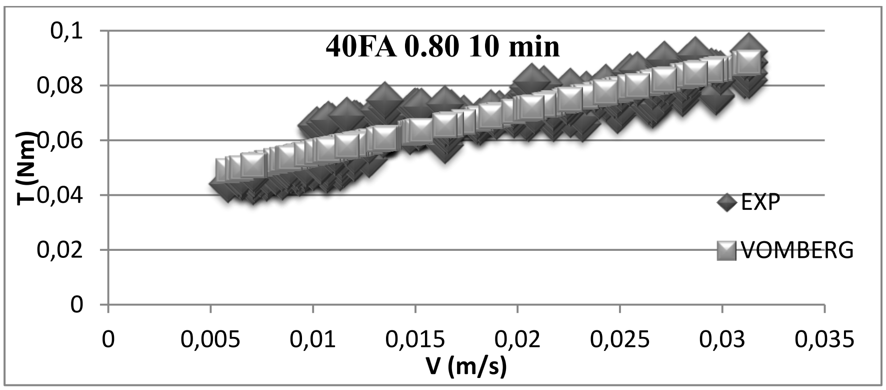

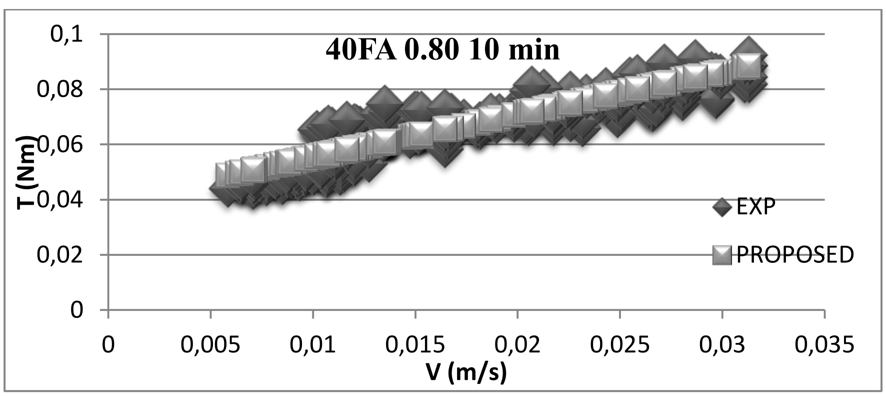

Figure A.24 (Continued)

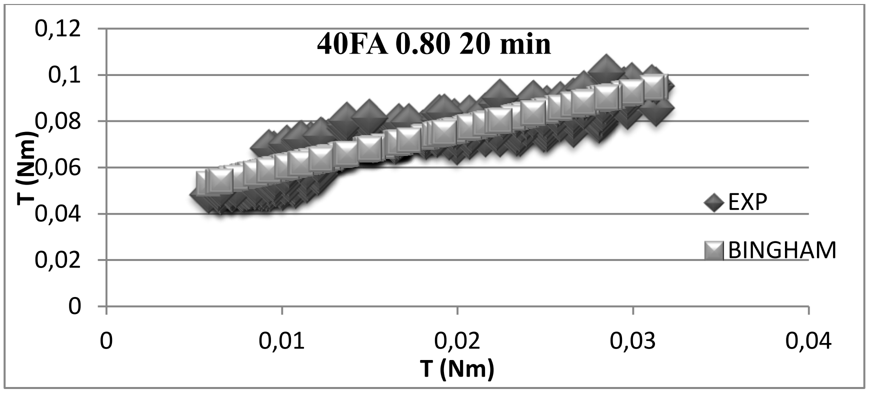

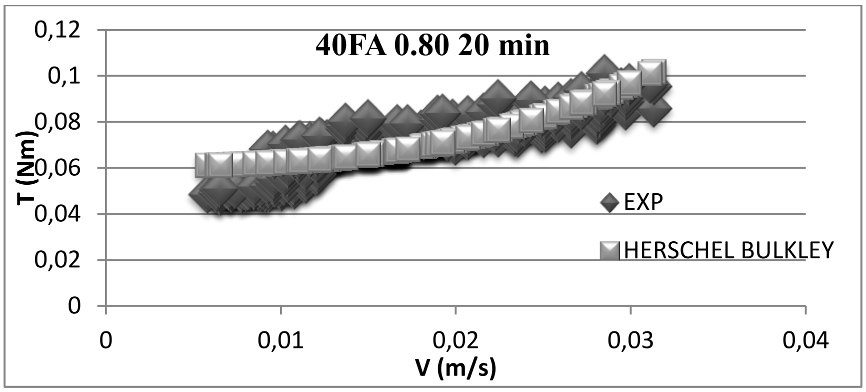

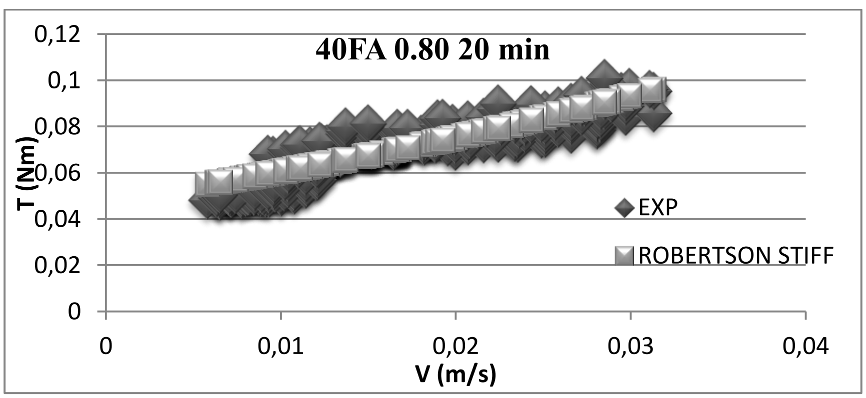

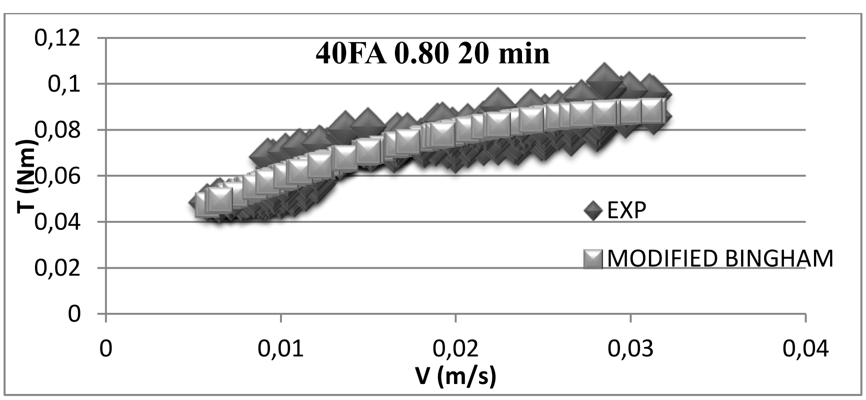

Figure A.25 Flow Models for 40FA0.8(20)

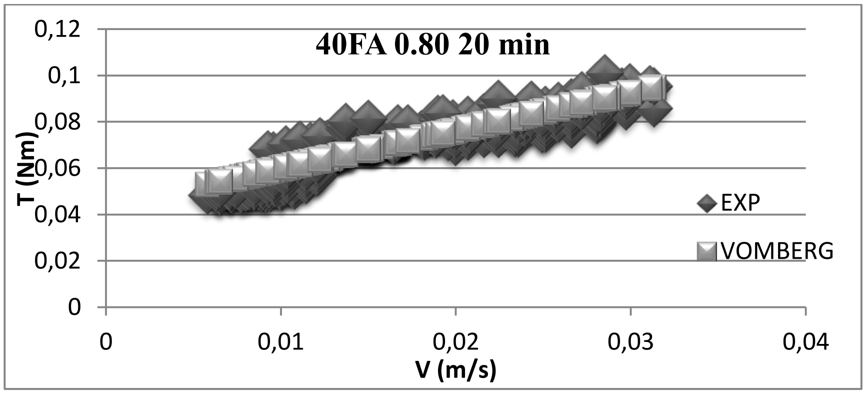

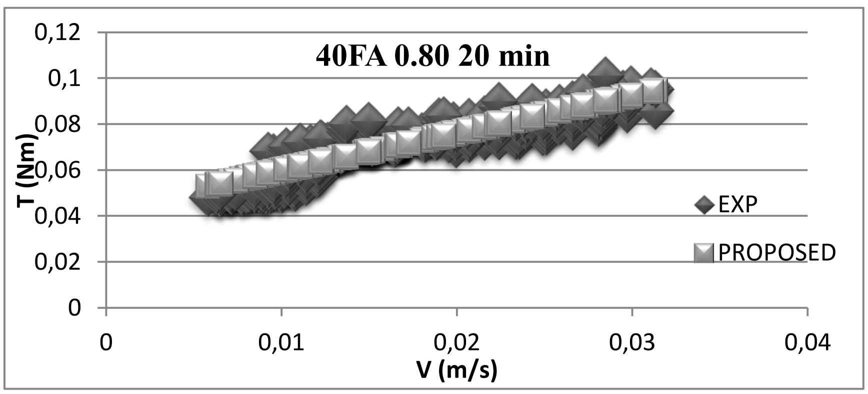

Figure A.25 (Continued)

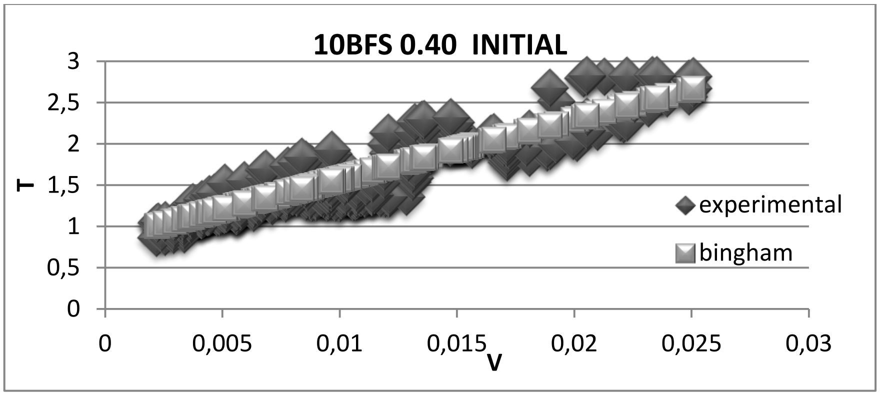

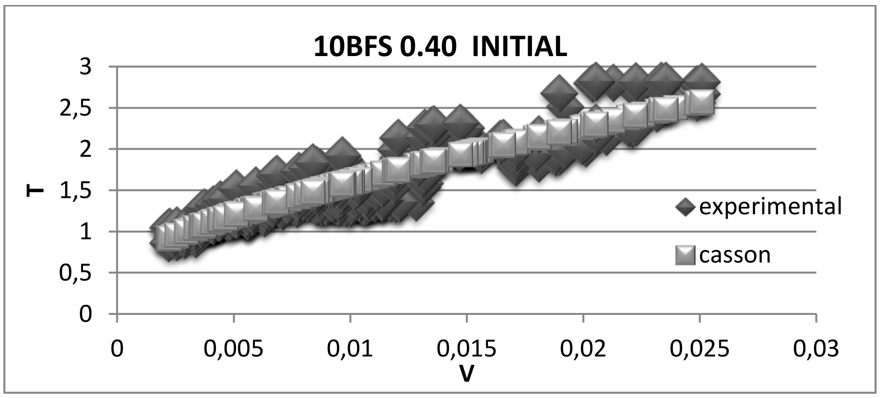

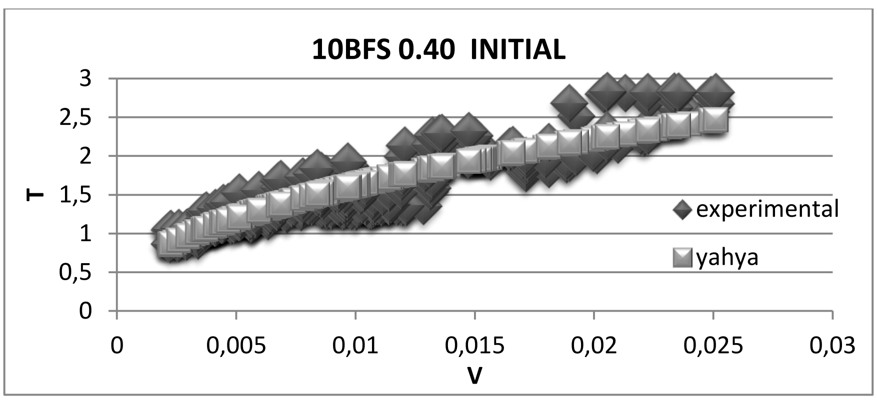

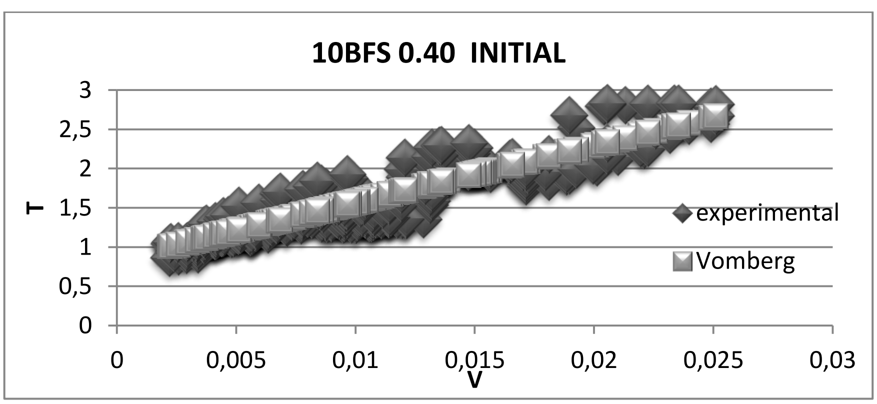

Figure A.26 Flow Models for 10BFS0.4

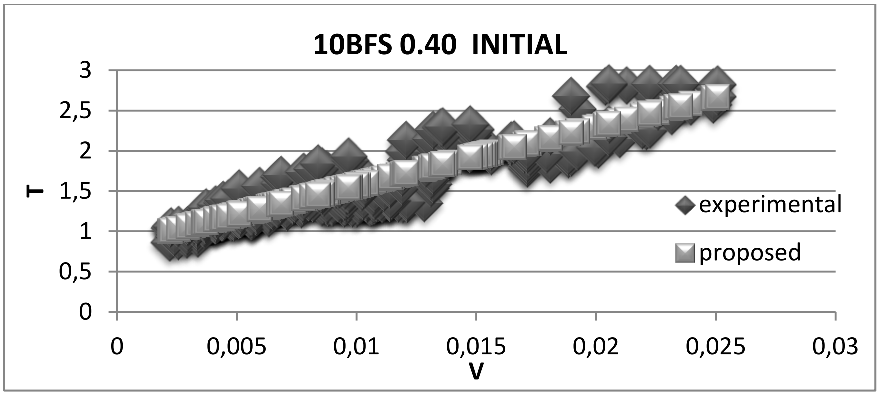

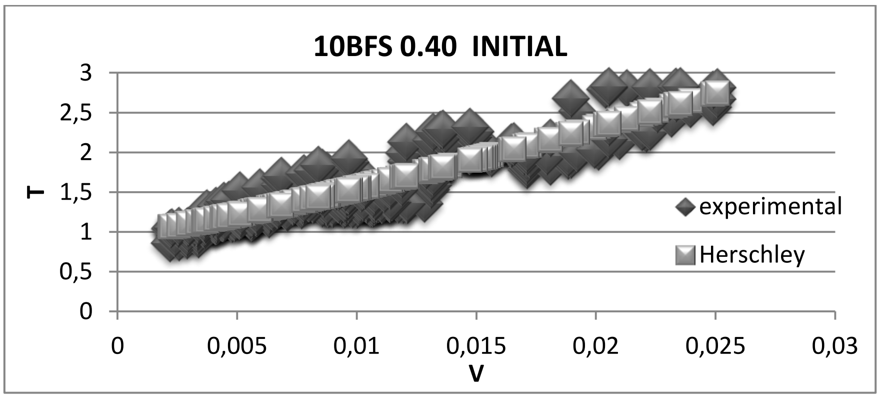

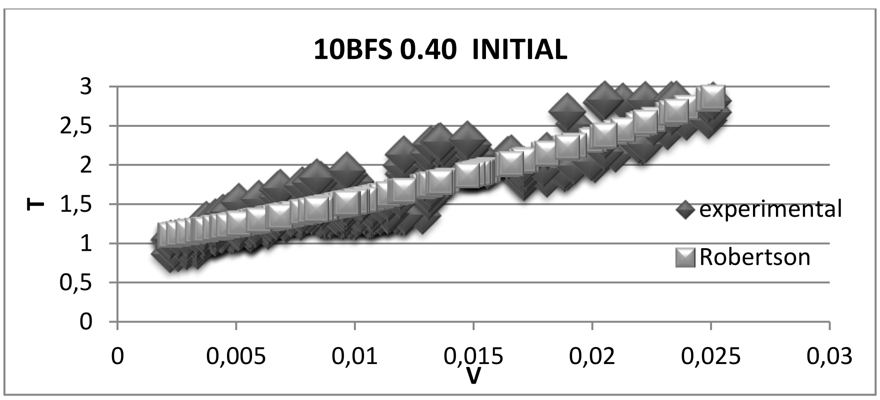

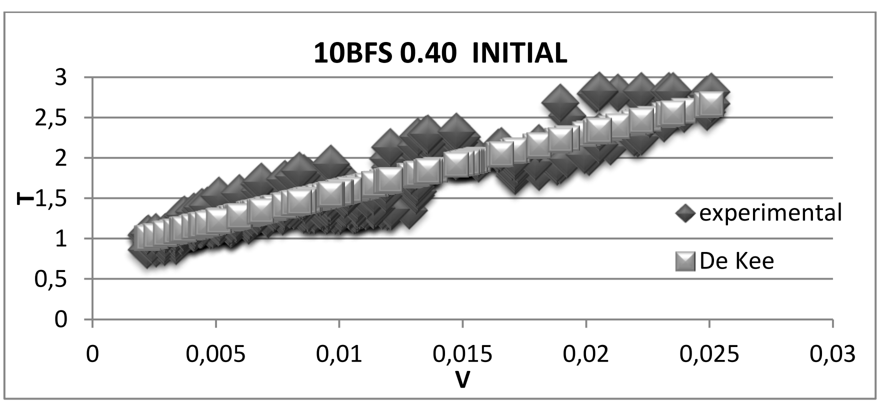

Figure A.26 (Continued)

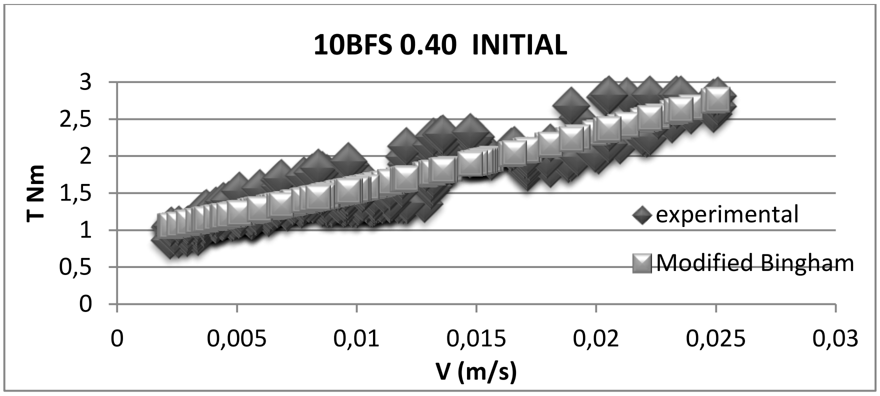

Figure A.26 (Continued)

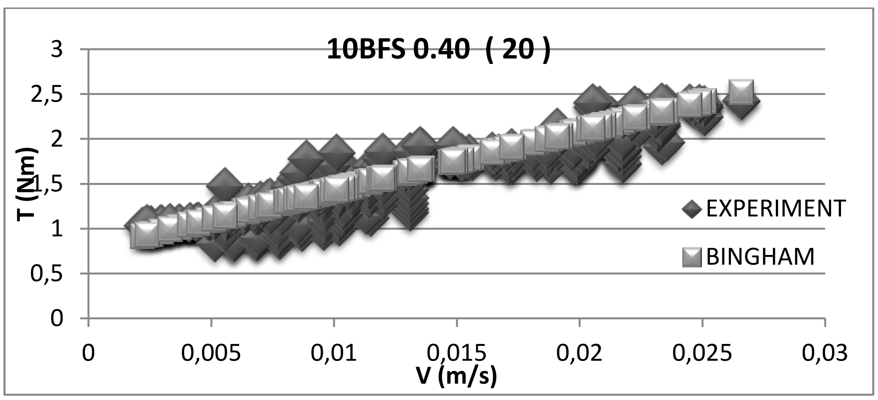

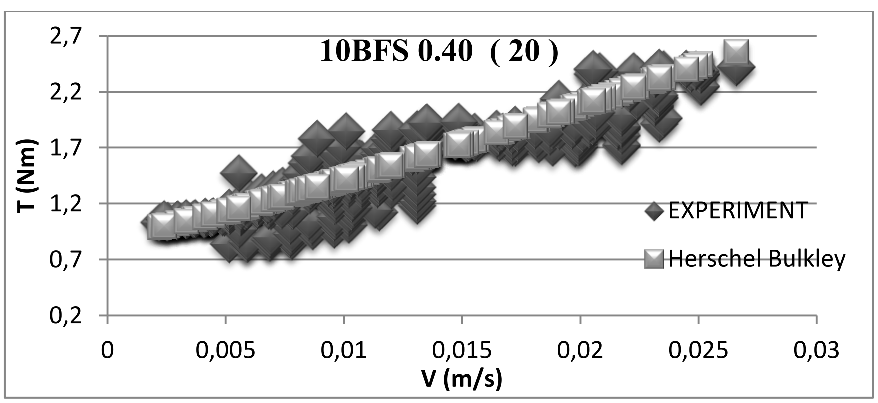

Figure A.27 Flow Models for for 10BFS0.4(20)

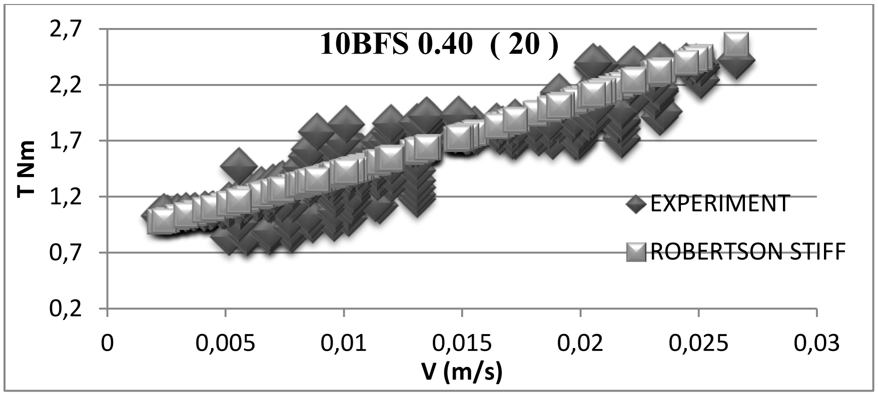

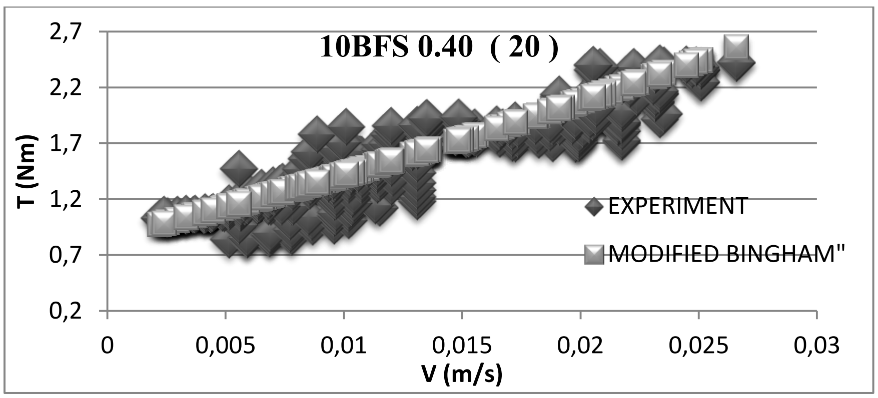

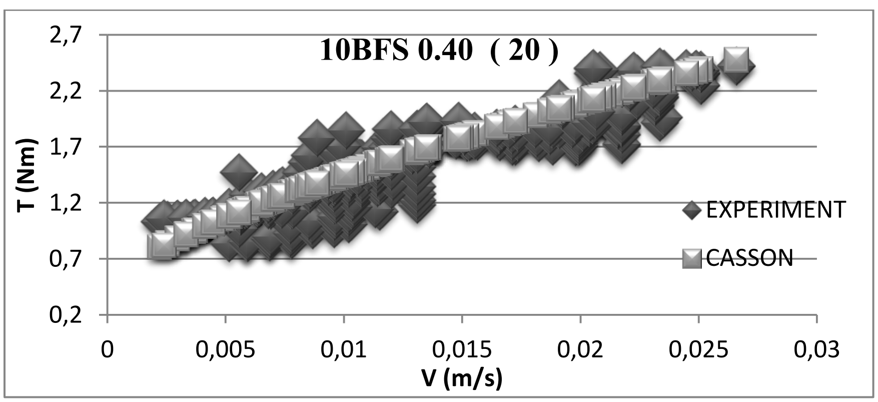

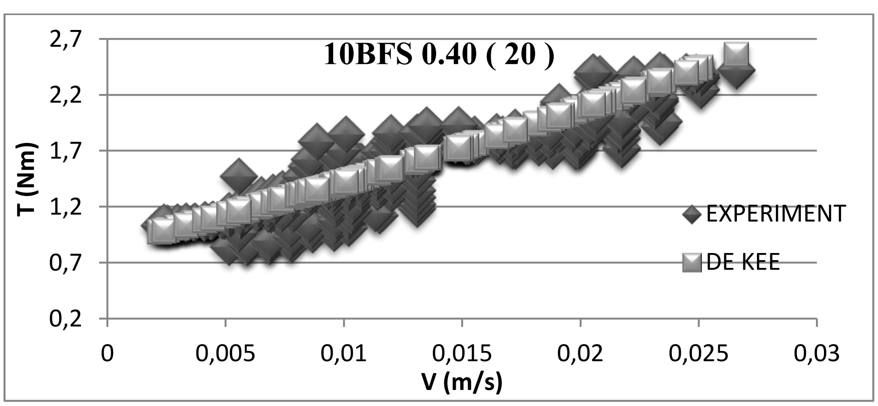

Figure A.27 (Continued)

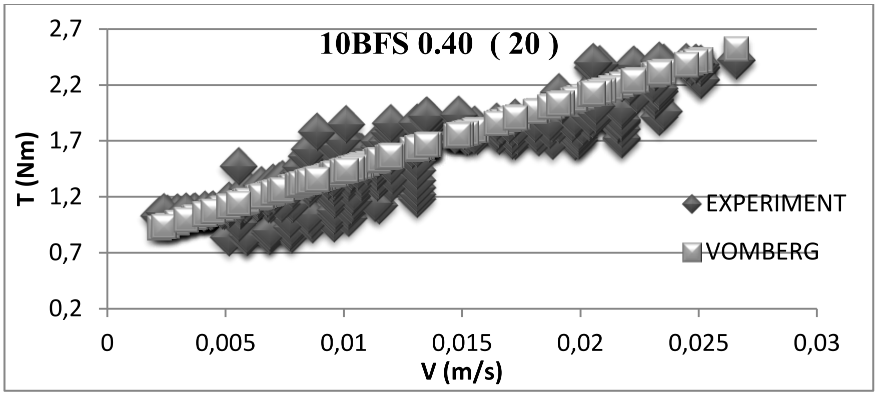

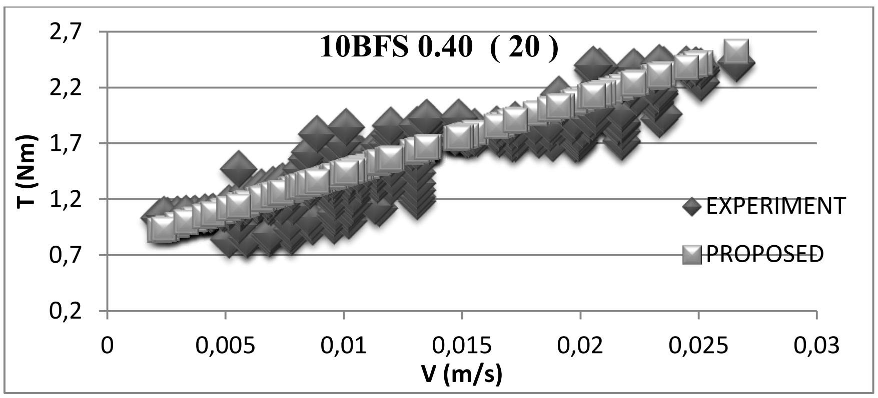

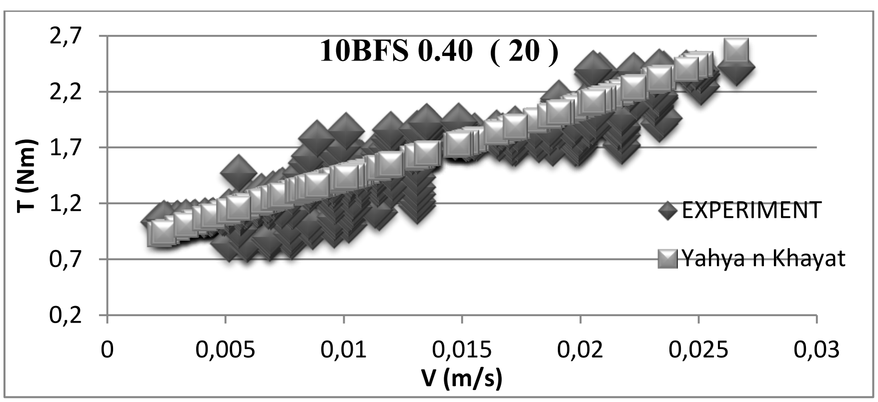

Figure A.27 (Continued)

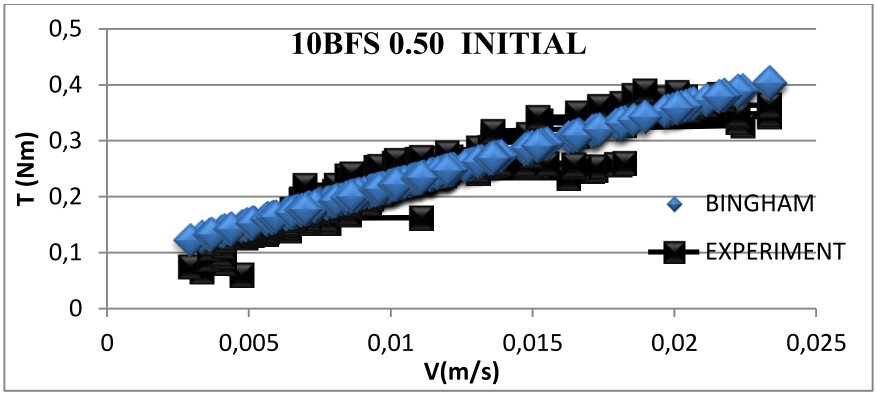

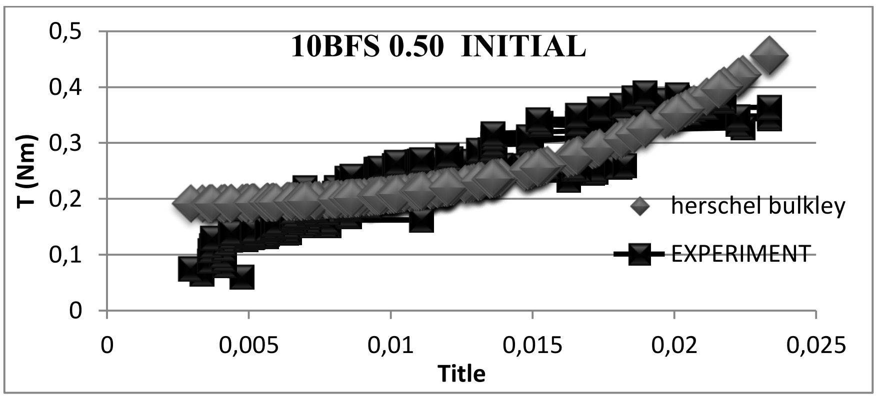

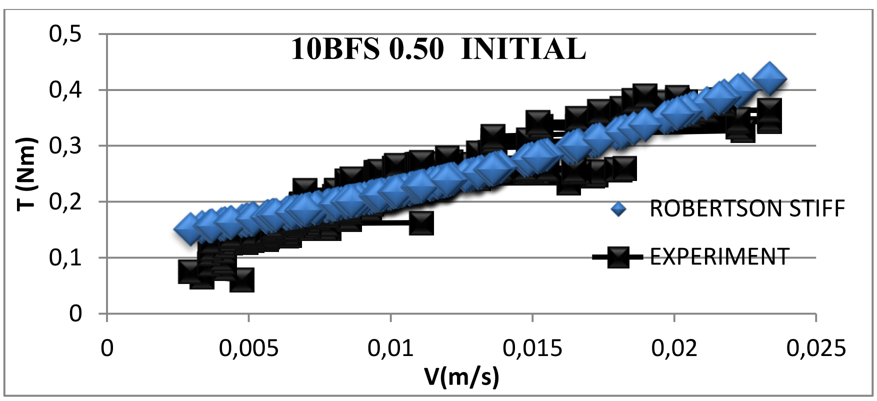

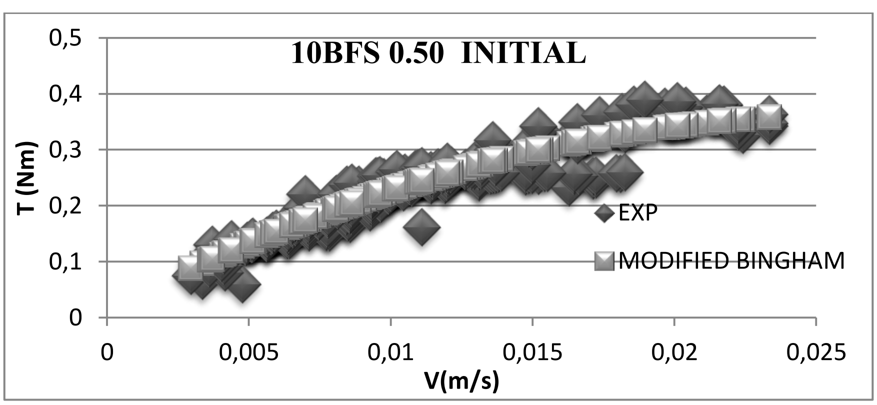

Figure A.28 Flow Models for 10BFS 0.5

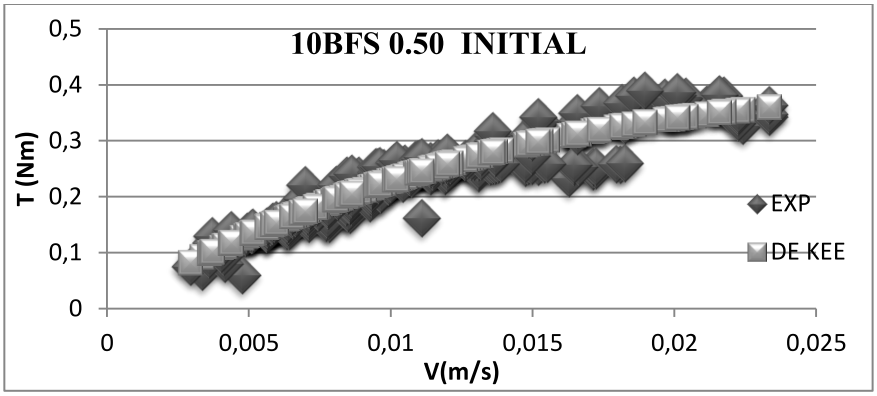

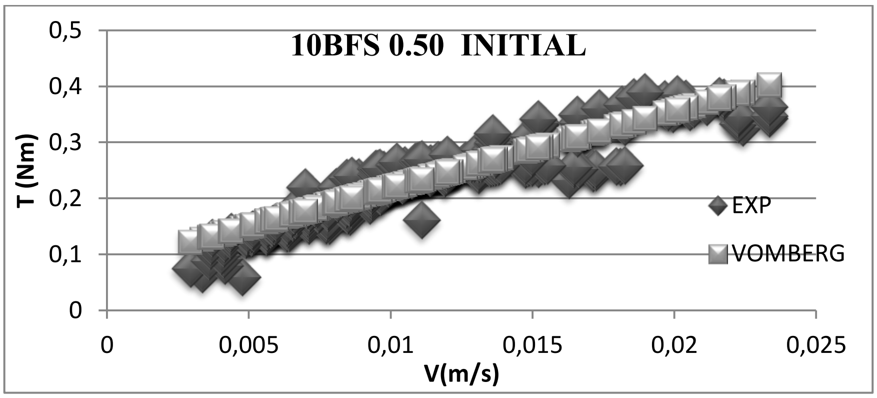

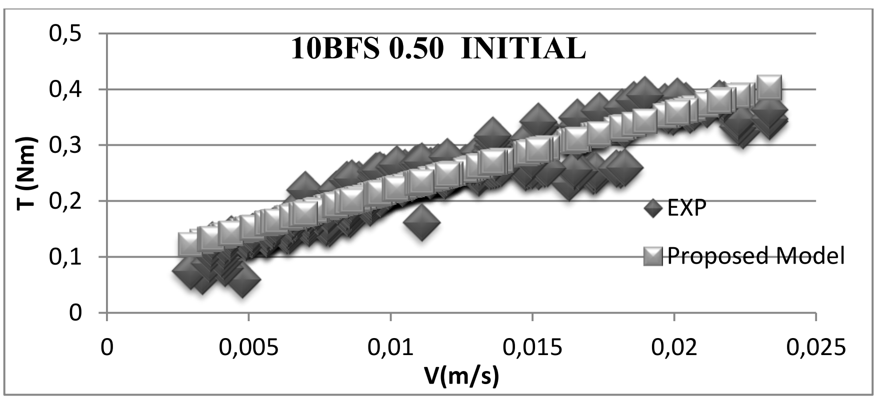

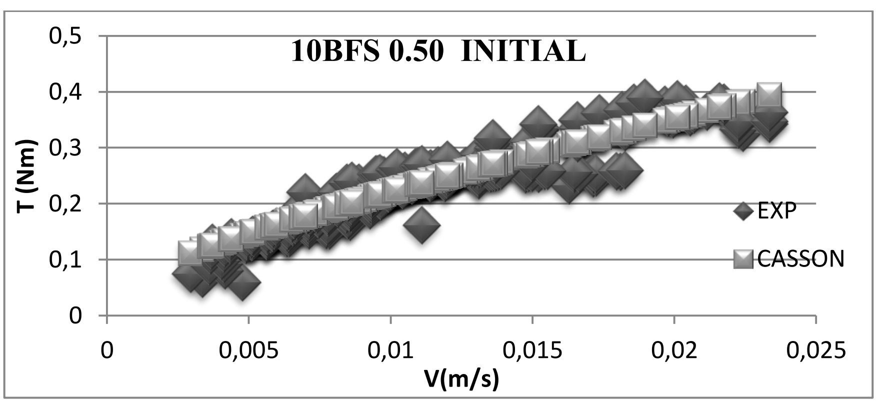

Figure A.28 (Continued)

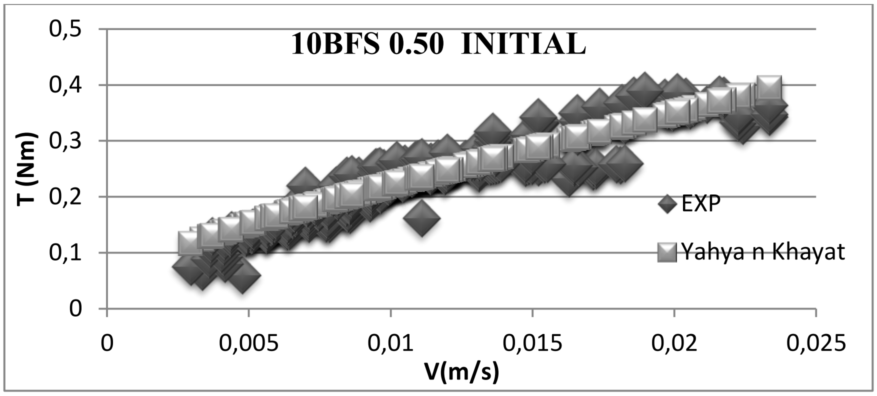

Figure A.28 (Continued)

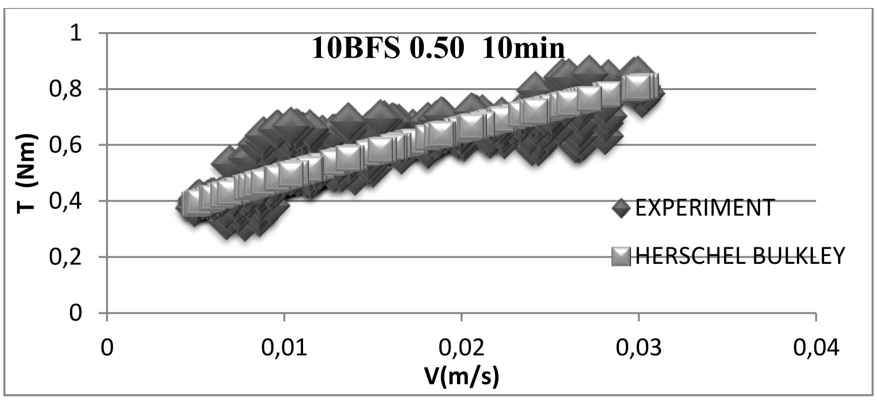

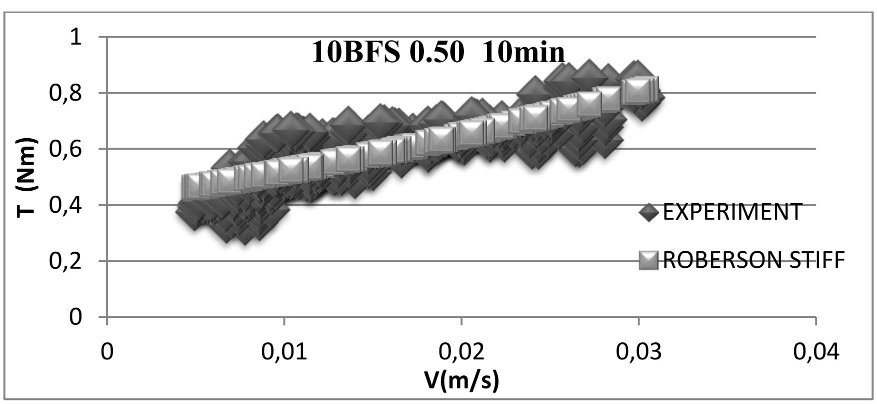

Figure A.29 Flow Models for 10BFS 0.5(10)

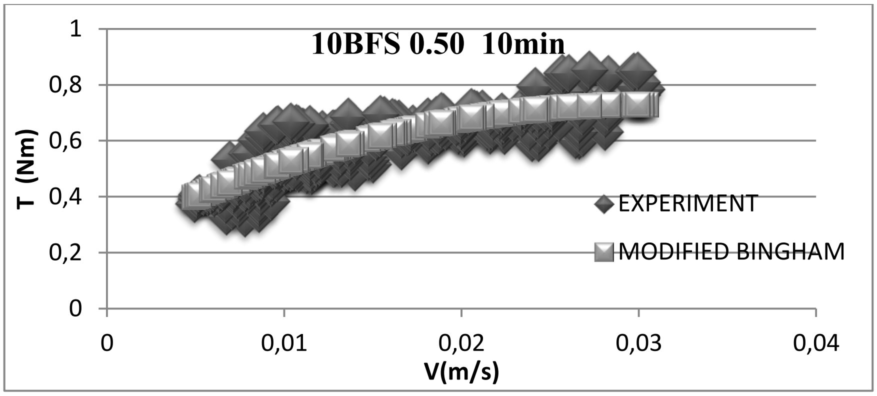

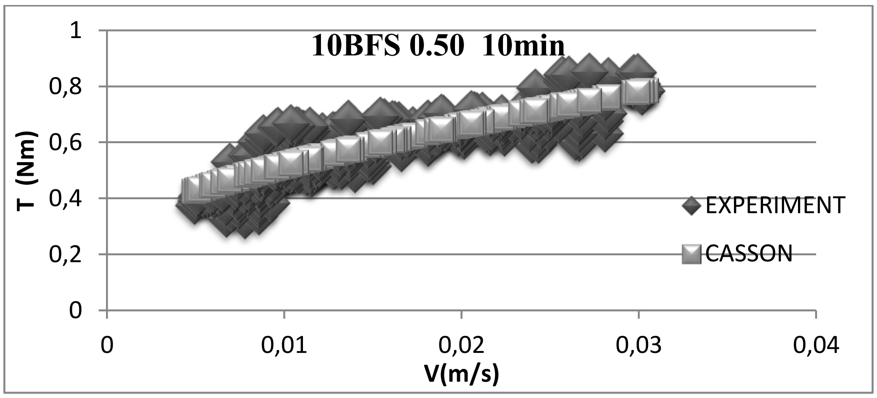

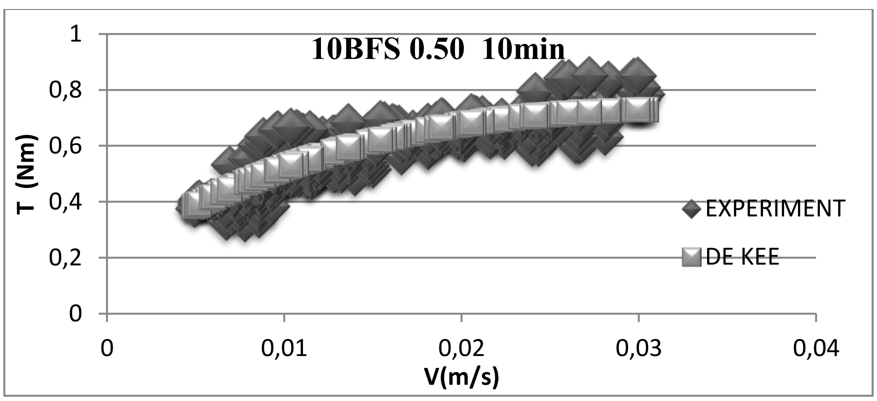

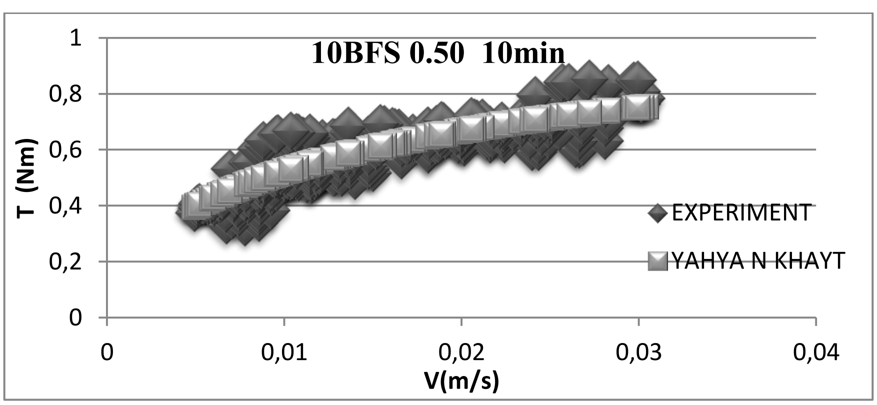

Figure A.29 (Continued)

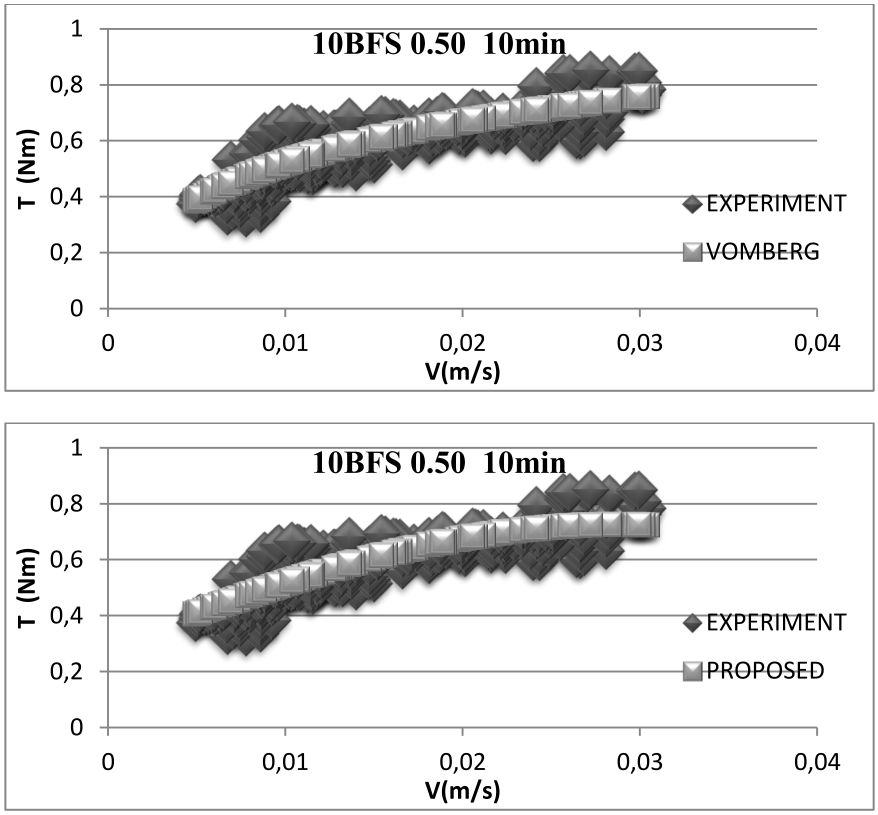

Figure A.29 (Continued)

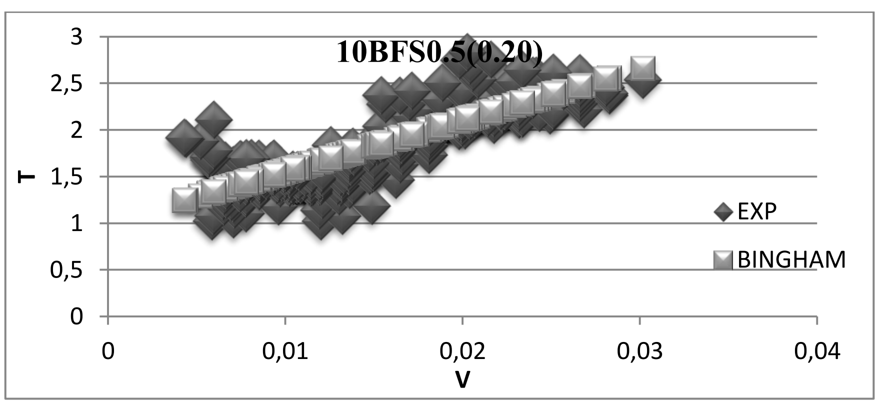

Figure A.30 Flow Models for 10BFS 0.5(20)

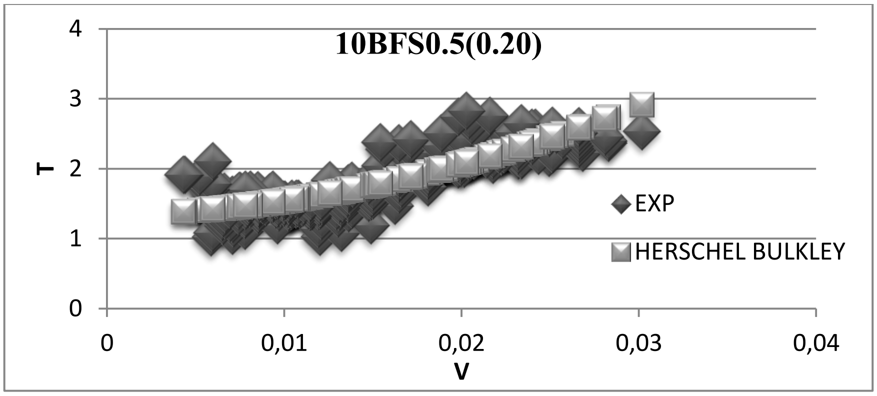

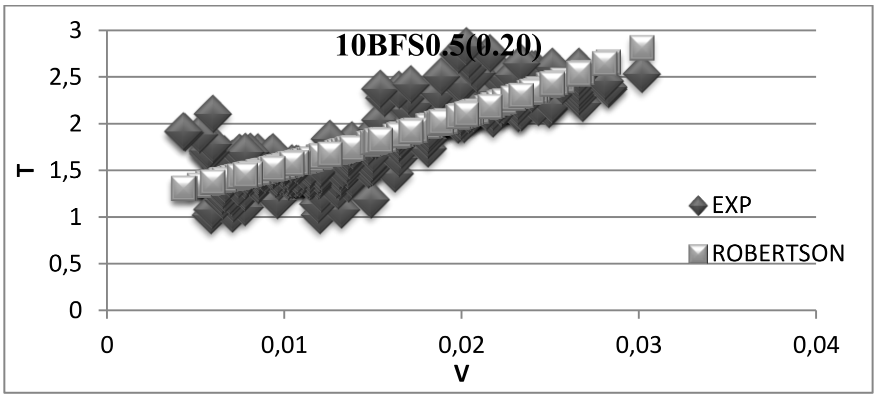

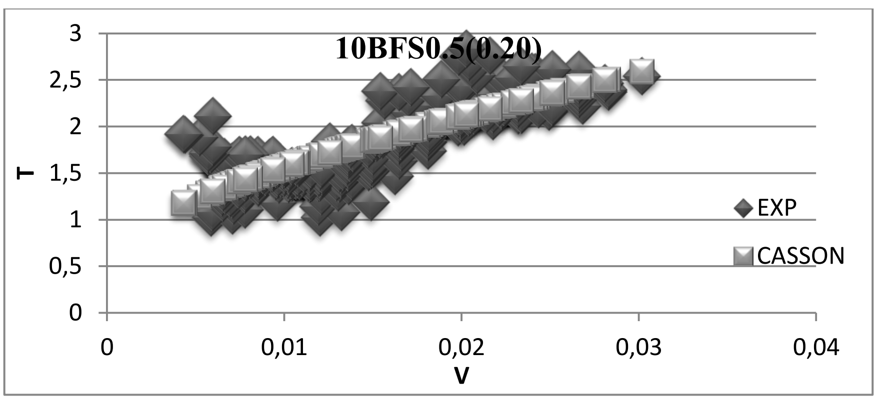

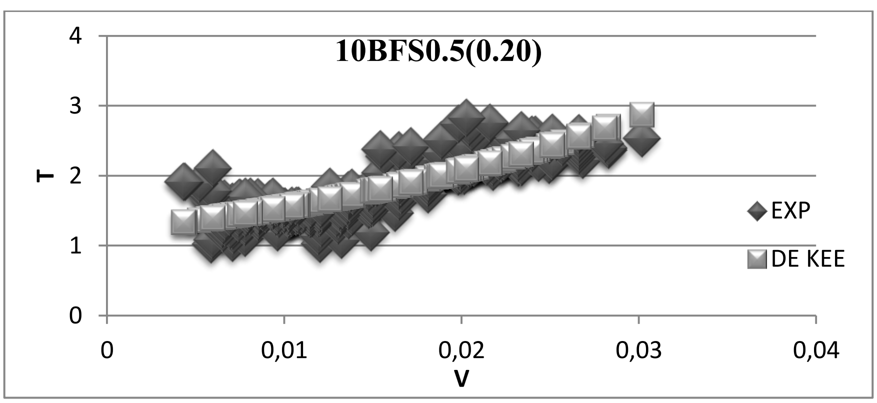

Figure A.30 (Continued)

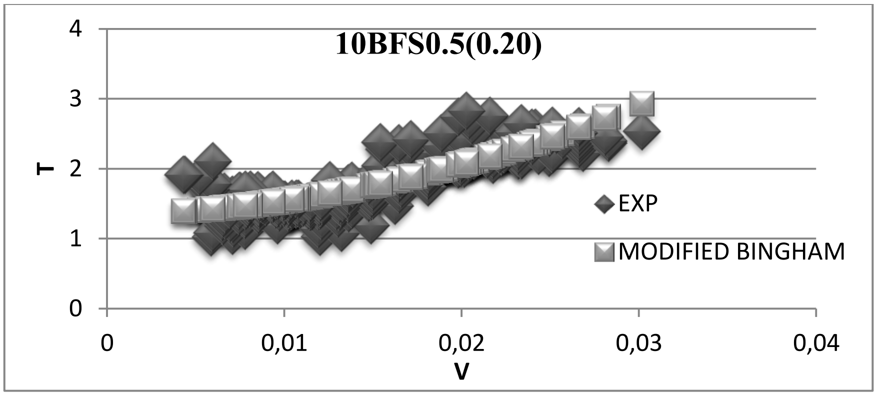

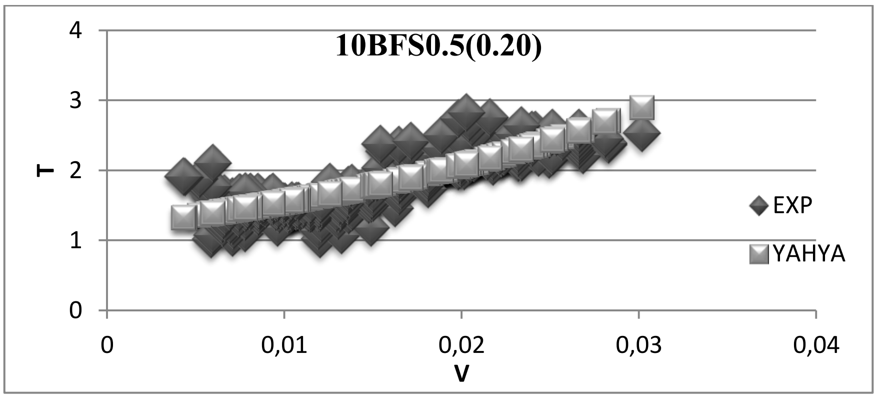

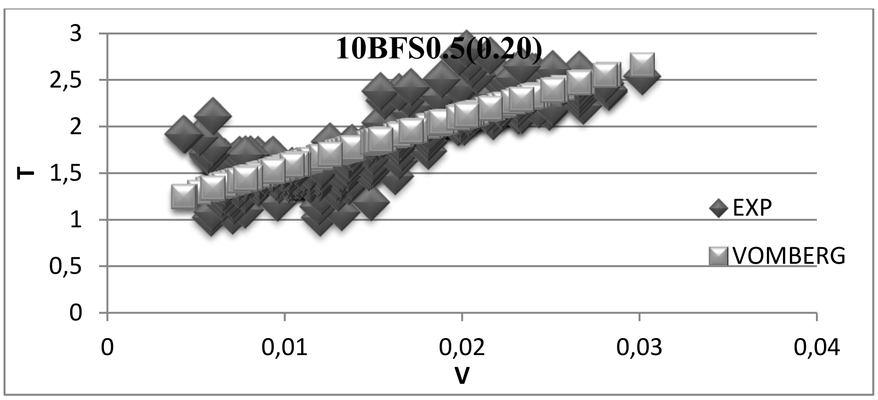

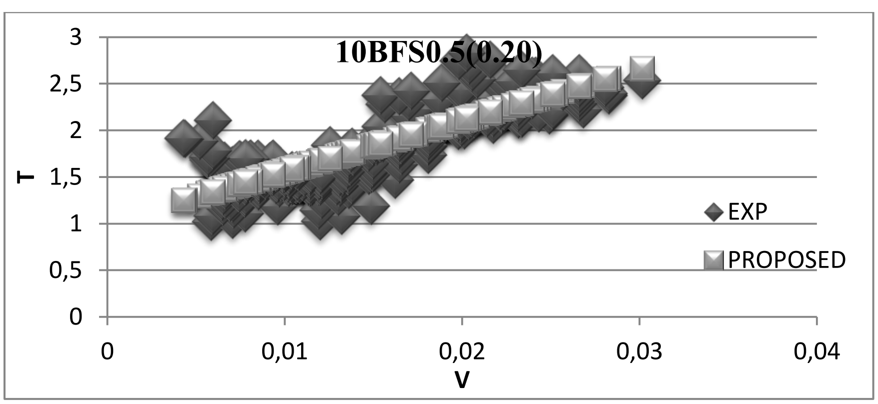

Figure A.30 (Continued)

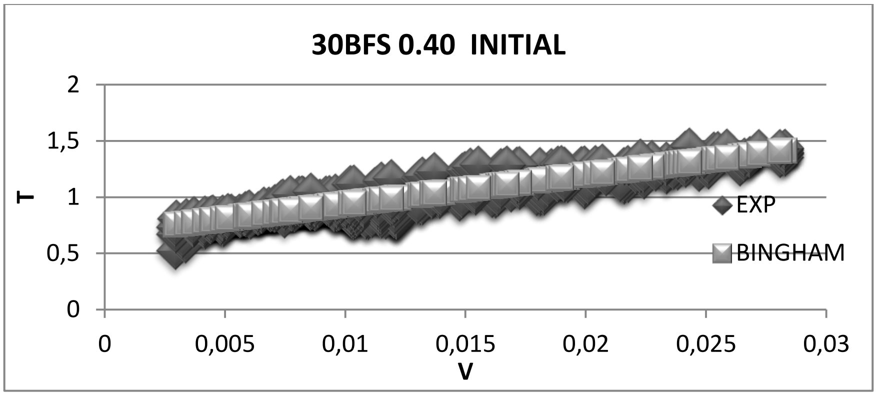

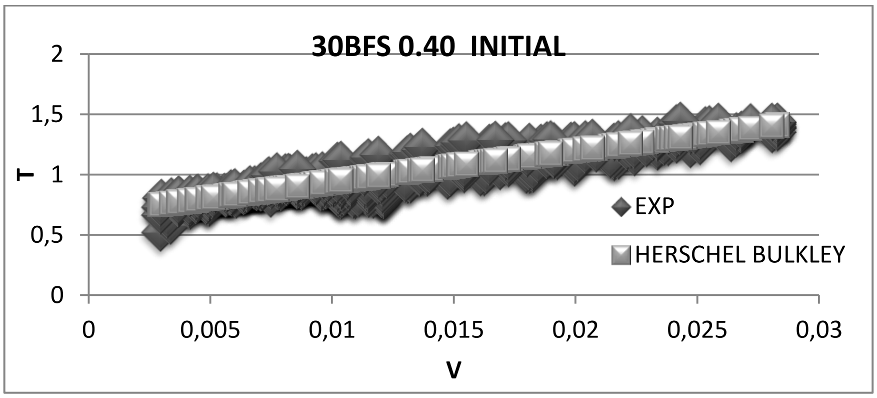

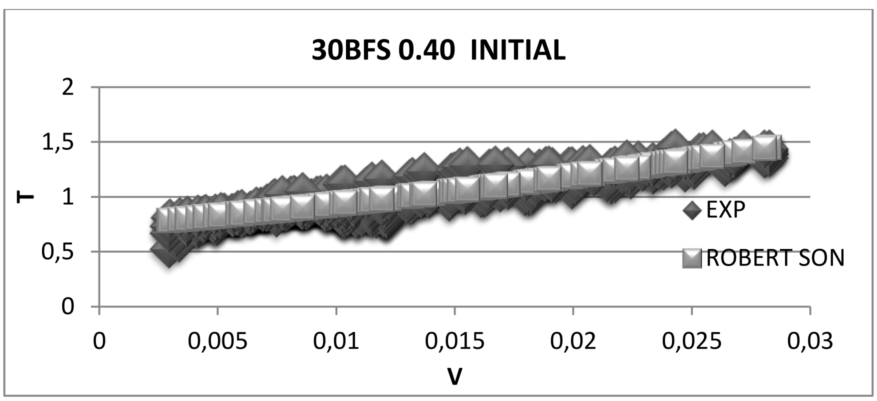

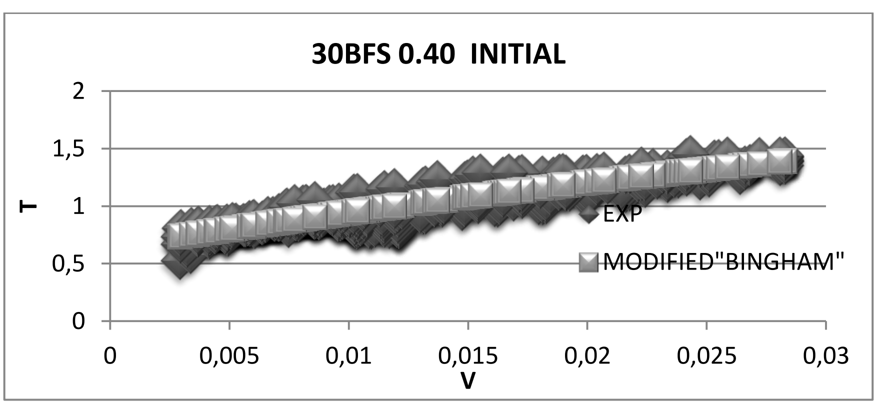

Figure A.31 Flow Models for 30BFS 0.4

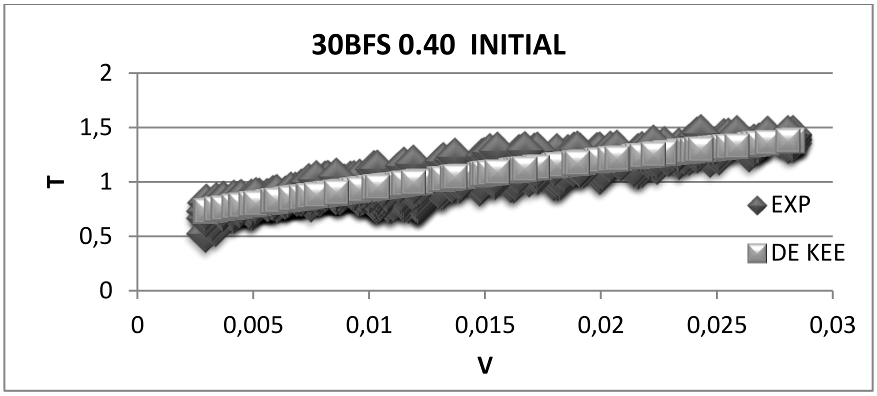

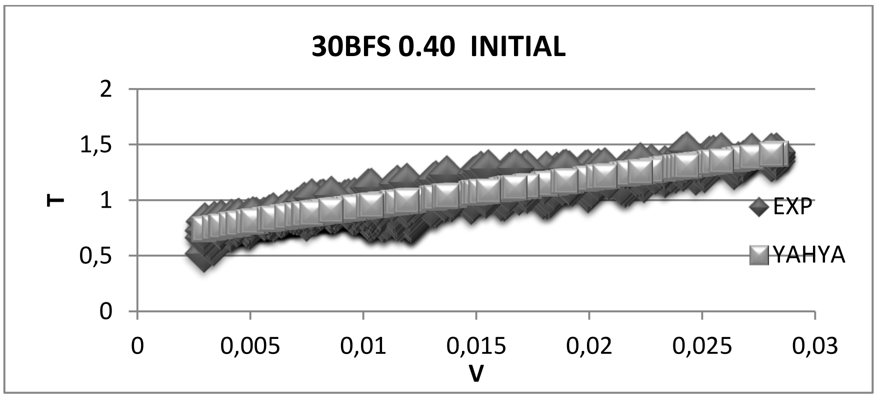

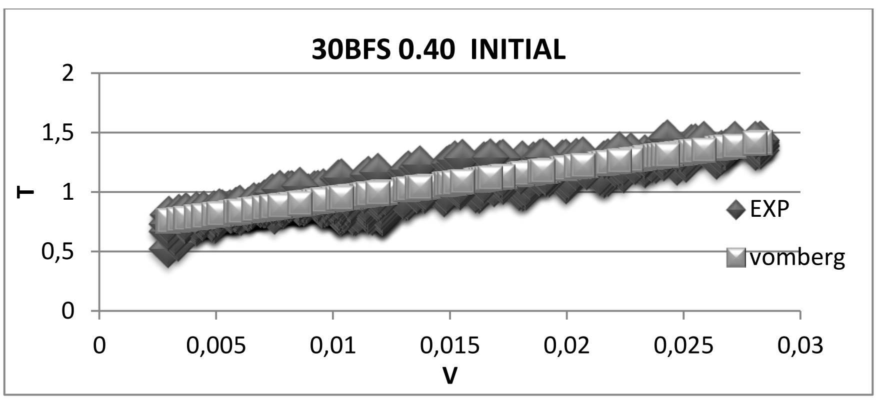

Figure A.31 (Continued)

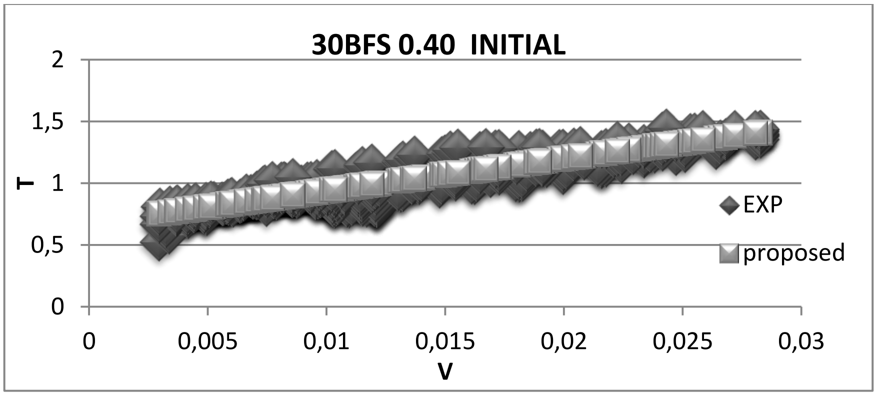

Figure A.31 (Continued)

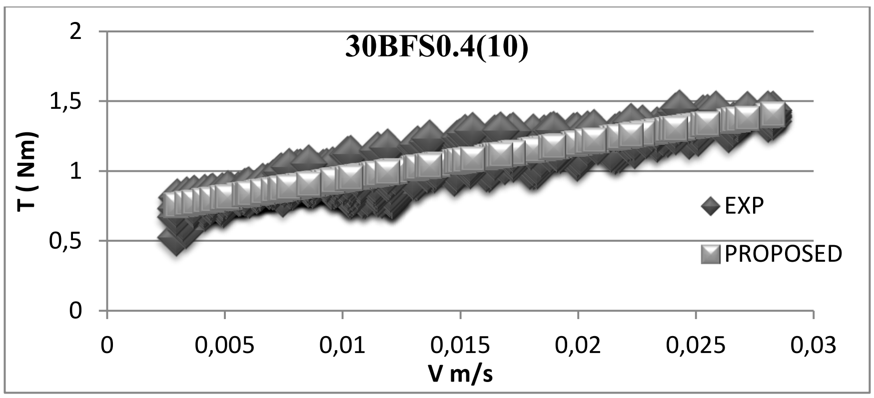

Figure A. 32 Flow Model for 30BFS 0.4(10)

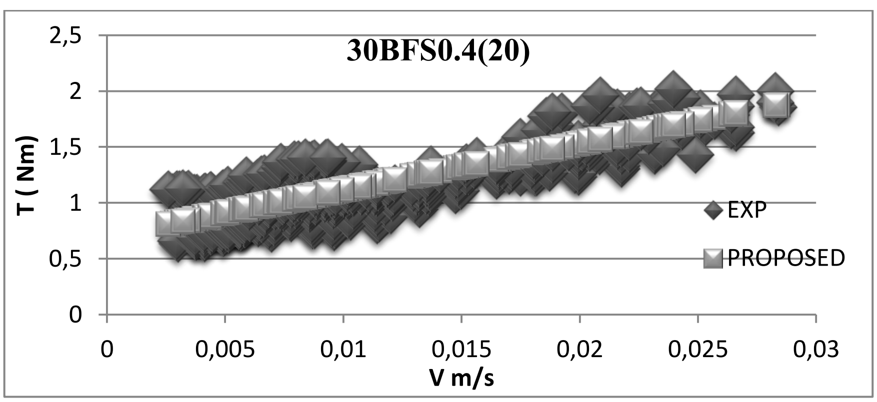

Figure A.33 Flow Models for 30BFS0.4(20)

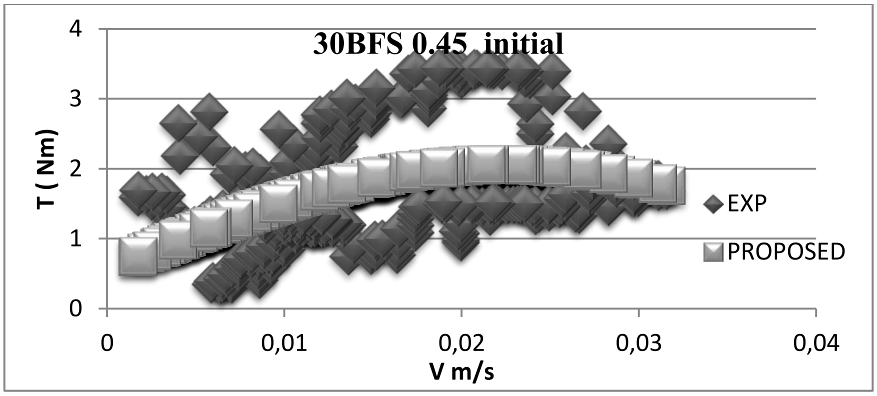

Figure A. 34 Flow model for 30BFS0.45

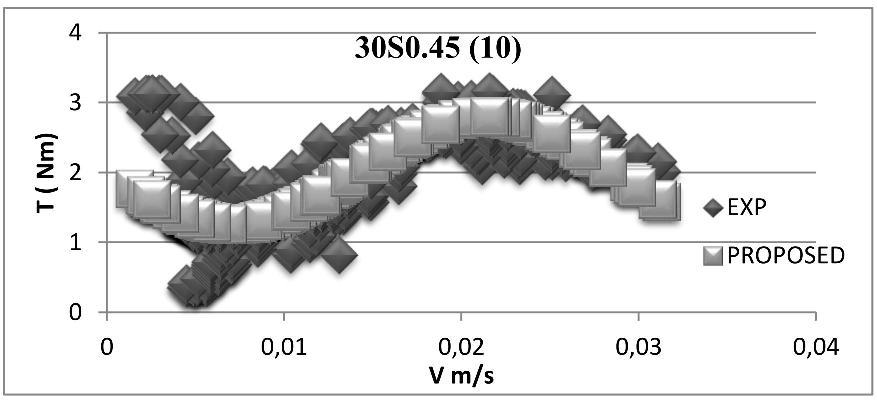

Figure A. 35 Flow model for 30BFS0.45(10)

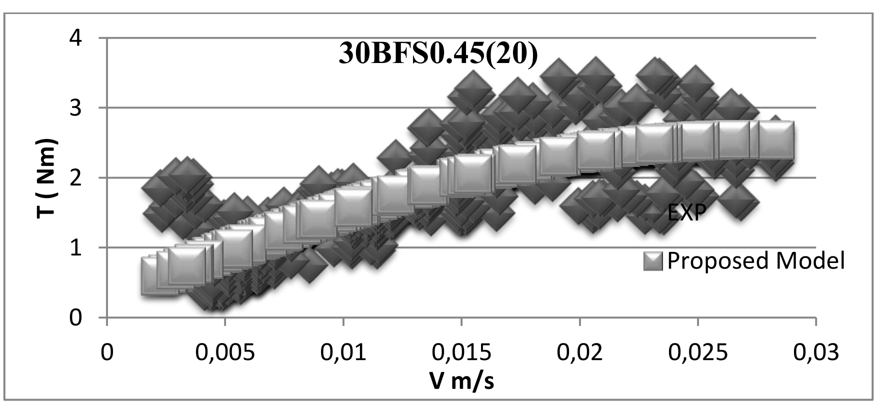

Figure A. 36 Flow model for 30BFS0.45(20)

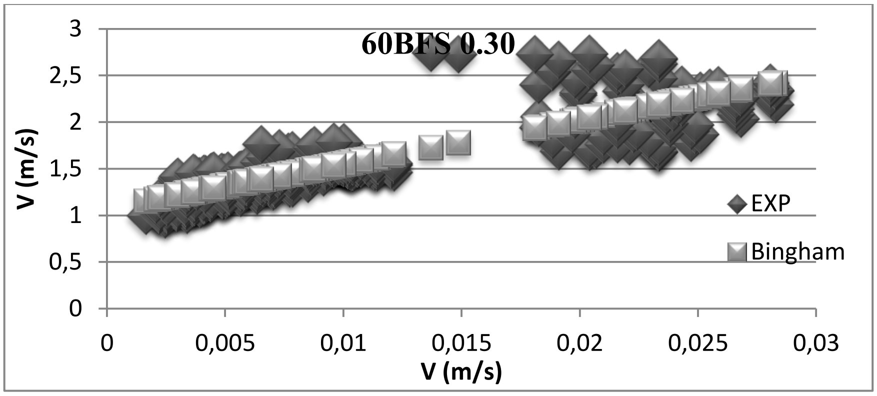

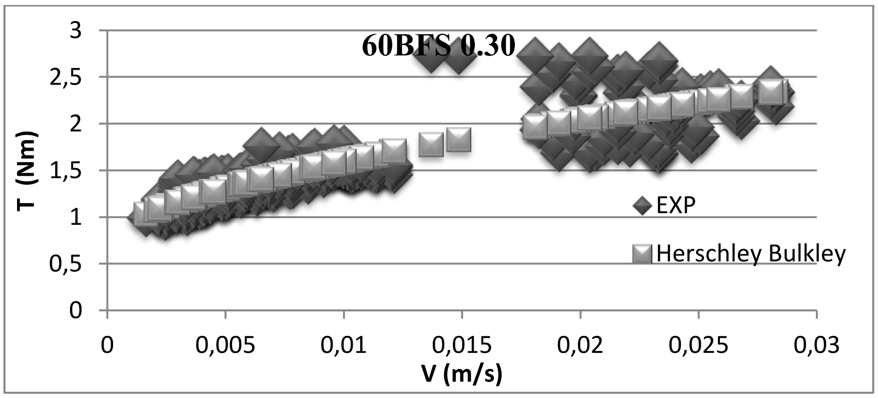

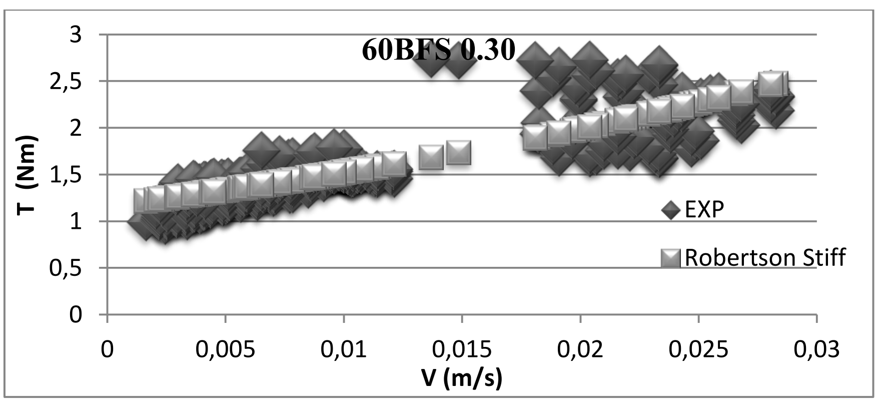

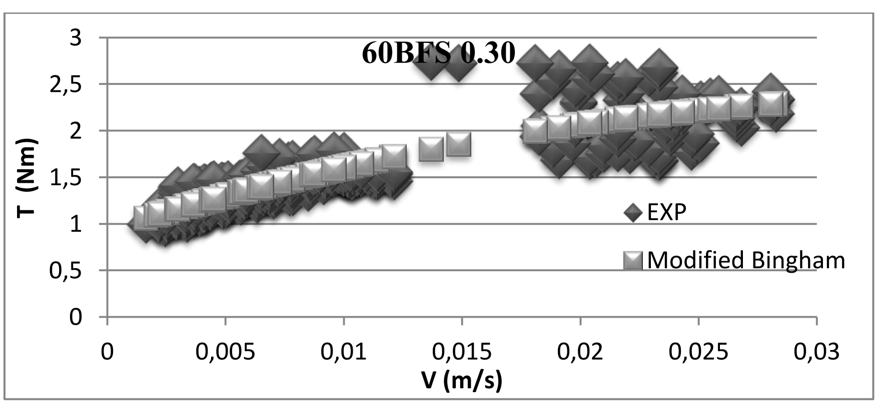

Figure A.37 Flow Models for 60BFS0.3

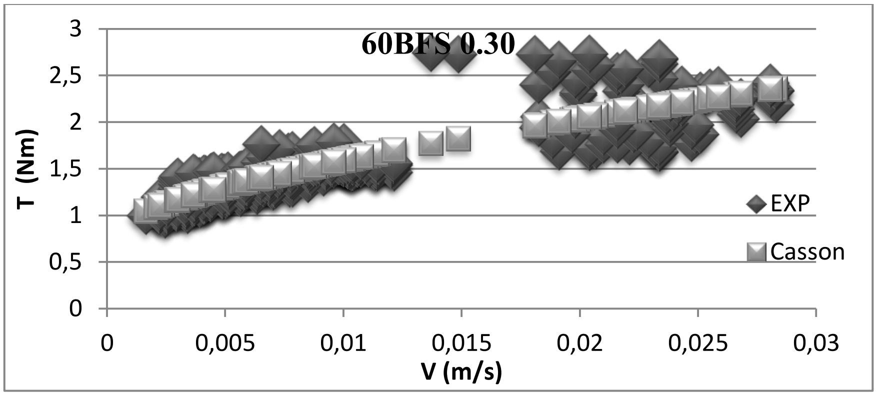

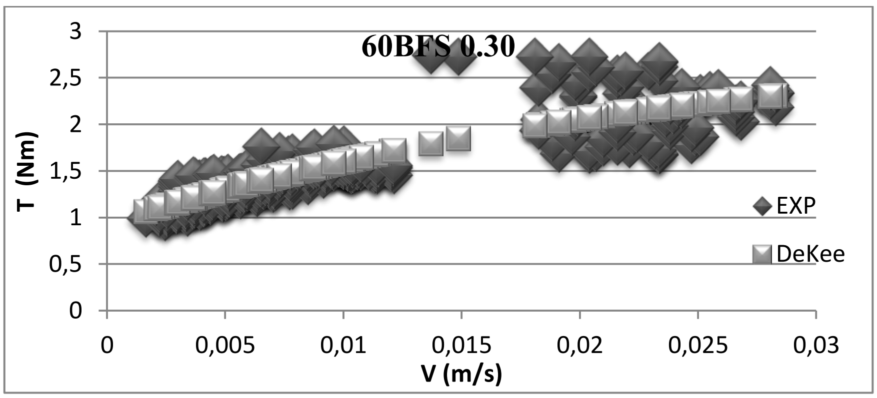

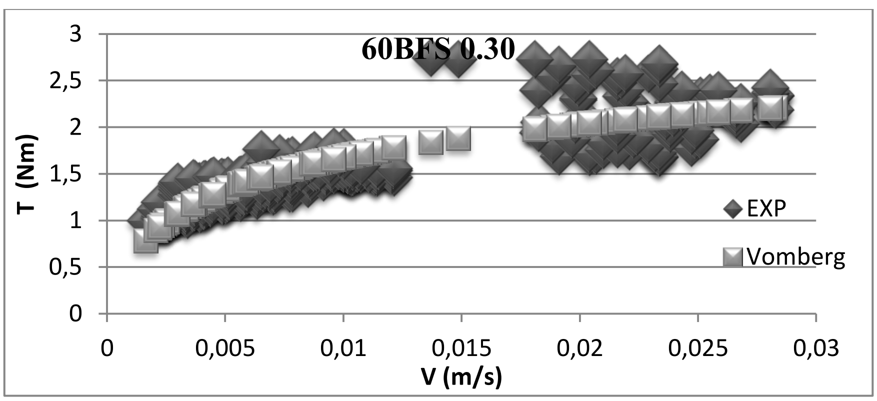

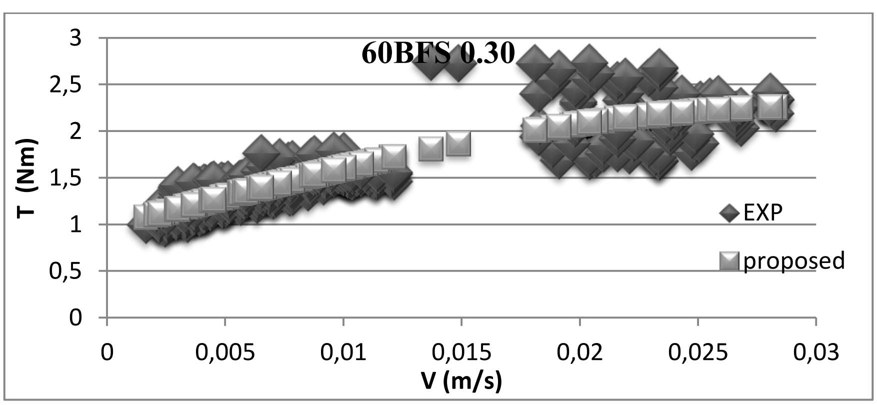

Figure A.37 (Continued)

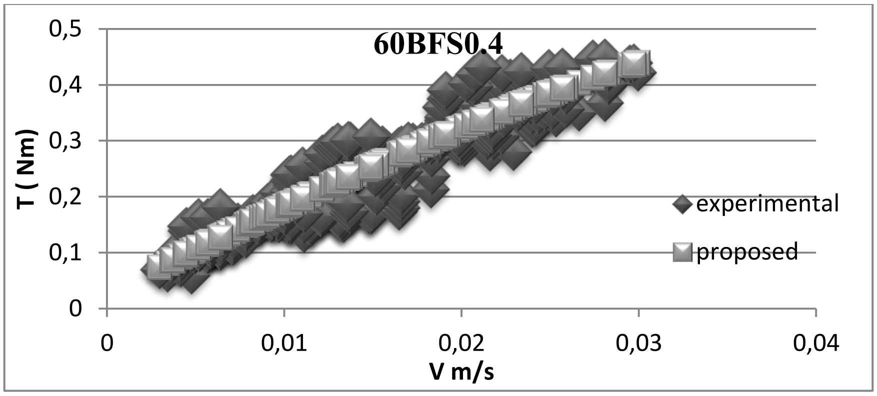

Figure A.38 Flow model for 60BFS 0.4

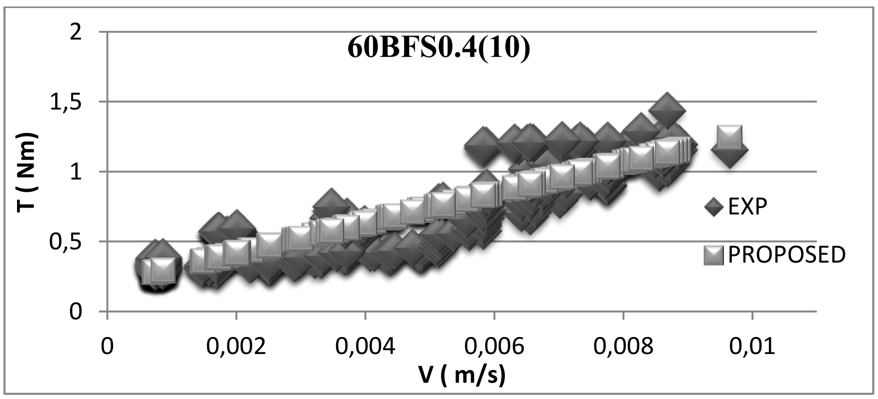

Figure A. 39 Flow model for 60BFS 0.4(10)

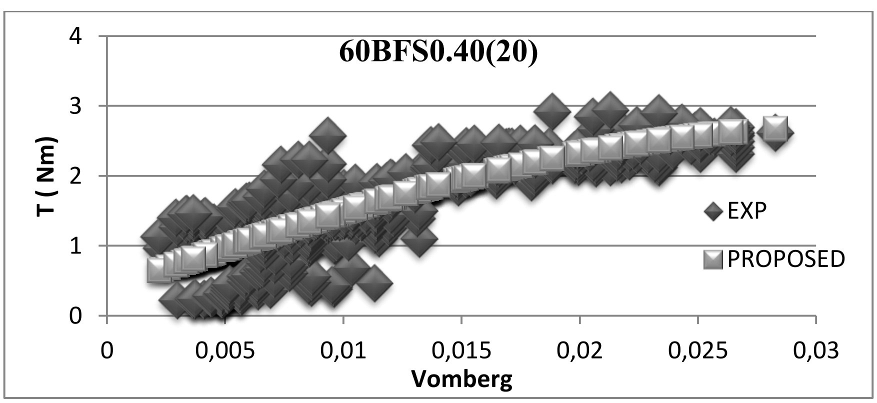

Figure A.40 Flow model for 60BFS 0.4(20)

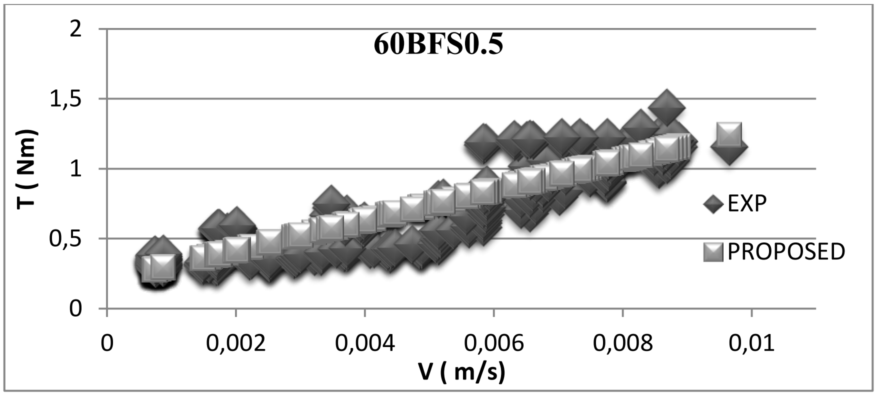

Figure A.41 Flow model for 60BFS 0.5

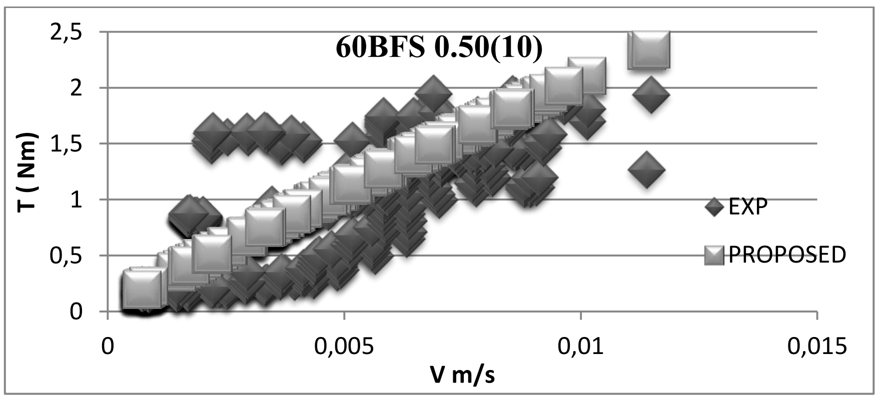

Figure A.42 Flow model for 60BFS 0.5 (10)

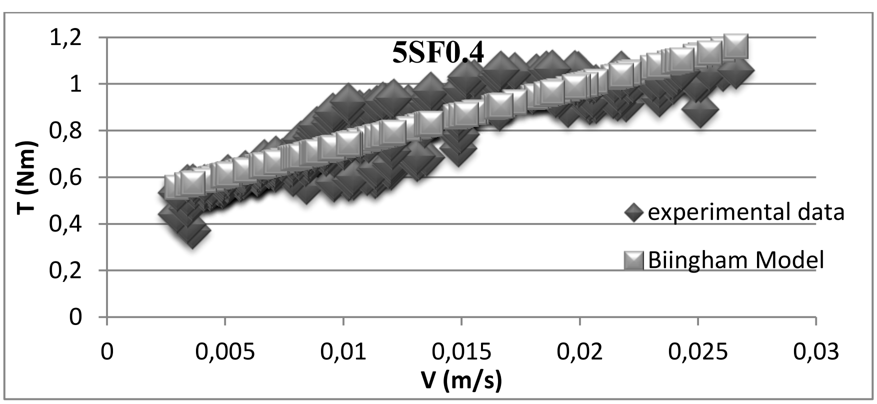

Figure A.43 Flow model for 5SF0.4

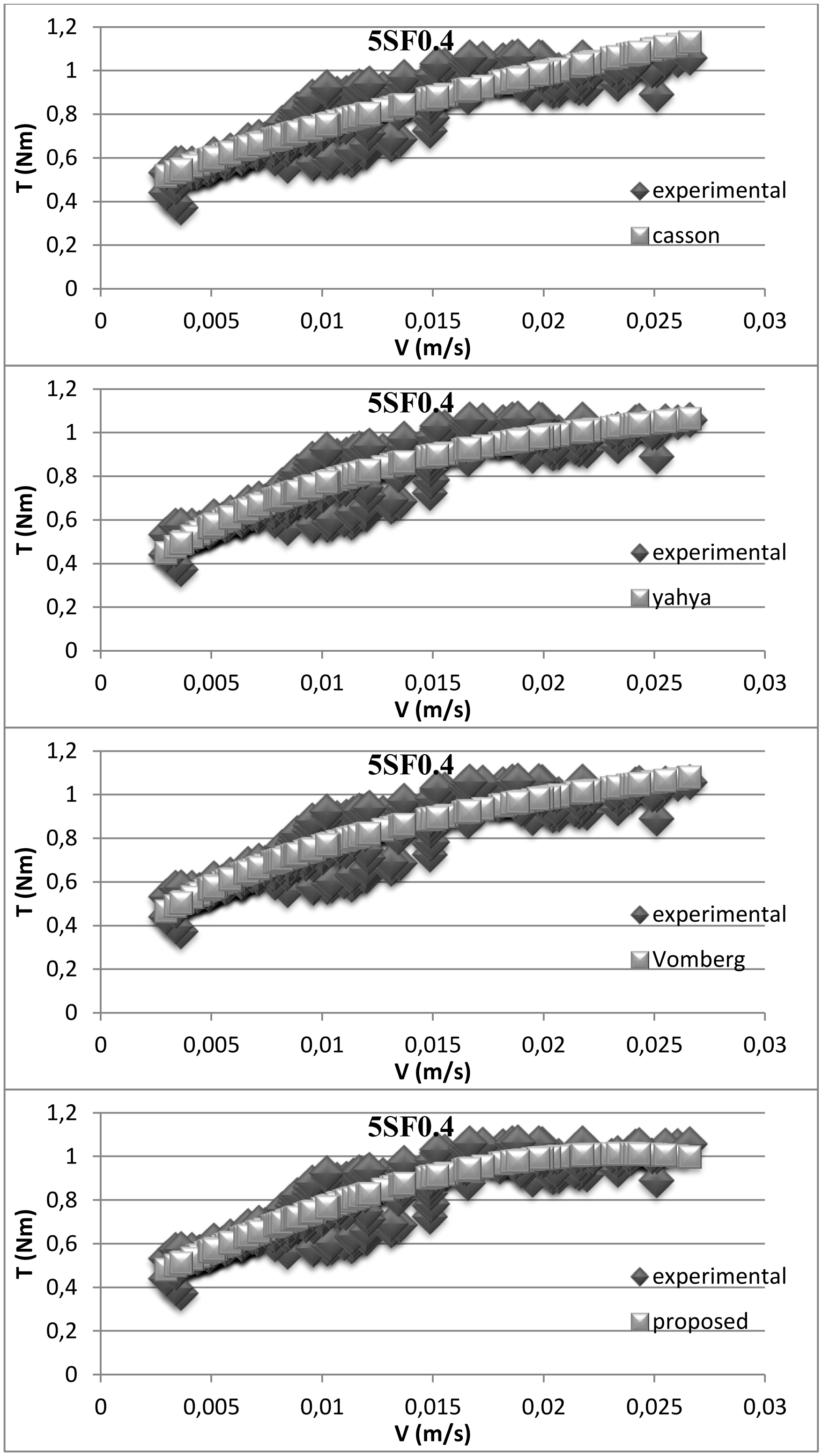

Figure A.43 (Continued)

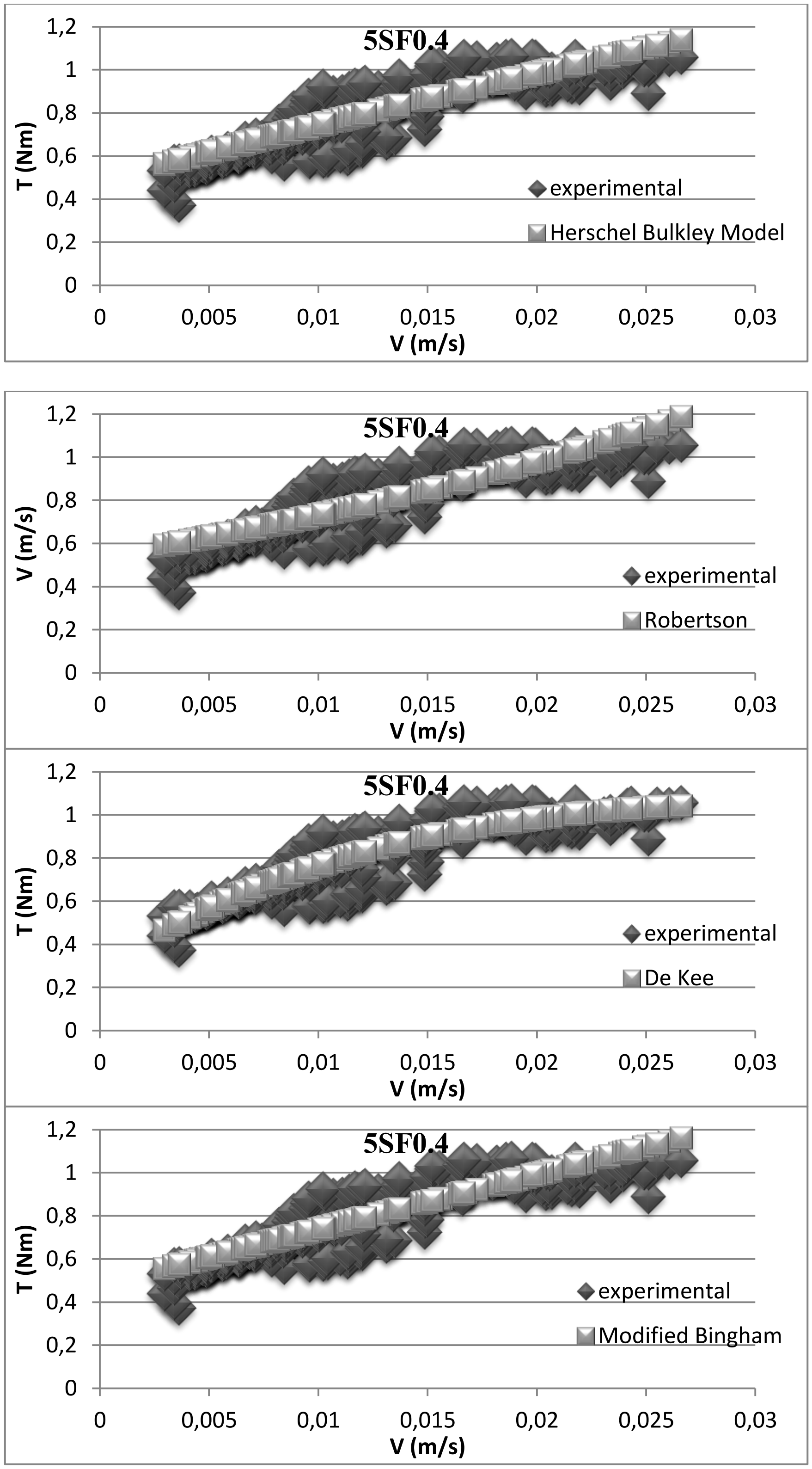

Figure A.43 (Continued)

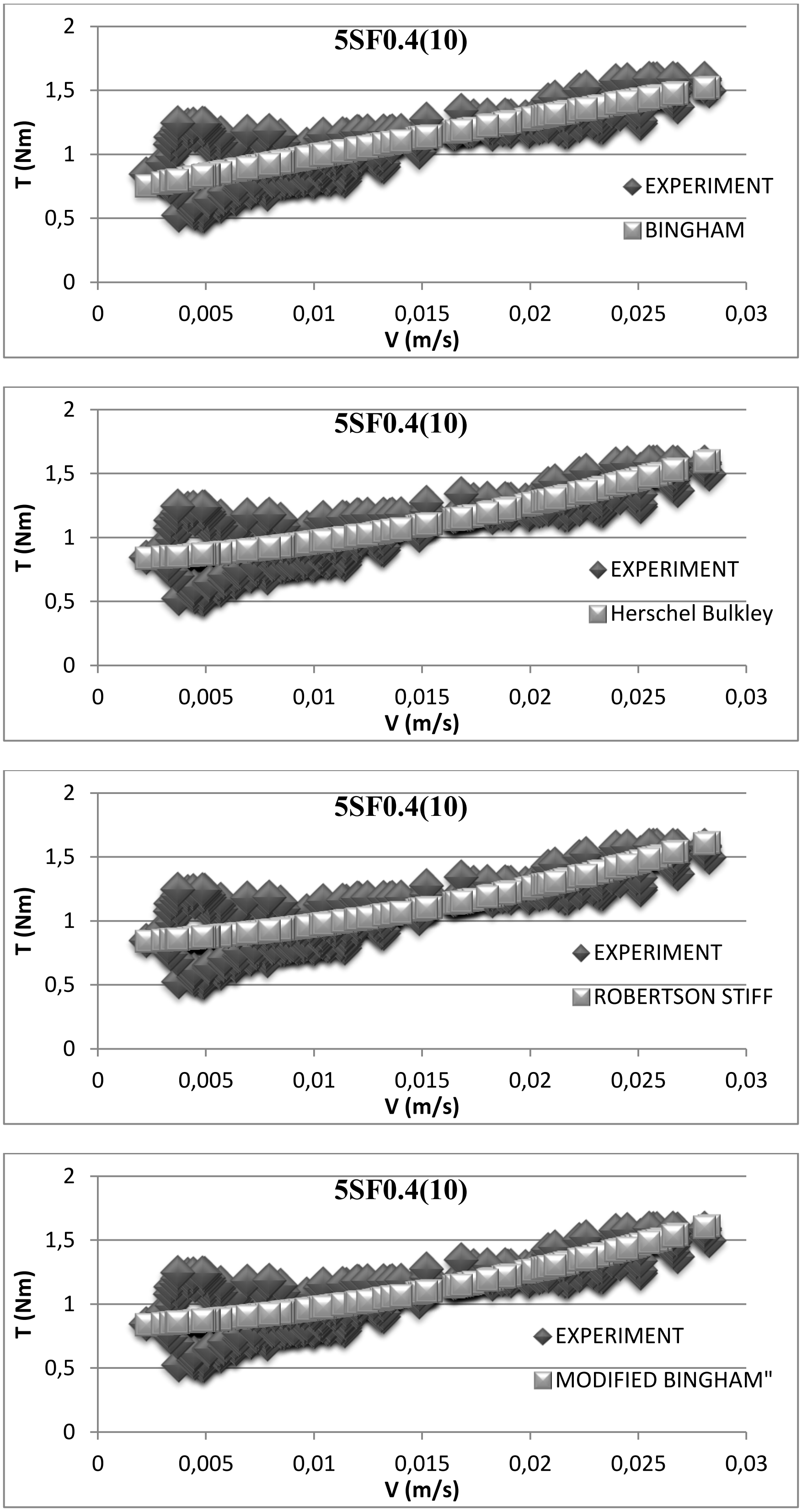

Figure A.44 Flow models for 5SF 0.4 (10)

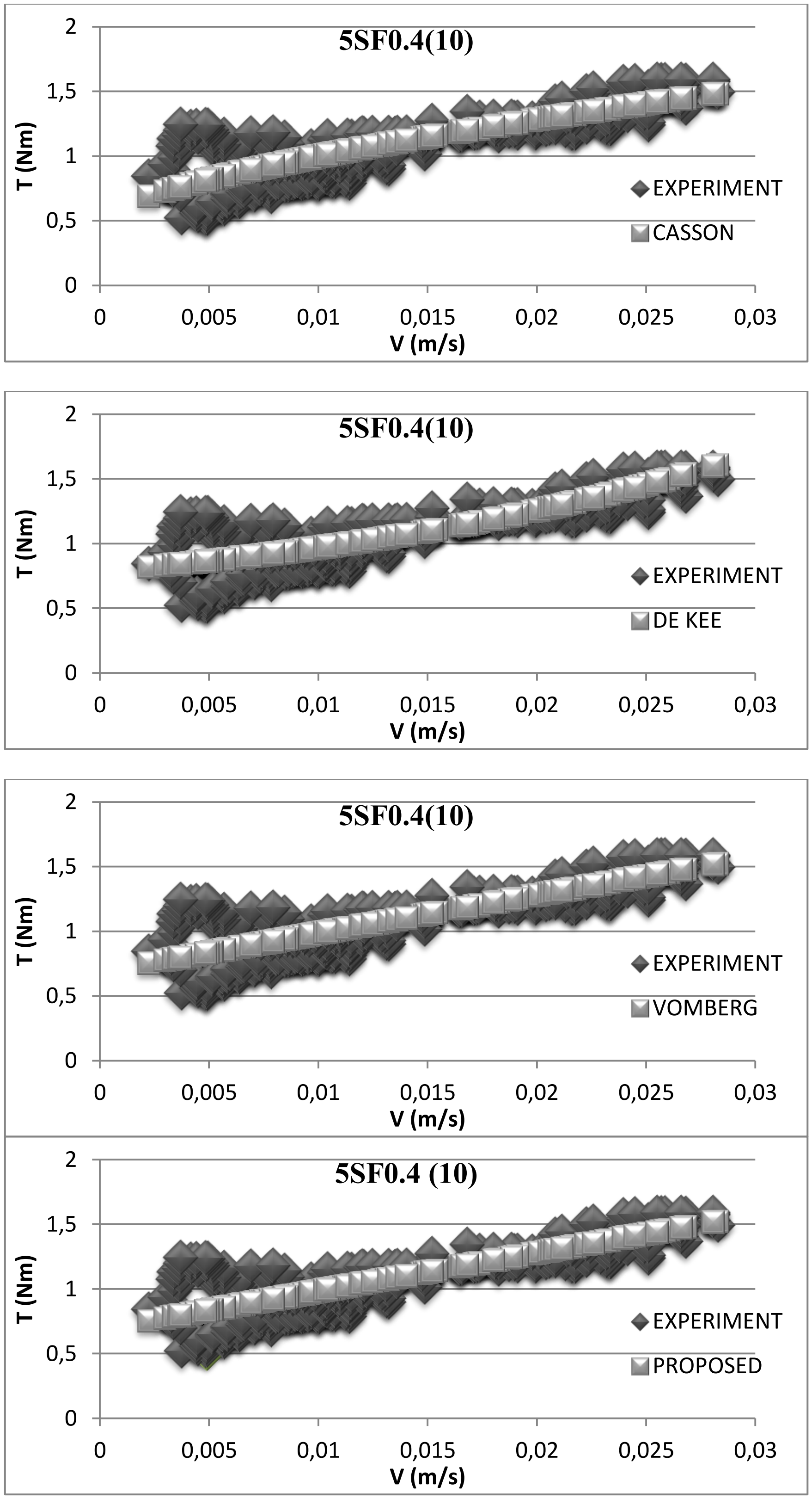

Figure A.44 (Continued)

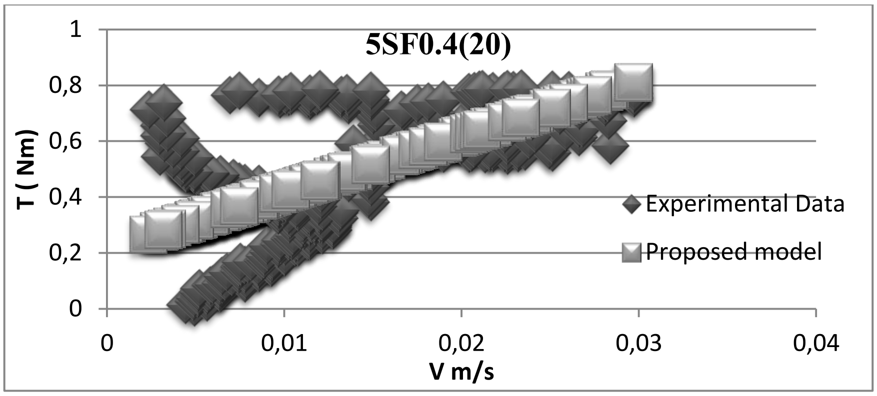

Figure A.45 Flow model for 5SF0.4(20)

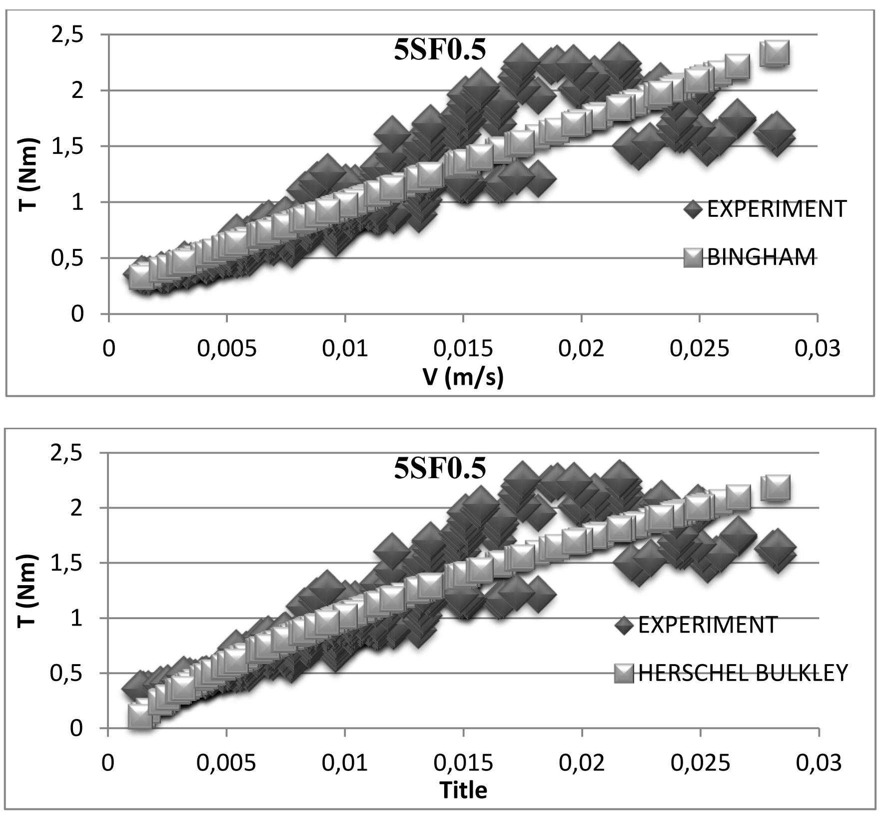

Figure A 46 Different flow models for 5SF 0.5

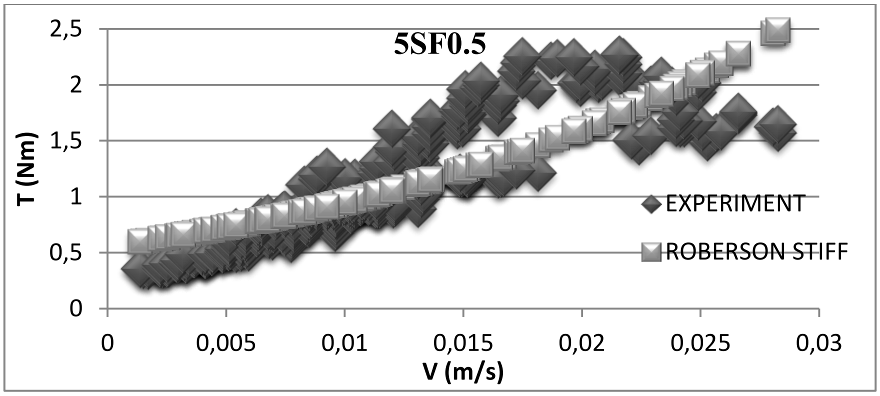

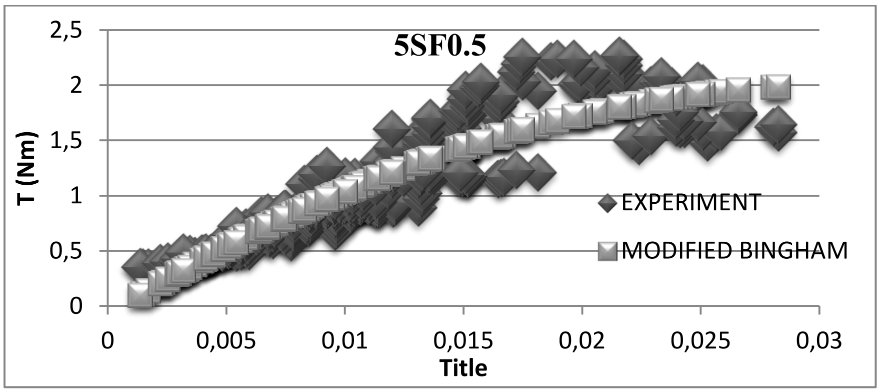

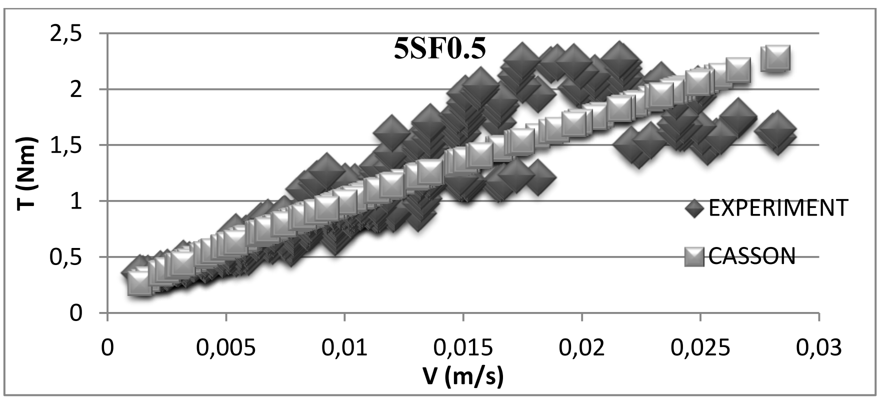

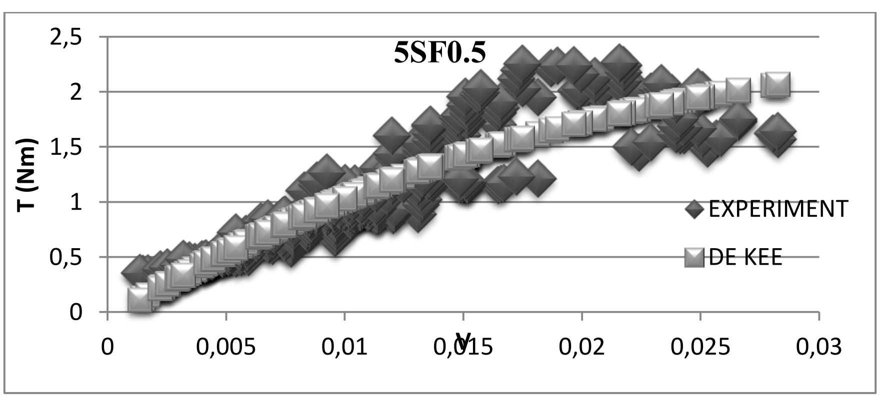

Figure A.46 (Continued)

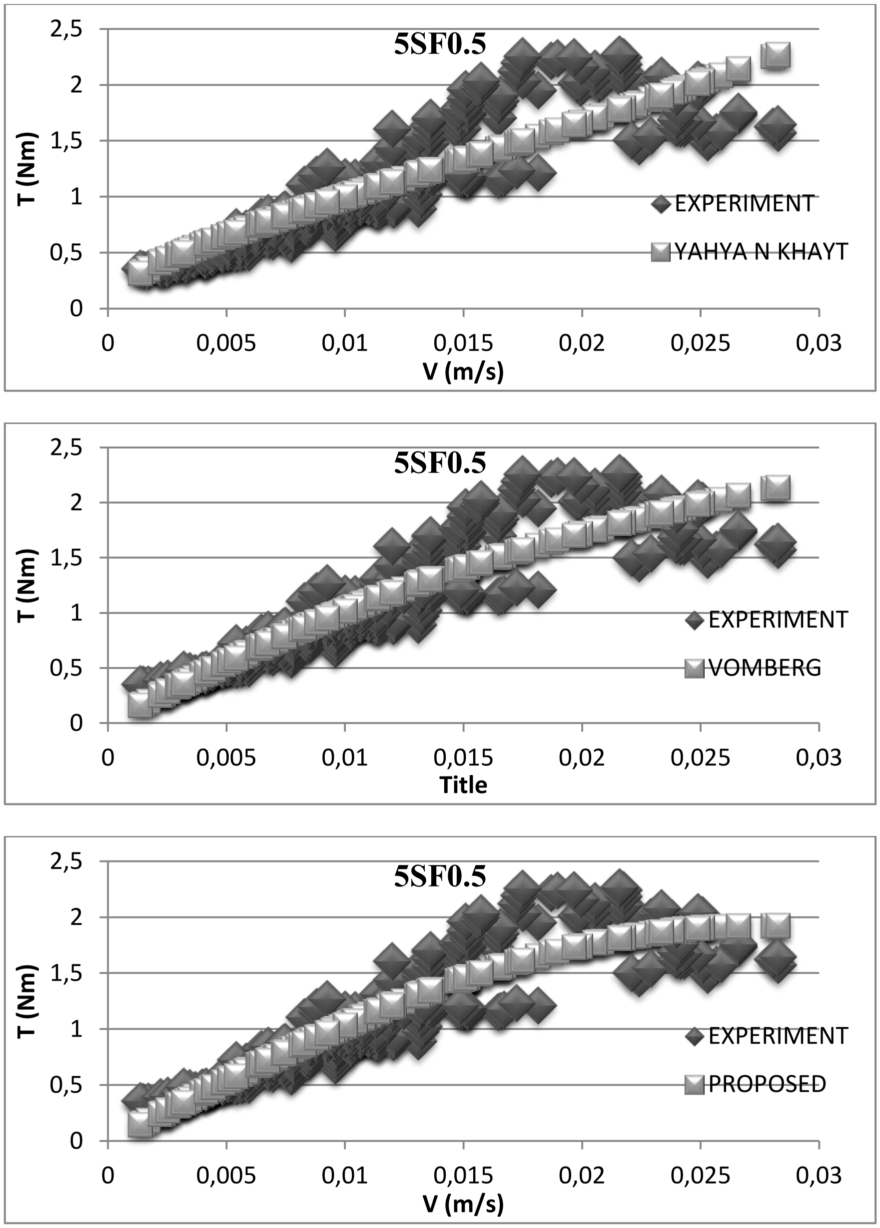

Figure A.46 (Continued)

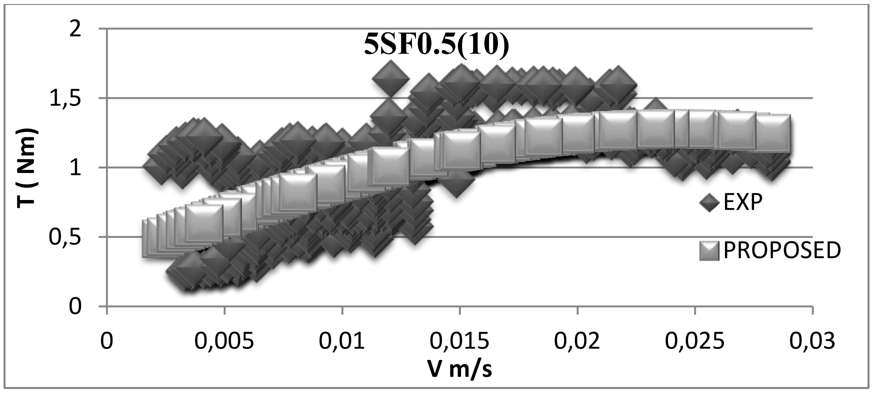

Figure A. 47 Flow Model for 5SF0.5(10)

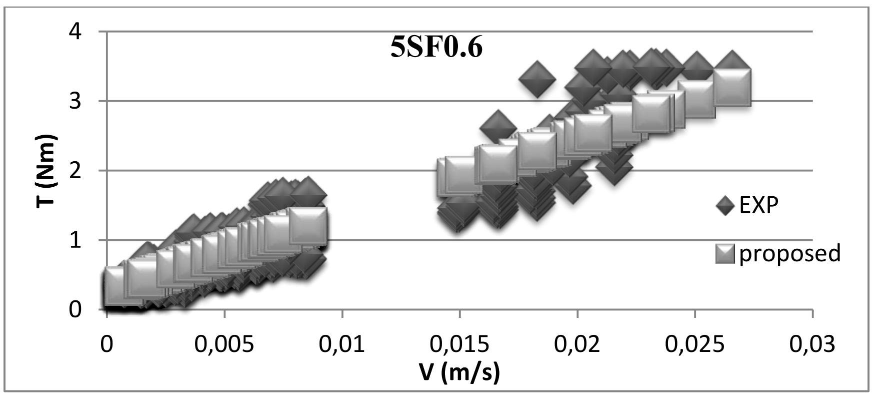

Figure A. 48 Flow Model for 5SF0.6

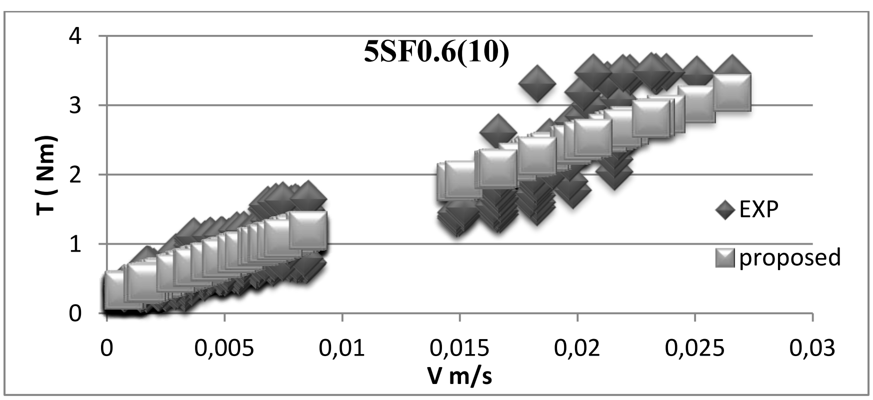

Figure A. 49 Flow Model for 5SF0.6(10)

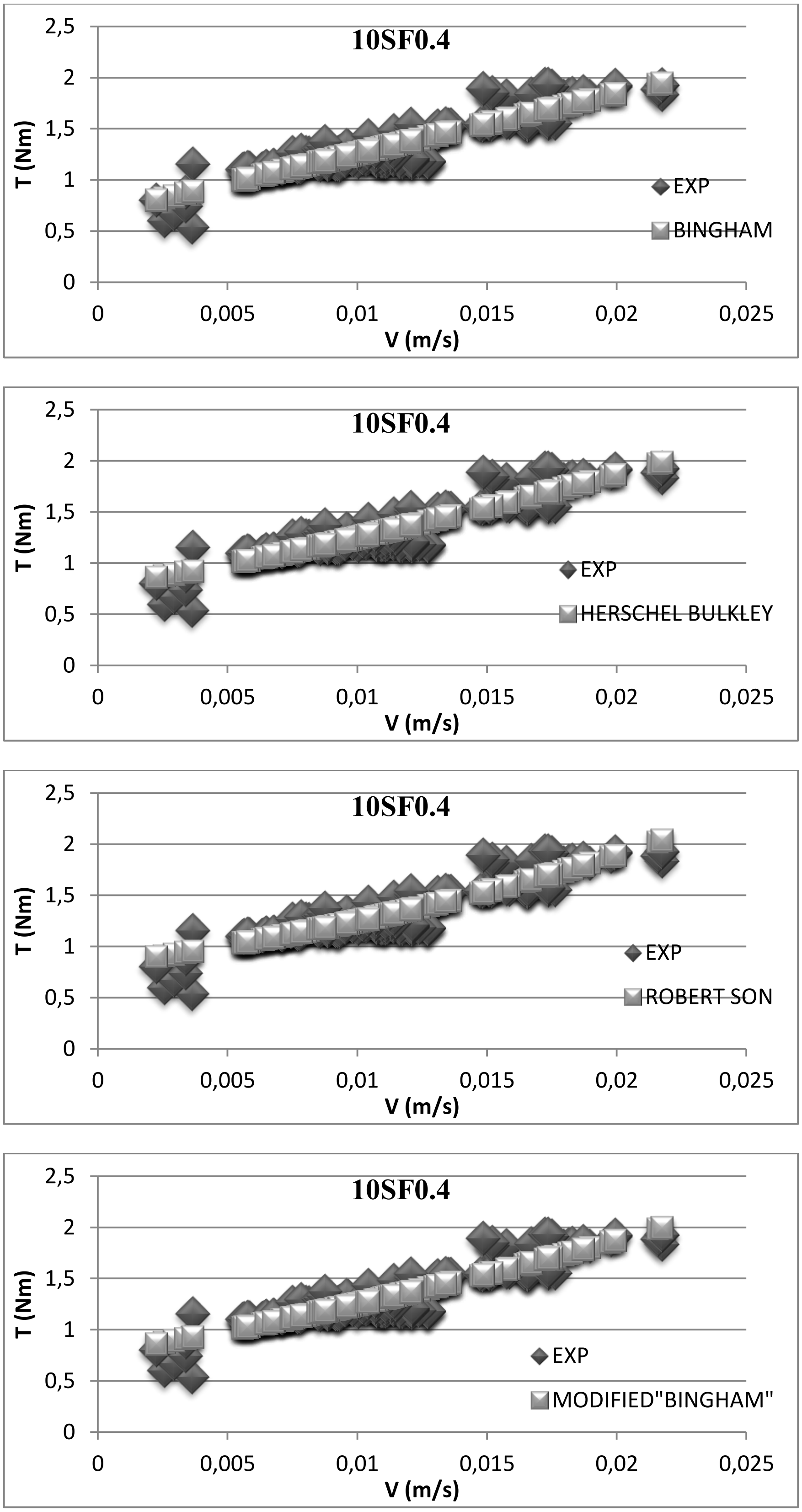

Figure A.50 Flow models for 10SF 0.4

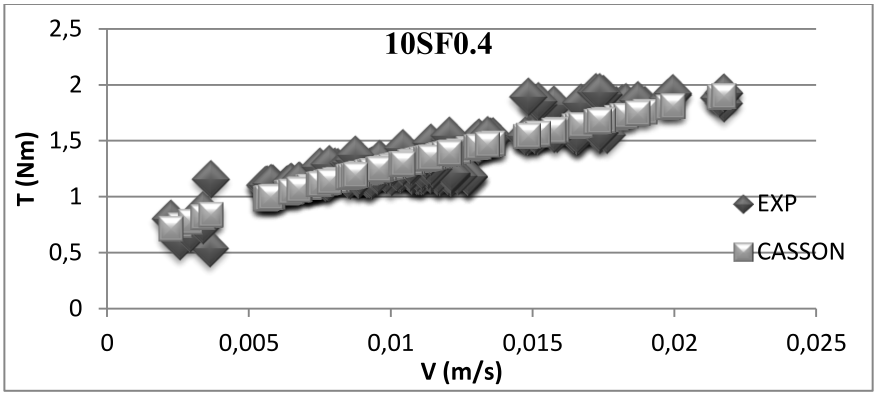

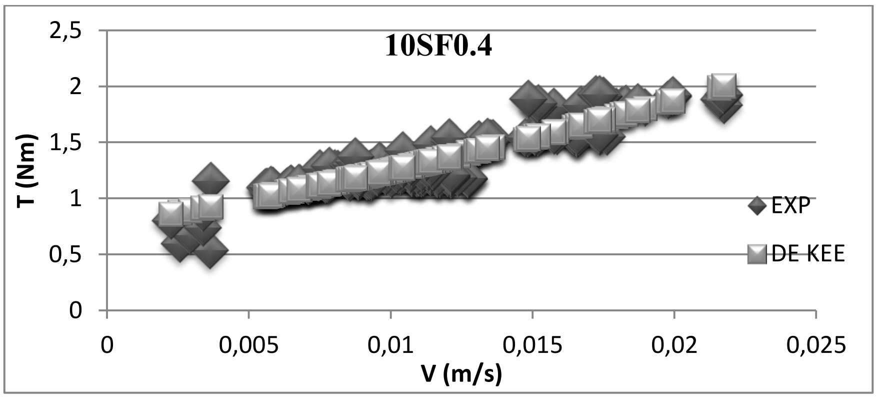

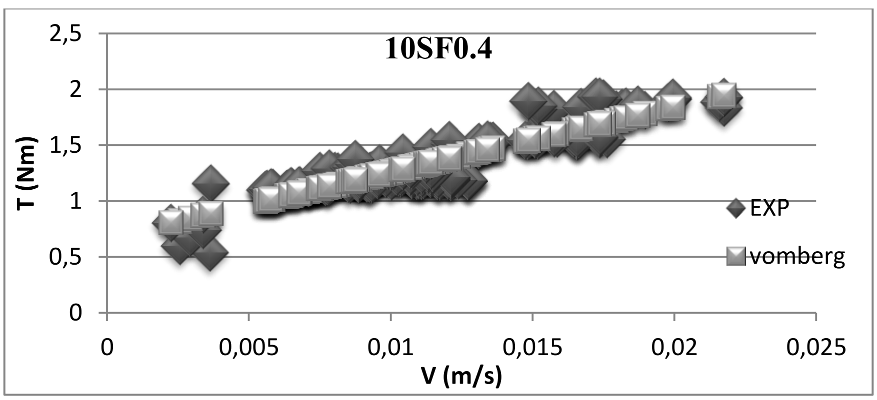

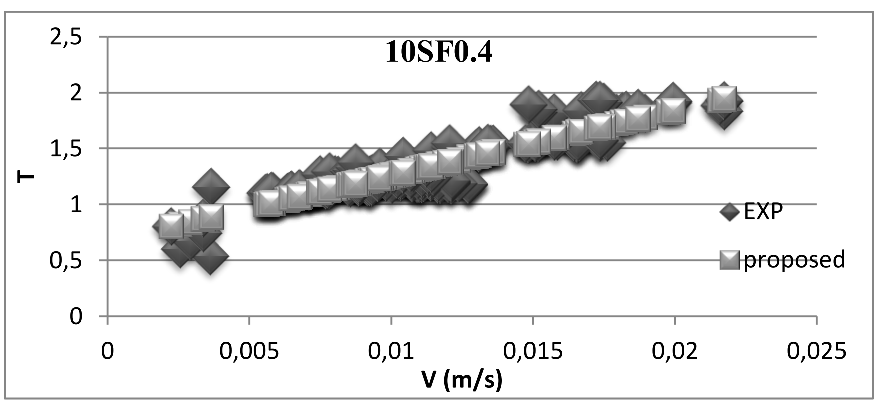

Figure A.50 (Continued)

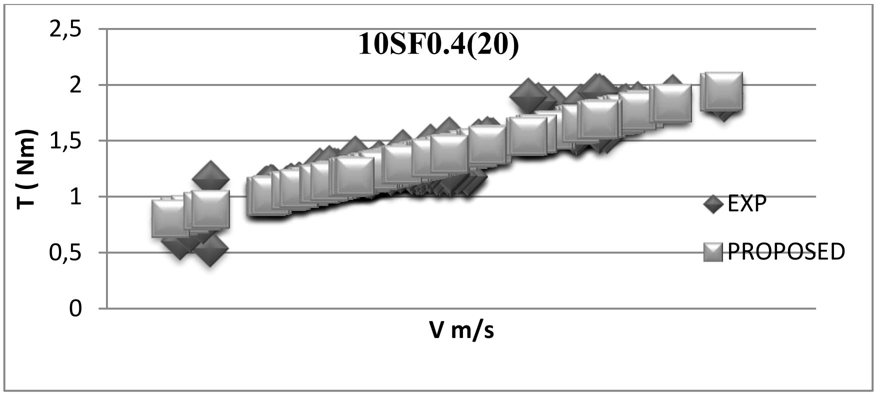

Figure A.51 Flow model for 10SF 0.4 (20)

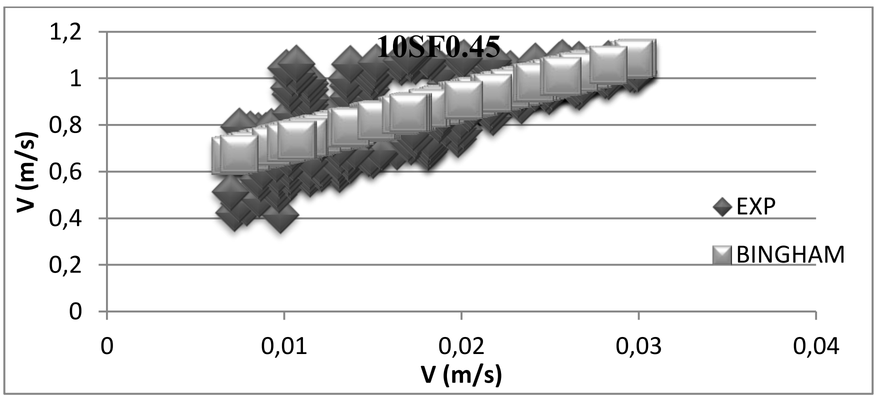

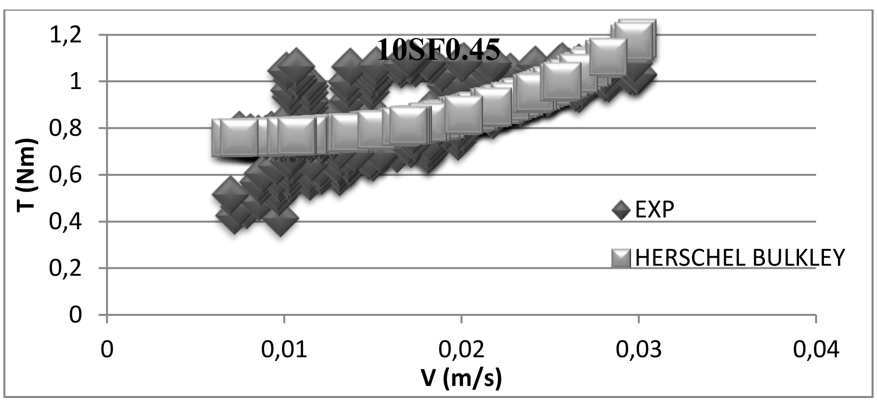

Figure A. 52 Flow model for 10SF 0.45

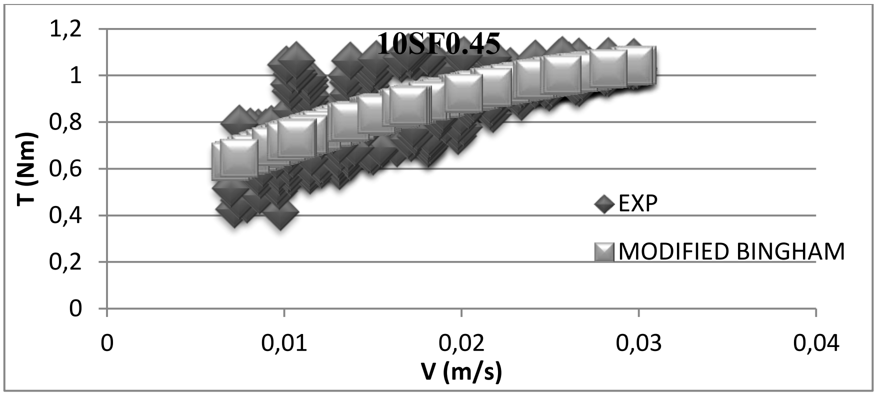

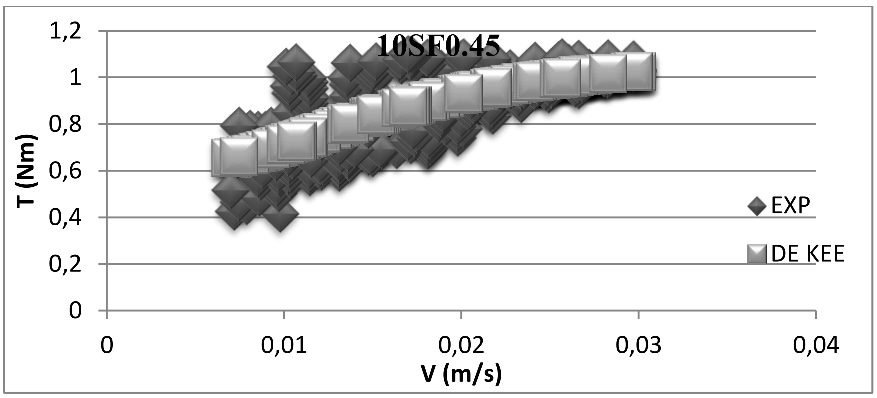

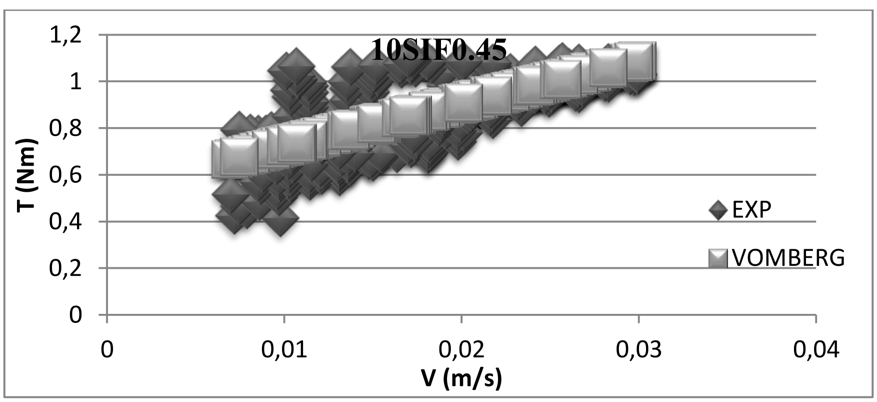

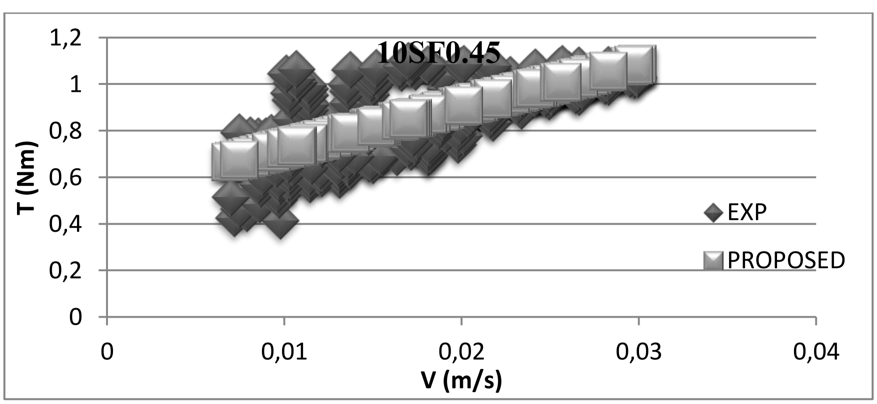

Figure A.52 Continued

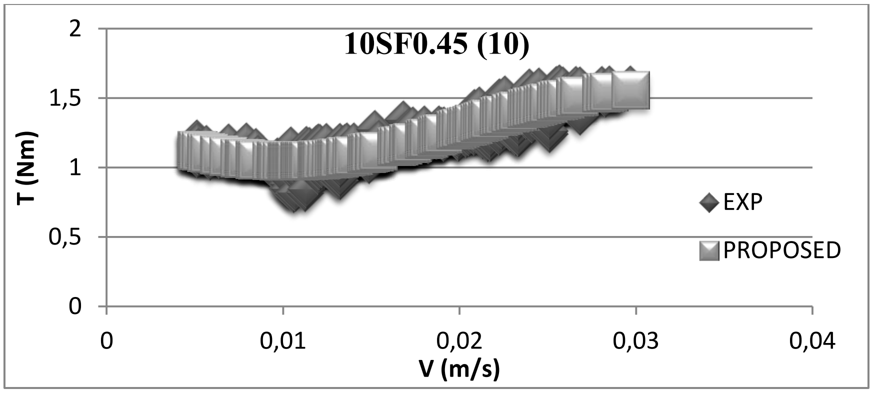

Figure A. 53 Flow model for 10 SF 0.45(10)

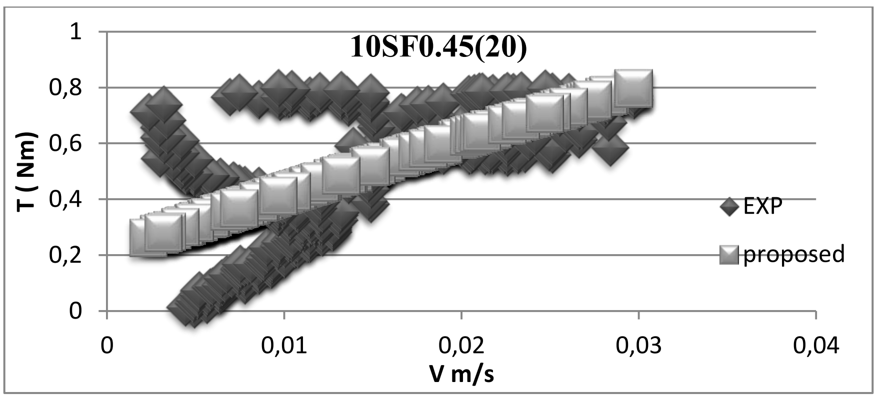

Figure A. 54 Flow model for 10 SF 0.45(20)

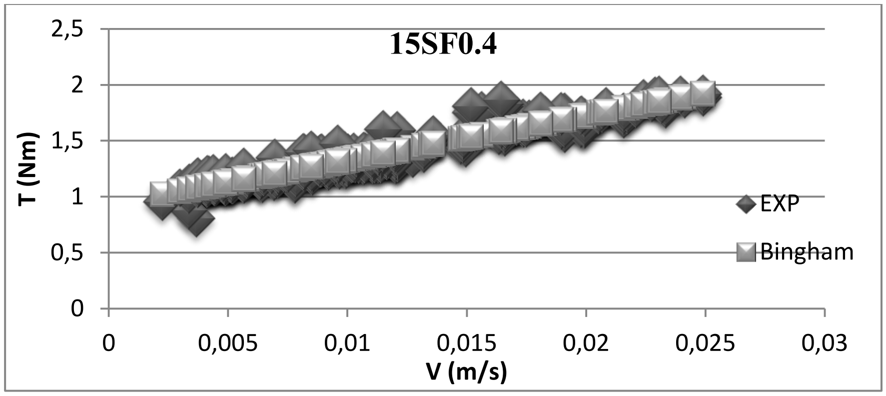

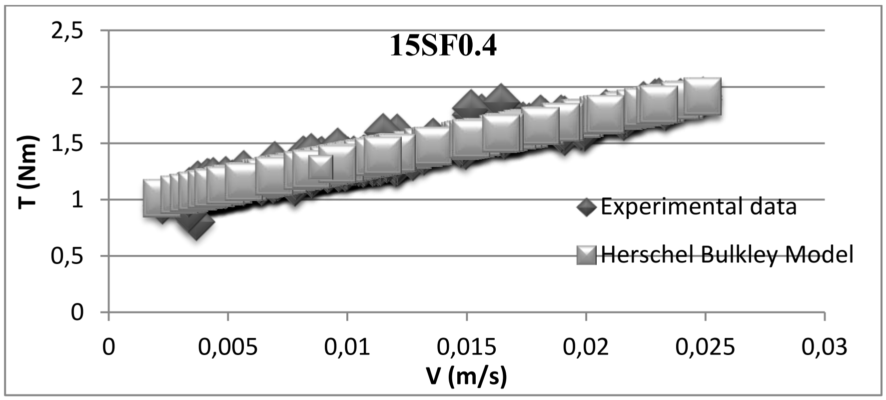

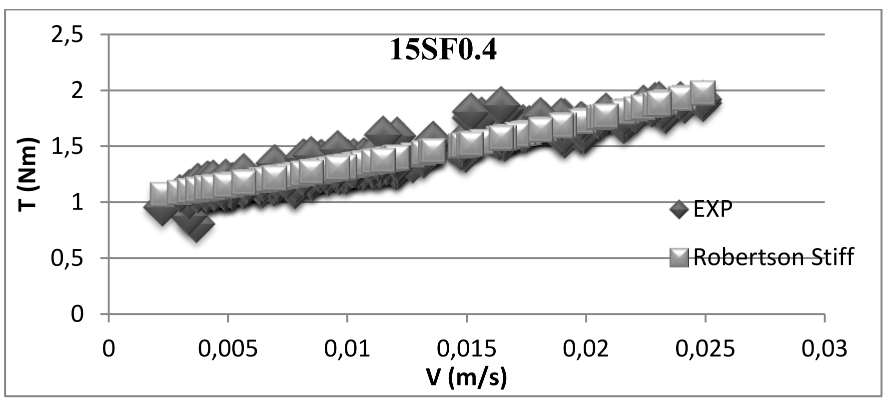

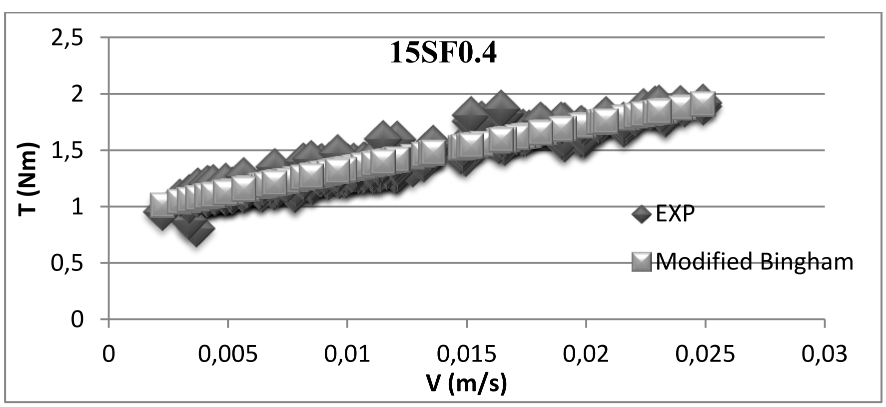

Figure A. 55 Flow models for 15 SF 0.4

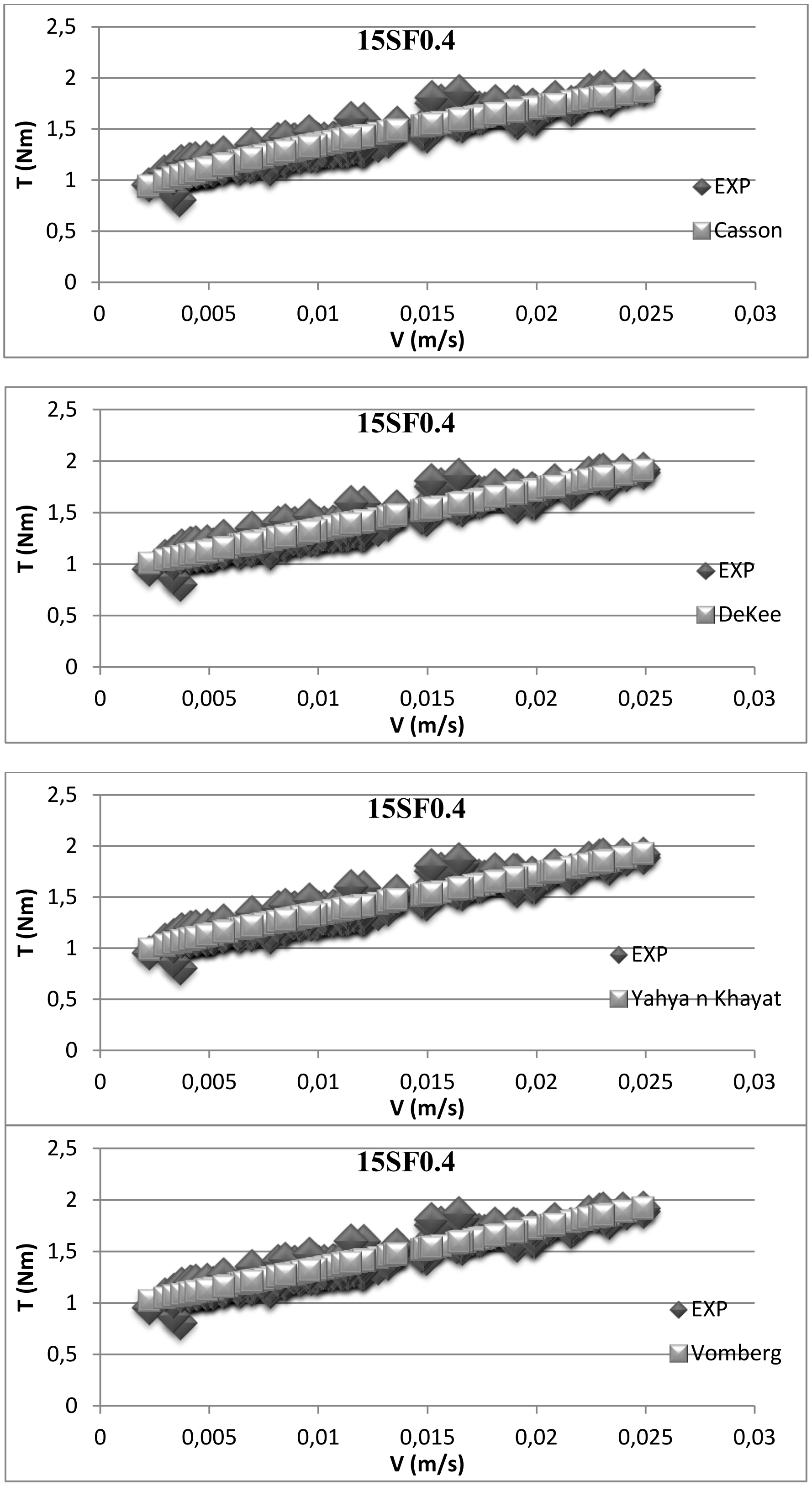

Figure A.55 (Continued)

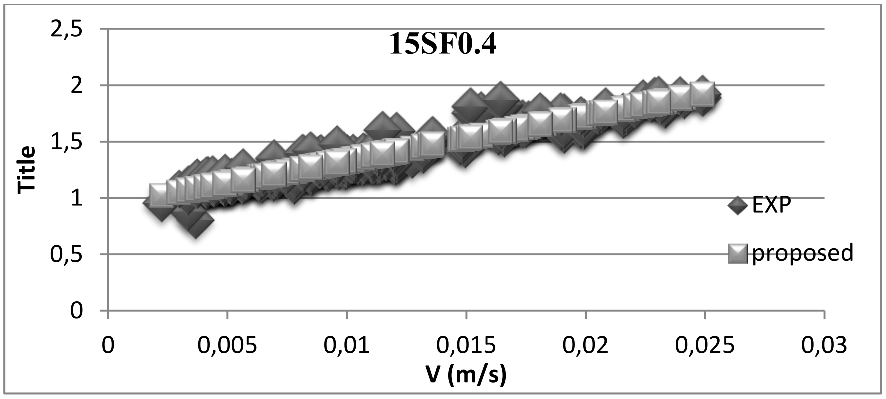

Figure A.55 (Continued)

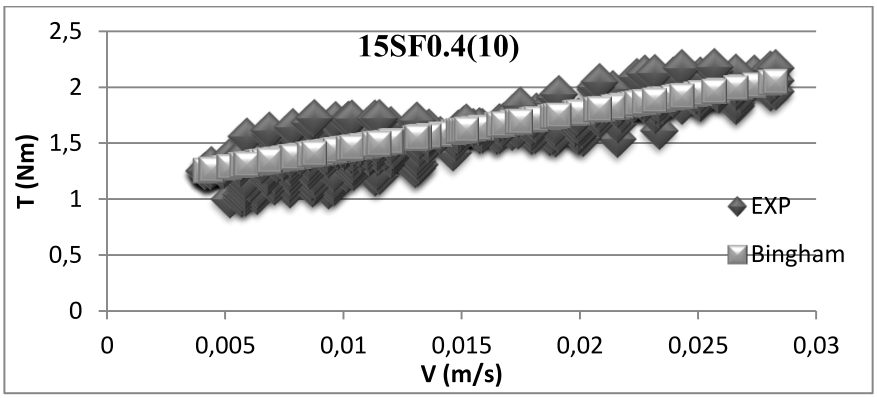

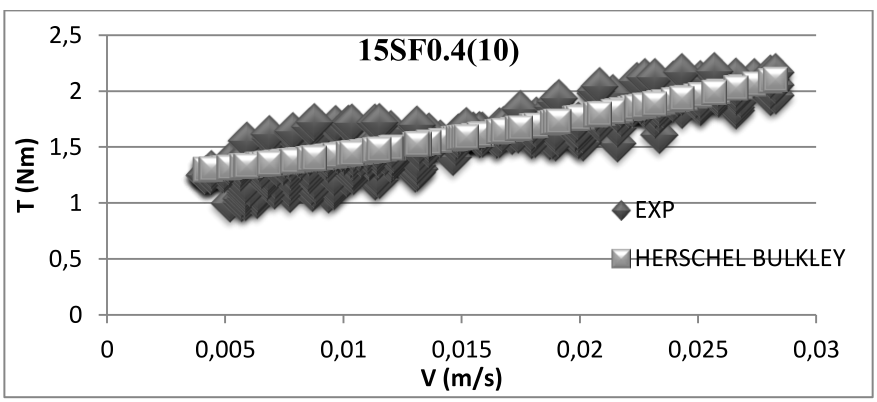

Figure A. 56 Flow models for 15SF0.4(10)

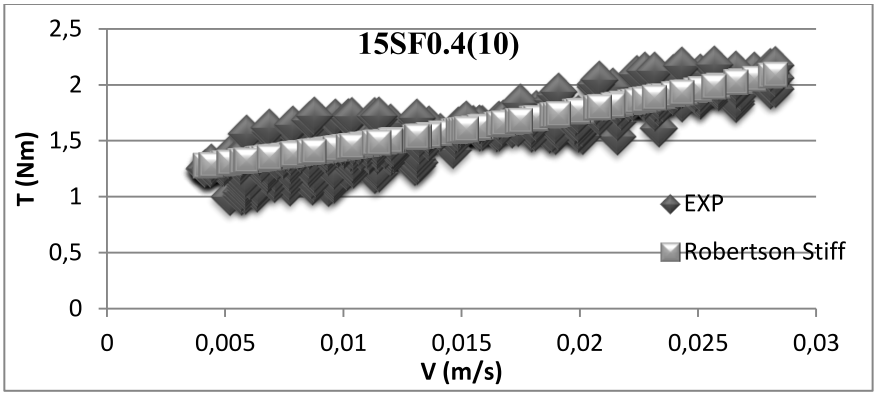

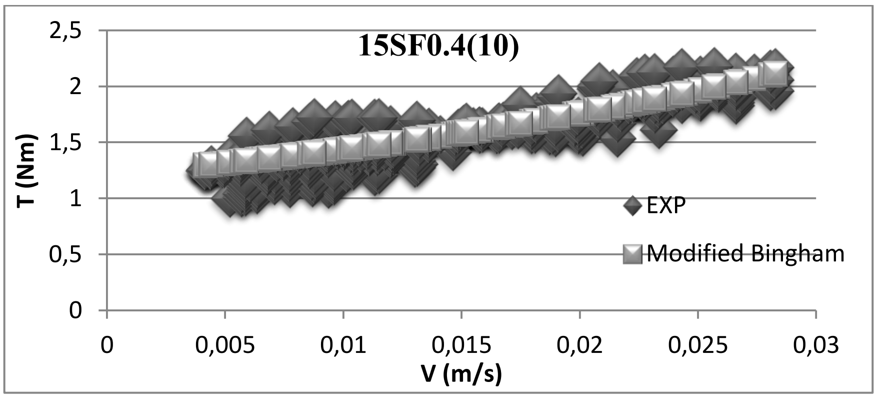

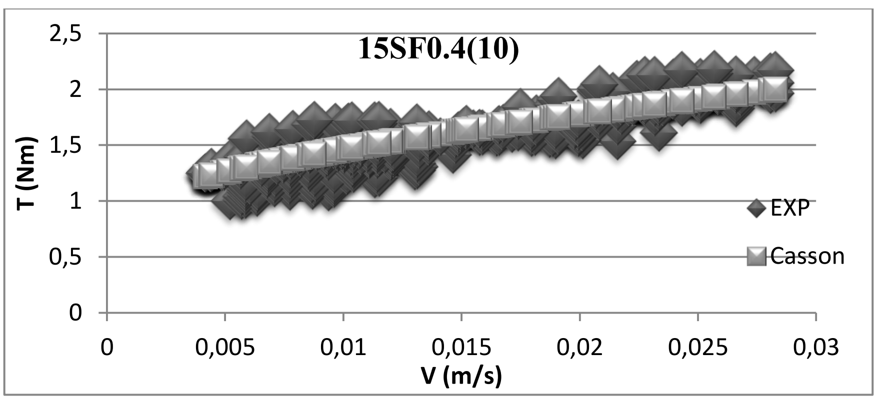

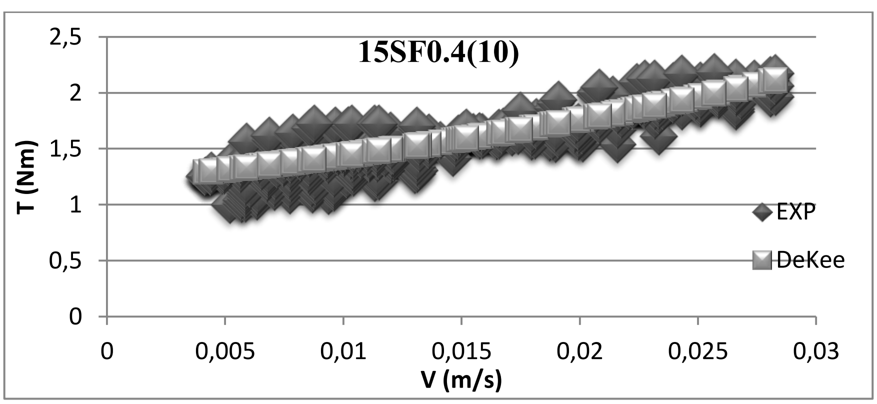

Figure A.56 Continued

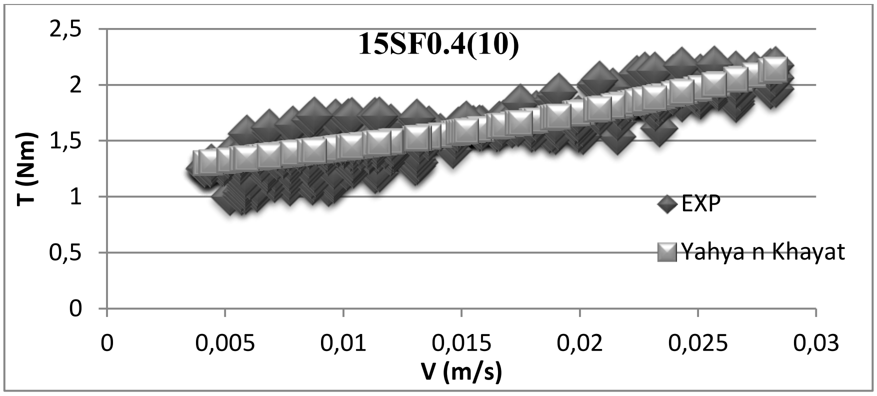

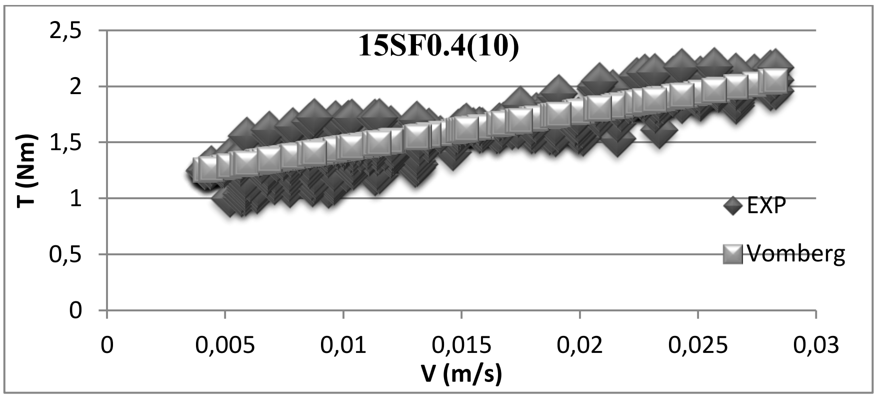

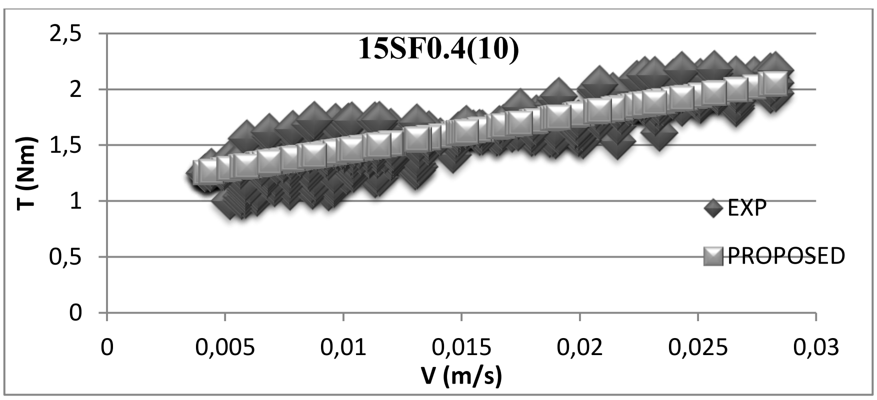

Figure A.56 (Continued)

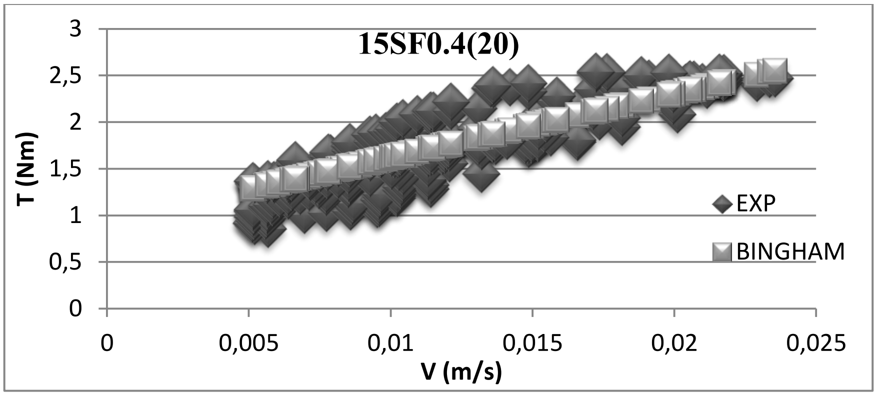

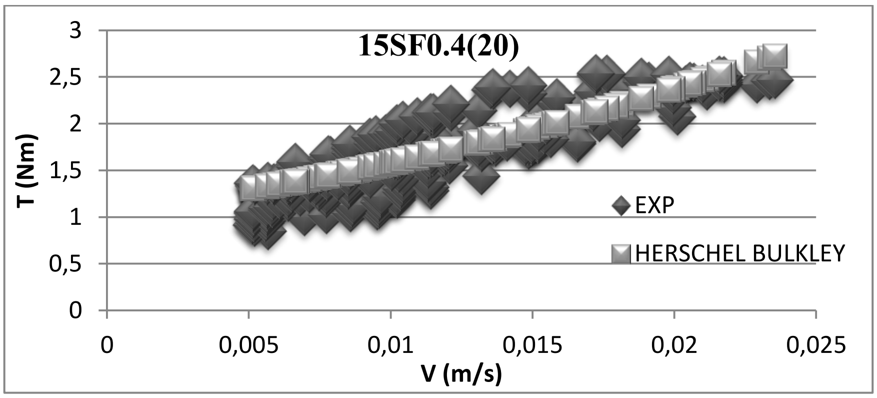

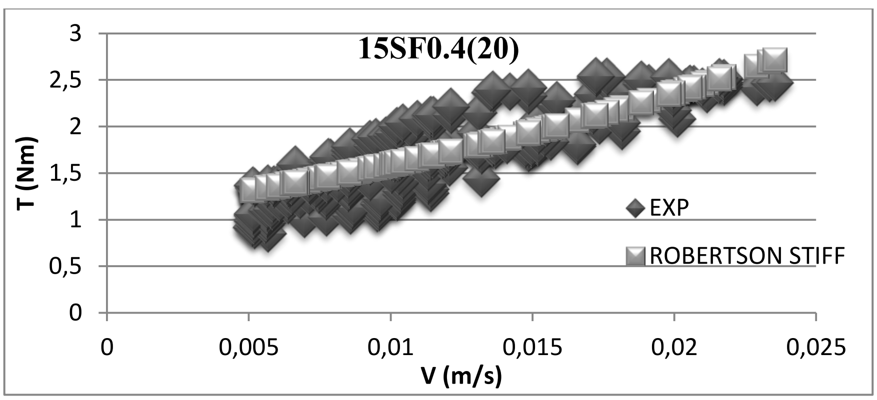

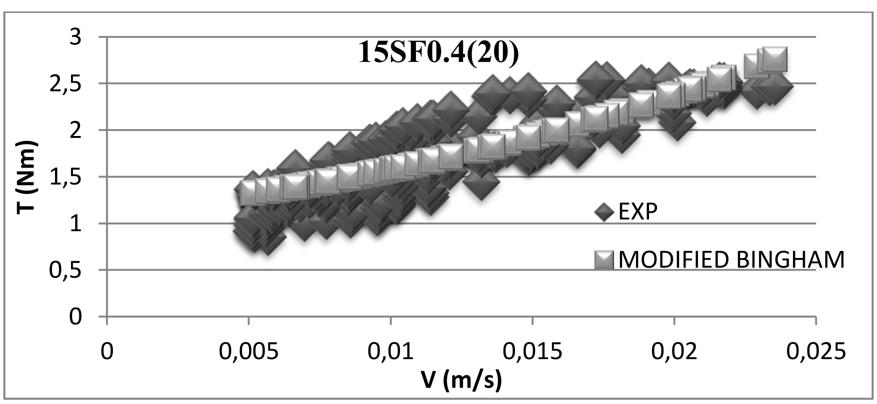

Figure A.57 Flow models for 15SF0.4(20)

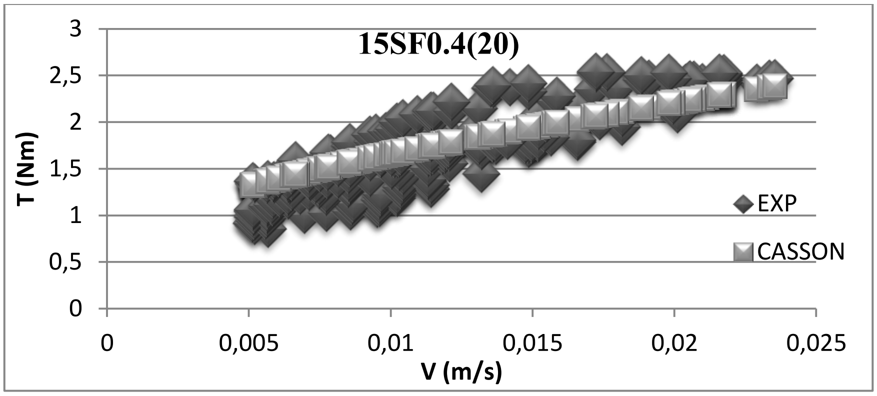

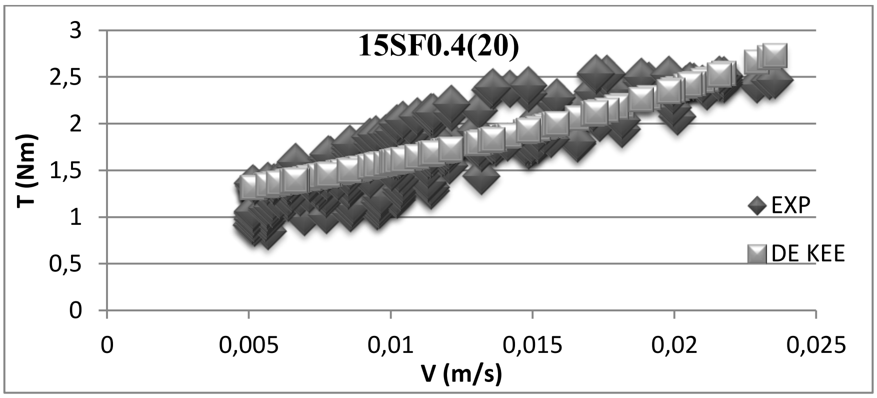

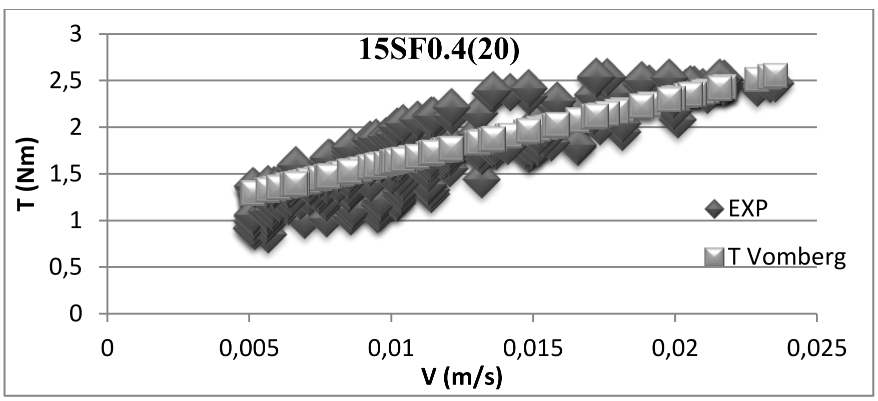

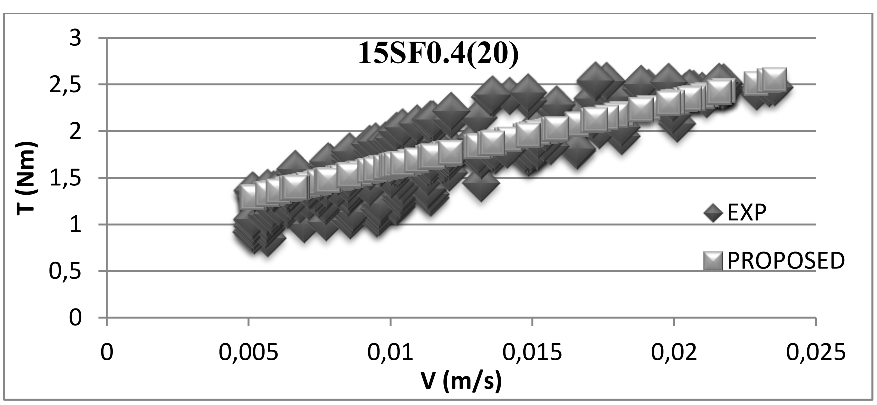

Figure A.57 (Continued)

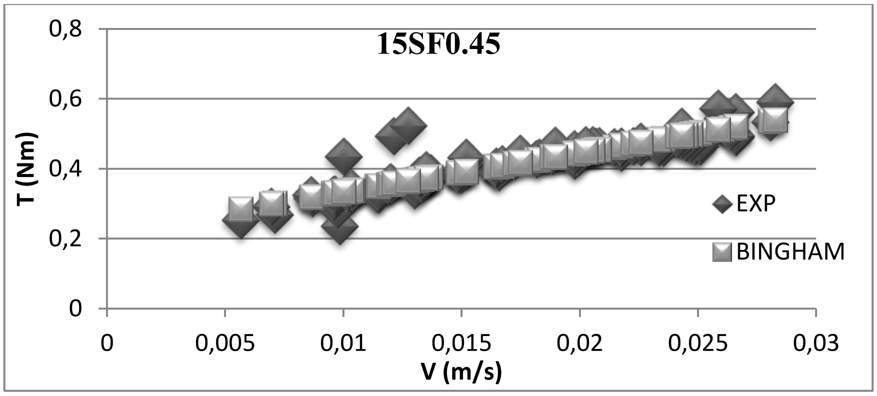

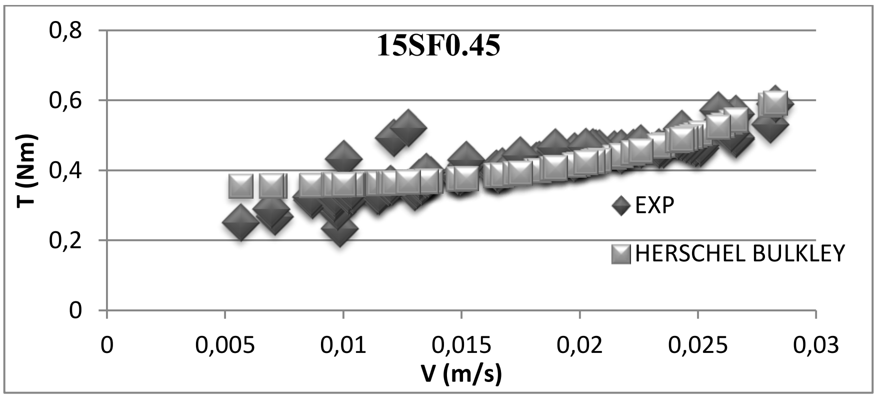

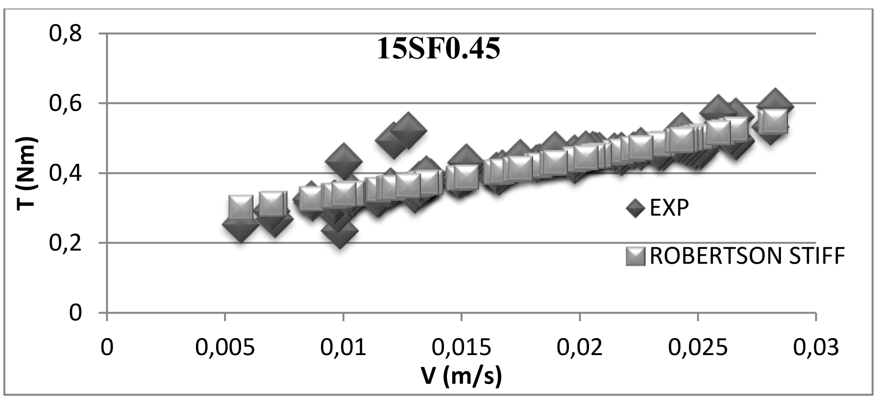

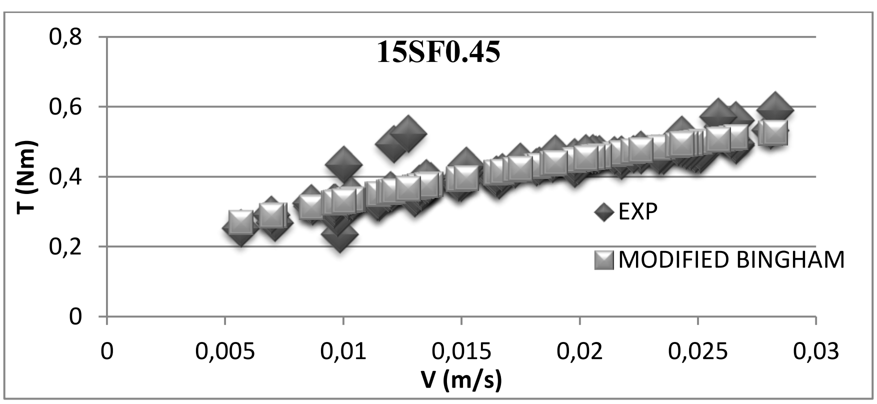

Figure A.58 Flow models for 15SF0.45

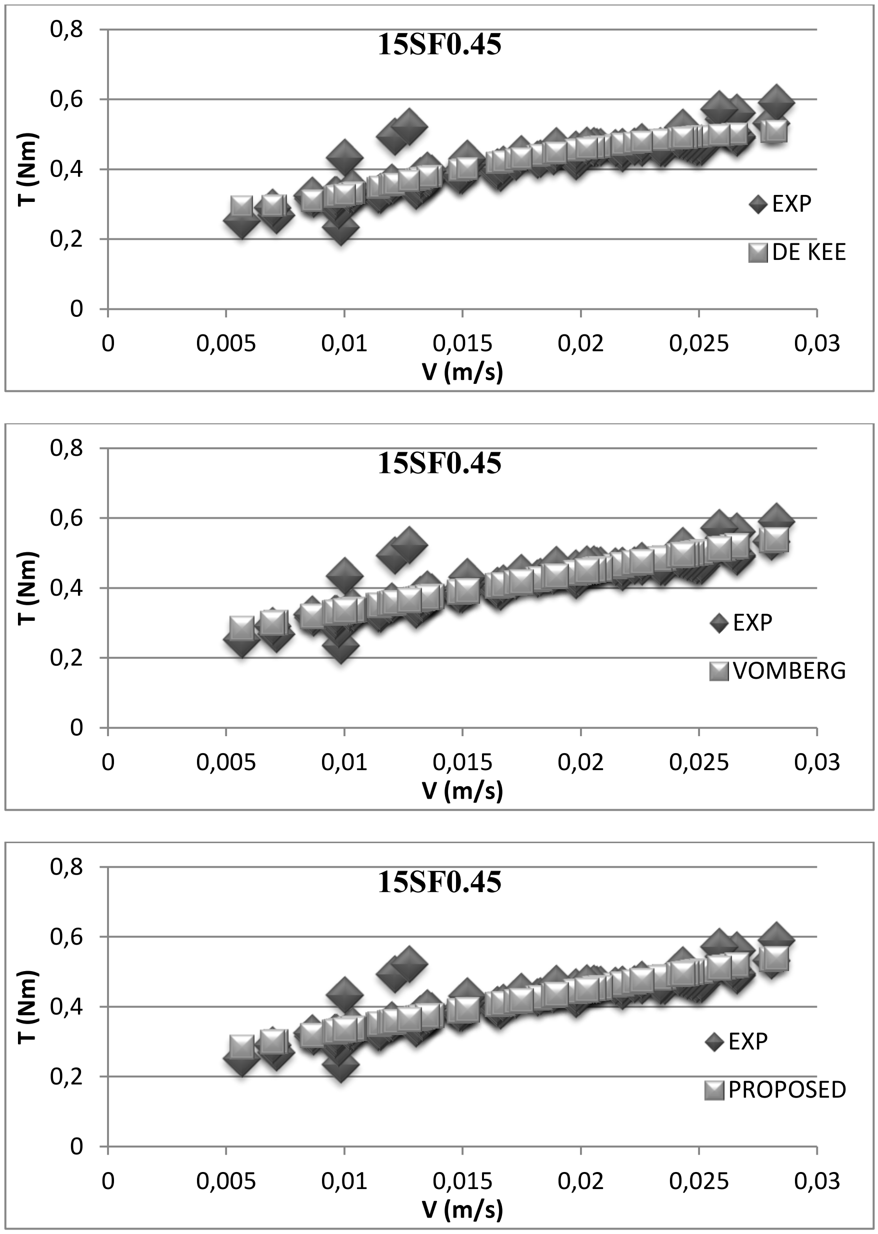

Figure A.58. (Continued)

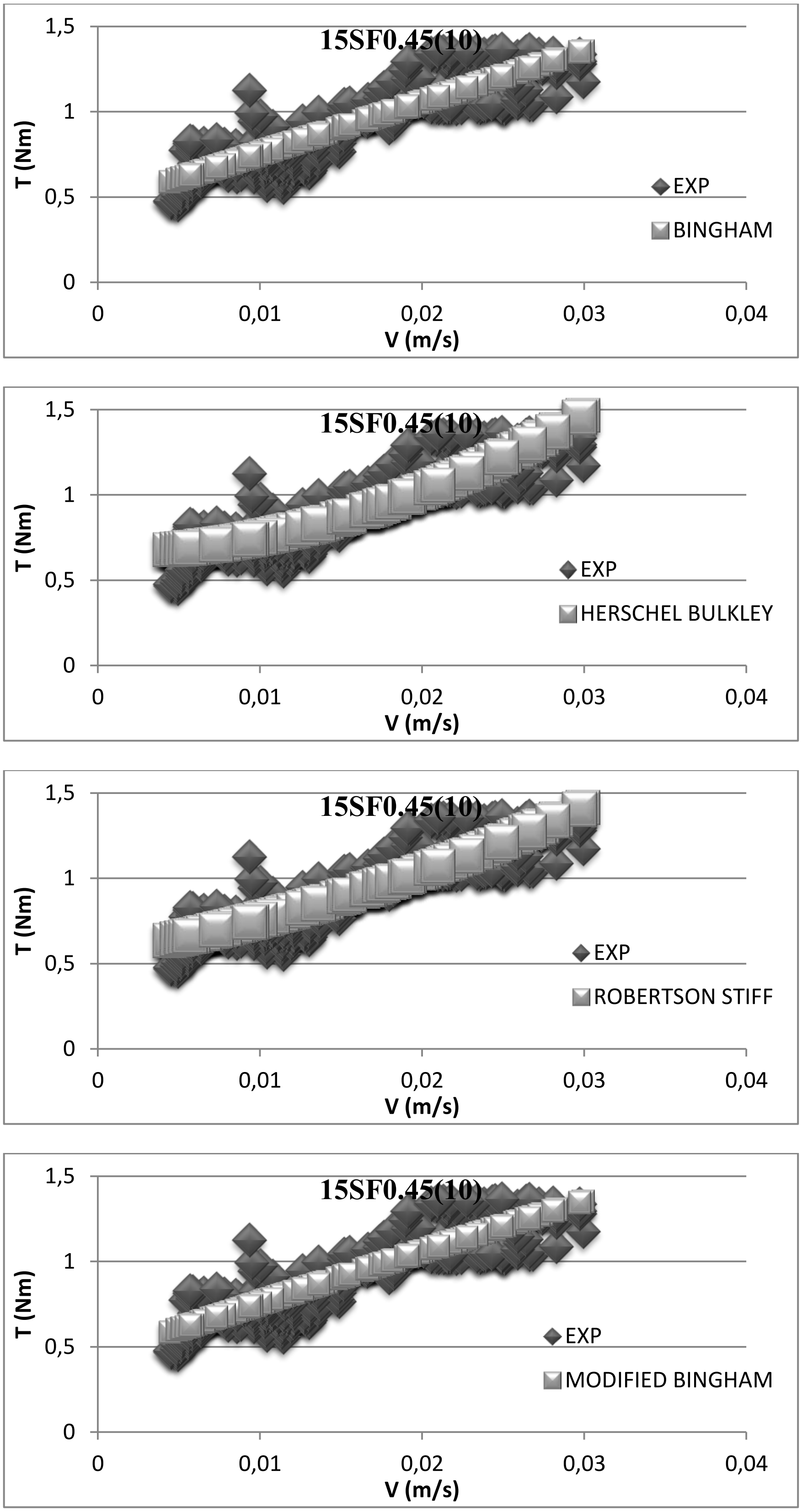

Figure A.59 Flow models for 15SF0.45(10)

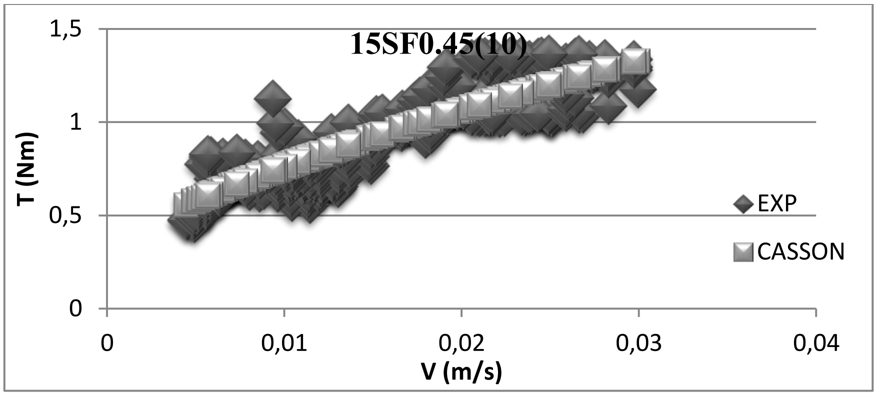

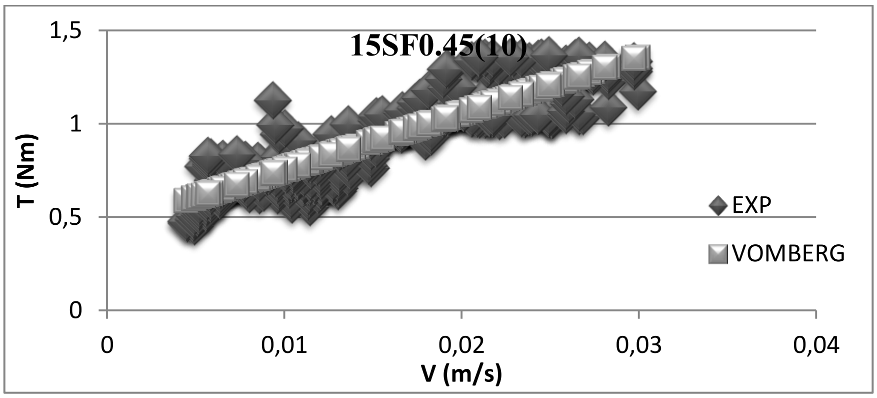

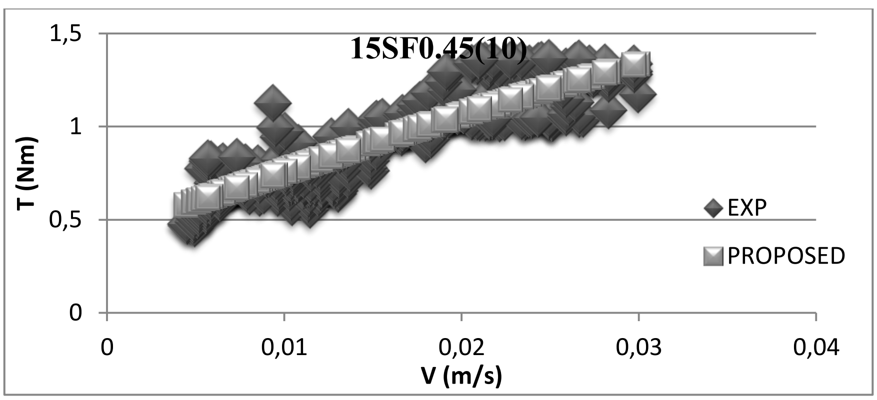

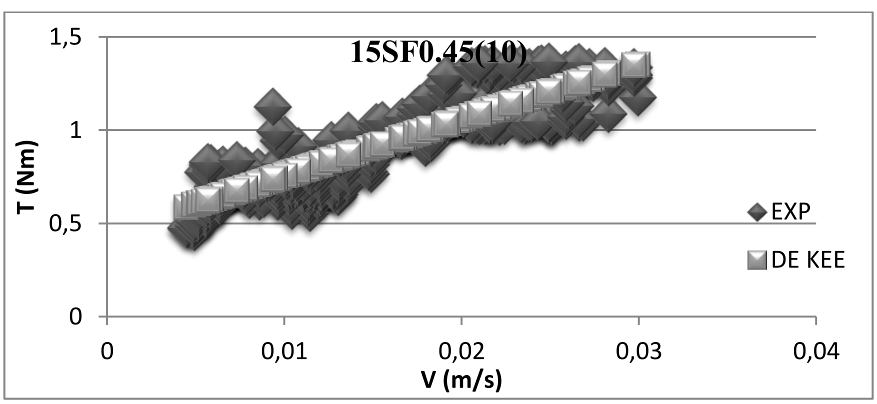

Figure A.59 (Continued)

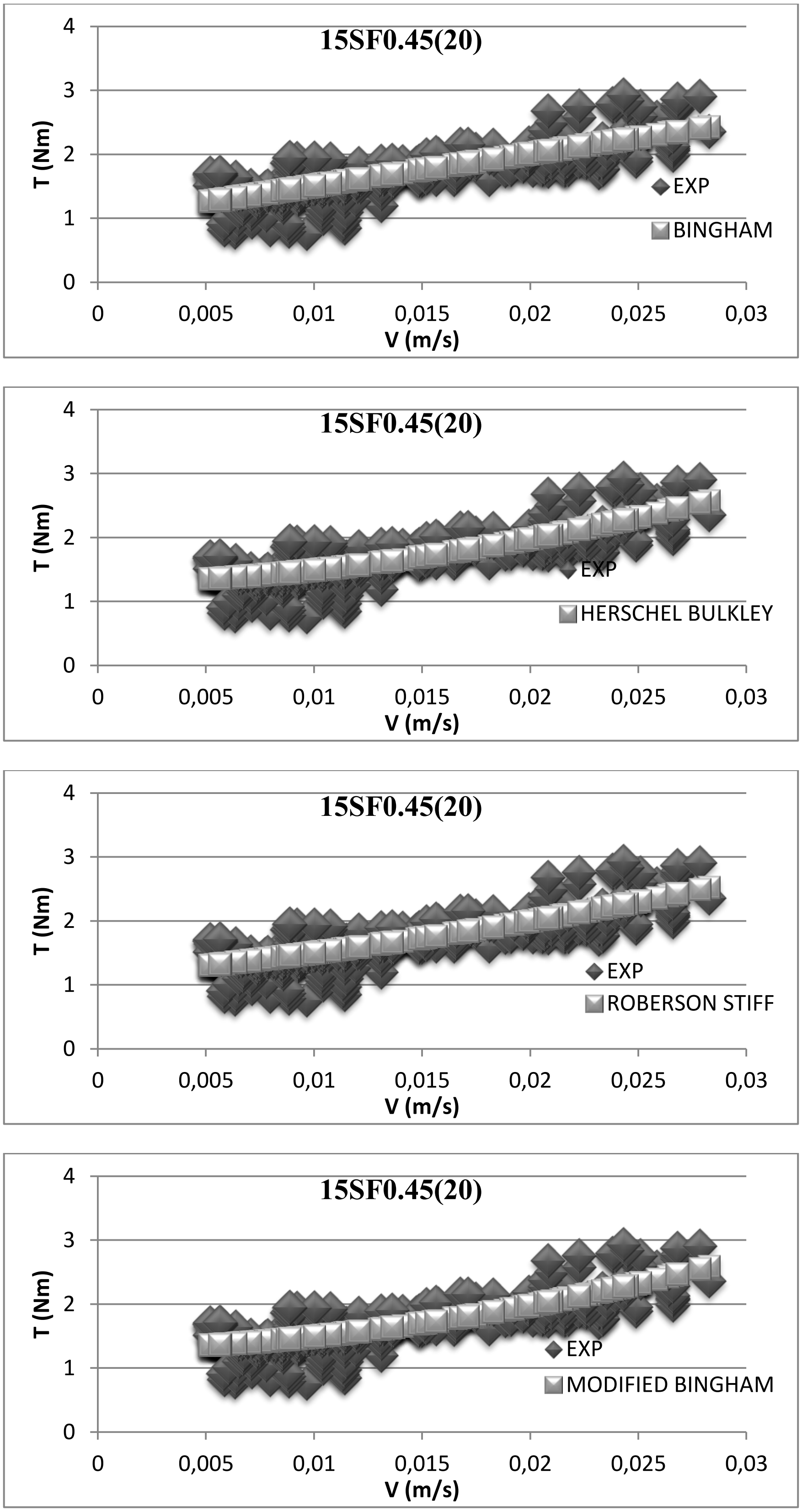

Figure A. 60 Flow models for 15SF 0.4 5(20)

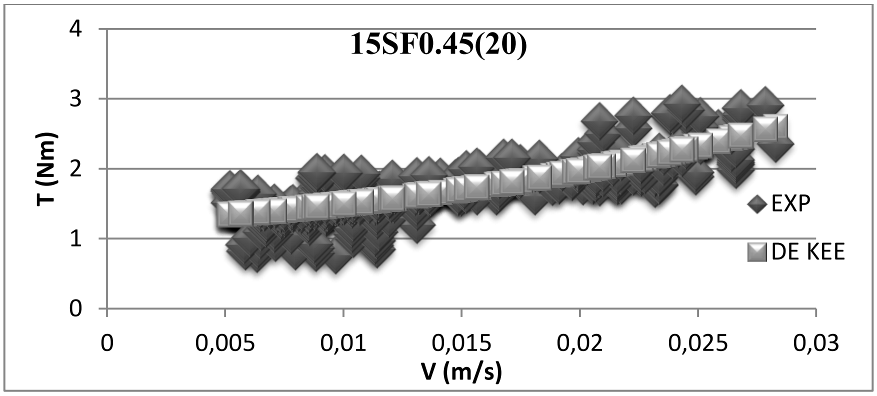

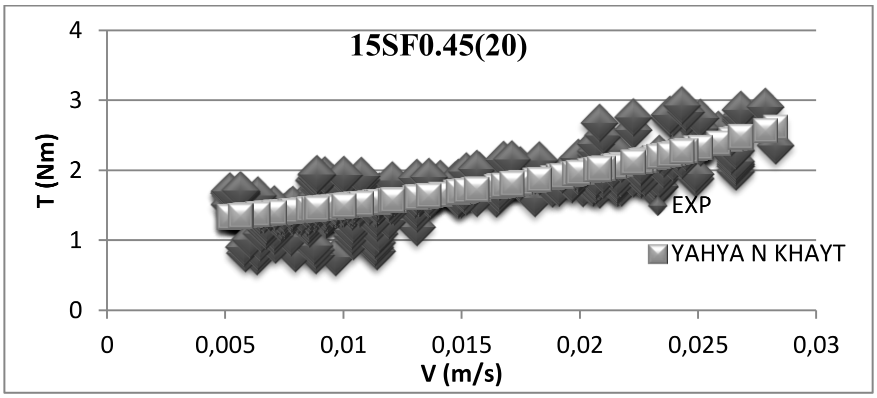

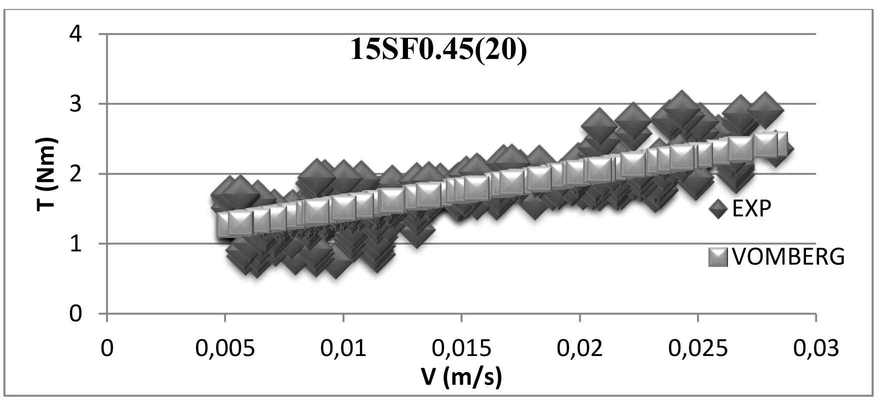

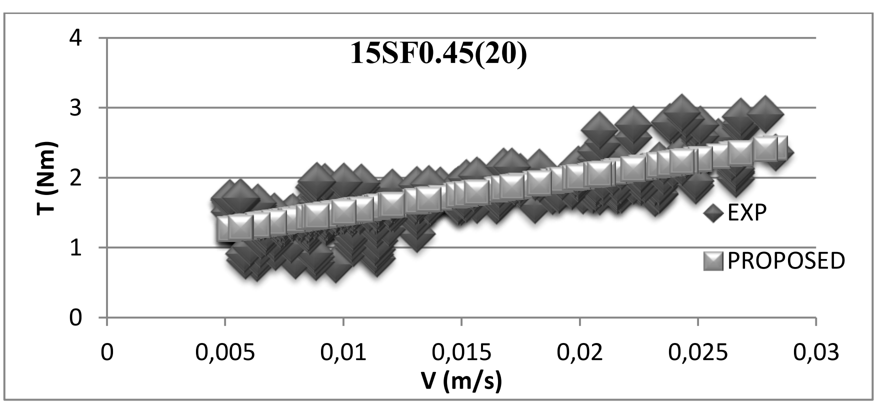

Figure A.60. (Continued)

CURRICULUM VITAE

Maria Idrees

Department of Civil Engineering

Middle East Technical University

Nationality: Pakistan

Email: mariyaidrees@gmail.com

Phone: +923454278291/+905356389425

Education

PhD Civil Engineering	Middle East Technical University, Ankara.
MSc Civil Engineering	University of Engineering and Technology Lahore, Pakistan
BSc Engineering	University of Engineering and Technology Lahore, Pakistan

Award:

90% Overseas Scholarship HEC Pakistan

Work Experience

Engineering Design Bureau	6 Months
Lecturer, University of Lahore	2 Years
Assistant Professor, University of Lahore	4 Months